

Understanding the genetic basis of resistance to European canker in apple

Thesis submitted for the degree of Doctor of Philosophy
School of Agriculture, Policy and Development

Ulrika Amanda Karlström

September 2023



Apple field at East Malling

Abstract

European canker, caused by the fungal pathogen *Neonectria ditissima*, is a devastating disease in commercial apple production. *N. ditissima* is principally a wood pathogen, which causes trunk cankers and dieback in apple orchards. Due to a lack of efficient cultural and chemical methods to control European canker, host resistance remains one of the most effective means of limiting disease spread. Despite its importance to the apple growing community, the genetic basis underlying this resistance is still not well understood which hinders efficient breeding of cultivars with improved tolerance to the disease. The work in this thesis was conducted to aid the development of apple cultivars with a high tolerance to infection by *N. ditissima*. This was done by exploring the genetics behind host resistance in apple scion germplasm as well as investigating the potential of developing apple cultivars with canker-suppressing endophytic microbiomes.

This thesis describes the identification of seven quantitative trait loci (QTL) associated with resistance to European canker in apple through Bayesian analysis. Single nucleotide polymorphism (SNP) haplotypes associated with resistant alleles for each QTL are also reported. The molecular basis of this quantitative resistance was further explored through a transcriptome analysis. The host response to *Neonectria* infection was studied in two partially tolerant cultivars; the scion variety 'Golden Delicious' and the rootstock cultivar 'M9'. Furthermore, a comparative transcriptome analysis of full-sibling apple genotypes carrying resistant and susceptible alleles at six resistance QTL was conducted to identify candidate genes underlying the quantitative resistance to this wood pathogen. Host resilience to plant pathogens is not only dependent on host resistance but can also be influenced by microbial communities colonising the phyllosphere. The work within this thesis therefore further explores the feasibility to breed apple cultivars amenable to endophyte colonization through a QTL analysis in a bi-parental population of apple.

Declaration of original authorship

I confirm that this is my own work and the use of all material from other sources has been properly and fully acknowledged.

Ulrika Amanda Karlström, 23/09/2023

Author contribution to published work

Karlström, A., Cabo-Medina, M., and Harrison, R. 2019. “Advances and challenges in apple breeding, vol. 2” in *Achieving Sustainable Cultivation of Temperate Zone Tree Fruits and Berries*, 217-260, ed G. A. Lang (Cambridge: Burleigh Dodds Science Publishing). Doi: 10.19103/AS.2018.0040.21

Amanda Karlström was responsible for the conception and content of the book chapter, extracts from which have been adapted and included in the introduction of this thesis.

Amanda Karlström drafted the original sections of the book chapter. M. Cabo-Medina and R. Harrison were responsible for the critical revision of the chapter. Amanda Karlström had an estimated percentage contribution of 80% to the original book chapter.

Karlström, A., Gómez-Cortecero, A., Nellist, C. F., Ordidge, M., Dunwell, J. M., & Harrison, R. J. 2022. Identification of novel genetic regions associated with resistance to European canker in apple. *BMC Plant Biology*, 22(1), 452.

<https://doi.org/10.1186/s12870-022-03833-0>

Amanda Karlström devised the study together with R.J Harrison. Amanda Karlström designed the experiments together with R.J Harrison, A. Gómez-Cortecero and C.F Nellist. Amanda Karlström was responsible for the experimental work with input from A. Gómez-Cortecero and C.F Nellist. Amanda Karlström was responsible for data analysis and interpretation. Amanda Karlström wrote the first draft of the manuscript. All authors critically reviewed the manuscript and approved the final version of the manuscript. Amanda Karlström had an estimated percentage contribution of 85% to the paper.

Karlström, A., Gómez-Cortecero, A., Connell, J., Nellist, C. F., Ordidge, M., Dunwell, J. M., & Harrison, R. J. Transcriptome analysis provide insights in resistance to European canker and reveal candidate resistance genes.

Amanda Karlström was responsible for the conception of the study together with R.J Harrison and A. Gómez-Cortecero. Amanda Karlström designed the experiments together with R.J Harrison, C.F Nellist and A. Gómez-Cortecero. A. Gómez-Cortecero and Amanda Karlström were responsible for the experiments and data collection. A. Gómez-Cortecero and J. Connell performed the processing of raw sequence data and alignment of reads to the apple genome. Amanda Karlström conducted the transcriptome analysis and interpreted the results. Amanda Karlström wrote the first draft of the manuscript. All authors critically reviewed the manuscript and approved the final version of the manuscript. Amanda Karlström had an estimated percentage contribution of 80% to the paper.

Karlström, A., Papp-Rupar, M., Passey, T. A., Deakin, G., & Xu, X. 2023. Quantitative trait loci associated with apple endophytes during pathogen infection. *Frontiers in Plant Science*, 14, 1054914.

This paper is based on a metabarcoding dataset and canker phenotypes from a previous publication (Papp-Rupar et al., 2022, doi:10.1094/PBIOMES-10-21-0061-R). X. Xu conceived the study. Amanda Karlström designed, planned and carried out the experiment together with X. Xu, T. Passey and M. Papp-Rupar. G. Deakin performed OTU clustering and taxonomy assignment of sequencing reads. Amanda Karlström produced the linkage map, carried out the QTL analysis and interpreted the results from the analysis. Amanda Karlström wrote the manuscript together with X. Xu. All authors contributed to the article and approved the final version. Amanda Karlström had an estimated percentage contribution of 60% to the paper.

Acknowledgments

First of all, I would like to thank my supervisor Richard Harrison for introducing me to apple breeding and giving me the opportunity to do a PhD. Thanks for always seeing the bigger picture and making research fun and inspiring. I would also like to thank my supervisors at University of Reading; Jim Dunwell and Matt Ordidge for their support and help with publications.

I would like to express gratitude to Antonio Gómez-Cortecero for passing on the knowledge of how to culture and successfully infect apple trees with *Neonectria*. But also, for never getting tired of talking about this pathogen. My thanks also go to all my colleagues, past and present, at East Malling for all your support and for making work enjoyable. I would especially want to thank Helen Cockerton for being so passionate about science and for loving to talk about quantitative genetics and statistics.

This thesis would not have been possible without the hard work from all the staff in the farm and glasshouse team at NIAB East Malling. I am grateful for your patience with me and for looking after all the trees. I am also grateful to all staff and interns at East Malling for their help with canker experiments.

My thanks go to the BBSRC for the funding of the project work, and to NIAB for allowing me to spend time working on the PhD alongside my job.

Finally, I would like to thank my parents for being an inspiration to do a PhD, despite some warnings against it. I am also very grateful to my siblings and friends for their love and support.

I would like to dedicate this work to my partner Robert and daughter Lilja. To Robert for being my best friend, my number one supporter and for always believing in me. To Lilja, whom has been nothing but a hindrance to me finishing this work since she arrived ten months ago, but who makes it all worth it.

Table of Contents

Abbreviations	10
Chapter 1: Introduction	12
The host: <i>Malus x domestica</i>	1
Apple production and breeding.....	2
<i>Advances and challenges in apple breeding</i>	3
The pathogen: <i>Neonectria ditissima</i>	17
Host infection.....	18
Host-pathogen interaction in plant disease	19
The <i>Malus</i> : <i>Neonectria</i> interaction	22
The role of the phyllosphere microbiome in plant disease	24
Aims of the project	26
References	28
Chapter 2: Identification of novel genetic regions associated with resistance to European canker in apple	64
Chapter 3: Transcriptome analysis provide insights in resistance to European canker and reveal candidate resistance genes	81
Chapter 4: Quantitative trait loci associated with apple endophytes during pathogen infection	125
Chapter 5: Discussion	138
The potential of improving resistance to <i>N. ditissima</i> in apple cultivation	2
Understanding the resistance response to <i>Neonectria</i> infection	4
How do host factors affect endophytes in the phyllosphere	6
References	8
Supplementary data for Chapter 2	151
Supplementary table 1: Mean and standard error for European canker phenotypes	1
Supplementary table 2: Broad sense heritability	2
Supplementary table 3: Summary of the selected haploblocks within QTL-regions	3
Supplementary table 5: Results from validation of haploblock alleles in biparental cross ..	4
Supplementary figure 1: Phenotypic distributions of canker phenotypes	7
Supplementary figure 2: BLUEs of the multiparental population for canker phenotypes .	10
Supplementary figure 3: Scree plot from the PCA of European canker data	11

Supplementary figure 4: Phenotypic distributions for progeny of 'Golden Delicious' x 'M9' for susceptibility to European canker	12
---	----

Supplementary data for Chapter 3..... 163

Supplementary table 1: Significantly enriched GO terms.....	1
Supplementary table 2: Significantly enriched KEGG terms	7
Supplementary table 3: Significantly enriched PFAM terms.....	12
Supplementary table 4: Genome positions and SNP haplotypes for resistance QTL.....	19
Supplementary table 5: Differentially expressed genes within QTL intervals.....	20
Supplementary table 6: Differentially expressed genes of particular interest.....	31
Supplementary figure 1: Overview of experimental units and sampling procedure	41

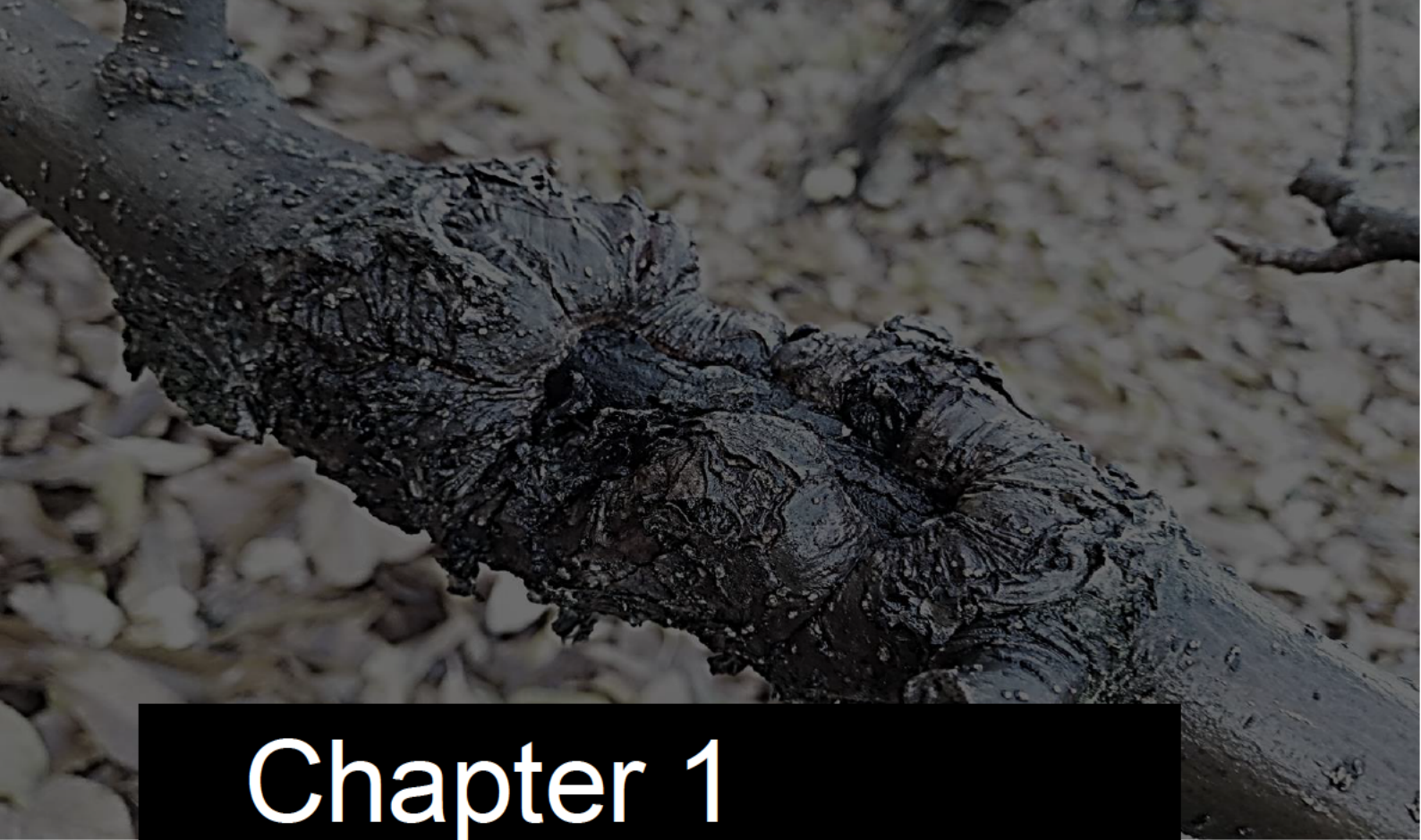
Supplementary data for Chapter 4..... 204

Supplementary table 1: Details of linkage map used for QTL analyses.....	1
Supplementary table 2: Description of phenotypes from 16s sequencing	2
Supplementary table 3: Description of phenotypes from ITS sequencing.....	4
Supplementary figure 1: Histograms showing endophyte trait distributions.....	6
Supplementary publication: <i>The influence of host genotypes on the endophytes in the leaf scar tissues of apple trees and correlation of the endophytes with apple canker (Neonectria ditissima) development</i>	7

Abbreviations

AUDPC	Area Under the Disease Progress Curve
Avr-gene	Avirulence gene
CC	Coiled coil (gene domain)
CIM	Composite interval mapping
DE	Differential expression
DEG	Differentially expressed gene
DNA	Deoxyribonucleic acid
ETI	Effector triggered immunity
FDR	False discovery rate
GD	'Golden Delicious' – apple cultivar
GWAS	Genome wide association study
HR	Hypersensitivity response
KW	Kruskal-Wallis test
LogFC	Log ₂ fold change
LRR	Leucine rich repeat
LRR-RLK	Leucine rich repeat containing receptor like kinase
MAMP	Microbe associated molecular pattern
MAS	Marker assisted selection
NLR	Nod-like receptor
OTU	Operational taxonomic unit
PAMP	Pathogen associated molecular pattern
PC	Principal component

PRR	Pattern recognition receptor
PTI	PAMP triggered immunity
R-gene	Resistance gene
RLK	Receptor like kinase
RNA	Ribonucleic acid
RNA-Seq	RNA sequencing
SNP	Single nucleotide polymorphism
SSR	Simple sequence repeat
TIR	Toll interleukin receptor 1 (gene domain)
Q-value	A p-value adjusted for the False Discovery Rate
QTL	Quantitative trait loci
QTL-R	Resistant allele at QTL
QTL-S	Susceptible allele at QTL
WAK	Wall associated kinase
WAKL	Wall associated kinase like



Chapter 1

Introduction

Introduction

1. The host: *Malus x domestica*

The cultivated apple, *Malus x domestica* Borkh (syn. *Malus pumila*) belongs to the subfamily Amygdaloideae of the Rosaceae family (Zhang et al., 2023). Apple is included in the tribe Malae within Amygdaloideae, which includes many species of horticultural importance, such as pear (*Pyrus communis*), loquat (*Eriobotrya japonica*), hawthorn (*Crataegus pinnatifida*), and quince (*Cydonia oblonga*) (Zhang et al., 2023). Phylogenetic studies based on genetic data suggest that the domestication of apple started in Central Asia from the species *Malus sieversii*, after which migration and trade brought the cultivated apple towards Europe during which hybridisations occurred with at least four wild species of *Malus*, particularly *Malus sylvestris* (Chen et al 2021., Cornille et al., 2012; Duan et al., 2017; Harrison & Harrison, 2011; Sun et al., 2020; Velasco et al., 2010). In a comparison of three *M. x domestica* reference genomes with those of *M. sylvestris* and *M. sieversii* it was shown that approximately 25-40 % of the domesticated apple's genome is likely to be derived from each of the two progenitor species (Sun et al., 2020). There are signs of directional selection for fruit related traits, such as fruit size, acidity and colour in the apple genome (Sun et al., 2020; Chen et al., 2021)

Most commercially grown apple varieties are functional diploids ($2n=34$), although triploids such as 'Jonagold' and 'Bramley's Seedling' also occur (Chagné et al., 2015). Domesticated apples are highly heterozygous due to gametophytic self-incompatibility and inbreeding depression (Spengler, 2019, Velasco et al., 2010). Genetic studies and breeding of this crop therefore relies on F1 progeny derived from heterozygous parents. The first whole genome assembly of apple was produced by Velasco et al in 2010 from a whole genome sequence of 'Golden Delicious' which has an estimated genome size of approximately 700 Mb. The sequencing of the apple genome revealed that it is likely the result of a genome wide duplication event of an ancestral 9-chromosome Rosaceae ancestor, resulting in homology between pairs of chromosomes (Velasco et al., 2010). Subsequent reference level apple genomes with improved quality include a doubled-haploid derivative of "Golden Delicious"

known as GDDH13 (Daccord et al 2017), a trihaploid line derived from ‘Hanfu’ (HFTH1, Zhang et al., 2019) and diploid ‘Gala’ (Sun et al., 2020).

There are twenty-five reported species of *Malus* and more than 7,000 varieties of domesticated apple described (Noiton & Alspach, 1996). The majority of existing *Malus* species originate from East Asia (Southern China, Northern Vietnam, Northern Laos), but wild *Malus* species are also found in Central Asia, North America and Europe (Chen et al., 2021). Interspecific crosses between *M. x domestica* and other species within the genus of *Malus* produce fertile offspring and have been used to introduce disease resistance and red flesh colour in the germplasm of the cultivated apple (Evans & James, 2003; Koller et al., 1994; Spengler, 2019; van Nocker & Gardiner, 2014)

2. Apple production and breeding

Apple is a commercially important crop in the United Kingdom, which grows both cider apples, culinary apples and dessert apples for fresh consumption, on a total area of ~14 thousand hectares (FAOSTAT, 2023). The UK dessert apple production constitutes approximately 40% of the total apple producing area but makes up 60% of the farm-gate value of all apples produced (£183 million in 2022, DefraStats, 2022; FAOSTAT, 2023). The most widely grown dessert cultivar in the UK is ‘Gala’, which is planted in 48% of all dessert apple orchards (DefraStats, 2022).

The following section provides further introduction to the global production of apple and to apple breeding. It consists of a pre-print of an excerpt from a book chapter by Karlström et al (2019) published in *Achieving sustainable cultivation of temperate zone tree fruits and berries* (DOI: 10.19103/AS.2018.0040.21). The section numbering has been changed in line with the rest of the thesis introduction.

Advances and challenges in apple breeding

Amanda Karlström, NIAB EMR and University of Reading, UK; Magdalena Cobo Medina, NIAB EMR and University of Nottingham, UK; and Richard Harrison, NIAB EMR, UK

2.1 Current production

Apple, *Malus × domestica* (Borkh), is one of the most important global fruit crops, both in terms of its cultural symbolism and with respect to the extent of production, which amounts to an average of 87 million tonnes of annual production globally for the years 2014–16 (FAOSTAT, 2018). Apple is primarily a temperate crop due to the chilling requirements for the initiation of blossoming (Heide and Prestrud, 2005), nevertheless there are varieties with lower requirements for chilling, which can be grown in subtropical climates (Labuschagné et al., 2002).

Global apple production has increased 117% between the mid-1980s and the mid-2010s (FAOSTAT, 2018). The growth in production is mainly attributed to a higher productivity per ha as the area utilised for apple production has increased by only 20% during the same period (FAOSTAT, 2018). As illustrated in Fig. 1, Asia surpassed Europe as the major apple-producing region of the world in the 1990s. Mainland China has been the major contributor to this large expansion of apple production in Asia and today represents 75% of the Asian production (Fig. 2). Any development towards a more sustainable cultivation of apple, either genetic or agronomic, will therefore have the most significant impact if adopted by commercial production in Asia.

Modern apple production systems are characterised by trees grown on dwarfing or semi-dwarfing rootstocks which allows for high-density planting. Such production systems have the benefit of earlier cropping trees and a higher production efficiency per ha (Robinson, 2007). Two clonally propagated dwarfing rootstocks, the varieties M9 and M26 (the M denoting 'Malling'), dominate the European and North American apple industry, although both were commercially released before 1950 and susceptible to certain pests and diseases (Marini et al., 2009, 2014, 2017). In China, 80–90% of apple production systems use seedlings from wild species of *Malus* (*M. sieversii*, *M. baccata*, *M. prunifolia* and *M. hupehensis*) as rootstocks. Due to genetic variation among the seedling rootstocks these

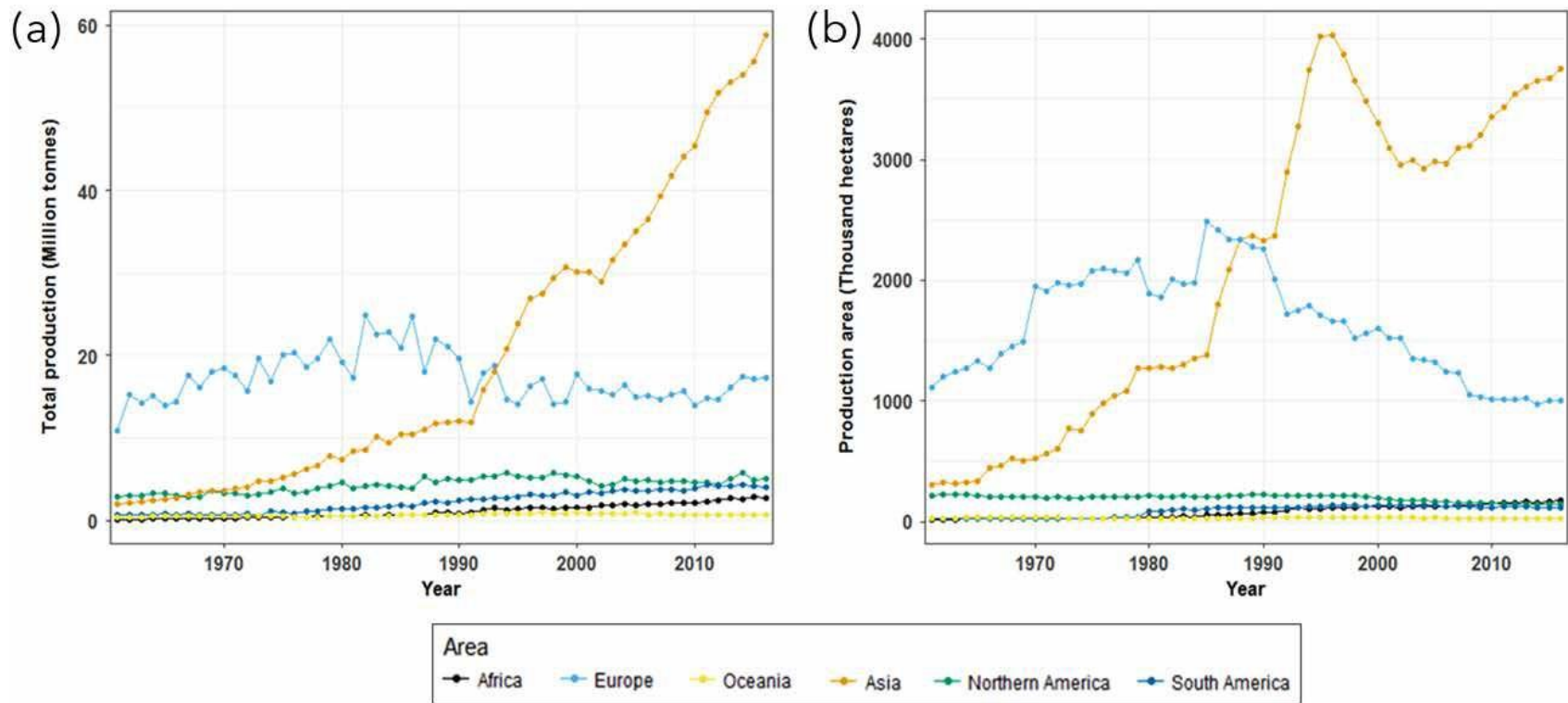
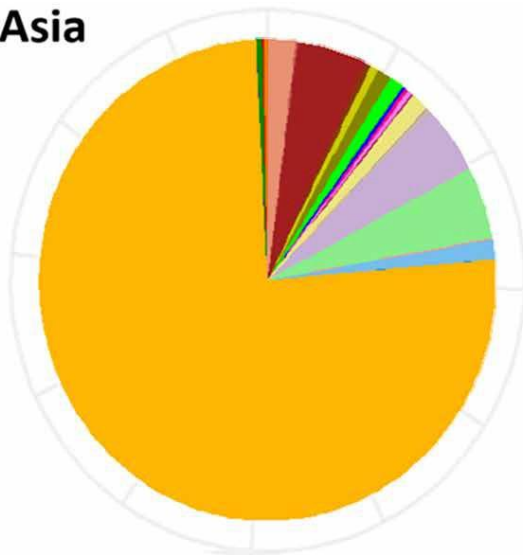
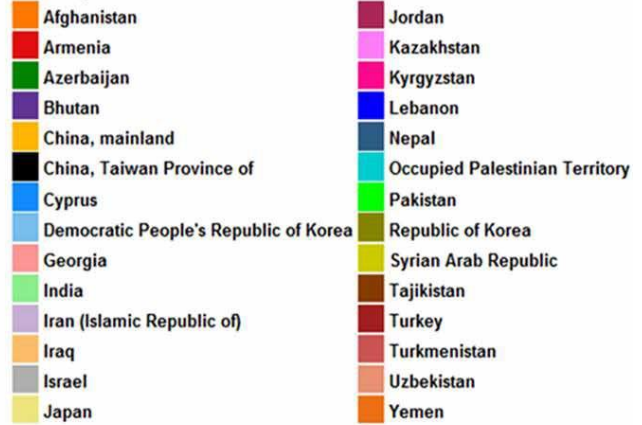


Figure 1 (a) The total annual production quantity of apple in million tonnes shown by continent. (b) Total area used for apple production in 1000 ha shown by continent. Source: data retrieved from the Food and Agriculture Organization of the United Nations (FAO) website, FAOSTAT (2018)

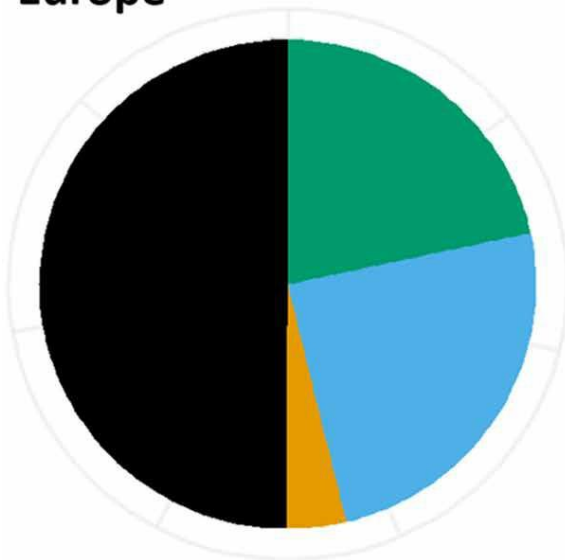
Asia



Country



Europe



Region



Figure 2 Breakdown of the total apple production quantity in 2016 by country and region in Asia and Europe, the two major apple producing regions of the world. Source: data retrieved from FAOSTAT (2018)

systems suffer from heterogeneity in vigour and a late onset of fruiting due to rootstock juvenility (Li et al., 2015).

While there is diversity in the apple scion varieties that are commercially grown, the genetic base from which they are derived is narrow (Bannier, 2011; Noiton and Alspach, 1996). A study which considered 500 apple varieties, predominantly with a Central European and/or US origin, found that 'Golden Delicious' occurred at least once in 51% of the pedigrees, whereas 'McIntosh' occurred in 35% of the varieties, 'Jonathan' in 31%, 'Cox's Orange Pippin' in 30%, 'Red Delicious' in 18% and 'James Grieve' in 15% (Bannier, 2011). The inclusion of these progenitor varieties and their derivatives in breeding programmes is principally attributed to their fruit quality, storability and cropping (Bannier, 2011). Because of the relatively narrow genetic pool of commercial apple production, negative traits originating from these founder varieties may be incorrectly attributed to be intrinsic to modern apple cultivation, rather than genetic weaknesses.

Novel apple varieties are released continuously, and there are currently 821 pending applications for *Malus domestica* variety registrations across 40 countries (CPVO, 2018). However, the adoption and spread of new varieties is limited due to a high degree of competition within the industry. Grower adoption of new varieties is also associated with a large financial risk as orchard establishment requires a high initial capital investment (Badiu et al., 2015) and there is therefore a need for growers to be reassured that there is a market demand for the variety once the trees begin to crop. For that reason the success of a novel variety tends to be reliant on the backing of grower associations and marketing organisations following extensive trialling. Many vigorously marketed apples are 'club' or 'managed' varieties for which exclusive rights to grow and sell the variety are licensed to specific grower organisations and nurseries. Such varieties are often granted patent and plant variety rights under a variety name or selection number and then trademarked and marketed under a separate name (Legun, 2015). Examples of club varieties are 'Cripps Pink' which is trademarked under the name Pink Lady® by Apple and Pear Australia Limited (APAL) and 'Scifresh', trademarked as Jazz® and owned and licensed by ENZAFRUIT International Ltd (Brown, 2009).

2.2 Current breeding of apple scions and rootstocks

As with other perennial tree crops, the breeding cycle of apple scions is long and the development of a new variety takes a minimum of 15–20 years (Fruitbreedomics, 2014a). This timeframe is further prolonged if germplasm with suboptimal fruit quality is used for the introduction of a new trait such as disease resistance (Flachowsky et al., 2011).

The most common breeding strategy in apple utilises controlled- pollinated crosses between elite selections or varieties to produce large full- sibling families, which are phenotypically evaluated in the field (Kumar, 2010). Genotypes which are considered to be outstanding are selected from the seedling trial and clonally propagated and planted in replicated advanced trials. The selected genotypes are thereafter assessed for fruit quality traits across multiple sites, years and harvests (Harshman et al., 2016). The breeding cycle is completed when elite clones, either from the advanced trials or after commercialisation, are used as breeding parents. The different stages of apple breeding are shown in Fig. 3. Due to the long juvenility phase (the period prior to reproductive maturity) of apple, a period of 4–7 years is required from when the initial cross is made until the progeny start to produce fruit and can be evaluated (Edge-Garza et al., 2015). The time and money invested in each

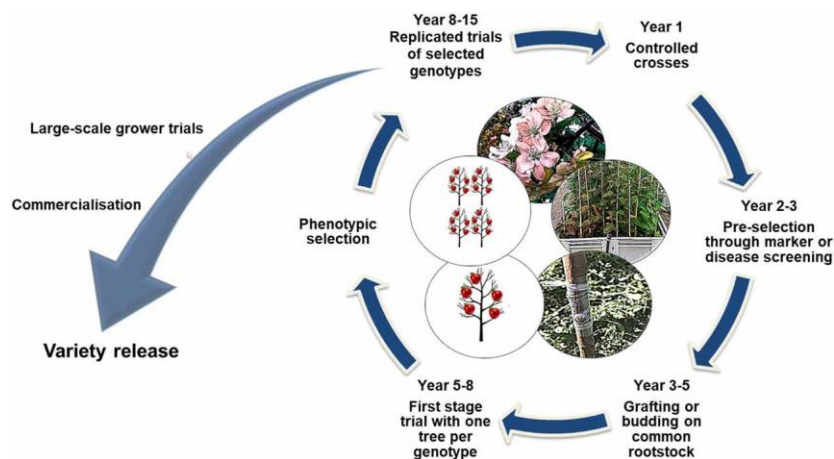


Figure 3 Illustration of a generalisation of the breeding cycle of apple, which can be seen as consisting of a population improvement cycle and a separate entity of variety development.

seedling that reaches cropping is therefore substantial (Edge-Garza et al., 2015; Ru et al., 2015). Hence, in breeding programmes with resistance to biotic stress as a major breeding objective, where possible, it is common to select for resistance at an early seedling stage (Kellerhals et al., 2017). A small percentage of individuals are moved forward to the advanced trialling stage, nevertheless the long period of trialling and the labour-intensive fruit phenotyping can contribute substantially to the costs of the breeding programme (Harshman et al., 2016).

Fruit quality traits, such as texture, attractiveness, aroma and storability, as well as tree productivity and consistent bearing are universally important breeding objectives of apple scion breeding programmes across the world (Centro de Pomaceas, 2019; Evans, 2011; Fruitbreedomics, 2012, 2013a,b,c; Johan Kriel, pers. comm.; Sansavini et al., 2004). In warmer regions with high exposure to sunlight, the development of varieties with low winter chilling requirement and fruits that are less prone to be damaged by sunburn are also priorities (Centro de Pomaceas, 2019; Johan Kriel, pers. comm.). Disease resistance objectives differ depending on region, with the major diseases being apple scab (*Venturia inaequalis*), powdery mildew, (*Podosphaera leucotricha*), fire blight (*Erwinia amylovora*) and European apple canker (*Neonectria ditissima*) (Fruitbreedomics, 2012, 2013a,b,c; Johan Kriel, pers. comm.; Sansavini et al., 2004). A major biotic constraint in apple growing regions in eastern Asia is Valsa canker, caused by the fungus *Valsa mali* (Abe et al., 2007). The genetic improvement of resistance levels to this pathogen is therefore a priority within this region (Abe et al., 2007; Tan et al., 2017a,b).

The breeding cycle for apple rootstocks can last even longer than for breeding for scion varieties due to the period of time required to replicate rooted material as well as extensive periods of trialling. The objectives of modern rootstock breeding programmes include vigour control of the scion (ranging from dwarfing to semi-invigorating depending on the target market), increased yield efficiency and precocity, good nursery performance (good production of liners in stoolbeds as well as adventitious rooting ability and grafting compatibility), resistance to woolly apple aphid (*Eriosoma lanigerum*), fire blight (*E. amylovora*), collar rot (*Phytophthora cactorum*), European apple canker (*N. ditissima*) and tolerance to the apple replant disease complex (Gregory et al., 2013).

2.3 Current genomic tools in apple

The first draft apple genome became available in 2010 (Velasco et al., 2010) and has since been a valuable resource of this economically important perennial crop and a crucial tool to advance the development of new and improved apple varieties. In 2017, a high-quality apple genome generated from a double haploid of 'Golden Delicious' was released, from a combination of long reads (PacBio) and short sequencing reads (Illumina). The new genome provides an excellent foundation for future genetic studies not only in apple but also for other species of Rosaceae (Daccord et al., 2017).

Simple sequence repeat (SSR) markers have been routinely utilised in apple research and breeding for decades. This is not surprising given their advantages: they are co-dominant, multi-allelic, abundant and, generally, are uniformly distributed (Gianfranceschi et al., 1998). A significant amount of progress in apple genetics has relied upon the utilisation of SSRs, for example, fine mapping of the rosy apple aphid resistance locus (Pagliarani et al., 2016), rootstock linkage map construction (Celton et al., 2009; Fernández-Fernández et al., 2012) as well as from the development of linkage maps of scion varieties (Liebhard et al., 2002, 2003; Kenis and Keulemans, 2005; N'Diaye et al., 2008; Ziya Motalebipour et al., 2015; Liu et al., 2016).

Several single nucleotide polymorphism (SNP) arrays have been developed specifically for apple. In 2012, the IRSC apple Infinium II 8K array became available. This was developed from a SNP-discovery panel consisting of 27 apple cultivars from around the world which were re-sequenced at low coverage (Chagné et al., 2012). Shortly after, a 20K Illumina apple array was developed using re-sequencing data from 13 apple cultivars and one crab apple species (Bianco et al., 2014). Both have been used to generate saturated linkage maps of an apple rootstock progeny (Antanaviciute et al., 2012), in genomic selection for fruit quality traits (Kumar et al., 2013) and in multiple studies to detect quantitative trait loci (QTL) for several traits including apple skin russeting (Falginella et al., 2015), sugar and soluble solid content (Guan et al., 2015) and budbreak and flowering time (Allard et al., 2016). These arrays have been useful for the generation of saturated genetic linkage maps and QTL detection. Nevertheless, these arrays also have certain limitations since the low- medium density of markers limits its applicability to genome-wide association studies (GWAS) (Bianco et al., 2016).

In 2016, the Axiom Apple 480K array was developed after high-depth re-sequencing of 63 different cultivars and two doubled haploids (Bianco et al., 2016). It became an important tool for GWAS, thanks to the high percentage of well-distributed and robust SNPs (Bianco et al., 2016). It was subsequently used for this purpose for the mapping of flowering and ripening periods in apples (Urrestarazu et al., 2017). There are also limitations to array-based genotyping, since the genotype calls often result in useless or unreliable data due to the high levels of off-target polymorphism in varieties which are absent from the initial discovery panel (Miller et al., 2013). Furthermore, as a closed genotyping system, limited by the discovery panel used, arrays often suffer from built-in ascertainment biases leading to limitations when applying some population genetic analyses (Albrechtsen et al., 2010).

There are several benefits of using genotyping-by-sequencing (GBS) technologies over microarray-based methods in apple, including a reduction of the ascertainment bias and as an opened genotyping system you can obtain genotypic data across the whole population (Elshire et al., 2011; Gardner et al., 2014). GBS methods provide a rapid tool to genotype breeding populations for several applications like GWAS and genomic selection (He et al., 2014). These sequencing technologies have been applied to map QTL for disease resistance to blue mould (Norelli et al., 2017), soft scald (McClure et al., 2016) and apple skin colour (Gardner et al., 2014), as well as for GWAS of scab and fruit quality traits (McClure et al., 2018). Some potential drawbacks of GBS are large proportion of missing data points due to low coverage of sequencing and management and analysis of a large amount of sequence data (Bhatia et al., 2013).

One of the latest technologies available to breeders is genome editing, a powerful method used for genome modification. The CRISPR/Cas9 system is one of the best-known techniques in this field since it allows for the targeted removal or addition of genes in a defined location. CRISPR/Cas9 has been applied in apple as a proof of concept to modify an apple phytoene desaturase (PDS) gene, essential for chlorophyll biosynthesis (Nishitani et al., 2016). PDS mutants showed the expected albino phenotype demonstrating the potential to modify the apple genome using CRISPR/Cas9 and how this could contribute to generate desired apple traits (Nishitani et al., 2016). CRISPR/Cas9 ribonucleoproteins have been used to silence DIPM-1, DIPM-2 and DIPM-4 in apple protoplasts to increase resistance to fire blight and proved that DNA-free genome editing can be performed on apple (Malnoy et al., 2016). Organisms obtained through novel mutagenesis techniques are not being regulated as genetically modified (GM) in the United States and Canada, while the Court of Justice of

the European Union has ruled that they are to be classified as GMOs and therefore subject to the same regulation as transgenic organisms (Judgement of 25 July 2018, Case C-528/16, ECLI:EU:C:2018:583).

The numerous advances in genomic tools have contributed to improvements for apple breeding, but there are several challenges to face in order to take advantage of these tools. Future challenges are related to the improvement of bioinformatic tools to facilitate the extraction of information from raw data and the improvement of algorithms for genotype calling (Gardner et al., 2014). Another challenge is to reduce the cost of genotyping to make it more affordable. The effectiveness of genomic tools is proven and the choice of the method is dependent on many factors but one of the most important and decisive is the price.

For the remainder of this chapter we will discuss scientific achievements and challenges within three areas of apple breeding which we consider to be central in order to ensure sustainable production in the future: (1) shortening the breeding cycle and improving selection to deliver better varieties to growers, (2) increasing the orchard productivity and resource-use efficiency through genetic means and (3) mitigating pre- and post-harvest losses through improved genetic approaches.

2.4 Shortening the breeding cycle and improving selection

There is a great potential to increase genetic gains in apple through shortening the breeding cycle and making selection more effective. The current constraints are mainly due to the long period of seedling juvenility and extensive trialling of advanced selections in traditional apple breeding.

Marker-assisted selection

The selection in apple breeding programmes has traditionally been based on phenotypic evaluations of performance (Ru et al., 2015; Ru, 2016). At the seedling trial stage, this requires the plant material to be evaluated to reach physical maturity before it can be assessed for fruit-related traits (Edge-Garza et al., 2015). The phenotypic selection of resistance to biotic stresses at this stage can also be highly laborious and costly depending on phenotyping protocol (Ru et al., 2015). Furthermore, the destructive nature of assessing tolerance to certain biotic stresses requires multiplying seedling plant material, which may

not be economically feasible. Owing to these factors apple is a good candidate for the implementation of genotyping technologies as tools to reduce the cost of plant phenotyping (van Nocker and Gardiner, 2014).

MAS is to date the most widely utilised genetic tool applied for apple seedling selection. In 2011–12, 43% of the apple breeding programmes in the European Union stated that they deployed markers in some way in their breeding programme, however only six of these programmes used markers to do progeny selection (Fruitbreedomics, 2014b). The traits for which predictive marker tests are available include fruit storability/ethylene biosynthesis (Edge-Garza et al., 2010), fruit acidity (Bai et al., 2012; Verma, 2014), bitter pit susceptibility (Kumar et al., 2013; Buti et al., 2015), fruit sweetness/fructose content (Guan et al., 2015), fruit skin and flesh colour (Cheng et al., 1996), fruit crispness (Verma, 2014), fruit firmness (Zhu and Barritt, 2008; Longhi et al., 2013; Nybom et al., 2013; Verma, 2014), scab resistance (Cheng et al., 1998; Vinatzer et al., 2004), powdery mildew resistance (Markussen et al., 1995; Evans and James, 2003) and fire blight resistance (Gardiner et al., 2012).

In a comparison of selection strategies in simulated data, Ru (2016) showed that incorporating marker information in the selection decision tended to increase the genetic gain compared to phenotype-only selection in scenarios where the proportion of genetic variance explained by the marker was higher than the broad-sense heritability of the trait. Empirical comparisons of MAS to phenotypic seedling selection in apple have been conducted for scab resistance (Tartarini et al., 2000), fruit storability/ethylene biosynthesis (Edge-Garza et al., 2010) and fruit firmness, acidity and crispness (Ru, 2016). The breeding value, defined as the component of a trait phenotype constituted by additive genetic effects, is commonly used as a measure of the value of an individual that is transferable to its offspring. A comparison of average estimate breeding value between seedlings selected through MAS or phenotypic selection for the traits such as fruit firmness, acidity and crispness indicated that the genetic gain was similar between the two selection strategies, although the variance of breeding values for MAS seedlings for firmness and crispness was lower (Ru, 2016). As mentioned by Ru, the use of genetic gain, defined as the

average increase in performance of all individuals per unit of time, might not be the best measure of response to selection in an apple breeding programme with the aim of selecting a few outstanding genotypes and not to improve the average population performance. In such a setting it might be preferred to look at the maximum breeding value achieved in a percentage of the highest performing progeny (Ru, 2016).

In calculations of the cost-efficiency of incorporating MAS in an apple breeding programme, Edge-Garza et al. (2015) concluded that maximum savings would be achieved if genotype-based culling of seedlings is performed at a stage where minimal routine seedling reductions are likely afterwards but before a large cost per seedling is incurred. The magnitude of savings in the cost scenarios of the same study were highly dependent on the proportion of seedlings that were culled after MAS. Traits that can be phenotyped at an early seedling stage, such as some disease screening, were not cost-effective to select for using markers (Edge-Garza et al., 2015).

2.5 Mitigating production losses and waste

Increases in apple yield can be greatly offset by the action of pests and diseases and through the development of physiological disorders. This is not only a concern in the pre-harvest stage of the production chain but also during post-harvest storage of the produce, as 8–10% of the total global apple production in 2011–13 was estimated to have been lost due to wastage between harvest and reaching the consumer (FAOSTAT, 2018). In order to reduce losses and waste, while at the same time lowering pesticide inputs, an emphasis will have to be placed on breeding varieties tolerant to biotic and abiotic stresses during all stages of production. Here we discuss biotic factors that are important in the commercial production of apple. The major focus of apple breeding and research has been on improving resistance to diseases occurring in the field, while relatively little attention has been given to tolerance towards storage diseases (Sansavini et al., 2004).

2.5.1 Pre-harvest

Increasing the resilience to field diseases has been of large importance in many apple breeding programmes, both for scion and rootstock varieties. Breeding efforts have mainly been focused on improving resistance to the two fungal pathogens apple scab, *Venturia inaequalis*, and powdery mildew, *Podosphaera leucotricha*, as well as the fire blight causing bacterium *Erwinia amylovora*. Varietal tolerance to the two major wood pathogens, the fungus *Neonectria ditissima* and bacterium *Valsa mali*, is recognised as being of high importance, but has received relatively little attention up until recently (Abe et al., 2007, 2011; Ghasemkhani et al., 2015b; Garkava-Gustavsson et al., 2016; Gómez-Cortecero et al., 2016). Resistance to the woolly apple aphid, *Eriosoma lanigerum*, has been an important objective for rootstock breeding and varieties with resistance from *Malus robusta* 'Robusta 5' (used as a parent in the Malling Merton series) and the variety 'Northern Spy' (parent in the Geneva-series) have been released (Bus et al., 2008).

Apple scab

Apple scab, *Venturia inaequalis*, causes brown lesions on leaves and fruits, making them unmarketable, and is considered the most economically damaging disease in apple (Vaillancourt and Hartman, 2000). In the early twentieth century, genetic resistance was recognised as a good control measure of the fungus, which led breeders to initiate crosses with wild apple species exhibiting resistance to the disease (Joshi et al., 2009). The apple scab pathosystem was also one of the first host–pathogen interactions in which the gene-for-gene model was demonstrated (Flor, 1971). A total of 20 different major resistance loci (denoted *Rvi1-20*) have since been identified in *Malus* germplasm (Clark et al., 2014). Avirulence alleles corresponding to 5 out of the 20 *Rvi* loci have been described in isolates of *V. inaequalis* (see Clark et al., 2014) or sources of resistance and interactions. The genomic location of several of these resistance genes have been published and markers developed (Cheng et al., 1998; Tartarini et al., 2000; Gyga et al., 2004; Patocchi et al., 2009). The *Rvi6* (previously denoted *Vf*) resistance, originating from *Malus floribunda* 821, is by far the most utilised source of resistance in the development of scab-resistant varieties (Gessler and Pertot, 2012). Furthermore, the majority of the commercially released *Rvi6*-resistant varieties have ancestry in the same resistant selections produced by the PRI Cooperation Program (Purdue University, Rutgers University and the University of Illinois) (Gessler and Pertot, 2012). There is an understanding that the genetic base of resistance needs to be broadened to avoid the selection of *V. inaequalis* pathotypes able to

overcome the *Rvi6* resistance (Parisi et al., 1993). There have therefore been attempts to use plant material with other, or polygenic resistance and to pyramid resistance genes in a single genotype (Kellerhals et al., 2009; Clark et al., 2014; Bastiaanse et al., 2016; Peil et al., 2007).

Apple powdery mildew

Apple powdery mildew, *Podosphaera leucotricha*, can be observed as a white layer of mycelia on leaves and shoots of apple. The pathogen can cause diminished shoot growth and flowering, fruit russeting and a general reduction in health due to reduced photosynthesis (Holb, 2017). Five sources of major resistance have been identified and markers segregating with the resistance developed: *PI₁* from *M. robusta* (Dunemann et al., 2007), *PI₂* from *Malus zumi* (Baumgartner et al., 2015), *PI_d* from 'D12' (James et al., 2004), *PI_m* from 'Mildew Immune Selection' (Bus et al., 2010) and *PI_w* from the ornamental crab apple 'White Angel' (Evans and James, 2003). In addition, there is evidence of polygenic resistance to *P. leucotricha* (Calenge and Durel, 2006; Stankiewicz- Kosyl et al., 2005). Alternative approaches that can be used in breeding for reduced incidence of powdery mildew are selection of loss-of-function mutations in susceptibility genes. *Mildew resistance locus o (Mlo)* genes are known to confer susceptibility to powdery mildew in a multitude of crops (Pessina et al., 2016a,b; Bracuto et al., 2017; Kusch and Panstruga, 2017). More than 20 *Mlo* gene homologues have been identified in the 'Golden Delicious' genome (Pessina et al., 2014). A knock-down mutation of one of these *Mlo* genes, *MdMLO19*, was shown to lead to a significant reduction of powdery mildew in apple (Pessina et al., 2016b). This finding supports the hypothesis that targeted mutation of susceptibility genes could be a feasible method to increase resistance to apple powdery mildew, as long as there are no pleiotropic effects which affect normal plant development. Furthermore, natural variations in alleles of *Mlo* genes could be exploited for resistance breeding (Pessina et al., 2017).

Fire blight

Fire blight, *Erwinia amylovora*, is caused by a gram-negative bacterium which produces blossom, rootstock and shoot blight in host trees (Norelli et al., 2003). Resistance towards the pathogen has been identified in both cultivated apple varieties and in wild apple accessions (Calenge et al., 2005; Durel et al., 2009; Le Roux et al., 2010; Emeriewen et al., 2017; Harshman et al., 2017). One of the resistant accessions described is the crab apple *Malus robusta* 'Robusta 5', from which a major resistance locus to *E.*

amylovora was discovered through linkage mapping (Peil et al., 2007). A putative resistance gene was subsequently identified within the locus, and designated *FB_MR5* (Fahrentropp et al., 2013). The effect of *FB_MR5* on the incidence of *E. amylovora* was verified by cloning the resistance gene into the susceptible variety 'Gala Galaxy', which rendered transgenic lines with significantly lower symptom development after artificial inoculations compared to the untransformed equivalents (Broggini et al., 2014; Kost et al., 2015). Resistance loci from the species *Malus arnoldiana* (Emeriewen et al., 2017), *Malus fusca* (Emeriewen et al., 2014) and the variety 'Evereste' (Durel et al., 2009) have also been mapped. The application of these varieties in scion breeding has been limited due to their poor fruit quality, which means that several generations of pseudo-backcrossing would be necessary to obtain a commercial variety (Kellerhals et al., 2008). Nevertheless, QTL from several varieties of cultivated apple have also been mapped (Calenge et al., 2005; Durel et al., 2009; Le Roux et al., 2010; van de Weg et al., 2018), which has enabled the development of molecular markers linked to a major resistance QTL on linkage group 7 in the variety 'Fiesta' (Khan et al., 2007).

European apple canker

European apple canker, *Neonectria ditissima*, is mainly a wood pathogen which causes trunk cankers, stem and branch lesions and dieback (Weber, 2014). The disease has become increasingly significant in recent years, particularly in apple growing regions with maritime temperate climates, where the high susceptibility of many modern varieties and limited effective control measures add to its prevalence (Beresford and Kim, 2011; Weber, 2014; Gómez-Cortecero et al., 2016). To date, there has been no report of any apple variety or species of *Malus* that exhibits complete immunity to *N. ditissima*. There is however germplasm that has exhibited partial resistance in experiments with controlled inoculations (van de Weg, 1989; Gelvonauskienė et al., 2007; Ghasemkhani et al., 2015a; Gómez-Cortecero et al., 2016). Breeding efforts to improve resistance in the germplasm have been limited, probably due to the highly polygenic nature of identified resistance and the large influence of environment on disease expression (Gómez-Cortecero et al., 2016). Nonetheless, there is ongoing research to map resistance QTL from 'Golden Delicious', *Malus robusta* 'Robusta 5', as well as from a multiparental breeding population (Peter Braun, pers. comm.; Vincent Bus, pers. comm.; Amanda Karlström, unpublished results)

3. The pathogen: *Neonectria ditissima*

Neonectria ditissima is a fungal pathogen able to cause disease in a wide range of hosts, including apple, pear (*Pyrus*) and other broad-leaved perennials such as species within *Fagus*, *Alnus*, *Populus*, *Aesculus*, *Corylus* and *Betula* (MacKenzie & Iskra, 2005; Walter et al., 2015).

The major symptoms of infection in the hosts are trunk cankers (fig. 4a), stem and branch lesions (fig. 4b and c) and dieback. In severe cases the lesions expand to girdle the whole main trunk and kill all branches above the point of the canker (Weber, 2014)

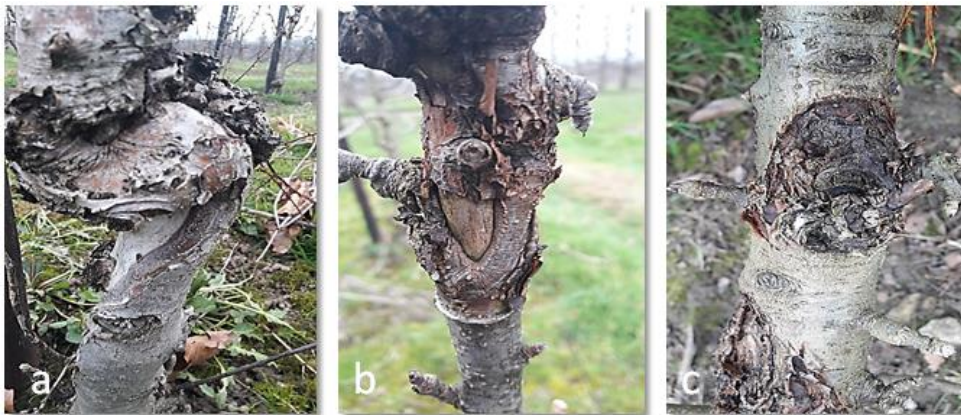


Figure 4. Symptoms of *N. ditissima* infection in seedlings of apple. **a** A trunk canker, almost girdling the stem of the tree, **b** Branch canker with a typical flaking, red-brown discoloration of epidermis and callus formation, **c** Lesion development in the area around a lateral branch

European apple canker is widespread in apple growing regions with temperate climate, including in Europe, North America, Chile, Australia, New Zealand, Japan and South Africa (Beresford & Kim, 2011; Weber, 2014). Areas with wet climate and mild temperatures are favourable for infection and the risk of disease is high in areas with rainfall on >30% of the days per month and an average temperature of 11-16°C for >8 hours per day (Beresford & Kim, 2011).

4. Host infection

N. ditissima is foremost a wood pathogen, which enters the host through any type of natural or artificial wounds such as leaf scars, pruning cuts or lenticels and cracks in the bark (Weber, 2014). In commercial pome fruit production one important source of disease spread is through infections originating from nursery propagation processes (Brown et al., 1994; McCracken et al., 2003). Such infections can remain symptomless until the trees are planted in the orchard, where subsequently the cankers develop (Wenneker et al., 2017)

The initial symptoms of infection by *N. ditissima* are a light brown discolouration and flaking of the epidermis, followed by necrosis of the underlying bark (Weber, 2014). During infection the hyphae of *N. ditissima* has been shown to colonize the cortex, phloem and xylem of apple (Ghasemkhani, 2015). During the development of the disease the woody tissues of the host also undergo changes in tissue structure. This has been shown in *Fraxinus mandshurica* var. *japonica* where it was found that the xylem vessels in the cankers were narrower than in healthy tissue and that necrotic areas were restricted to tissues in the vicinity of the canker (Sakamoto et al., 2004). *N. ditissima* is sometimes referred to as a necrotrophic fungi (Ghasemkhani, 2015; Weber & Dralle, 2013) although such a classification does not take into account that the fungus can reside latently in the host and it should therefore be considered hemibiotrophic (Salgado-Salazar et al., 2021)

The fungus spreads through conidia produced in pale yellow sporodochia or through ascospores which develop in a later stage of infection in bright red perithecia. Both the sporodochia and perithecia emerge on the surface of dead bark (Weber, 2014). The conidial spores produced by the asexual *Cylindrocarpon heteronema* occur in two forms; macroconidia and microconidia. Macroconidia are straight or slightly curved and 3-5 septate whereas the microconidia are ellipsoid or short cylindrical with one or no septa (Weber, 2014). In New Zealand, both conidia and ascospores have been shown to be present in apple orchards throughout the year when rainfall occurred (Amponsah et al., 2015). There is therefore a year-round risk of infection in conducive environments.

5. Host-pathogen interaction in plant disease

The interaction between a pathogen and its plant host is specific to each host-pathogen system. To maximise the effectiveness of resistance breeding it is therefore important to understand the causes of successful or unsuccessful host colonization by a pathogen and how the plant immune system functions.

Pathogen recognition is the first frontier of the plant immune system. Several models have been used to conceptualise how pathogens are recognised by the plant immune system and these models develop as the molecular and biochemical understanding of plant-pathogen interactions grow (van der Burgh & Joosten, 2019). The gene-for-gene model was first described by H.H Flor in the mid-20th century, when he detailed a gene-for-gene interaction between resistance (*R*) genes in the host and avirulence (*Avr*) genes in the pathogen (Kaur et al., 2021). According to the model the recognition of the *Avr* protein by its corresponding *R* protein results in a plant immune response, whereas the absence of either of the two genes results in disease (Jones & Dangl, 2006). The gene-for-gene model was further extended to the zig-zag model, which illustrates the evolutionary arms race between plants and pathogens (Jones & Dangl, 2006). The zig-zag model incorporates the fact that certain microbes have adapted to a particular plant host and are able to elicit virulence factors, denoted effectors, that interfere with immunity (Cui et al., 2015). This enables the pathogen to successfully infect the host and cause disease. Nevertheless, during the host-pathogen co-evolution the plant immune system has also developed more specialised recognition systems to intercept the pathogen effectors and induce immune responses (Toruño et al., 2016). The zig-zag model makes a distinction between plant immune receptors that recognise a wide group of pathogens (usually denoted pattern recognition receptors, PRRs) and specialised immune receptors which identify effectors from a specific pathogen (*R-gene* proteins). The model also highlights the immune response triggered by the identification of these different sets of receptors, with PRRs inducing so called PAMP triggered immunity (PTI) and *R-genes* inducing Effector-triggered immunity (ETI) (Jones & Dangl, 2006). In several plant-pathosystems the initial responses observed in the plant during ETI are a burst of oxidative species and the induction of localised plant cell death in the host, a mechanism referred to as hypersensitivity response (HR) (Jones & Dangl, 2006). This type of response confines biotrophic pathogens to their site of infection and deprives them of a nutrient source (Govrin & Levine, 2000; Jones & Dangl, 2006). Necrotrophic or hemibiotrophic plant-pathogens, such as *N. ditissima*, can on the

contrary benefit from plant-pathogen interactions where host cell death is induced. The necrotrophic pathogen may therefore produce defense triggering elicitors, which can either be unspecific or host specific (Toruño et al., 2016). Although HR is a well-described resistance mechanism in leaf and non-lignified plant tissue, its function in woody plant tissue has not been reported.

During ETI, but also PTI, phytohormone signalling of salicylic acid (SA), jasmonic acid (JA) and ethylene (ET) is triggered (Delaney et al., 1994). These signalling compounds activate the subsequent transcription of pathogenesis related genes (Nandi et al., 2003; Rahman et al., 2014). The SA-pathway is generally associated with immunity responses towards biotrophic pathogens, while JA and ET are associated with immunity to necrotrophic pathogens (Nandi et al., 2003; Thomma et al., 1998; Tsuda & Katagiri, 2010). A clear distinction between PTI and ETI does not exist as they induce overlapping downstream immune responses and there is emerging evidence that PTI is required for a normal ETI response (Chang et al., 2022).

Although the zig-zag model is widely accepted, there have been recent calls to classify plant immune responses based on the site of pathogen recognition, a so called 'spatial immunity model' (Kanyuka & Rudd, 2019; Thomma et al., 2011; van der Burgh & Joosten, 2019). The distinction between extracellular and intracellular immune receptors is proposed by these authors due to a blurry line between what constitutes a PRR and R-gene protein, as well a lack of clear distinction between PAMPs and effectors.

The cell surface immune receptors (CSIRs) include a wide range of receptors that are able to intercept a large number of invasion molecules in the extracellular space, including PAMPs, danger associated molecular patterns (DAMPs) and effectors (Kanyuka & Rudd, 2019). The CSIRs include the large group of receptor-like kinases (RLKs), which contain a ligand-binding extracellular domain and an intracellular kinase domain. The most well-characterised group of RLKs are the leucine rich repeat-containing RLKs (LRR-RLKs). Examples of well-studied LRR-RLKs are FLS2 in Arabidopsis, Xa21 in rice and EFR in Arabidopsis. These receptor proteins recognise conserved pathogen patterns such as the flg22 peptide derived from bacterial flagellin (FLS2), the elf18 peptide derived from the bacterial EF-Tu protein (EFR) and the *Xanthomonas* derived peptide Ax21 (Xa21) (Ngou et al., 2022; Park et al., 2010)

Wall Associated Receptor-like Kinases (WAKs) are a subgroup of RLKs, which recently has been emerging as having an important role in many plant-pathogen interactions, particularly when it comes to fungal pathogens (Stephens et al., 2022). Another subgroup of the RLKs are

lectin receptor-like kinases (LecRLKs), which all contain an extracellular lectin domain. The LecRLKs are grouped based on the structure of their lectin domain, which influences the type of ligands they bind to. The majority of LecRLKs that have a reported role in plant pathogen recognition belong to the L (legume)-type LecRLKs, which can recognize complex glucose, mannose, hormones, and microbial invasion pattern (Sun et al., 2020). The G (GNA-related/S-locus)-type LecRLKs (G-LecRLKs) have lectin-domains with a specificity for binding mannose. G-type LecRLKs have only relatively recently been linked to pathogen recognition in a few plant-pathogen interaction (Bao et al., 2023; Luo et al., 2020; Ma et al., 2023; Pi et al., 2023).

Chitin, a constituent of fungal cell walls, is the most well-described fungal elicitor recognised by CSIRs (Desaki et al., 2018; Kouzai et al., 2014; Ngou et al., 2022). The plant receptors able recognise chitin contain Lysine motif (LysM) sites that bind to the chitin fragments (Kaku and Shibuya, 2016). Additional fungal elicitors that are intercepted by plants include oligogalacturonides from fungal cell walls, fungal toxin, effectors and endopolygalacturonase (Ngou et al., 2022)

The Intracellular Immune Receptors (IIRs) detect the presence or activity of pathogen elicitors inside the host cell. The majority of described IIRs encode receptor proteins which share some conserved structural domains, a nucleotide-binding domain (NB) and leucine-rich-repeats (LRR) and this class of genes is therefore referred to as NB-LRRs or NLRs (NOD-like receptors). The plant NLRs are further divided into two subclasses depending on their N-terminal domain: a coiled-coil (CC) or Toll interleukin receptor 1 (TIR) (Lolle et al., 2020). Gene prediction of NLRs in plant genomes indicates an abundance of genes within this class. In domesticated apple the number of predicted NLRs exceeds 1,000, which is high in relation to its genome size (Arya et al., 2014; Borrelli et al., 2018).

6. The *Malus*: *Neonectria* interaction

The molecular interaction between the *Malus* host and *N. ditissima* is still unraveling. Studies by Salgado-Salazar et al (2021) and Gomez-Cortecero (2019) have used genomic and transcriptomic data from *N. ditissima* to understand the chemical weaponry used by the fungus to infect its hosts. Both studies showed that *N. ditissima* can use a combination of Carbohydrate-Active enZymes (CAZymes), clusters of genes involved in secondary metabolism and effectors to infect woody species.

CAZymes are enzymes responsible for breaking down complex carbohydrates and polysaccharides into smaller products, and is divided into classes depending on their function (Rafiei et al., 2021). Among the groups, Glycoside hydrolases (GHs) accounted for the largest proportion of the CAZymes identified in *Neonectria* (Gómez-Cortecero, 2019; Salgado-Salazar et al., 2021). GHs cleave glycosidic bonds between carbohydrate molecules or between a carbohydrate and a non-carbohydrate group and can thus act in degrading cell walls. This class of enzymes have therefore been shown to be important virulence factors for many plant pathogens. (Rafiei et al., 2021). The predicted secretome of *N. ditissima* also contained other CAZyme groups that are known to function in cell-wall degradation, including polysaccharide lyases, auxiliary activity enzymes and carbohydrate binding modules (Gómez-Cortecero, 2019; Salgado-Salazar et al., 2021). The majority of the CAZymes predicted to be secreted by *N. ditissima* were significantly up-regulated during canker infection (Gómez-Cortecero 2019).

Several gene clusters associated with secondary metabolism were identified among the predicted proteins in *N. ditissima* (Gómez-Cortecero, 2019; Salgado-Salazar et al., 2021). These were predominantly gene clusters predicted to be Nonribosomal peptide synthetases (NPRS) or clusters with Polyketide synthetases (PKS). NPRS and PKS have been linked to plant pathogen virulence factors, including; a polyketide synthase gene cluster required for pathogenicity of *Pseudocercospora fijiensis* on banana (Thomas et al., 2021), the AM-toxin, produced by the apple pathotype of *Alternaria alternata* (Meena & Samal, 2019) and NPS6, which is required for the pathogenicity of multiple fungal pathogens (Oide et al., 2006).

Gómez-Cortecero (2019) found that a total of 44 putative effector proteins were differentially expressed in *N. ditissima* when comparing gene expression in mycelia samples with fungal tissue in infected wood. Out of these putative effectors, 18 were up-regulated during infection.

The studies by Salgado-Salazar et al and Gomez-Cortecero highlight how *Neonectria* utilises a wide range of CAZymes to modulate plant cell walls, which is a common infection strategy by hemibiotrophic/necrotrophic pathogens with a broad host range (Rafiei et al., 2021). Furthermore, *N. ditissima* can produce secondary metabolites that potentially acts as toxins or in other ways increase the virulence of the fungus. Gómez-Cortecero also showed that effector proteins are expressed during infection and may have a role in infection.

The host side of the *Malus: Neonectria* interaction is still largely unknown, although there are ongoing efforts to further the understanding of the molecular mechanisms underlying resistance to this fungus. There are no reported sources of complete immunity to *N. ditissima* in *Malus* germplasm (Bus et al., 2019; Garkava-Gustavsson et al., 2016; Gómez-Cortecero et al., 2016; Karlström et al., 2022; Skytte af Sättra et al., 2023), hence researchers have focused on describing the number of genetic loci involved in tolerance and identifying genetic regions with a large effect on resistance (Bus et al., 2021; Bus et al., 2019; Skytte af Sättra et al., 2023). Bus et al (2019) were the first to describe a QTL associated with resistance to *N. ditissima* by mapping QTL in a biparental population from the cross 'M9' x *Malus* 'Robusta 5'. The QTL, denoted *Rnd1*, is located on chromosome 14 from the hybrid crab-apple *Malus* 'Robusta 5'. *Rnd1* was the only resistance loci reported in the study, however Bus et al used low-density SSR markers for QTL identification and there may therefore be additional QTL segregating in the population which were not closely linked to a genetic marker. Bus et al (2021) and Skytte af Sättra et al (2023) studied the segregation of resistance from apple scion cultivars in two different biparental populations and both identified QTL on chromosome 8 and 16 of the apple genome. Skytte af Sättra et al found an additional two QTL on chromosome 1 and 15 in the population derived from a cross between 'Aroma' x 'Discovery'. All the identified QTL in scion germplasm had small-moderate effects on tolerance to European canker. The multiple number of QTL of lesser effect indicate that there are multiple mechanisms of resistance that together result in a slower spread of the disease in woody tissue.

Ghasemkhani (2015) compared the transcriptomes of one canker susceptible ('Prima') and one tolerant apple cultivar ('Jonathan') during *N. ditissima* infection and found 1055 genes that were differentially expressed between the two cultivars in infected tissue. The differentially expressed genes included a putative NLR (*RPM1*-like), a LRR-RLK (*BAK1*-like), UDP-glucosyltransferases, glutathione transferases as well as transcription factors and genes involved in the phenylpropanoid pathway and secondary metabolism. Only limited results and

methods have been published from this study, hence the full picture of the molecular response in apple to *N. ditissima* infection remains elusive.

7. The role of the phyllosphere microbiome in plant disease

Plants are colonised by fungal and bacterial microorganisms, both below and above-ground. The phyllosphere refers to the total above-ground plant compartments when viewed as a habitat for microorganisms, whereas the microbial habitat within the root-area is called the rhizosphere (Compant et al., 2016). Microbes inhabiting non-infected plant tissue are divided into epiphytes and endophytes, depending on whether they are present on the external plant surface or within plant tissues. Epiphytes and endophytes can be neutral, commensal or beneficial to the plant host, but these groups also include pathogens in their latent phase as well as dormant saprobes (Compant et al., 2016).

The plant microbiome has been shown to contribute to plant fitness in terms of growth promotion, nutrient uptake, stress tolerance but also resistance to pathogens (Trivedi et al., 2020). Most of the research on how microbiome assembly can shape plant disease outcomes has been done on rhizospheres (Gu et al., 2020; Gu et al., 2022; Wen et al., 2022). However, the role of the phyllosphere in plant: pathogen interactions is starting to emerge. Liu et al (2023) showed how a few key microbial taxa in the phyllosphere had a disease suppressive effect on rice false smut (*Ustilaginoidea virens*) and that the suppression of *U. virens* was associated with a reduction in leucine in the rice panicles. Similarly, (Li et al., 2022) studied the difference in leaf epi- and endophyte composition between healthy and diseased citrus leaves and showed how microbes associated with the phyllosphere microbiome shift had antagonistic effects on the pathogen *Diaporthe citri*. There are several proposed mechanisms of the phyllosphere microbiota-mediated pathogen suppression; antagonistic inter-species interaction, competition for nutrients, changes in host metabolism, priming of the plant immune system and mediating plant-plant crosstalk (Gu et al., 2020; Zhan et al., 2022).

The phyllosphere microbial community is shaped by both exogenous and plant endogenous factors. Exogenous factors include light, temperature, moisture and rainfall, geographical location, CO₂, nutrient availability and biotic stresses, whereas the endogenous factors include host species or host genotype within species and developmental stage of the host (Trivedi et al., 2020). The host factors that influence the assembly process of phyllosphere microbial

communities are still not fully understood. Horton et al (2014) conducted a Genome Wide Association Study (GWAS) to study the plant loci responsible for differences in phyllosphere composition and found that genes involved in defense response or had kinase activity were enriched in loci with GWAS hits. Other plant host factors shown to influence the phyllosphere include genes involved in cytokinin and ethylene signalling and cuticle formation (Bodenhausen et al., 2014; Gupta et al., 2022)

In search for possible biocontrol agents against *N. ditissima*, the role of the apple endophytic community in relation to *N. ditissima* infection has also been studied (Liu et al., 2020; Olivieri et al., 2021; Papp-Rupar et al., 2022, 2023). Endophytes with biocontrol potential towards *N. ditissima* have been isolated and tested against the pathogen (Liu et al., 2020; Papp-Rupar et al., 2023). Olivieri et al (2021) showed that susceptible and tolerant *Malus* genotypes differed in endophyte composition and diversity indices. Furthermore, Papp-Rupar et al (2022) reported the impacts of apple host genotype on endophyte assembly in trees infected with *N. ditissima*. The previous research indicates a potential of employing beneficial microorganisms from the *Malus* phyllosphere to suppress European canker. It also highlights that host genotype plays an important role in the three-way interaction between the host, *N. ditissima* and microbiome. A better understanding of the host genetic factors that influence endophyte assembly could be used to breed apple cultivars prone to associations with *N. ditissima* suppressing microbes. This could also help unveil what causes *N. ditissima* to shift from the endophytic latent phase to pathogenic.

8. Aims of the project

Host resistance remains one of the most effective means of controlling European canker in apple. Despite its importance to the apple growing community, the genetic basis underlying this resistance is still not well understood which hinders efficient breeding of cultivars with improved tolerance to the disease. The work in this thesis was conducted to aid the development of apple cultivars with a high tolerance to infection by *N. ditissima*. This was partly done by exploring the genetics behind host resistance in apple scion germplasm. Knowledge of the apple loci that influence resistance could be used to develop genetic markers to be utilised in breeding programmes, while comprehension of the genes involved could provide targets for gene-editing. Moreover, the potential of developing apple cultivars with a canker-suppressing endophytic microbiome was investigated.

This thesis is presented as a collection of two published papers, and one manuscript covering the following topics;

1. Identification of novel genetic regions associated with resistance to European canker in apple (Karlstrom et al., 2022)

This work aimed to describe resistance QTL in apple germplasm that is relevant for modern breeding programmes. Several phenotyping methods were used to determine the level of resistance of individuals in a multiparental population. Furthermore, phenotypic data from a biparental population derived from a cross between 'Golden Delicious' x 'M9' was used to validate the effect of SNP-haplotypes within the QTL.

2. Transcriptome analysis provide insights in resistance to European canker and reveal candidate resistance genes (submitted, 2023)

This study was conducted to shine light on the type of molecular mechanisms that underly quantitative disease resistance to *N. ditissima* in *Malus*. Transcriptome data from RNA sequencing of infected stems of 'Golden Delicious' and 'M9' was used to understand the global response to the pathogen. Additionally, this work aims to identify the genes underlying the QTL identified in Karlstrom et al (2022). To this end, a comparative transcriptome analysis of full-sibling apple genotypes carrying resistant (QTL-R) and susceptible (QTL-S) alleles was conducted.

3. Quantitative trait loci associated with apple endophytes during pathogen infection (Karlstrom et al., 2023)

The aim of this study was to identify genetic regions that promote host-microbial associations with *N. ditissima* suppressive endophytes. This information can be used to inform breeding of new cultivars with disease suppressive microbiomes and to facilitate the identification of genes that promote associations with beneficial microorganisms. The work is based on a previous publication by Papp-Rupar et al (2022), in which it was shown that apple genotype has a significant effect on the abundance of several bacterial and fungal endophyte taxa. The amplicon sequencing data from wood endophytes in the prior study was used together with SNP marker data to study QTL influencing the phyllosphere microbiome assembly.

References

- Abe, K., Kotoda, N., Kato, H. and Soejima, J. (2007). Resistance sources to Valsa canker (*Valsa ceratosperma*) in a germplasm collection of diverse *Malus* species (*Valsa ceratosperma*). *Plant Breeding* 126(4), 449–53. doi:10.1111/j. 1439-0523.2007.01379.x.
- Abe, K., Kotoda, N., Kato, H. and Soejima, J. (2011). Genetic studies on resistance to Valsa canker in apple: Genetic variance and breeding values estimated from intra- and inter-specific hybrid progeny populations. *Tree Genetics and Genomes* 7(2), 363–72. doi:10.1007/s11295-010-0337-3.
- Albrechtsen, A., Nielsen, F. C. and Nielsen, R. (2010). Ascertainment biases in SNP chips affect measures of population divergence. *Molecular Biology and Evolution* 27(11), 2534–47. doi:10.1093/molbev/msq148.
- Allard, A., Bink, M. C. A. M., Martinez, S., Kelner, J. J., Legave, J. M., di Guardo, M., Di Pierro, E. A., Laurens, F., van de Weg, E. W. and Costes, E. (2016). Detecting QTLs and putative candidate genes involved in budbreak and flowering time in an apple multiparental population. *Journal of Experimental Botany* 67(9), 2875–88. doi:10.1093/jxb/erw130.
- Amponsah, N. T., Scheper, R. W. A., Fisher, B. M., Walter, M., Smits, J. M., & Jesson, L. K. (2017). The effect of wood age on infection by *Neonectria ditissima* through artificial wounds on different apple cultivars. *New Zealand plant protection*, 70, 97-105.
- Antanaviciute, L., Fernández-Fernández, F., Jansen, J., Banchi, E., Evans, K. M., Viola, R., Velasco, R., Dunwell, J. M., Troggio, M. and Sargent, D. J. (2012). Development of a dense SNP-based linkage map of an apple rootstock progeny using the *Malus* Infinium whole genome genotyping array. *BMC Genomics* 13, 203. doi:10.1186/1471-2164-13-203.
- Arya, P., Kumar, G., Acharya, V., & Singh, A. K. (2014). Genome-wide identification and expression analysis of NBS-encoding genes in *Malus x domestica* and expansion of NBS genes family in Rosaceae. *Plos One*, 9(9), e107987. <https://doi.org/10.1371/journal.pone.0107987>

Badiu, D., Arion, F., Muresan, I., Lile, R. and Mitre, V. (2015). Evaluation of economic efficiency of apple orchard investments. *Sustainability* 7(8), 10521–33. doi:10.3390/su70810521.

Bai, Y., Dougherty, L., Li, M., Fazio, G., Cheng, L. and Xu, K. (2012). A natural mutation-led truncation in one of the two aluminium-activated malate transporter-like genes at the *Ma* locus is associated with low fruit acidity in apple. *Molecular Genetics and Genomics*: MGG 287(8), 663–78. doi:10.1007/s00438-012-0707-7.

Bannier, H.-J. (2011). Moderne apfelzüchtung: Genetische verarmung und tendenzen zur inzucht. *Erwerbs-Obstbau* 52(3–4), 85–110. doi:10.1007/s10341-010-0113-4.

Bao, Y., Li, Y., Chang, Q., Chen, R., Wang, W., Zhang, Q., Chen, S., Xu, G., Wang, X., Cui, F., Dou, D., & Liang, X. (2023). A pair of G-type lectin receptor-like kinases modulates *nlp20*-mediated immune responses by coupling to the RLP23 receptor complex. *Journal of Integrative Plant Biology*, 65(5), 1312–1327. <https://doi.org/10.1111/jipb.13449>

Bastiaanse, H., Bassett, H. C. M., Kirk, C., Gardiner, S. E., Deng, C., Groenworld, R., Chagné, D. and Bus, V. G. (2016). Scab resistance in ‘Geneva’ apple is conditioned by a resistance gene cluster with complex genetic control. *Molecular Plant Pathology* 17(2), 159–72. doi:10.1111/mpp.12269.

Baumgartner, I. O., Patocchi, A., Frey, J. E., Peil, A. and Kellerhals, M. (2015). Breeding elite lines of apple carrying pyramided homozygous resistance genes against apple scab and resistance against powdery mildew and fire blight. *Plant Molecular Biology Reporter* 33(5), 1573–83. doi:10.1007/s11105-015-0858-x.

Beresford, R. M. and Kim, K. S. (2011). Identification of regional climatic conditions favorable for development of European canker of apple. *Phytopathology* 101(1), 135–46. doi:10.1094/PHYTO-05-10-0137.

Bhatia, D., Wing, R. A. and Singh, K. (2013). Genotyping by sequencing its implications and benefits. *Crop Improvement* 40(2), 101–11.

Bianco, L., Cestaro, A., Sargent, D. J., Banchi, E., Derdak, S., Di Guardo, M., Salvi, S., Jansen, J., Viola, R., Gut, I., et al. (2014). Development and validation of a 20K single nucleotide polymorphism (SNP) whole genome genotyping array for apple (*Malus × domestica* Borkh). *PLoS ONE* 9(10), e110377. doi:10.1371/journal.pone.0110377.

Bianco, L., Cestaro, A., Linsmith, G., Muranty, H., Denancé, C., Théron, A., Poncet, C., Micheletti, D., Kerschbamer, E., Di Pierro, E. A., et al. (2016). Development and validation of the Axiom® Apple480K SNP genotyping array. *The Plant Journal: for Cell and Molecular Biology* 86(1), 62–74. doi:10.1111/tpj.13145.

Bodenhausen, N., Bortfeld-Miller, M., Ackermann, M., & Vorholt, J. A. (2014). A synthetic community approach reveals plant genotypes affecting the phyllosphere microbiota. *PLoS Genetics*, 10(4), e1004283. <https://doi.org/10.1371/journal.pgen.1004283>

Borrelli, G. M., Mazzucotelli, E., Marone, D., Crosatti, C., Michelotti, V., Valè, G., & Mastrangelo, A. M. (2018). Regulation and evolution of NLR genes: A close interconnection for plant immunity. *International Journal of Molecular Sciences*, 19(6). <https://doi.org/10.3390/ijms19061662>

Bracuto, V., Appiano, M., Ricciardi, L., Göl, D., Visser, R. G. F., Bai, Y. and Pavan, S. (2017). Functional characterization of the powdery mildew susceptibility gene *SmMLO1* in eggplant (*Solanum melongena* L.). *Transgenic Research* 26(3), 323–30. doi:10.1007/s11248-016-0007-9.

Broggini, G. A. L., Wöhner, T., Fahrentrapp, J., Kost, T. D., Flachowsky, H., Peil, A., Hanke, M. V., Richter, K., Patocchi, A. and Gessler, C. (2014). Engineering fire blight resistance into the apple cultivar ‘Gala’ using the *FB_MR5* CC-NBS-LRR resistance gene of *Malus × robusta* 5. *Plant Biotechnology Journal* 12(6), 728–33. doi:10.1111/pbi.12177.

Brown, A. E., Muthumeenakshi, S., Swinburne, T. R., & Li, R. (1994). Detection of the source of infection of apple trees by *Cylindrocarpum heteronema* using DNA polymorphisms. *Plant Pathology*, 43(2), 338–343. <https://doi.org/10.1111/j.1365-3059.1994.tb02693.x>

Brown, S. K. (2009). Making sense of new apple varieties, trademarks and clubs: Current status. *New York Fruit Quarterly* 17(3): 9–12.

Bus, V. G. M., Chagné, D., Bassett, H. C. M., Bowatte, D., Calenge, F., Celton, J.-M., Durel, C.-E., Malone, M. T., Patocchi, A., Ranatunga, A. C., et al. (2008). Genome mapping of three major resistance genes to woolly apple aphid (*Eriosoma lanigerum* Hausm.). *Tree Genetics and Genomes* 4(2), 223–36. doi:10.1007/s11295-007-0103-3.

Bus, V. G. M., Bassett, H. C. M., Bowatte, D., Chagné, D., Ranatunga, C. A., Ulluwishewa, D., Wiedow, C. and Gardiner, S. E. (2010). Genome mapping of an apple scab, a powdery mildew

and a woolly apple aphid resistance gene from open-pollinated mildew immune selection. *Tree Genetics and Genomes* 6(3), 477–87. doi:10.1007/s11295-009-0265-2.

Bus, V. G. M., Scheper, R. W. A., Walter, M., Campbell, R. E., Kitson, B., Turner, L., Fisher, B. M., Johnston, S. L., Wu, C., Deng, C. H., Singla, G., Bowatte, D., Jesson, L. K., Hedderley, D. I., Volz, R. K., Chagné, D., & Gardiner, S. E. (2019). Genetic mapping of the European canker (*Neonectria ditissima*) resistance locus Rnd1 from *Malus* 'Robusta 5.' *Tree Genetics & Genomes*, 15(2), 25. <https://doi.org/10.1007/s11295-019-1332-y>

Bus, V., Singla, G., Horner, M., Jesson, L., Walter, M., Kitson, B., López-Girona, E., Kirk, C., Gardiner, S., Chagné, D., & Volz, R. (2021). Preliminary genetic mapping of fire blight and European canker resistances in two apple breeding families. *Acta Horticulturae*, 1307, 199–204. <https://doi.org/10.17660/ActaHortic.2021.1307.31>

Buti, M., Poles, L., Caset, D., Magnago, P., Fernández-Fernández, F., Colgan, R. J., Velasco, R. and Sargent, D. J. (2015). Identification and validation of a QTL influencing bitter pit symptoms in apple (*Malus × domestica*). *Molecular Breeding* 35(1). doi:10.1007/s11032-015-0258-9.

Calenge, F. and Durel, C.-E. (2006). Both stable and unstable QTLs for resistance to powdery mildew are detected in apple after four years of field assessments. *Molecular Breeding* 17(4), 329–39. doi:10.1007/s11032-006-9004-7.

Calenge, F., Drouet, D., Denancé, C., van de Weg, W. E., Brisset, M. N., Paulin, J. P. and Durel, C. E. (2005). Identification of a major QTL together with several minor additive or epistatic QTLs for resistance to fire blight in apple in two related progenies. *Theoretical and Applied Genetics* 111(1), 128–35. doi:10.1007/s00122-005-2002-z.

Celton, J.-M., Tustin, D. S., Chagné, D. and Gardiner, S. E. (2009). Construction of a dense genetic linkage map for apple rootstocks using SSRs developed from *Malus* ESTs and *Pyrus* genomic sequences. *Tree Genetics and Genomes* 5(1), 93–107. doi:10.1007/s11295-008-0171-z.

Centro de Pomaceas. 2019. Programa mejoramiento genético. Available at: <http://pomaceas.utralca.cl/investigacion/programa-mejoramiento-genetico>.

Chagné, D., Crowhurst, R. N., Troggio, M., Davey, M. W., Gilmore, B., Lawley, C., Vanderzande, S., Hellens, R. P., Kumar, S., Cestaro, A., et al. (2012). Genome-wide SNP

detection, validation, and development of an 8K SNP array for apple. *PLoS ONE* 7(2), e31745. doi:10.1371/journal.pone.0031745.

Chagné, D., Kirk, C., Whitworth, C., Erasmuson, S., Bicknell, R., Sargent, D. J., Kumar, S., & Troggio, M. (2015). Polyploid and aneuploid detection in apple using a single nucleotide polymorphism array. *Tree Genetics & Genomes*, 11(5), 94. <https://doi.org/10.1007/s11295-015-0920-8>

Chang, M., Chen, H., Liu, F., & Fu, Z. Q. (2022). PTI and ETI: convergent pathways with diverse elicitors. *Trends in Plant Science*, 27(2), 113–115. <https://doi.org/10.1016/j.tplants.2021.11.013>

Chen, P., Li, Z., Zhang, D., Shen, W., Xie, Y., Zhang, J., ... & Guan, Q. (2021). Insights into the effect of human civilization on *Malus* evolution and domestication. *Plant Biotechnology Journal*, 19(11), 2206–2220. <https://doi.org/10.1111/pbi.13648>

Cheng, F. S., Weeden, N. F. and Brown, S. K. (1996). Identification of co-dominant RAPD markers tightly linked to fruit skin color in apple. *Theoretical and Applied Genetics* 93(1–2), 222–7. doi:10.1007/BF00225749.

Cheng, F. S., Weeden, N. F., Brown, S. K., Aldwinckle, H. S., Gardiner, S. E. and Bus, V. G. (1998). Development of a DNA marker for *Vm*, a gene conferring resistance to apple scab. *Genome* 41(2), 208–14. doi:10.1139/g98-020.

Clark, M. D., Luby, J. J. and Bradeen, J. M. (2014). Characterizing the host response and genetic control of resistance in ‘Honeycrisp’ to apple scab (*Venturia inaequalis*). *European Journal of Plant Pathology* 140(1), 69–81.

Compant, S., Saikkonen, K., Mitter, B., Campisano, A., & Mercado-Blanco, J. (2016). Editorial special issue: soil, plants and endophytes. *Plant and Soil*, 405(1–2), 1–11. <https://doi.org/10.1007/s11104-016-2927-9>

Cornille, A., Gladioux, P., Smulders, M. J. M., Roldán-Ruiz, I., Laurens, F., Le Cam, B., Nersesyan, A., Clavel, J., Olonova, M., Feugey, L., Gabrielyan, I., Zhang, X.-G., Tenailon, M. I., & Giraud, T. (2012). New insight into the history of domesticated apple: secondary contribution of the European wild apple to the genome of cultivated varieties. *PLoS Genetics*, 8(5), e1002703. <https://doi.org/10.1371/journal.pgen.1002703>

CPVO. (2018). Community Plant Variety Office (CPVO) statistics database. Available at: http://cpvoextranet.cpvo.europa.eu/DENOMINATIONS_WEB/UK/PAGE_statistics.htm (Accessed on 14 June 2018).

Cui, H., Tsuda, K., & Parker, J. E. (2015). Effector-triggered immunity: from pathogen perception to robust defense. *Annual Review of Plant Biology*, 66, 487–511. <https://doi.org/10.1146/annurev-arplant-050213-040012>

Daccord, N., Celton, J. M., Linsmith, G., Becker, C., Choisne, N., Schijlen, E., van de Geest, H., Bianco, L., Micheletti, D., Velasco, R., et al. (2017). High-quality de novo assembly of the apple genome and methylome dynamics of early fruit development. *Nature Genetics* 49(7), 1099–106. doi:10.1038/ng.3886.

Department for Environment, Food & Rural Affairs. (2022). Horticulture Statistics 2022 (Updated 30 October 2023). Retrieved from: <https://www.gov.uk/government/statistics/latest-horticulture-statistics/horticulture-statistics-2022>

Delaney, T. P., Uknes, S., Vernooij, B., Friedrich, L., Weymann, K., Negrotto, D., Gaffney, T., Gut-Rella, M., Kessmann, H., Ward, E., & Ryals, J. (1994). A central role of salicylic Acid in plant disease resistance. *Science*, 266(5188), 1247–1250. <https://doi.org/10.1126/science.266.5188.1247>

Desaki, Y., Miyata, K., Suzuki, M., Shibuya, N., & Kaku, H. (2018). Plant immunity and symbiosis signaling mediated by LysM receptors. *Innate Immunity*, 24(2), 92–100. <https://doi.org/10.1177/1753425917738885>

Duan, N., Bai, Y., Sun, H., Wang, N., Ma, Y., Li, M., Wang, X., Jiao, C., Legall, N., Mao, L., et al. (2017). Genome re-sequencing reveals the history of apple and supports a two-stage model for fruit enlargement. *Nature Communications* 8(1), 249. doi:10.1038/s41467-017-00336-7.

Dunemann, F., Peil, A., Urbanietz, A. and Garcia-Libreros, T. (2007). Mapping of the apple powdery mildew resistance gene PI1 and its genetic association with an NBS-LRR candidate resistance gene. *Plant Breeding* 126(5), 476–81. doi:10.1111/j.1439-0523.2007.01415.x.

Durel, C. E., Denancé, C. and Brisset, M. N. (2009). Two distinct major QTL for resistance to fire blight co-localize on linkage group 12 in apple genotypes ‘Evereste’ and *Malus floribunda* clone 821. *Genome* 52(2), 139–47. doi:10.1139/g08-111.

Edge-Garza, D. A., Peace, C. P. and Zhu, Y. (2010). Enabling marker-assisted seedling selection in the Washington apple breeding program. *Acta Horticulturae* 859(859), 369–73. doi:10.17660/ActaHortic.2010.859.44.

Edge-Garza, D. A., Luby, J. J. and Peace, C. (2015). Decision support for cost-efficient and logistically feasible marker-assisted seedling selection in fruit breeding. *Molecular Breeding* 35(12), 223. doi:10.1007/s11032-015-0409-z.

Elshire, R. J., Glaubitz, J. C., Sun, Q., Poland, J. A., Kawamoto, K., Buckler, E. S. and Mitchell, S. E. (2011). A robust, simple genotyping-by-sequencing (GBS) approach for high diversity species. *PLoS ONE* 6(5), e19379. doi:10.1371/journal.pone.0019379.

Emeriewen, O., Richter, K., Kilian, A., Zini, E., Hanke, M., Malnoy, M. and Peil, A. (2014). Identification of a major quantitative trait locus for resistance to fire blight in the wild apple species *Malus fusca*. *Molecular Breeding* 34(2), 407–19. doi:10.1007/s11032-014-0043-1.

Emeriewen, O. F., Peil, A., Richter, K., Zini, E., Hanke, M. and Malnoy, M. (2017). Fire blight resistance of *Malus × arnoldiana* is controlled by a quantitative trait locus located at the distal end of linkage group 12. *European Journal of Plant Pathology* 148(4), 1011–8. doi:10.1007/s10658-017-1152-6.

Evans, K. (2011). Apple breeding in the Pacific Northwest. In: XIII Eucarpia Symposium on Fruit Breeding and Genetics. *Acta Horticulturae* 976, 75–8. doi:10.17660/ActaHortic.2013.976.6.

Evans, K. (2017). *Achieving Sustainable Cultivation of Apples*. Cambridge, UK: Burleigh Dodds Science Publishing Limited.

Evans, K. M. and James, C. M. (2003). Identification of SCAR markers linked to *PI-w* mildew resistance in apple. *Theoretical and Applied Genetics* 106(7), 1178–83. doi:10.1007/s00122-002-1147-2.

Fahrentrapp, J., Broggin, G. A. L., Kellerhals, M., Peil, A., Richter, K., Zini, E. and Gessler, C. (2013). A candidate gene for fire blight resistance in *Malus × robusta* 5 is coding for a CC–NBS–LRR. *Tree Genetics and Genomes* 9(1), 237–51. doi:10.1007/s11295-012-0550-3.

Falginella, L., Cipriani, G., Monte, C., Gregori, R., Testolin, R., Velasco, R., Troggio, M. and Tartarini, S. (2015). A major QTL controlling apple skin russeting maps on the linkage group

12 of 'Renetta Grigia di Torriana'. *BMC Plant Biology* 15, 150. doi:10.1186/s12870-015-0507-4.

FAOSTAT. (2018). Food and Agriculture Organization of the United Nations. Available at: <http://www.fao.org/faostat/en/>(Accessed on 14 June 2018).

Fernández-Fernández, F., Antanaviciute, L., van Dyk, M. M., Tobutt, K. R., Evans, K. M., Rees, D. J. G., Dunwell, J. M. and Sargent, D. J. (2012). A genetic linkage map of an apple rootstock progeny anchored to the *Malus* genome sequence. *Tree Genetics and Genomes* 8(5), 991–1002. doi:10.1007/s11295-012-0478-7.

Flachowsky, H., Le Roux, P. M., Peil, A., Patocchi, A., Richter, K. and Hanke, M. V. (2011). Application of a high-speed breeding technology to apple (*Malus × domestica*) based on transgenic early flowering plants and marker-assisted selection. *New Phytologist* 192(2), 364–77. doi:10.1111/j.1469-8137.2011.03813.x.

Flor, H. H. (1971). Current status of the gene-for-gene concept. *Annual Review of Phytopathology* 9(1), 275–96. doi:10.1146/annurev.py.09.090171.001423.

Fruitbreedomics. (2012). DAY 1 - Stakeholder Day - Conferences 1, 2 - Welcome - Jaroslav Vacha and Jan Blazek (video file). 9 April 2012. Available at: <https://vimeo.com/63414205>.

Fruitbreedomics. (2013a). CONF. 15 D. 1 -New apple cultivars released at the research institute of horticulture Skierniewice. Mariusz Lewandowski (Poland) (video file). 5 April 2013. Retrieved from: <https://vimeo.com/63414205>.

Fruitbreedomics. (2013b). CONF. 10 D. 1 -Progress in Better3fruit's apple and pear breeding program- Inge de Wit – Better3fruit (Belgium). (video file). 5 April 2013. Available at: <https://vimeo.com/63413153>.

Fruitbreedomics. (2013c). CONF. 12 D. 1 -Advances in CRA-FRF pear and apple breeding- Gianluca Baruzzi – CRA-FRF (Italy). (video file). 5 April 2013. Available at: <https://vimeo.com/63413152> 12 D, 1.

Fruitbreedomics. (2014a). C5 D1 – Molecular markers on breeding: Apple – Dr. M. Kellerhals – (Agroscope, Switzerland) – FB 3rd A. Meeting - Zürich 2014. (video file). 10 April 2014. Available at: <https://vimeo.com/91614678>.

Fruitbreedomics. (2014b). C8 D1 – MAB Transfer – Dr. François Laurens (INRA, France) – FB 3rd A. Meeting – Zürich 2014. video file. Available at: <https://vimeo.com/91614738>.

Gardiner, S. E., Norelli, J. L., de Silva, N., Fazio, G., Peil, A., Malnoy, M., Horner, M., Bowatte, D., Carlisle, C., Wiedow, C., et al. (2012). Putative resistance gene markers associated with quantitative trait loci for fire blight resistance in *Malus* 'Robusta 5' accessions. *BMC Genetics* 13, 25. doi:10.1186/1471-2156-13-25.

Gardner, K. M., Brown, P., Cooke, T. F., Cann, S., Costa, F., Bustamante, C., Velasco, R., Troggio, M. and Myles, S. (2014). Fast and cost-effective genetic mapping in apple using next-generation sequencing. *G3* (Bethesda, Md.) 4(9), 1681–7. doi:10.1534/g3.114.011023.

Garkava-Gustavsson, L., Ghasemkhani, M., Zborowska, A., Englund, J.-E., Lateur, M. and van de Weg, E. (2016). Approaches for evaluation of resistance to European canker (*Neonectria ditissima*) in apple. *Acta Horticulturae* 1127(1127), 75–82. doi:10.17660/ActaHortic.2016.1127.14.

Gelvonauskienė, D., Sasnauskas, A. and Gelvonauskis, B. (2007). The breeding of apple tree resistant to European canker (*Nectria galligena* bres.) scientific works of the Lithuanian Institute of Horticulture and Lithuanian University of Agriculture. *Sodininkyste ir Darzininkyste* 26(3).

Gessler, C. and Pertot, I. (2012). *Vf* scab resistance of *Malus*. *Trees* 26(1), 95–108. doi:10.1007/s00468-011-0618-y.

Ghasemkhani M. (2015). Resistance against fruit tree canker in apple vol. 77. Sueciae: Doctoral thesis, Swedish University of Agricultural Sciences, Alnarp, Sweden / *Acta Universitatis Agriculturae*; 2015. p. 64.

Ghasemkhani, M., Liljeroth, E., Sehic, J., Zborowska, A. and Nybom, H. (2015a). Cut-off shoots method for estimation of partial resistance in apple cultivars to fruit tree canker caused by *Neonectria ditissima*. *Acta Agriculturae Scandinavica, Section B – Soil and Plant Science* 65(5), 412–21.

Ghasemkhani, M., Sehic, J., Ahmadi-Afzadi, M., Nybom, H. and Garkava-Gustavsson, L. (2015b). Screening for partial resistance to fruit tree canker in apple cultivars. *Acta Horticulturae* 1099(1099), 687–90. doi:10.17660/ActaHortic.2015.1099.84.

Garkava-Gustavsson, L., Ghasemkhani, M., Zborowska, A., Englund, J. E., Lateur, M., & van de Weg, E. (2016). Approaches for evaluation of resistance to European canker (*Neonectria ditissima*) in apple. *Acta Horticulturae*, 1127, 75–82. <https://doi.org/10.17660/ActaHortic.2016.1127.14>

Gianfranceschi, L., Seglias, N., Tarchini, R., Komjanc, M. and Gessler, C. (1998). Simple sequence repeats for the genetic analysis of apple. *Theoretical and Applied Genetics* 96(8), 1069–76. doi:10.1007/s001220050841.

Gómez-Cortecero, A., Saville, R. J., Scheper, R. W. A., Bowen, J. K., Agripino De Medeiros, H., Kingsnorth, J., Xu, X. and Harrison, R. J. (2016). Variation in host and pathogen in the *Neonectria/Malus* interaction; toward an understanding of the genetic basis of resistance to European canker. *Frontiers in Plant Science* 7, 1365. doi:10.3389/fpls.2016.01365.

Gómez-Cortecero, A. (2019). The molecular basis of pathogenicity of *Neonectria ditissima* [Doctoral dissertation]. University of Reading.

Govrin, E. M., & Levine, A. (2000). The hypersensitive response facilitates plant infection by the necrotrophic pathogen *Botrytis cinerea*. *Current Biology*, 10(13), 751–757. [https://doi.org/10.1016/s0960-9822\(00\)00560-1](https://doi.org/10.1016/s0960-9822(00)00560-1)

Gu, S., Wei, Z., Shao, Z., Friman, V.-P., Cao, K., Yang, T., Kramer, J., Wang, X., Li, M., Mei, X., Xu, Y., Shen, Q., Kümmerli, R., & Jousset, A. (2020). Competition for iron drives phytopathogen control by natural rhizosphere microbiomes. *Nature Microbiology*, 5(8), 1002–1010. <https://doi.org/10.1038/s41564-020-0719-8>

Gu, Y., Banerjee, S., Dini-Andreote, F., Xu, Y., Shen, Q., Jousset, A., & Wei, Z. (2022). Small changes in rhizosphere microbiome composition predict disease outcomes earlier than pathogen density variations. *The ISME Journal*, 16(10), 2448–2456. <https://doi.org/10.1038/s41396-022-01290-z>

Guan, Y., Peace, C., Rudell, D., Verma, S. and Evans, K. (2015). QTLs detected for individual sugars and soluble solids content in apple. *Molecular Breeding* 35(6), 135. doi:10.1007/s11032-015-0334-1.

Gupta, R., Elkabetz, D., Leibman-Markus, M., Sayas, T., Schneider, A., Jami, E., Kleiman, M., & Bar, M. (2022). Cytokinin drives assembly of the phyllosphere microbiome and promotes

disease resistance through structural and chemical cues. *The ISME Journal*, 16(1), 122–137. <https://doi.org/10.1038/s41396-021-01060-3>

Gygax, M., Gianfranceschi, L., Liebhard, R., Kellerhals, M., Gessler, C. and Patocchi, A. (2004). Molecular markers linked to the apple scab resistance gene *Vbj* derived from *Malus baccata* jackii. *Theoretical and Applied Genetics* 109(8), 1702–9. doi:10.1007/s00122-004-1803-9.

Harshman, J. M., Evans, K. M. and Hardner, C. M. (2016). Cost and accuracy of advanced breeding trial designs in apple. *Horticulture Research* 3, 16008. doi:10.1038/hortres.2016.8.

Harshman, J. M., Evans, K. M., Allen, H., Potts, R., Flamenco, J., Aldwinckle, H. S., Wisniewski, M. E. and Norelli, J. L. (2017). Fire blight resistance in wild accessions of *Malus sieversii*. *Plant Disease* 101, 1738–45.

He, J., Zhao, X., Laroche, A., Lu, Z. X., Liu, H. and Li, Z. (2014). Genotyping-by-sequencing (GBS), an ultimate marker-assisted selection (MAS) tool to accelerate plant breeding. *Frontiers in Plant Science* 5, 484. doi:10.3389/fpls.2014.00484.

Heide, O. M. and Prestrud, A. K. (2005). Low temperature, but not photoperiod, controls growth cessation and dormancy induction and release in apple and pear. *Tree Physiology* 25(1), 109–14. doi:10.1093/treephys/25.1.109.

Holb, I. J. (2017). Categorization of apple cultivars based on seasonal powdery mildew disease progression in two disease management systems over 12 years. *Trees* 31(6), 1905–17. doi:10.1007/s00468-017-1595-6.

Horton, M. W., Bodenhausen, N., Beilsmith, K., Meng, D., Muegge, B. D., Subramanian, S., Vetter, M. M., Vilhjálmsson, B. J., Nordborg, M., Gordon, J. I., & Bergelson, J. (2014). Genome-wide association study of *Arabidopsis thaliana* leaf microbial community. *Nature Communications*, 5, 5320. <https://doi.org/10.1038/ncomms6320>

James, C. M., Clarke, J. B. and Evans, K. M. (2004). Identification of molecular markers linked to the mildew resistance gene *PI-d* in apple. *Theoretical and Applied Genetics* 110(1), 175–81. doi:10.1007/s00122-004-1836-0.

Jones, J. D. G., & Dangl, J. L. (2006). The plant immune system. *Nature*, 444(7117), 323–329. <https://doi.org/10.1038/nature05286>

Joshi, S. G., Soriano, J. M., Kortstee, A., Schaart, J. G., Krens, F.A. Jacobsen, E. and Schouten, H. J. (2009). Development of cisgenic apples with durable resistance to apple scab. *Acta Horticulturae* 839(839), 403–6. doi:10.17660/ActaHortic.2009.839.53

Kanyuka, K., & Rudd, J. J. (2019). Cell surface immune receptors: the guardians of the plant's extracellular spaces. *Current Opinion in Plant Biology*, 50, 1–8. <https://doi.org/10.1016/j.pbi.2019.02.005>

Karlström, A., Cabo-Medina, M., and Harrison, R. (2019). “Advances and challenges in apple breeding, vol. 2” in *Achieving Sustainable Cultivation of Temperate Zone Tree Fruits and Berries*, ed G. A. Lang (Cambridge: Burleigh Dodds Science Publishing). doi: 10.19103/AS.2018.0040.21

Karlström, A., Gómez-Cortecero, A., Nellist, C. F., Ordidge, M., Dunwell, J. M., & Harrison, R. J. (2022). Identification of novel genetic regions associated with resistance to European canker in apple. *BMC Plant Biology*, 22(1), 452. <https://doi.org/10.1186/s12870-022-03833-0>

Karlström, A., Papp-Rupar, M., Passey, T. A., Deakin, G., & Xu, X. (2023). Quantitative trait loci associated with apple endophytes during pathogen infection. *Frontiers in Plant Science*, 14, 1054914.

Kaur, B., Bhatia, D., & Mavi, G. S. (2021). Eighty years of gene-for-gene relationship and its applications in identification and utilization of R genes. *Journal of Genetics*, 100(2), 50. <https://doi.org/10.1007/s12041-021-01300-7>

Kellerhals, M., Patocchi, A., Duffy, B. and Frey, J. (2008). Modern approaches for breeding high quality apples with durable resistance to scab, powdery mildew and fire blight. In: Boos, M. (Ed.), *Ecofruit – 13th International Conference on Cultivation Technique and Phytopathological Problems in Organic Fruit-Growing: Proceedings to the Conference from 18–20 February 2008 at Weinsberg/Germany*, pp. 226–31.

Kellerhals, M., Spuhler, M., Duffy, B., Patocchi, A. and Frey, J. E. (2009). Selection efficiency in apple breeding. *Acta Horticulturae* 814(814), 177–84. doi:10.17660/ActaHortic.2009.814.22.

Kellerhals, M., Schütz, S. and Patocchi, A. (2017). Breeding for host resistance to fire blight. *Journal of Plant Pathology: An International Journal of the Italian Phytopathological Society* 99(Special Issue), 37–43.

- Kenis, K. and Keulemans, J. (2005). Genetic linkage maps of two apple cultivars (*Malus domestica* Borkh.) based on AFLP and microsatellite markers. *Molecular Breeding* 15(2), 205–19. doi:10.1007/s11032-004-5592-2.
- Khan, M. A., Durel, C. E., Duffy, B., Drouet, D., Kellerhals, M., Gessler, C. and Patocchi, A. (2007). Development of molecular markers linked to the 'Fiesta' linkage Group 7 major QTL for fire blight resistance and their application for marker-assisted selection. *Genome* 50(6), 568–77. doi:10.1139/g07-033.
- Koller, B., Gianfranceschi, L., Seglias, N., McDermott, J., & Gessler, C. (1994). DNA markers linked to *Malus floribunda* 821 scab resistance. *Plant Molecular Biology*, 26(2), 597–602. <https://doi.org/10.1007/BF00013746>
- Kost, T. D., Gessler, C., Jänsch, M., Flachowsky, H., Patocchi, A. and Broggini, G. A. (2015). Development of the first cisgenic apple with increased resistance to fire blight. *PLoS ONE* 10(12), e0143980. doi:10.1371/journal.pone.0143980.
- Kouzai, Y., Mochizuki, S., Nakajima, K., Desaki, Y., Hayafune, M., Miyazaki, H., Yokotani, N., Ozawa, K., Minami, E., Kaku, H., Shibuya, N., & Nishizawa, Y. (2014). Targeted gene disruption of *OsCERK1* reveals its indispensable role in chitin perception and involvement in the peptidoglycan response and immunity in rice. *Molecular Plant-Microbe Interactions*, 27(9), 975–982. <https://doi.org/10.1094/MPMI-03-14-0068-R>
- Kumar, S., Chagné, D., Bink, M. C. A. M., Volz, R. K., Whitworth, C. and Carlisle, C. (2012). Genomic selection for fruit quality traits in apple (*Malus × domestica* Borkh.). *PLoS ONE* 7(5), e36674. doi:10.1371/journal.pone.0036674.
- Kumar, S., Garrick, D. J., Bink, M. C., Whitworth, C., Chagné, D. and Volz, R. K. (2013). Novel genomic approaches unravel genetic architecture of complex traits in apple. *BMC Genomics* 14, 393. doi:10.1186/1471-2164-14-393.
- Kusch, S. and Panstruga, R. (2017). mlo-based resistance: An apparently universal 'weapon' to defeat powdery mildew disease. *Molecular Plant-Microbe Interactions: MPMI* 30(3), 179–89. doi:10.1094/MPMI-12-16-0255-CR.
- Labuschagné, I. F., Louw, J. H., Schmidt, K. and Sadie, A. (2002). Genetic variation in chilling requirement in apple progeny. *Journal of the American Society for Horticultural Science* 127(4), 663–72. doi:10.21273/JASHS.127.4.663.

- Le Roux, P.-M. F., Khan, M. A., Broggini, G. A. L., Duffy, B., Gessler, C. and Patocchi, A. (2010). Mapping of quantitative trait loci for fire blight resistance in the apple cultivars 'Florina' and 'Nova Easygro'. *Genome* 53(9), 710–22. doi:10.1139/G10-047
- Legun, K. A. (2015). Club apples: A biology of markets built on the social life of variety. *Economy and Society* 44(2), 293–315. doi:10.1080/03085147.2015.1013743.
- Li, H., Wan, Y., Wang, M., Han, M. and Huo, X. (2015). History, status and prospects of the apple industry in China. *Journal of the American Pomological Society* 69(4), 174–85.
- Liebhard, R., Gianfranceschi, L., Koller, B., Ryder, C. D., Tarchini, R., van de Weg, E. and Gessler, C. (2002). Development and characterisation of 140 new microsatellites in apple (*Malus × domestica* Borkh.). *Molecular Breeding* 10(4), 217–41. doi:10.1023/A:1020525906332.
- Liebhard, R., Koller, B., Patocchi, A., Kellerhals, M., Pfammatter, W., Jermini, M. and Gessler, C. (2003). Mapping quantitative field resistance against apple scab in a 'fiesta' × 'discovery' progeny. *Phytopathology* 93(4), 493–501. doi:10.1094/PHYTO.2003.93.4.493.
- Liu, Z., Bao, D., Liu, D., Zhang, Y., Ashraf, M. A. and Chen, X. (2016). Construction of a genetic linkage map and QTL analysis of fruit-related traits in an F1 Red Fuji × Hongrou apple hybrid. *Open Life Sciences* 11(1). doi:10.1515/biol-2016-0063.
- Liu, J., Ridgway, H. J., & Jones, E. E. (2020). Apple endophyte community is shaped by tissue type, cultivar and site and has members with biocontrol potential against *Neonectria ditissima*. *Journal of Applied Microbiology*, 128(6), 1735–1753. <https://doi.org/10.1111/jam.14587>
- Liu, X., Matsumoto, H., Lv, T., Zhan, C., Fang, H., Pan, Q., Xu, H., Fan, X., Chu, T., Chen, S., Qiao, K., Ma, Y., Sun, L., Wang, Q., & Wang, M. (2023). Phyllosphere microbiome induces host metabolic defence against rice false-smut disease. *Nature Microbiology*, 8(8), 1419–1433. <https://doi.org/10.1038/s41564-023-01379-x>
- Li, P.-D., Zhu, Z.-R., Zhang, Y., Xu, J., Wang, H., Wang, Z., & Li, H. (2022). The phyllosphere microbiome shifts toward combating melanose pathogen. *Microbiome*, 10(1), 56. <https://doi.org/10.1186/s40168-022-01234-x>

Lolle, S., Stevens, D., & Coaker, G. (2020). Plant NLR-triggered immunity: from receptor activation to downstream signaling. *Current Opinion in Immunology*, 62, 99–105. <https://doi.org/10.1016/j.coi.2019.12.007>

Longhi, S., Hamblin, M. T., Trainotti, L., Peace, C. P., Velasco, R. and Costa, F. (2013). A candidate gene based approach validates *Md-PG1* as the main responsible for a QTL impacting fruit texture in apple (*Malus × domestica* Borkh). *BMC Plant Biology* 13, 37. doi:10.1186/1471-2229-13-37.

Luo, X., Wu, W., Liang, Y., Xu, N., Wang, Z., Zou, H., & Liu, J. (2020). Tyrosine phosphorylation of the lectin receptor-like kinase LORE regulates plant immunity. *The EMBO Journal*, 39(4), e102856. <https://doi.org/10.15252/emj.2019102856>

MacKenzie, M., & Iskra, A. J. (2005). The first report of beech bark disease in ohio comes nineteen years after the first report of the initiating scale. *Plant Disease*, 89(2), 203. <https://doi.org/10.1094/PD-89-0203A>

Ma, L., Haile, Z. M., Sabbadini, S., Mezzetti, B., Negrini, F., & Baraldi, E. (2023). Functional characterization of MANNANOSE-BINDING LECTIN 1, a G-type lectin gene family member, in response to fungal pathogens of strawberry. *Journal of Experimental Botany*, 74(1), 149–161. <https://doi.org/10.1093/jxb/erac396>

Malnoy, M., Viola, R., Jung, M. H., Koo, O. J., Kim, S., Kim, J. S., Velasco, R. and Nagamangala Kanchiswamy, C. (2016). DNA-free genetically edited grapevine and apple protoplast using CRISPR/Cas9 ribonucleoproteins. *Frontiers in Plant Science* 7, 1904. doi:10.3389/fpls.2016.01904.

Marini, R. P., Black, B. and Crassweller, R. M. (2009). Performance of ‘golden delicious’ apple on 23 rootstocks at 12 locations: A five-year summary of the 2003 NC-140 dwarf rootstock trial. *Journal of the American Pomological Society* 63(3), 115–27.

Marini, R. P., Black, B., Crassweller, R. M., Domoto, P. A., Hampson, C., Moran, R., Robinson, T., Stasiak, M. and Wolfe, D. (2014). Performance of ‘Golden Delicious’ apple on 23 rootstocks at eight locations: A ten year summary of the 2003 NC-140 dwarf apple rootstock trial. *Journal of the American Pomological Society* 68(2), 54–68.

Marini, R. P., Crassweller, R. M., Autio, W., Moran, R., Robinson, T. L., Cline, J., Wolfe, D. and Parra-Quezada, R. (2017). The interactive effects of early season temperatures, crop density

and rootstock on average fruit weight of 'Golden Delicious' apple. *Acta Horticulturae* 1177(1177), 189–94. doi:10.17660/ActaHortic.2017.1177.26.

Markussen, T., Kruger, J., Schmidt, H. and Dunemann, F. (1995). Identification of PCR-based markers linked to the powdery-mildew-resistance gene *PI1* from *Malus robusta* in cultivated apple. *Plant Breeding* 114(6), 530–4. doi:10.1111/j.1439-0523.1995.tb00850.x.

McClure, K. A., Gardner, K. M., Toivonen, P. M., Hampson, C. R., Song, J., Forney, C. F., DeLong, J., Rajcan, I. and Myles, S. (2016). QTL analysis of soft scald in two apple populations. *Horticulture Research* 3, 16043. doi:10.1038/hortres.2016.43.

McClure, K. A., Gardner, K. M., Douglas, G. M., Song, J., Forney, C. F., DeLong, J., Fan, L., Du, L., Toivonen, P. M. A., Somers, D. J., et al. (2018). A genome-wide association study of apple quality and scab resistance. *The Plant Genome* 11(1). doi:10.3835/plantgenome2017.08.0075.

McCracken, A. R., Berrie, A., Barbara, D. J., Locke, T., Cooke, L. R., Phelps, K., Swinburne, T. R., Brown, A. E., Ellerker, B., & Langrell, S. R. H. (2003). Relative significance of nursery infections and orchard inoculum in the development and spread of apple canker (*Nectria galligena*) in young orchards. *Plant Pathology*, 52(5), 553–566. <https://doi.org/10.1046/j.1365-3059.2003.00924.x>

Meena, M., & Samal, S. (2019). Alternaria host-specific (HSTs) toxins: An overview of chemical characterization, target sites, regulation and their toxic effects. *Toxicology Reports*, 6, 745–758. <https://doi.org/10.1016/j.toxrep.2019.06.021>

Miller, A. J., Matasci, N., Schwaninger, H., Aradhya, M. K., Prins, B., Zhong, G. Y., Simon, C., Buckler, E. S. and Myles, S. (2013). Vitis phylogenomics: Hybridization intensities from a SNP array outperform genotype calls. *PLoS ONE* 8(11), e78680. doi:10.1371/journal.pone.0078680.

Nandi, A., Kachroo, P., Fukushige, H., Hildebrand, D. F., Klessig, D. F., & Shah, J. (2003). Ethylene and jasmonic acid signaling affect the NPR1-independent expression of defense genes without impacting resistance to *Pseudomonas syringae* and *Peronospora parasitica* in the *Arabidopsis ssi1* mutant. *Molecular Plant-Microbe Interactions*, 16(7), 588–599. <https://doi.org/10.1094/MPMI.2003.16.7.588>

N'Diaye, A., van de Weg, W. E., Kodde, L. P., Koller, B., Dunemann, F., Thiermann, M., Tartarini, S., Gennari, F. and Durel, C. E. (2008). Construction of an integrated consensus map of the apple genome based on four mapping populations. *Tree Genetics and Genomes* 4(4), 727–43. doi:10.1007/s11295-008-0146-0.

Ngou, B. P. M., Ding, P., & Jones, J. D. G. (2022). Thirty years of resistance: Zig-zag through the plant immune system. *The Plant Cell*, 34(5), 1447–1478. <https://doi.org/10.1093/plcell/koac041>

Nishitani, C., Hirai, N., Komori, S., Wada, M., Okada, K., Osakabe, K., Yamamoto, T. and Osakabe, Y. (2016). Efficient genome editing in apple Using a CRISPR/Cas9 system. *Scientific Reports* 6, 31481. doi:10.1038/srep31481.

Noiton, D. A. M. and Alspach, P. A. (1996). Founding clones, inbreeding, coancestry, and status number of modern apple cultivars. *Journal of the American Society for Horticultural Science* 121(5), 773–82. doi:10.21273/JASHS.121.5.773.

Norelli, J. L., Jones, A. L. and Aldwinckle, H. S. (2003). Fire blight management in the twenty-first century: using new technologies that enhance host resistance in apple. *Plant Disease* 87(7), 756–65.

Norelli, J. L., Wisniewski, M. and Droby, S. (2014). Identification of a QTL for postharvest disease resistance to *Penicillium expansum* in *Malus sieversii*. *Acta Horticulturae* 1053(1053), 199–203. doi:10.17660/ActaHortic.2014.1053.21.

Norelli, J. L., Wisniewski, M., Fazio, G., Burchard, E., Gutierrez, B., Levin, E. and Droby, S. (2017). Genotyping-by-sequencing markers facilitate the identification of quantitative trait loci controlling resistance to *Penicillium expansum* in *Malus sieversii*. *PLoS ONE* 12(3), e0172949. doi:10.1371/journal.pone.0172949.

Nybom, H., Ahmadi-Afzadi, M., Sehic, J. and Hertog, M. (2013). DNA marker-assisted evaluation of fruit firmness at harvest and post-harvest fruit softening in a diverse apple germplasm. *Tree Genetics and Genomes* 9(1), 279–90. doi:10.1007/s11295-012-0554-z.

Oide, S., Moeder, W., Krasnoff, S., Gibson, D., Haas, H., Yoshioka, K., & Turgeon, B. G. (2006). *NPS6*, encoding a nonribosomal peptide synthetase involved in siderophore-mediated iron metabolism, is a conserved virulence determinant of plant pathogenic ascomycetes. *The Plant Cell*, 18(10), 2836–2853. <https://doi.org/10.1105/tpc.106.045633>

Olivieri, L., Saville, R. J., Gange, A. C., & Xu, X. (2021). Apple endophyte community in relation to location, scion and rootstock genotypes and susceptibility to European canker. *FEMS Microbiology Ecology*, 97(10). <https://doi.org/10.1093/femsec/fiab131>

Pagliarani, G., Dapena, E., Miñarro, M., Denancé, C., Lespinasse, Y., Rat-Morris, E., Troglio, M., Durel, C. E. and Tartarini, S. (2016). Fine mapping of the rosy apple aphid resistance locus *Dp-fl* on linkage group 8 of the apple cultivar 'Florina'. *Tree Genetics and Genomes* 12(3), 56. doi:10.1007/s11295-016-1015-x.

Papp-Rupar, M., Karlstrom, A., Passey, T., Deakin, G., & Xu, X. (2022). The influence of host genotypes on the endophytes in the leaf scar tissues of apple trees and correlation of the endophytes with apple canker (*Neonectria ditissima*) development. *Phytobiomes Journal*. <https://doi.org/10.1094/PBIOMES-10-21-0061-R>

Papp-Rupar, M., Olivieri, L., Saville, R., Passey, T., Kingsnorth, J., Fagg, G., McLean, H., & Xu, X. (2023). From Endophyte Community Analysis to Field Application: Control of Apple Canker (*Neonectria ditissima*) with *Epicoccum nigrum* B14-1. *Agriculture*, 13(4), 809. <https://doi.org/10.3390/agriculture13040809>

Parisi, L., Lespinasse, Y., Guillaumes, J. (1993). A new race of *Venturia inaequalis* virulent to apples with resistance due to the Vf gene. *Phytopathology* 83(5), 533–7. doi:10.1094/Phyto-83-533.

Park, C.-J., Han, S.-W., Chen, X., & Ronald, P. C. (2010). Elucidation of XA21-mediated innate immunity. *Cellular Microbiology*, 12(8), 1017–1025. <https://doi.org/10.1111/j.1462-5822.2010.01489.x>

Patocchi, A., Frei, A., Frey, J. E. and Kellerhals, M. (2009). Towards improvement of marker assisted selection of apple scab resistant cultivars: *Venturia inaequalis* virulence surveys and standardization of molecular marker alleles associated with resistance genes. *Molecular Breeding* 24(4), 337–47. doi:10.1007/s11032-009-9295-6.

Peil, A., Garcia-Libreros, T., Richter, K., Trognitz, F. C., Trognitz, B., Hanke, M.-V. and Flachowsky, H. (2007). Strong evidence for a fire blight resistance gene of *Malus robusta* located on linkage group 3. *Plant Breeding* 126(5), 470–5. doi:10.1111/j.1439-0523.2007.01408.x.

Pessina, S., Pavan, S., Catalano, D., Gallotta, A., Visser, R. G., Bai, Y., Malnoy, M. and Schouten, H. J. (2014). Characterization of the MLO gene family in Rosaceae and gene expression analysis in *Malus domestica*. *BMC Genomics* 15, 618. doi:10.1186/1471-2164-15-618.

Pessina, S., Lenzi, L., Perazzolli, M., Campa, M., Dalla Costa, L., Urso, S., Valè, G., Salamini, F., Velasco, R. and Malnoy, M. (2016a). Knockdown of MLO genes reduces susceptibility to powdery mildew in grapevine. *Horticulture Research* 3, 16016. doi:10.1038/hortres.2016.16.

Pessina, S., Angeli, D., Martens, S., Visser, R. G., Bai, Y., Salamini, F., Velasco, R., Schouten, H. J. and Malnoy, M. (2016b). The knock-down of the expression of *MdMLO19* reduces susceptibility to powdery mildew (*Podosphaera leucotricha*) in apple (*Malus domestica*). *Plant Biotechnology Journal* 14(10), 2033–44. doi:10.1111/pbi.12562.

Pessina, S., Palmieri, L., Bianco, L., Gassmann, J., van de Weg, E., Visser, R. G. F., Magnago, P., Schouten, H. J., Bai, Y., Riccardo Velasco, R., et al. (2017). Frequency of a natural truncated allele of *MdMLO19* in the germplasm of *Malus domestica*. *Molecular Breeding: New Strategies in Plant Improvement* 37(1), 7. doi:10.1007/s11032-016-0610-8.

Phipps, J. B., Robertson, K. R., Rohrer, J. R., & Smith, P. G. (1991). Origins and evolution of subfam. Maloideae (Rosaceae). *Systematic Botany*, 16(2), 303. <https://doi.org/10.2307/2419283>

Pi, L., Zhang, Y., Wang, J., Wang, N., Yin, Z., & Dou, D. (2023). A G-type lectin receptor-like kinase in *Nicotiana benthamiana* enhances resistance to the fungal pathogen *Sclerotinia sclerotiorum* by complexing with CERK1/LYK4. *Phytopathology Research*, 5(1), 27. <https://doi.org/10.1186/s42483-023-00182-0>

Rafiei, V., Vélèz, H., & Tzelepis, G. (2021). The role of glycoside hydrolases in phytopathogenic fungi and oomycetes virulence. *International Journal of Molecular Sciences*, 22(17). <https://doi.org/10.3390/ijms22179359>

Rahman, A., Kuldau, G. A., & Uddin, W. (2014). Induction of salicylic acid-mediated defense response in perennial ryegrass against infection by *Magnaporthe oryzae*. *Phytopathology*, 104(6), 614–623. <https://doi.org/10.1094/PHYTO-09-13-0268-R>

- Robinson, T. L. (2007). Effects of tree density and tree shape on apple orchard performance. *Acta Horticulturae* 732(732), 405–14. doi:10.17660/ActaHortic.2007.732.61.
- Ru, S. (2016). Theoretical and empirical evaluation of efficiency of marker-assisted seedling selection in Rosaceae tree fruit breeding. (Doctoral dissertation). Washington State University.
- Ru, S., Main, D., Evans, K. and Peace, C. (2015). Current applications, challenges, and perspectives of marker-assisted seedling selection in Rosaceae tree fruit breeding. *Tree Genetics and Genomes* 11(1), 8. doi:10.1007/s11295-015-0834-5.
- Sakamoto, Y., Yamada, Y., Sano, Y., Tamai, Y., & Funada, R. (2004). Pathological anatomy of Nectria canker on *Fraxinus mandshurica* var. *japonica*. *IAWA Journal*, 25(2), 165–174. <https://doi.org/10.1163/22941932-90000358>
- Salgado-Salazar, C., Skaltsas, D. N., Phipps, T., & Castlebury, L. A. (2021). Comparative genome analyses suggest a hemibiotrophic lifestyle and virulence differences for the beech bark disease fungal pathogens *Neonectria faginata* and *Neonectria coccinea*. *G3* (Bethesda, Md.), 11(4). <https://doi.org/10.1093/g3journal/jkab071>
- Sansavini, S., Donati, F., Costa, F. and Tartarini, S. (2004). Advances in apple breeding for enhanced fruit quality and resistance to biotic stresses: New varieties for the European market. *Journal of Fruit and Ornamental Plant Research* 12.
- Skytte af Sättra, J., Odilbekov, F., Ingvarsson, P. K., van de Weg, E., & Garkava-Gustavsson, L. (2023). Parametric mapping of QTL for resistance to European canker in apple in 'Aroma' × 'Discovery.' *Tree Genetics & Genomes*, 19(2), 12. <https://doi.org/10.1007/s11295-023-01587-w>
- Spengler, R. N. (2019). Origins of the apple: the role of megafaunal mutualism in the domestication of *Malus* and Rosaceous trees. *Frontiers in Plant Science*, 10, 617. <https://doi.org/10.3389/fpls.2019.00617>
- Stankiewicz-Kosyl, M., Pitera, E. and Gawronski, S. W. (2005). Mapping QTL involved in powdery mildew resistance of the apple clone U 211. *Plant Breeding* 124(1), 63–6.
- Stephens, C., Hammond-Kosack, K. E., & Kanyuka, K. (2022). WAKsing plant immunity, waning diseases. *Journal of Experimental Botany*, 73(1), 22–37. <https://doi.org/10.1093/jxb/erab422>

Sun, X., Jiao, C., Schwaninger, H., Chao, C. T., Ma, Y., Duan, N., Khan, A., Ban, S., Xu, K., Cheng, L., Zhong, G.-Y., & Fei, Z. (2020). Phased diploid genome assemblies and pan-genomes provide insights into the genetic history of apple domestication. *Nature Genetics*, 52(12), 1423–1432. <https://doi.org/10.1038/s41588-020-00723-9>

Sun, Y., Qiao, Z., Muchero, W., & Chen, J.-G. (2020). Lectin Receptor-Like Kinases: The Sensor and Mediator at the Plant Cell Surface. *Frontiers in Plant Science*, 11, 596301. <https://doi.org/10.3389/fpls.2020.596301>

Tan, Y., Shen, F., Chen, R., Wang, Y., Wu, T., Li, T., Xu, X., Han, Z. and Zhang, X. (2017a). Candidate genes associated with resistance to Valsa canker identified via quantitative trait loci in apple. *Journal of Phytopathology* 165(11–12), 848–57.

Tan, Y., Lv, S., Liu, X., Gao, T., Li, T., Wang, Y., Wu, T., Zhang, X., Han, Y., Korban, S. S., et al. (2017b). Development of high-density interspecific genetic maps for the identification of QTLs conferring resistance to *Valsa ceratosperma* in apple. *Euphytica* 213(1), 10. doi:10.1007/s10681-016-1790-3.

Tartarini, S., Sansavini, S., Vinatzer, B., Gennari, F. and Domizi, C. (2000). Efficiency of marker assisted selection (MAS) for the *Vf* scab resistance gene. *Acta Horticulturae* 538, 549–52.

Thomas, E., Noar, R. D., & Daub, M. E. (2021). A polyketide synthase gene cluster required for pathogenicity of *Pseudocercospora fijiensis* on banana. *Plos One*, 16(10), e0258981. <https://doi.org/10.1371/journal.pone.0258981>

Thomma, B. P., Eggermont, K., Penninckx, I. A., Mauch-Mani, B., Vogelsang, R., Cammue, B. P., & Broekaert, W. F. (1998). Separate jasmonate-dependent and salicylate-dependent defense-response pathways in Arabidopsis are essential for resistance to distinct microbial pathogens. *Proceedings of the National Academy of Sciences of the United States of America*, 95(25), 15107–15111. <https://doi.org/10.1073/pnas.95.25.15107>

Thomma, B. P. H. J., Nürnberger, T., & Joosten, M. H. A. J. (2011). Of PAMPs and effectors: the blurred PTI-ETI dichotomy. *The Plant Cell*, 23(1), 4–15. <https://doi.org/10.1105/tpc.110.082602>

Toruño, T. Y., Stergiopoulos, I., & Coaker, G. (2016). Plant-Pathogen Effectors: Cellular Probes Interfering with Plant Defenses in Spatial and Temporal Manners. *Annual Review of Phytopathology*, 54, 419–441. <https://doi.org/10.1146/annurev-phyto-080615-100204>

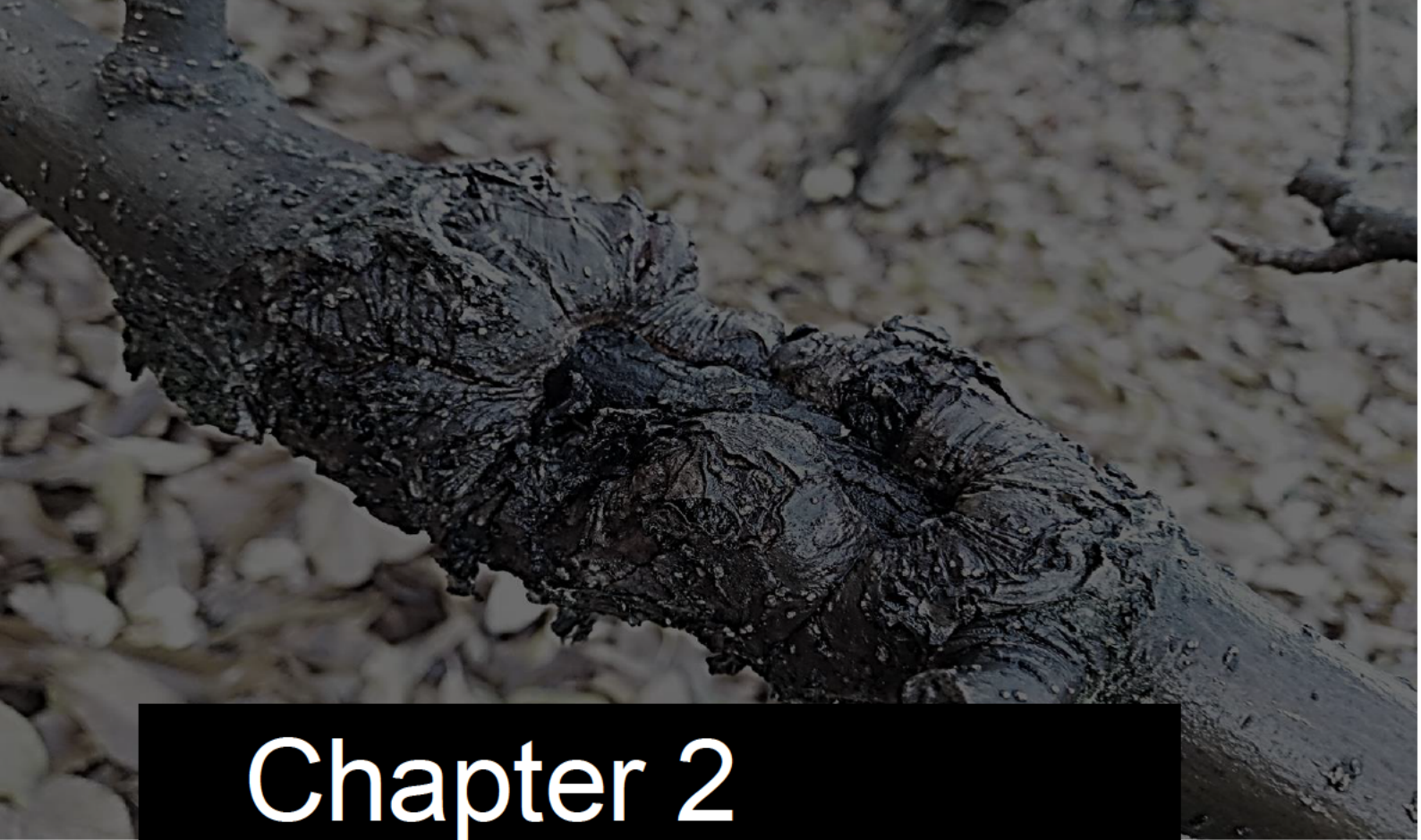
- Trivedi, P., Leach, J. E., Tringe, S. G., Sa, T., & Singh, B. K. (2020). Plant-microbiome interactions: from community assembly to plant health. *Nature Reviews. Microbiology*, 18(11), 607–621. <https://doi.org/10.1038/s41579-020-0412-1>
- Tsuda, K., & Katagiri, F. (2010). Comparing signaling mechanisms engaged in pattern-triggered and effector-triggered immunity. *Current Opinion in Plant Biology*, 13(4), 459–465. <https://doi.org/10.1016/j.pbi.2010.04.006>
- Urrestarazu, J., Muranty, H., Denancé, C., Leforestier, D., Ravon, E., Guyader, A., Guisnel, R., Feugey, L., Aubourg, S., Celton, J. M., et al. (2017). Genome-wide association mapping of flowering and ripening periods in apple. *Frontiers in Plant Science* 8, 1923. doi:10.3389/fpls.2017.01923.
- Vaillancourt, L. J. and Hartman, J. R. (2000). Apple scab. Plant Health Instructor.
- van de Weg, W. E. (1989). Screening for resistance to *Nectria galligena* Bres. in cut shoots of apple. *Euphytica* 42(3), 233–40. doi:10.1007/BF00034459.
- van de Weg, E., Di Guardo, M., Jansch, M., Socquet-Juglard, D., Costa, F., Baumgartner, I., Broggini, G. A. L., Kellerhals, M., Troggio, M., Laurens, F., et al. (2018). Epistatic fire blight resistance QTL alleles in the apple cultivar ‘Enterprise’ and selection X-6398 discovered and characterized through pedigree-informed analysis. *Molecular Breeding* 38(1), 5. doi:10.1007/s11032-017-0755-0.
- Cvan der Burgh, A. M., & Joosten, M. H. A. J. (2019). Plant immunity: thinking outside and inside the box. *Trends in Plant Science*, 24(7), 587–601. <https://doi.org/10.1016/j.tplants.2019.04.009>
- van Nocker, S. and Gardiner, S. E. (2014). Breeding better cultivars, faster: Applications of new technologies for the rapid deployment of superior horticultural tree crops. *Horticulture Research* 1, 14022. doi:10.1038/hortres.2014.22.
- Velasco, R., Zharkikh, A., Affourtit, J., Dhingra, A., Cestaro, A., Kalyanaraman, A., Fontana, P., Bhatnagar, S. K., Troggio, M., Pruss, D., et al. (2010). The genome of the domesticated apple (*Malus × domestica* Borkh.). *Nature Genetics* 42(10), 833–9. doi:10.1038/ng.654.

- Verma, S. (2014). A predictive genetic knowledge for apple 'fresh sensation' provides information to increase breeding efficiency in Washington. (Doctoral dissertation). Available from ProQuest Dissertations and Theses database. (UMI No. 3628891).
- Vinatzer, B. A., Patocchi, A., Tartarini, S., Gianfranceschi, L., Sansavini, S. and Gessler, C. (2004). Isolation of two microsatellite markers from BAC clones of the *Vf* scab resistance region and molecular characterization of scab-resistant accessions in *Malus* germplasm. *Plant Breeding* 123(4), 321–6. doi:10.1111/j.1439-0523.2004.00973.x.
- Walter, M., Glaister, M. K., Clarke, N. R., Lutz, H. V., Eld, Z., & Amponsah, N. T. (2015). Are shelter belts potential inoculum sources for *Neonectria ditissima* apple tree infections? *New Zealand Plant Protection*, 240 227–240.
- Weber, R. W. S. (2014). Biology and control of the apple canker fungus *Neonectria ditissima* (syn. *N. galligena*) from a Northwestern European perspective. *Erwerbs-Obstbau* 56(3), 95–107. doi:10.1007/s10341-014-0210-x.
- Weber, R. W. S., & Dralle, N. (2013). Fungi Associated with Blossom-End Rot of Apples in Germany. *European Journal of Horticultural Science*, 78, 97–105.
- Wenneker, M., de Jong, P. F., Joosten, N. N., Goedhart, P. W., & Thomma, B. P. H. J. (2017). Development of a method for detection of latent European fruit tree canker (*Neonectria ditissima*) infections in apple and pear nurseries. *European Journal of Plant Pathology*, 148(3), 631–635. <https://doi.org/10.1007/s10658-016-1115-3>
- Wen, T., Xie, P., Penton, C. R., Hale, L., Thomashow, L. S., Yang, S., Ding, Z., Su, Y., Yuan, J., & Shen, Q. (2022). Specific metabolites drive the deterministic assembly of diseased rhizosphere microbiome through weakening microbial degradation of autotoxin. *Microbiome*, 10(1), 177. <https://doi.org/10.1186/s40168-022-01375-z>
- Zhan, C., Matsumoto, H., Liu, Y., & Wang, M. (2022). Pathways to engineering the phyllosphere microbiome for sustainable crop production. *Nature Food*, 3(12), 997–1004. <https://doi.org/10.1038/s43016-022-00636-2>
- Zhang, L., Hu, J., Han, X., Li, J., Gao, Y., Richards, C. M., ... & Cong, P. (2019). A high-quality apple genome assembly reveals the association of a retrotransposon and red fruit colour. *Nature communications*, 10(1), 1494.

Zhang, L., Morales-Briones, D. F., Li, Y., Zhang, G., Zhang, T., Huang, C. H., ... & Ma, H. (2023). Phylogenomics insights into gene evolution, rapid species diversification, and morphological innovation of the apple tribe (Maleae, Rosaceae). *New Phytologist*, 240(5), 2102-2120.

Zhu, Y. and Barritt, B. H. (2008). *Md-ACS1* and *Md-ACO1* genotyping of apple (*Malus × domestica* Borkh.) breeding parents and suitability for marker-assisted selection. *Tree Genetics and Genomes* 4(3), 555–62. doi:10.1007/s11295-007-0131-z.

Ziya Motalebipour, E., Kafkas, S., Özongun, Ş. and Atay, A. N. (2015). Construction of dense genetic linkage maps of apple cultivars Kaşel-41 and Williams' Pride by simple sequence repeat markers. *Turkish Journal of Agriculture and Forestry = Turk tarim ve ormancilik dergisi* 39, 967–75.



Chapter 2

Identification of novel genetic regions associated with resistance to European canker in apple

This chapter describes the identification of resistance QTL to *Neonectria ditissima* through a pedigree-based analysis in a population consisting of apple germplasm relevant for modern breeding programmes. Several phenotyping methods were used to determine the level of resistance of the individuals in the multiparental population. Furthermore, phenotypic data from a biparental population derived from a cross between 'Golden Delicious' x 'M9' was used to validate the effect of SNP-haplotypes within the QTL.

RESEARCH ARTICLE

Open Access



Identification of novel genetic regions associated with resistance to European canker in apple

Amanda Karlström^{1,2*} , Antonio Gómez-Cortecero¹, Charlotte F. Nellist¹ , Matthew Ordidge² , Jim M. Dunwell²  and Richard J. Harrison³ 

Abstract

Background: European canker, caused by the fungal pathogen *Neonectria ditissima*, is an economically damaging disease in apple producing regions of the world – especially in areas with moderate temperatures and high rainfall. The pathogen has a wide host range of hardwood perennial species, causing trunk cankers, dieback and branch lesions in its hosts. Although apple scion germplasm carrying partial resistance to the disease has been described, little is still known of the genetic basis for this quantitative resistance.

Results: Resistance to *Neonectria ditissima* was studied in a multiparental population of apple scions using several phenotyping methods. The studied population consists of individuals from multiple families connected through a common pedigree. The degree of disease of each individual in the population was assessed in three experiments: artificial inoculations of detached dormant shoots, potted trees in a glasshouse and in a replicated field experiment. The genetic basis of the differences in disease was studied using a pedigree-based analysis (PBA). Three quantitative trait loci (QTL), on linkage groups (LG) 6, 8 and 10 were identified in more than one of the phenotyping strategies. An additional four QTL, on LG 2, 5, 15 and 16 were only identified in the field experiment. The QTL on LG2 and 16 were further validated in a biparental population. QTL effect sizes were small to moderate with 4.3 to 19% of variance explained by a single QTL. A subsequent analysis of QTL haplotypes revealed a dynamic response to this disease, in which the estimated effect of a haplotype varied over the field time-points.

Conclusions: This study describes the first identified QTL associated with resistance to *N. ditissima* in apple scion germplasm. The results from this study show that QTL present in germplasm commonly used in apple breeding have a low to medium effect on resistance to *N. ditissima*. Hence, multiple QTL will need to be considered to improve resistance through breeding.

Keywords: *Neonectria ditissima*, European canker, *Malus x domestica*, Apple, Disease resistance

Background

European apple canker, caused by the fungal pathogen *Neonectria ditissima*, infects a wide range of hosts, including apple (*Malus* spp.), pear (*Pyrus* spp.) and a

range of other broad-leaved perennial species [1, 2]. The disease is widespread in apple orchards in regions with temperate and wet climates [3, 4].

N. ditissima is foremost a wood pathogen, which enters the host through natural or artificial wounds such as leaf scars, pruning cuts or lenticels and cracks in the bark [3]. The disease symptoms are trunk cankers, branch lesions and die-back. In severe cases the lesions expand to girdle the whole main trunk of the

*Correspondence: Amanda.Karlstrom@nlab.com

¹ NIAB, Lawrence Weaver Rd, Cambridge CB3 0LE, UK
Full list of author information is available at the end of the article



© The Author(s) 2022. **Open Access** This article is licensed under a Creative Commons Attribution 4.0 International License, which permits use, sharing, adaptation, distribution and reproduction in any medium or format, as long as you give appropriate credit to the original author(s) and the source, provide a link to the Creative Commons licence, and indicate if changes were made. The images or other third party material in this article are included in the article's Creative Commons licence, unless indicated otherwise in a credit line to the material. If material is not included in the article's Creative Commons licence and your intended use is not permitted by statutory regulation or exceeds the permitted use, you will need to obtain permission directly from the copyright holder. To view a copy of this licence, visit <http://creativecommons.org/licenses/by/4.0/>. The Creative Commons Public Domain Dedication waiver (<http://creativecommons.org/publicdomain/zero/1.0/>) applies to the data made available in this article, unless otherwise stated in a credit line to the data.

tree and kill all branches above the point of the canker [5].

European canker control strategies are removal of infected wood through pruning and the limitation of new infections through the application of fungicides when wound incidence is high [1, 6]. Genetic variation in *N. ditissima* resistance has been documented in commercial apple varieties of *Malus x domestica*, wild species of *Malus* as well as in apple rootstocks [5, 7–9]. Previous studies of the inheritance of canker resistance in apple progenies demonstrate that the resistance is inherited quantitatively [7], though QTLs of major effect might be present too [10]. The relative levels of resistance of mature trees of parental cultivars correspond well with the relative levels of juvenile full-sib families, indicating that juvenile material may be used in inheritance studies [10]. The crab apple accession *Malus robusta* ‘Robusta 5’ has shown tolerance to infection by *N. ditissima* in multiple studies [7, 11]. Bus et al. [12] genetically mapped a QTL for disease incidence from ‘Robusta 5’ in a bi-parental cross between the apple rootstock ‘M9’ x ‘Robusta 5’. In the study, a single medium effect size QTL on linkage group 14 was identified by mapping the disease incidence in segregating progeny genotyped with simple-sequence repeats (SSR)-markers. This QTL accounted for around 40% of the variance in disease, but the variance explained was dependent upon the phenotyping method [12]. Although there are commercial scion cultivars tolerant to apple canker, there is no published information on which chromosomal regions control the quantitative resistance found in this germplasm.

The response of plants to disease has shown temporal variation in several plant-microbe interactions [13–17]. The dynamic QTL methods in these studies analyses the phenotypic variation at different times during infection, whereas conventional methods would analyse the cumulative disease phenotype at the end. In these studies, resistance QTL were uniquely identified at different stages of disease or plant development, indicating that the genes controlling the response to disease have temporal expression patterns. This type of, so called, dynamic response has not been reported for interactions with wood pathogens.

In the present study, the genetic basis of resistance to *N. ditissima* in apple scion germplasm was studied through QTL mapping in a multiparental population using a pedigree-based Bayesian analysis [18]. Three phenotyping strategies (field, potted trees and shoots) were used to determine whether rapid phenotyping methods can replace field experiments for QTL discovery.

Results

Phenotypic analysis

The multiparental population showed a normal distribution of disease levels to European canker in all measured phenotypes, apart from %HTA and %CB which was skewed towards 100%. Disease distribution in individual families is shown in Suppl. Fig. 1A–H. Mean values for each family and European canker phenotype are shown in Supplementary Table 1. A comparison of phenotypes for parental apple genotypes and a standard set of cultivars with known resistance to European canker is shown in Supplementary Fig. 2.

All genotypes exhibited disease symptoms upon infection, hence there was no evidence of complete resistance to this disease in the genotypes studied. The overall infection success across all inoculation points of the artificial inoculations was >95% in all three phenotyping experiments.

The broad sense heritability (H^2) from the different phenotyping events and measurements is shown in Supplementary Table 2 and correlations between these are shown in Fig. 1. The canker phenotypes recorded from detached shoots and potted trees resulted in lower estimates of heritability than data from the field experiment, 0.16, 0.46 and 0.54–0.76, respectively (Suppl. Table 2).

Within the field experiment, the Pearson correlation for genotypic BLUEs of canker lesion size was relatively low between 5 and 11 months post inoculation (mpi, $r = 0.45$, $p < 0.001$). The highest correlation was observed between the two later time-points (8 and 11 mpi, $r = 0.78$, $p < 0.001$). The BLUEs from the potted tree experiment had a low correlation with the susceptibility in the other phenotyping experiments (see Fig. 1). The shoot experiment had a higher correlation to the early stage of field infection at 5 mpi ($r = 0.44$, $p < 0.001$), compared to the two later time-points (Fig. 1A). Canker Index (CI) had a moderate correlation to percent cankered branches (%CB, $r = 0.42$, $p < 0.001$) but was not correlated to the other phenotypes. The relationship between different European canker phenotypes is also visualised in the biplot for the correlation matrix PCA (Fig. 1B). The first and second principal component from the PCA explained 41.6 and 17.3% of the variance, respectively (Suppl. Fig. 3). The loadings from field 5, 8, 11 mpi, shoot and potted tree experiment are clustered together, indicating a high degree of correlation between these variables for the two first principal components. Loadings from these variables also show a positive correlation to PC1 ($r = 0.19$ – 0.43), whereas percent healthy tree area (%HTA) is negatively correlated to the same PC ($r = -0.42$). Nevertheless, the potted tree data had the highest correlation ($r = 0.84$)

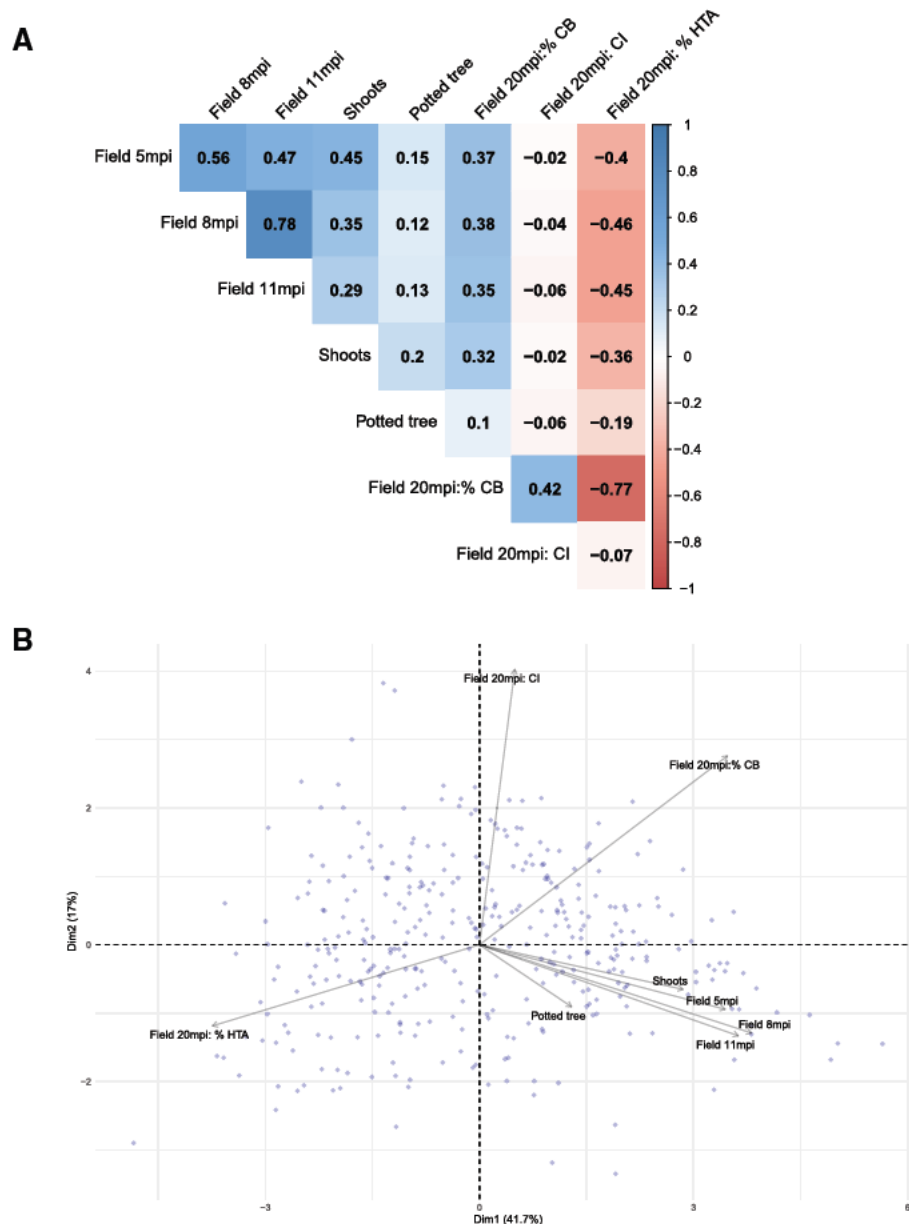


Fig. 1 Correlation matrix and principal component analysis (PCA) of phenotypic susceptibility data to European canker in a multiparental population of apple. **a** Correlation matrix showing Pearson's correlation coefficient of phenotype data. **b** PCA biplot for the first and second component. The length of the arrows approximates the variance of the variables, whereas the angles between them (cosine) approximate their correlations

to PC3, to which 12% of the total variation was attributed. The CI loading was largely uncorrelated to PC1 ($r = 0.05$) but had a strong negative correlation to PC2 ($r = -0.70$).

A correlation between %HTA and the total number of branches per tree was observed ($r = 0.27$, data not shown), A similar negative correlation was found for %CB ($r = -0.28$). Surprisingly, there was also a weak

positive correlation between 5 mpi and number of branches ($r = 0.17$).

Identification of QTL associated with resistance

The Bayesian QTL mapping analysis revealed a total of seven linkage groups involved in the response to European canker (Fig. 2 and Table 1). There was positive ($2\lnBF > 2$) or strong evidence ($2\lnBF > 5$) for a QTL in

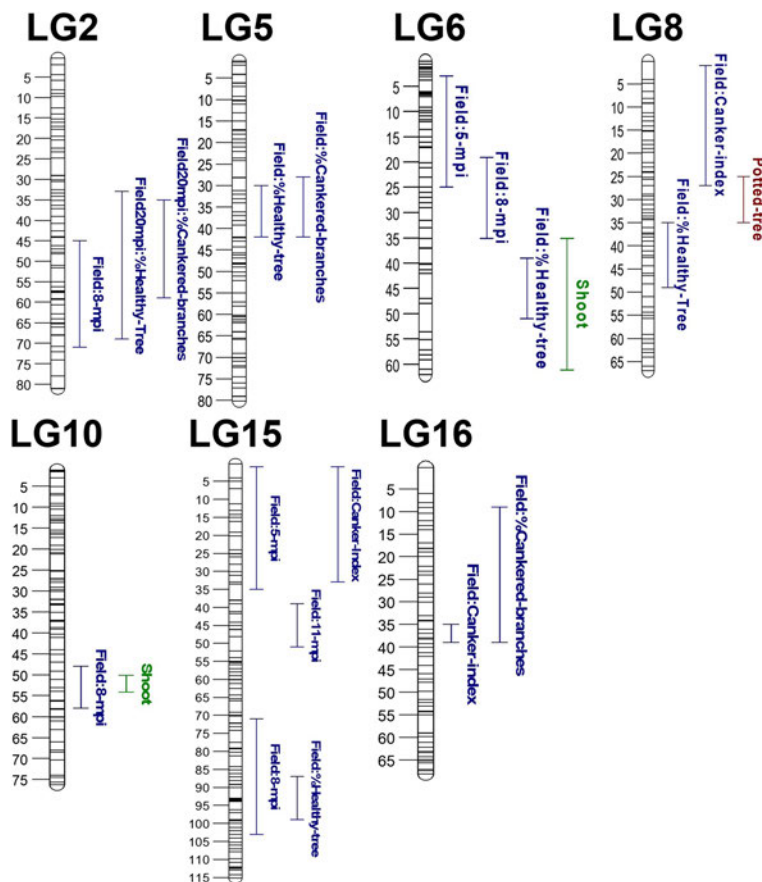


Fig. 2 QTL regions identified to be associated with resistance to European apple canker. The figure shows QTL intervals from each measured phenotype. Different colours indicate distinct phenotyping experiments

more than one phenotyping experiment for three of the LGs: 6, 8 and 10. For the remaining four LGs there was strong evidence for a QTL in one of the phenotyping events at the linkage group level. The variance attributed to individual QTL was small to moderate with effect sizes of 5 to 19%.

There was strong evidence for a QTL on LG6 in both the shoot experiment and at 5 mpi in the field ($2\ln BF = 9.4$ and 7.3 , respectively). There was also positive evidence ($2\ln BF > 2$) for a QTL on this linkage group at 8 mpi (Table 1). However, two separate QTL regions on LG6 were indicated, depending on the analysed phenotype (Fig. 2). There was no positive evidence for the presence of more than one QTL in the output from FlexQTL. The FlexQTL analysis showed that QTL on LG6 had a larger effect at the earlier stage of field infection, as the QTL explained 15% of the variation in shoots and at 5 mpi, but less than 7% at later field time-points.

A QTL on LG8 was identified in data for %HTA ($2\ln BF = 2.1$), CI ($2\ln BF = 5.6$), and the potted tree experiment ($2\ln BF = 2.1$). Hence, this QTL was found

in more than one type of experiment. Depending on phenotype, the variance attributed to this QTL ranged between 9.3–15%. A third QTL, located on LG10, was positively identified using two types of phenotyping methods. There was positive evidence for this QTL in the field 8 mpi and in the shoot experiment ($2\ln BF = 2.5$ and 2.1 , respectively).

A QTL on LG5 was positively identified in data from the field experiment at 20 mpi but was not identified at earlier time-points nor in the other phenotyping experiments. There was strong evidence ($2\ln BF = 7.9$) for a QTL on LG5 for %HTA and positive evidence ($2\ln BF = 4.4$) for %CB. Hence, this QTL was only identified after a prolonged period of infection.

The variance attributed to QTL on LG15 was the highest among all discovered QTL, with an effect size of 19 and 17.5% at 8 and 11 mpi respectively. Nevertheless, the effect of this QTL was much lower at 5 mpi (5.5%). Three regions on LG15 were identified to have an association with the susceptibility to canker depending on phenotype (Fig. 2). However, there was no positive

Table 1 Summary of the results from the quantitative trait loci (QTL) mapping of resistance to European canker with the FlexQTL software. QTL regions reported consist of successive 2-cM bins with two times the natural log of Bayes factors (2lnBF) greater than 2

LG	Phenotyping event	2lnBF for whole LG	QTL region (cM)	QTL mode (cM)	Estimated effect (%)
2	Field 5 mpi ^a	< 2	–	–	–
	Field 8 mpi	6.5	45–71	61	7.9
	Field 11 mpi	< 2	–	–	–
	Field 20 mpi - % Healthy tree	4.7	33–69	49	7.1
	Field 20 mpi - % Cankered branches	4.8	35–59	43	7.1
	Field 20 mpi - Canker Index	< 2	–	–	–
	Shoot	< 2	–	–	–
	Potted tree	< 2	–	–	–
	Consensus region	–	45–57	–	–
5	Field 5 mpi	< 2	–	–	–
	Field 8 mpi	< 2	–	–	–
	Field 11 mpi	< 2	–	–	–
	Field 20 mpi - % Healthy tree	7.9	30–42	36	6.1
	Field 20 mpi - % Cankered branches	3.5	28–42	34	4.3
	Field 20 mpi - Canker Index	< 2	–	–	–
	Shoot	< 2	–	–	–
	Potted tree	< 2	–	–	–
	Consensus region	–	30–42	–	–
6	Field 5 mpi	7.3	3–25	13	15.0
	Field 8 mpi	2.1	19–35	29	6.2
	Field 11 mpi	< 2	–	–	–
	Field 20 mpi - % Healthy tree	< 2	–	–	–
	Field 20 mpi - % Cankered branches	< 2	–	–	–
	Field 20 mpi - Canker Index	< 2	–	–	–
	Shoot	9.4	35–61	37	14.7
	Potted tree	< 2	–	–	–
	Consensus region	–	19–25	–	–
8	Field 5 mpi	< 2	–	–	–
	Field 8 mpi	< 2	–	–	–
	Field 11 mpi	< 2	–	–	–
	Field 20 mpi - % Healthy tree	2.1	35–49	35	7.1
	Field 20 mpi - % Cankered branches	< 2	–	–	–
	Field 20 mpi - Canker Index	2.2	1–27	7.0	5.0
	Shoot	< 2	–	–	–
	Potted tree	2.1	25–35	29	15.0
	Consensus region	–	25–27	–	–
10	Field 5 mpi	< 2	–	–	–
	Field 8 mpi	2.5	48–58	50	5.0
	Field 11 mpi	< 2	–	–	–
	Field 20 mpi - % Healthy tree	< 2	–	–	–
	Field 20 mpi - % Cankered branches	< 2	–	–	–
	Field 20 mpi - Canker Index	< 2	–	–	–
	Shoot	2.1	50–54	52	12.9
	Potted tree	< 2	–	–	–
	Consensus region	–	50–54	–	–

Table 1 (continued)

LG	Phenotyping event	2lnBF for whole LG	QTL region (cM)	QTL mode (cM)	Estimated effect (%)
15	Field 5 mpi	2.1	1–35	27	5.5
	Field 8 mpi	5.7	71–103	81	19.0
	Field 11 mpi	4.4	39–51	45	17.5
	Field 20 mpi - % Healthy tree	2.2	87–99	95	17.3
	Field 20 mpi - % Cankered branches	<2	–	–	–
	Field 20 mpi - Canker Index	2.5	1–33	13.0	5.0
	Shoot	<2	–	–	–
	Potted tree	<2	–	–	–
	Consensus region	–	1–39, 87–99	–	–
16	Field 5 mpi	<2	–	–	–
	Field 8 mpi	<2	–	–	–
	Field 11 mpi	<2	–	–	–
	Field 20 mpi - % Healthy tree	<2	–	–	–
	Field 20 mpi - % Cankered branches	6	7–37	29	10.0
	Field 20 mpi - Canker Index	4.3	35–47	43.0	5.0
	Shoot	<2	–	–	–
	Potted tree	<2	–	–	–
	Consensus region	–	35–37	–	–

^a mpi Months post inoculation

evidence for the presence of more than one QTL in the analysis.

A further two QTL were identified on LG2 and LG16. The QTL analysis did not discern any obvious temporal patterns in effect sizes for these QTL.

Haplotype analysis

A haplotype analysis was conducted to understand which haplotypes contributed to resistance to *N. ditissima* at different stages of infection. The effect of all haploblocks within the QTL regions was tested on lesion size data at 5, 8 and 11 mpi in the field. The haploblocks (HB) with the most significant effect on canker lesion size from each QTL region and the number of unique haplotypes within the multiparental population are shown in Supplementary Table 3. Haplotype alleles for each HB are shown in Supplementary Table 4.

Figure 3 shows the estimated percent deviation from the mean of resistant and susceptible/neutral haploblock alleles for the three time-points. Haplotypes were only included if they were present in a parent segregating for European canker resistance at that QTL locus, as haplotype effects from non-segregating parents could not be reliably estimated. A total of 33 haploblock alleles were present in segregating parents across all seven genetic regions.

The estimated effects of some haplotypes varied over the three time-points (Fig. 3). For HB5, the percent deviation from the mean more than doubled over the assessed time-period for two out of three resistant haplotypes (Fig. 3). Furthermore, the allele HB15-shared-R2 had a susceptible effect on lesion size at 5 mpi but a resistant effect at 11 mpi, with –8 and –11% deviation from mean for individuals with one or two copies, respectively, of the haplotype. The resistant alleles HB16-Aroma-R and HB16-Sel1-R also showed increased effects on resistance with time.

The haplotype alleles with the largest negative effects on lesion size were found within HB2, HB6, HB15 and HB16 (Fig. 3). The effect of HB6-shared-R, which ranged between –7.4 to –13.5%, was similar across time-points and for individuals carrying one or two copies of the allele. This haplotype was inherited from four of the parents, Gala, Golden Delicious, EM-Selection-2 and EM-Selection-4 and could be traced back to the unknown parent of ‘Golden Delicious’. The origin of the haplotype HB15-shared-R was traced back to ‘Golden Delicious’ and ‘Jonathan’. The resistant effect of HB15-shared-R increased with time and was estimated to reduce lesion size with –8 and –12% at 11 mpi for individuals with one or two copies, respectively, of the haplotype. HB15-shared-R segregated in two of the parents, Golden

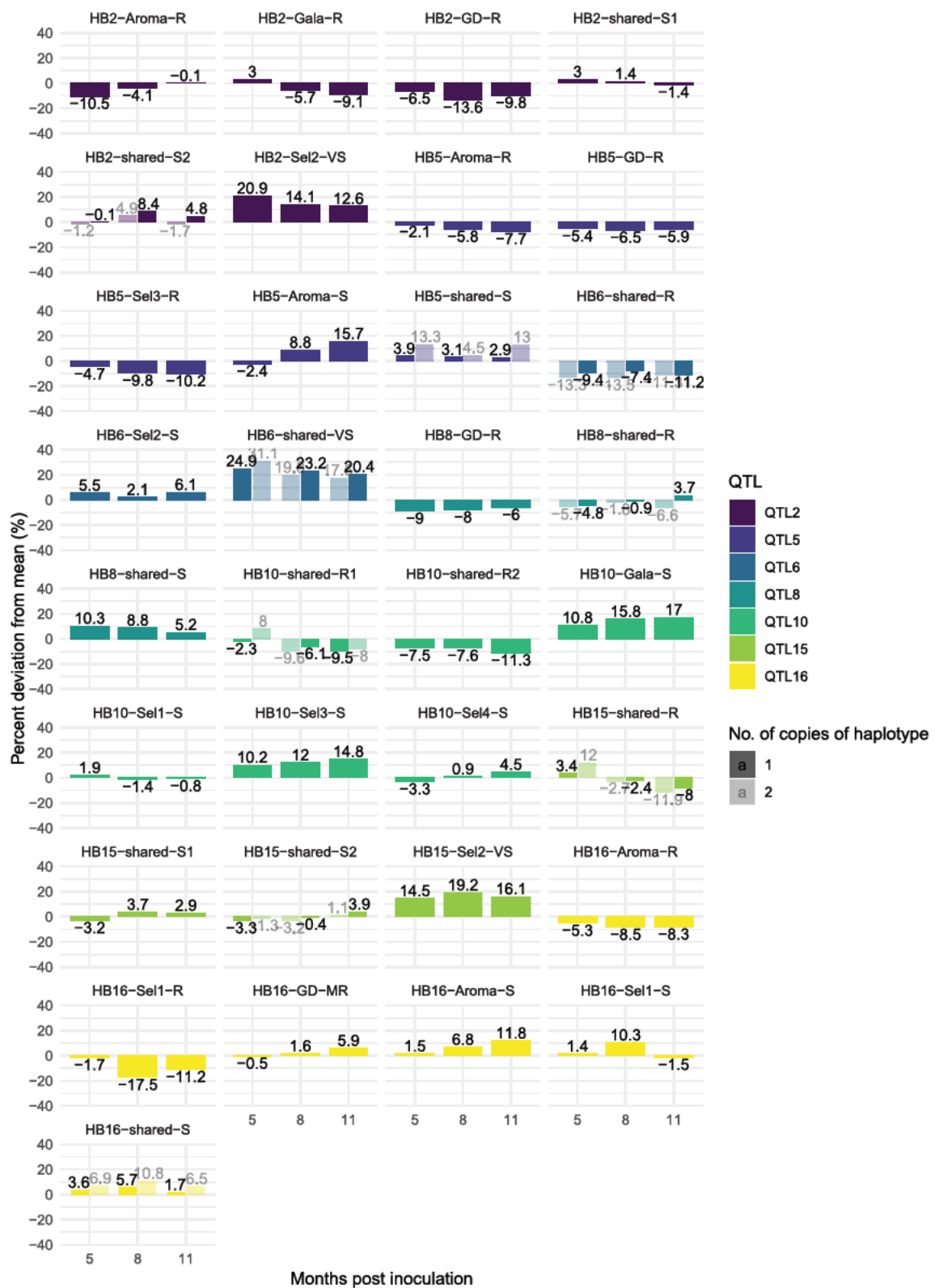


Fig. 3 Estimated percent deviation from mean lesion size at 5, 8 and 11 months post inoculation for individuals with 1 or 2 copies of haplotypes. The haplotypes shown are present in at least one parent that segregates for resistance to European apple canker at the QTL-locus. Haplotypes denoted R have a resistant effect while S and VS have susceptible and very susceptible effects

Delicious and EM-Selection-4. This haplotype was also present in a third parent (EM-Selection-1), which had two alleles with a resistant effect on lesion size at this locus.

Three haploblock alleles were associated with large increases in lesion size: HB2-Sel2-VS, HB6-shared-VS and HB15-Sel3-VS (Fig. 3). Individuals heterozygous for HB2-Sel2-VS had an estimated +13–21% increase in lesion size, depending on time-point. The origin of this haplotype could not be traced further back than to the unreleased selection ‘EM002’ due to the lack of available material in the germplasm collection (Fig. 5). HB6-shared-VS was associated with an up to +31% increase in lesion size compared to the mean (Fig. 3). The allele was inherited from the three parents Gala, EM-Selection-3 and EM-Selection-4, of which EM-Selection-3 was homozygous for the haplotype. Hence, HB6-shared-VS only segregated in the family MDX061. This allele was present in many of the founding cultivars, including ‘Delicious’, ‘Jonathan’, and ‘Ingrid-Marie.’

Validation of haplotype effects in a biparental population

A significant haplotype-trait association was identified for two of the seven QTL regions in progeny from a ‘Golden Delicious’ x ‘M9’ cross. Based on the results from the multiparental population, QTL on five LG were expected to segregate in ‘Golden Delicious’: LG 2, 5, 8, 15 and 16. The segregation of resistance loci in ‘M9’ was not previously known. Mean Area Under Disease Progression Curve (AUDPC) and disease distribution for haploblock alleles for which ‘Golden Delicious’ segregates are shown in supplementary Table 5 and Fig. 4, respectively. The distribution of disease phenotypes in the ‘Golden Delicious’ x ‘M9’ progeny is shown in Supplementary Fig. 4.

The haplotype ‘HB2-shared-S2’ was inherited from both parents and was associated with an increase in AUDPC (Fig. 4). There was a significant effect of this haplotype ($p = 0.02$) in data from the detached shoot experiment. Additionally, the haplotype ‘HB16-GD-MR’ was confirmed to be associated with resistance to European canker in the detached shoot experiment ($p = 0.017$). Individuals with one copy of this allele had a reduction in mean AUDPC with 28 and 118 units in the potted tree and shoot experiment, respectively. No haploblock alleles had a significant effect on AUDPC in the potted tree experiment.

Progeny with the allele ‘HB8-GD-R’ had a reduced mean AUDPC with 94, and 22 units, respectively, in the potted tree and shoot experiment. Nevertheless, the effect of this haplotype was non-significant ($p = 0.058$).

Surprisingly, progeny with the haplotype ‘HB5-GD-R’ had a higher mean AUDPC compared to individuals that inherited the susceptible allele ‘HB6-shared-S’ in both experiments (Suppl. Table 5).

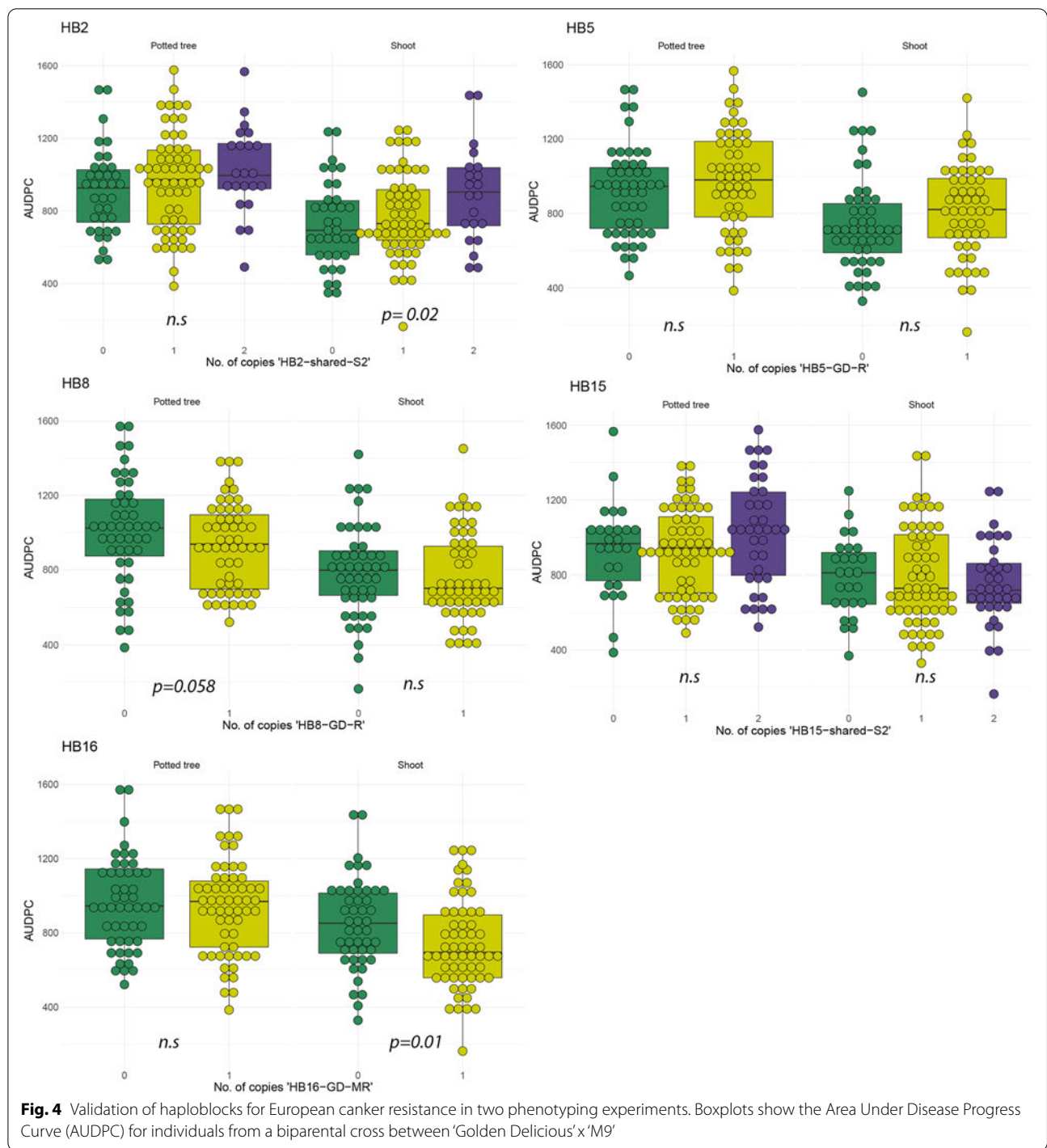
The proportion of variation attributed to significant haplotypes was low, with 4.5–5.4% variance explained by single haplotypes in the detached shoot experiment. The total variance due to significant haplotypes was 10% in this experiment.

Discussion

Identified resistance loci widely distributed in apple scion germplasm

Seven linkage groups were shown to be associated with the level of resistance to European apple canker in a multiparental scion population. Three of these QTL were identified in more than one experiment using the same population: the QTLs on LG6, LG8 and LG10. Furthermore, the effect of the most significant haploblocks from two of the QTL-regions (HB2 and HB16) were validated in separate experiments with a biparental population derived from a cross between ‘Golden Delicious’ and ‘M9’. Thus, five out of the seven QTL-regions were confirmed in more than one experiment. All the identified QTL had small to moderate effects on disease expression. The effects of the identified QTL exhibited two different patterns: increased effect with time and stable effects across time-points. The phenotypes from the potted tree and shoot experiment were considered to mimic early-stage disease responses, as these experiments ended within a few months after commencement.

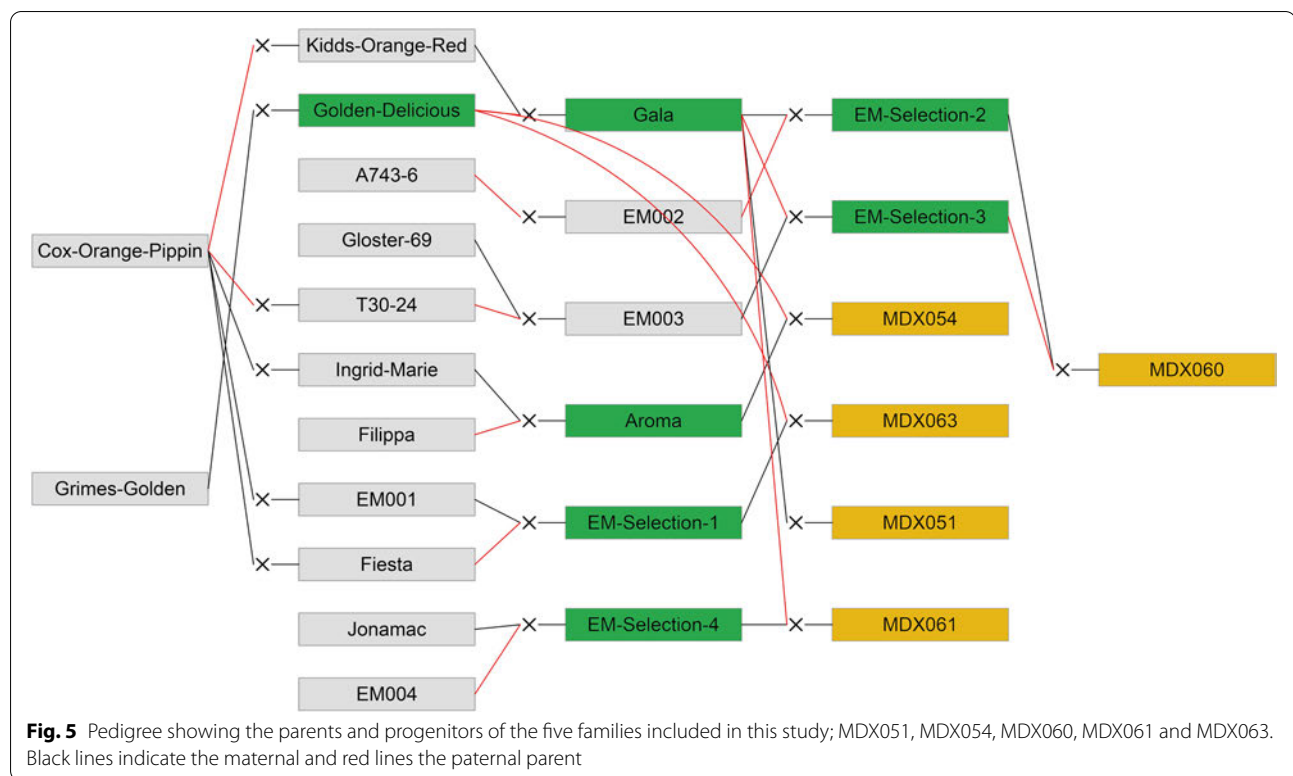
This study reveals that resistance loci to European apple canker are present in apple germplasm commonly found as parents and grandparents in modern breeding programmes. Four haplotypes, HB2-GD-R, HB6-shared-R, HB10-shared-R1 and HB15-shared-R, with the largest resistance effects, are all present in ‘Golden Delicious’, a cultivar that has been reported to feature in the pedigree of 51% out of 500 modern apple varieties with Central-European and US origin [19]. However, the resistance loci on LG6 and LG10 from ‘Golden Delicious’ could not be identified in a bi-parental population derived from this cultivar as it does not segregate at these positions. Resistant haplotypes described in this study are also shared by varieties that have been reported to be moderately tolerant to *N. ditissima* in previous studies, such as ‘Santana’ (HB 2, 6, 10), ‘Priscilla’ (HB 2 and 6), ‘Elstar’ (HB 2, 6, 10) and ‘Jonathan’ (HB 10, 15 and 16) [8, 20, 21]. Several of the identified resistant haplotypes in this study were inherited from the Swedish cultivar ‘Aroma’, which has been reported to show a medium level of resistance [7, 9]. These haplotypes are derived from the founding parent



'Filippa' and unlikely to be widespread in germplasm outside of Scandinavia.

Interestingly, the QTL-region on LG15 has also been shown to be associated with increased resistance to the fungal wood pathogen *Valsa mali* [22]. In the study, the

resistant locus was mapped on LG15 of the parent 'Jonathan', a cultivar that is also predicted by us to segregate for resistance to *N. ditissima* at this locus. This suggests that this locus may have a wider role in the resistance to wood pathogens in apple.



Evidence of dynamic QTL effects in resistance to European apple canker

Disease development after infection by *N. ditissima* is a slow process, often characterised by a prolonged symptomless period followed by necrotic lesions that spread within the bark. During the initial stage of infection there is no macroscopic visible resistance response from the host tree; however, as time progresses, some host genotypes develop callus around the boundaries of the canker lesion [3]. By mapping lesion size data from each time-point, we were able to study the dynamics of genetic effects during *N. ditissima* colonisation. This showed a temporal pattern in effects of QTL and its related SNP haplotypes. The distinction between early and late response is supported by the correlation of disease phenotypes, with a higher correlation between the detached shoot, potted tree and 5 mpi in the field compared to phenotypes from the later field time-points.

The results show evidence of two QTL, on LG5 and LG16, with larger genetic effects at the later stages of disease development. These later responses may be involved in cell-wall modifications and lignin deposition [23–26] and might be expected to be conferred by different groups of genes.

Phenotyping methods

This study involved replicated assessments of resistance to European canker using three types of plant material

(dormant shoots, actively growing trees in pots and field planted trees) and four types of phenotypes (lesion size, healthy tree area, percent branches with canker and number of canker lesions). It was evident from the PCA biplot (Fig. 1b) that there was a positive correlation between lesion size, irrespective of plant material used. As the two first components in the PCA explained most of the variation (59%), it can be assumed that these methods assess similar types of pathogen responses. This is supported by the evidence for a QTL on LG6 and LG10 in both canker lesion data from the field and the shoot experiment. Nevertheless, only three out of seven QTL could be positively identified in more than one experiment. This may be due to the relatively small effect sizes of identified QTL, which has the implication that they sometimes fall below the threshold of detection [27]. The low heritability of the detached shoot experiment ($H^2 = 0.16$), compared to the other phenotyping methods, indicates a large degree of variation between replicates within this experiment. This is in concordance with previous studies using this type of phenotyping assay [28, 29]. Data from the potted tree experiment only revealed one QTL with positive evidence and had a relatively low correlation to the other canker lesion phenotypes, despite reports that similar experiments could provide sufficient resolution to differentiate between susceptible and resistant varieties [28, 30]. One

influencing factor could be the timing of inoculations, as the potted trees in our experiment were inoculated while actively growing, whereas the other studies inoculated closer to leaf-fall. Generally, it can be concluded that long term experiments are needed to fully capture all resistance responses to European canker in apple and rapid phenotyping methods are therefore not able to replace field experiments.

The canker index (CI) used in this study provides information on the number of secondary canker lesions that had developed 20 mpi. The phenotype correlations and PCA indicate that CI is largely uncorrelated to all other phenotypic traits except for %CB. This would suggest that infection and colonization provide information on different components of resistance. This finding is in accordance with research by Garkava-Gustafsson et al. [28] but contradicts results from by Wenneker et al. [30], where moderate-strong correlations were found between infection percentage and colonization. The discrepancies between the different studies might be due to differences in experimental approaches, and neither of the other studies used trees which had already been infected with canker.

The correlation observed between %HTA and %CB and total number of tree branches suggest a relationship between tree vigour and canker tolerance. The identification of a QTL on LG5, which was only revealed from %HTA and %CB data, could therefore be influenced by tree growth. Indeed, this linkage group has previously been associated to tree growth traits in apple [31, 32]. Nonetheless, there was a significant effect of individual haplotypes from this QTL region on canker lesion size at 11 mpi, indicating a direct effect on pathogen colonization.

Conclusions

The results from this study show that QTL present in commonly used apple breeding germplasm have a low to medium effect on resistance to *N. ditissima*. Hence, multiple QTL will need to be considered to improve resistance through breeding. As phenotyping of resistance to European apple canker is time-consuming and costly, marker-assisted selection would greatly benefit the selection process. Genomic prediction uses methods of simultaneously estimating the effect of a large set of markers distributed across the genome, and would therefore provide a good alternative for the selection of a multi-QTL trait such as resistance to European apple canker [33, 34]. Medium effect apple canker QTL could be incorporated in the genomic prediction model to achieve higher prediction accuracies for this trait [35, 36].

Methods

Plant material

A multiparental population, comprising 317 individuals from four full-sib and one half-sib family and their parents were used for this study (Fig. 5, Supp. Table 1). The families were chosen based on a subset of progeny from each family showing segregation for resistance to European apple canker [7]. The experiments were carried out while the trees were juvenile.

The phenotyping of resistance to *N. ditissima* was performed by carrying out three types of experiments, namely, artificial inoculations of field planted trees, potted trees in the glasshouse and detached shoots.

Seven replicate grafts were made from each member of the population, along with the parental genotypes. All genotypes were grafted onto 'M9' EMLA rootstocks. Grafted plants were grown in 2L pots in polytunnels before planting out four plants for field experiments (after 9 months) and including three plants in potted tree experiments (after 7 months). The plant material used to propagate the trees were sourced from NIAB, East Malling, UK (in the case of seedling families and unnamed selections) and the National Fruit Collection, Brogdale, UK (for named varieties).

Neonectria ditissima inoculum

N. ditissima isolate Hg199 was used for all pathogenicity screens. Hg199 has been shown to be highly pathogenic on apple [7]. Inoculum for each pathogenicity screen was prepared according to Gomez-Cortecero et al. [7]. A concentration of 10^5 macroconidia/ml was used in all experiments. Inoculation points that did not result in lesions were handled as missing data, to obtain more accurate estimates of disease spread across all the inoculation points within one replicate.

Resistance phenotyping

Field experiment

The field experiment was conducted in a randomised complete block design in a field in East Malling, UK with four replicates trees per genotype. The varieties 'Cox Orange Pippin' (susceptible), 'Jonathan' (medium resistant), and 'Santana' (medium resistant) were included in the experiments as references.

Artificial leaf scar inoculations were conducted following 12 months of establishment in November, 2018. Inoculations were conducted as per Gómez-Cortecero et al. [7] with a few modifications. Five artificial leaf scars were inoculated per tree, with each leaf scar positioned on a separate branch. Individual inoculations within a tree were considered as pseudo-replicates; each was marked to allow repeated measurements. An inoculum

volume of 6 μ l at was pipetted onto each artificial leaf-scar wound and covered with petroleum jelly (Vaseline) after absorption. Each pseudo-replicate within a block was inoculated with the same source of inoculum. Conidial germination rate was determined as per Walter et al. [37] and ranged between 50 and 86% for different inoculation days.

Canker lesion development was measured with digital calipers at the maximum length of the lesion at three time-points, five, eight and eleven mpi. Lesions that reached the full length of the branch were recorded as missing data. A final assessment of the field experiment was conducted at 20 mpi, in which the following three phenotypes were recorded; percent branch area with foliage (healthy tree area; %HTA), percentage of all branches with cankers (cankered branches, %CB), and number of cankers. The number of cankers included the sites of inoculation as well as secondary canker lesions on the tree. A canker index (CI) was thereafter calculated by dividing number of cankers with the number of branches on each tree. Trees that were completely covered with canker (5.8% of all trees) were removed from the canker index as it was not possible to count individual cankers.

Potted tree experiment

The experiment was conducted between August–November of 2018. Potted trees were placed in glasshouse compartments with misting lines set to maintain a relative humidity above 80%. Trees were drip-irrigated throughout the experiment. Glasshouse compartments were equipped with supplementary lighting (SON-T 400w) set at 16:8 light:dark hours. A chilling-fan ensured a maximum temperature of 22°C.

Two artificial leaf scar wounds (pseudo-replicates) were inoculated on the main leader of each tree using the inoculation method above, with an inoculum volume of 3 μ l. Each pseudo-replicate within a block was inoculated with the same source of inoculum. Conidial germination rate of the inoculum was determined as described above and ranged between 50 and 99% for different inoculation days.

The first measurements of lesion length were conducted 21 and 23 dpi for the top and bottom inoculation points respectively. Developing lesions were thereafter measured weekly for 7 weeks.

Detached shoot experiment

The phenotyping of detached shoots was repeated in 2 years, with three replicate shoots/year. For each experiment, one-year dormant shoots were collected from trees of each of the members of the multiparental population. Shoots were collected from three different trees, to avoid pseudo-replication. All shoots were 60 (\pm 10) cm long. The shoots were wrapped in damp tissue paper and stored at

4°C until the start of each experiment, when they were placed in wet floral foam (Oasis®) in large trays. The shoots were regularly supplied with water but not nutrients.

The experiments were carried out between February–May in year 1 (2017) and January–April in year 2 (2018) in a glasshouse compartment. Light and relative humidity were controlled in the same manner as for the potted tree experiment. Throughout the experiment the shoots were refreshed by cutting off approximately a centimeter at the bottom-ends with secateurs.

The inoculations of the two experiments were conducted as per Gomez et al. [7] with a few modifications. Two leaf buds, the eighth and the fourteenth counting basipetally, were inoculated per shoot. An inoculum volume of 3 μ l was pipetted onto each of the two leaf-scar wounds. Due to low lesion development following inoculation in year 2, the leaf-scars were re-inoculated 28 days after the initial inoculation.

Lesion lengths were recorded weekly, using digital calipers, after the first symptoms appeared. The lesion lengths were measured in six assessments in year 1 (between 23 and 58 dpi) and in seven assessments in year 2 (between 27 and 70 dpi).

Phenotypic data

The area under the disease progression curve (AUDPC) was calculated for each genotype in the potted tree and detached shoot experiment using the R package ‘agricolae’ [38], whereas lesion size at five, eight and eleven mpi were used for the analysis of the field experiment. Cumulative data were used for the potted tree and shoot experiment rather than individual time-points as these experiments were carried out within a limited time-frame, and no differences were therefore expected between time-points.

Spatial corrections were assessed for the field and potted tree experiment using the package ‘SpATS’ in R (version 4.0.4; R Core Team, 2013) to remove variation due to tree position [39]. In the SpATS model, genotype and replicate were included as fixed effects and spatial coordinates within the field/glasshouse compartment (row and column) were included as random effects. Best Linear Unbiased Estimates (BLUEs) for each genotype were thereafter generated using the SpATS model. BLUEs for the detached shoot experiment were obtained with the R package ‘lme4’ [40] with genotype, year and lesion position as fixed effects, while tray nested within replicate were included as random effects. Broad sense heritability (H^2) was calculated in SpATS. All data were either log or arcsin transformed to ensure a normal distribution of residuals in the estimation of BLUEs. Back-transformed values were used for the analysis in FlexQTL for all phenotypes except

%HTA and %CB, which remained arcsin transformed due to being skewed towards 100%.

Principal component analysis was performed using the function ‘prcomp’ in R, using scaled and centred BLUEs for each phenotypic trait.

Genotypic data

DNA was extracted from flash-frozen leaf tissue of all genotypes in the multiparental population, including their parents and progenitors (Fig. 1). The DNA was extracted using EconoSpin® All-In-One Silica Membrane Mini Spin Columns (Epoch Life Science) according to the protocol for the DNeasy plant mini kit (Qiagen). The buffers used for extraction were according to Lamour and Finley [41].

The population was genotyped on the Illumina Infinium® 20k SNP array [42]. The genotypes for each marker were assigned using GenomeStudio Genotyping Module 2.0 (Illumina). A subset of SNPs were selected after filtering by the software ASSiST [42] and based on the absence of null-alleles in a previous set of 25 mapping populations and 400 pedigreed cultivars and breeding selections studied in the EU FruitBreedomics project [43]. SNP data curation and haplotype assignment were carried out according to Vanderrzande et al. [44]. Approximately 6000 SNP markers passed the quality control and were used to form 1083 haploblocks, distributed with 1 cM spacing across all chromosomes.

QTL analysis

The QTL analysis was performed through Markov chain Monte Carlo (MCMC)-based Bayesian approach as embedded in the software FlexQTL™ (www.flexqtl.nl) as described by Bink et al. [18, 45–47]. The probability model used in the software is described in Bink et al. [18]. The analyses were conducted using haplotype data, phenotypic BLUEs and a consensus genetic linkage map based on 21 full-sib families [48]. Each QTL analysis had a MCMC chain of 200,000 iterations with a thinning of 200. The effective sample size in the parameter file was set to 100. To ensure reproducible results, multiple FlexQTL™ runs were conducted. Additional runs were made with different settings for 1) starting seed, 2) allowed maximum number of QTLs included in models (5, 10), 3) prior for expected number of QTLs (3, 5). QTL effects were set to being additive with a normal prior distribution and a (co) variance matrix with a random, diagonal structure. QTL positions were reproducible across the different settings. Furthermore, all the runs converged, and had effective chain size > 100 for all parameters [18]. Results are shown from the FlexQTL™ run with 10 maximum QTL and a prior of 5 QTL.

Two times the natural log of Bayes factors (2lnBF) was generated by FlexQTL™ and used to determine the level of significance of a QTL, where a 2lnBF of > 2, 5, and 10 indicates a positive, strong, or decisive presence of a QTL, respectively [18, 46, 47]. QTLs are assumed to be true if they had at least strong evidence for one QTL against no QTL on that linkage group (LG) within one experiment, or if they had at least positive evidence in two or more independent phenotyping experiments.

The QTL intervals were defined as regions covered by a continuous set of 2 cM bin intervals with 2lnBF > 2. QTL intervals are reported for any QTL with at least positive evidence.

The proportion of phenotypic variation explained by each assumed true QTL was calculated using FlexQTL™ output and the formula: $h^2 = V_{QTL} / V_P$, where V_{QTL} = additive variance of a QTL and V_P = total phenotypic variance.

Haplotype analysis

The effect of single haplotypes on the canker phenotype at different time-points was estimated as follows. The size of haploblocks was reset in FlexQTL so that no recombinations occurred within assigned haploblocks in the multiparental population. The significance of haploblocks within the QTL regions was assessed in the software ASReml-R Version 4 (VSN International Ltd) to compare haplotype effects across time-points. A REML-analysis with the following model was used to test the significance of QTL-haploblocks:

$$y = \mu + Xb + Za + e,$$

where y is a vector of observed BLUEs, X is the incidence matrix of fixed effects, b is a vector of fixed effects (in this case maternal/paternal haplotype), a is the vector of random effects (apple genotypes), Z is the design matrix of random effects and e is the residual error. The covariance structure for genotype effect was calculated using genomic information (i.e. $N(0, G\sigma_a^2)$), where σ_a^2 is the additive genetic variance and G the genomic relationship matrix. The genomic relationship matrix was constructed in R-package rrBLUP [49]. An inverse of the genomic relationship matrix was used in the asreml model.

The degree by which a haploblock can explain observed phenotypic variation was tested for each haploblock within the QTL region using a Wald statistic on the asreml-model. Maternally and paternally inherited haploblocks were tested separately. The haploblock with lowest p -value for each QTL was selected for further analysis.

The model above is expected to identify in which haploblocks the parental genotypes are segregating.

However, it does not fully estimate the effect of haplotypes that may have been inherited from both maternal and paternal parents. Therefore, the number of copies of each haplotype (0, 1 or 2) within the selected haploblocks was included as a single fixed effect in the asreml-model described above. Only full-sib families were included in the haplotype analysis.

Validation of haploblock effects

Disease phenotypes from 145 progeny resulting from the cross ‘Golden Delicious’ x ‘M9’ (GDxM9) were used to validate the effect of identified haploblocks. The cross progeny was phenotyped for resistance to *N. ditissima* in two separate detached shoot experiments and one potted tree experiment, as described above. Three replicate shoots were phenotyped in each of the two detached shoot experiments, whereas two replicate trees were used in the potted tree experiment. The lengths of canker lesions were measured in seven assessments in the detached shoot experiments (between 15 and 59 dpi) and in six assessments in the potted tree experiment (between 12 and 66 dpi). Marginal AUDPC means for each genotype was calculated using R-package ‘emmeans’ from a linear model with replicate and year as fixed effects. The genotyping and haplotype phasing of the GDxM9 family was performed as described for the multiparental population. A linear model was used to test the significance of each haplotype on AUDPC for each haploblock. A multi-QTL linear model with all of the significant haplotypes was thereafter fitted for both experiments to estimate variance attributed to each haplotype.

Abbreviations

AUDPC: Area Under Disease Progress Curve; BLUE: Best Linear Unbiased Estimate; CB: Canker Branches; CI: Canker Index; HB: Haploblock; HTA: Healthy Tree Area; LG: Linkage Group; MCMC: Markov Chain Monte Carlo; PBA: Pedigree Based Analysis; PCA: Principal Component Analysis; QTL: Quantitative Trait Loci.

Supplementary Information

The online version contains supplementary material available at <https://doi.org/10.1186/s12870-022-03833-0>.

Additional file 1: Supplementary Fig. 1A-1H. Phenotypic distributions for each European canker phenotype by family. **Supplementary Fig. 2.** Best Linear Unbiased Estimates (BLUEs) of parents and standard varieties. **Supplementary Fig. 3.** Scree plot from the principal component analysis of European canker phenotypes. **Supplementary Fig. 4.** Phenotypic distributions for progeny of ‘Golden Delicious’ x ‘M9’.

Additional file 2: Supplementary Table 1. Mean and standard error for European canker phenotypes. **Supplementary Table 2.** Broad sense heritability for resistance to European apple canker in the multiparental population. **Supplementary Table 3.** Summary of the selected haploblocks within QTL-regions. **Supplementary Table 4.** Haploblock alleles from parents segregating at QTL locus. **Supplementary Table 5.** Mean, standard error and significance of haploblock alleles in ‘M9’ x ‘Golden Delicious’ cross progeny.

Additional file 3: Online resource 1. Haplotype data used for analysis in FlexQTL.

Additional file 4: Online resource 2. Phenotypic data used for QTL analysis and linkage map.

Additional file 5: Online resource 3. SNP data of multiparental population.

Acknowledgments

The authors would like to gratefully thank Eric van de Weg (Wageningen University and Research) for advice on the analysis in FlexQTL as well as critically reviewing the manuscript. We would like to acknowledge the staff in the NIAB farm and glasshouse department at East Malling for assistance and support. A special thanks to Graham Caspell (Farm Manager, NIAB at East Malling) for all advice on the field experiment. This work was funded by the Biotechnology and Biological Sciences Research Council (BBSRC BB/P000851/1).

Authors’ contributions

RJH and AK devised the study. AK, AGC, CFN and RJH designed the experiments. AK performed the experimental work with input from AGC and CFN. AK performed all data analysis. All authors (AK, RJH, CFN, AGC, MO and JMD) conceived and drafted the manuscript. All authors have read and approved the manuscript.

Funding

This work was funded by the Biotechnology and Biological Sciences Research Council (BBSRC BB/P000851/1). The funders had no role in study design, data collection and analysis, decision to publish, or preparation of the manuscript.

Availability of data and materials

Haplotype data used for the QTL identification and BLUEs of European canker phenotypes for all individuals and linkage map are provided as supplementary Online resource 1 and 2. The SNP data used as a part of this study is available in online resource 3. The data presented in the study are deposited in the Genome Database for Rosaceae repository (https://www.rosaceae.org/publication_datasets, accession number tFGDR1057) and European Variation Archive (<https://www.ebi.ac.uk/eva/?eva-study=PRJEB54689>, accession number PRJEB54689).

Declarations

Ethics approval and consent to participate

Not applicable.

Consent for publication

Not applicable.

Competing interests

The authors have no relevant financial or non-financial interests to disclose.

Author details

¹NIAB, Lawrence Weaver Rd, Cambridge CB3 0LE, UK. ²University of Reading, School of Agriculture, Policy and Development, Reading RG6 7EU, UK. ³Wageningen University and Research, 6708 PB, Wageningen, Netherlands.

Received: 16 February 2022 Accepted: 9 September 2022

Published online: 21 September 2022

References

- Walter M, Stevenson OD, Amponsah NT, Scheper RWA, Rainham DG, Hornblow CG, et al. Control of *Neonectria Ditisissima* with copper based products in New Zealand. *NZPP*. 2015;68:241–9.
- Walter M, Glaister MK, Clarke NR, von Lutz HV, Eld Z, Amponsah NT, et al. Are shelter belts potential inoculum sources for *Neonectria ditissima* apple tree infections? *N Z Plant Prot*. 2015;240:227–40.

3. Weber RWS. Biology and control of the apple canker fungus *Neonectria ditissima* (Syn. *N. Galligena*) from a Northwestern European perspective. *Erwerbs-Obstbau*. 2014;56:95–107.
4. Beresford RM, Kim KS. Identification of regional climatic conditions favorable for development of European canker of apple. *Phytopathology*. 2011;101:135–46.
5. Ghasemkhani M. Resistance against fruit tree canker in apple, vol. 77. Suecia: Doctoral thesis, Swedish University of Agricultural Sciences, Alnarp, Sweden / Acta Universitatis Agriculturae; 2015. p. 64.
6. Walter M, Campbell RE, Amponsah NT, Scheper RWA, Butler RC. Evaluation of biological and agrichemical products for control of *Neonectria ditissima* conidia production. *NZPP*. 2017;70:87–96.
7. Gómez-Cortecero A, Saville RJ, Scheper RWA, Bowen JK, Agripino De Medeiros H, Kingsnorth J, et al. Variation in host and pathogen in the *Neonectria/Malus* interaction; toward an understanding of the genetic basis of resistance to European canker. *Front Plant Sci*. 2016;7:1365.
8. van de Weg WE. Screening for resistance to *Nectria Galligena* Bres. In cut shoots of apple. *Euphytica*. 1989;42:233–40.
9. Garkava-Gustavsson L, Zborowska A, Sehic J, Rur M, Nybom H, Englund JE, et al. Screening of apple cultivars for resistance to European canker, *Neonectria ditissima*. *Acta Hort*. 2013:529–36. <https://www.journal.nzpps.org/index.php/nzpp/article/view/137>.
10. van de Weg E. Breeding for resistance to *Nectria Galligena*; differences in resistance between seedling populations. Integrated control of pome fruit diseases. *IOBC Bull*. 1989;12(6):137–45.
11. Bus VGM, Bassett HCM, Bowatte D, Chagné D, Ranatunga CA, Ulluwishewa D, et al. Genome mapping of an apple scab, a powdery mildew and a woolly apple aphid resistance gene from open-pollinated mildew immune selection. *Tree Genet Genomes*. 2010;6:477–87.
12. Bus VGM, Scheper RWA, Walter M, Campbell RE, Kitson B, Turner L, et al. Genetic Mapping of the European Canker (*Neonectria ditissima*) Resistance Locus *Rnd1* from *Malus* 'Robusta 5'. *Tree Genet Genomes*. 2019;15:25.
13. Chang L, Guo Z, Mu P. Genetic mapping and QTL analysis associated with fusarium head blight resistance at different developmental stages in wheat (*Triticum Aestivum* L) using recombinant inbred lines. *Pak J Bot*. 2018;50:2215–21.
14. Li J, Lindqvist-Kreuzer H, Tian Z, Liu J, Song B, Landeo J, et al. Conditional QTL underlying resistance to late blight in a diploid potato population. *Theor Appl Genet*. 2012;124:1339–50.
15. Li YB, Wu CJ, Jiang GH, Wang LQ, He YQ. Dynamic analyses of Rice blast resistance for the assessment of genetic and environmental effects. *Plant Breed*. 2007;126:541–7.
16. Welz HG, Schechert AW, Geiger HH. Dynamic gene action at QTLs for resistance to *Setosphaeria turcica* in maize. *Theor Appl Genet*. 1999;98:1036–45.
17. Mohler V, Stadlmeier M. Dynamic QTL for adult plant resistance to powdery mildew in common wheat (*Triticum Aestivum* L.). *J Appl Genet*. 2019;60:291–300.
18. Bink MCAM, Jansen J, Madduri M, Voorrips RE, Durel CE, Kouassi AB, et al. Bayesian QTL analyses using pedigreed families of an outcrossing species, with application to fruit firmness in apple. *Theor Appl Genet*. 2014;127:1073–90.
19. Bannier HJ. Moderne Apfelzüchtung: Genetische Verarmung Und Tendenzen Zur Inzucht. *Erwerbs-Obstbau*. 2011;52:85–110.
20. Amponsah NT, Scheper RWA, Fisher BM, Walter M, Smits JM, Jesson LK. The effect of wood age on infection by *Neonectria ditissima* through artificial wounds on different apple cultivars. *N Z Plant Prot*. 2017;70:97–105.
21. Wenneker M, de Jong PF, Joosten NN, Goedhart PW, Thomma BPHJ. Development of a method for detection of latent European fruit tree canker (*Neonectria ditissima*) infections in apple and pear nurseries. *Eur J Plant Pathol*. 2017;148:631–5.
22. Tan Y, Shen F, Chen R, Wang Y, Wu T, Li T, et al. Candidate genes associated with resistance to Valsa canker identified via quantitative trait loci in apple. *J Phytopathol*. 2017;165:848–57.
23. Xie M, Zhang J, Tschaplinski TJ, Tuskan GA, Chen J-G, Muchero W. Regulation of lignin biosynthesis and its role in growth-defense tradeoffs. *Front Plant Sci*. 2018;9:1427.
24. Lionetti V, Fabri E, De Caroli M, Hansen AR, Willats WGT, Piro G, et al. Three pectin Methyltransferase inhibitors protect Cell Wall integrity for Arabidopsis immunity to Botrytis. *Plant Physiol*. 2017;173:1844–63.
25. Lee M-H, Jeon HS, Kim SH, Chung JH, Roppolo D, Lee H-J, et al. Lignin-based barrier restricts pathogens to the infection site and confers resistance in plants. *EMBO J*. 2019;38:e101948.
26. Yan Q, Si J, Cui X, Peng H, Chen X, Xing H, et al. The soybean Cinnamate 4-hydroxylase gene *GmC4H1* contributes positively to plant defense via increasing lignin content. *Plant Growth Regul*. 2019;88:139–49.
27. Würschum T. Mapping QTL for agronomic traits in breeding populations. *Theor Appl Genet*. 2012;125:201–10.
28. Garkava-Gustavsson L, Ghasemkhani M, Zborowska A, Englund JE, Lateur M, van de Weg E. Approaches for evaluation of resistance to European canker (*Neonectria ditissima*) in apple. *Acta Hort*. 2016:75–82.
29. Scheper RWA, Fisher BM, Taylor T, Hedderley DI. Detached shoot treatments cannot replace whole-tree assays when phenotyping for apple resistance to *Neonectria ditissima*. *New Zealand Plant Protection*. 2018;71:151–7.
30. Wenneker M, Goedhart PW, van der Steeg P, van de Weg E, Schouten HJ. Methods for the quantification of resistance of apple genotypes to European fruit tree canker caused by *Neonectria ditissima*. *Plant Dis*. 2017;101(12):2012–9.
31. Harrison N, Harrison RJ, Barber-Perez N, Cascant-Lopez E, Cobo-Medina M, Lipska M, et al. A new three-locus model for rootstock-induced dwarfing in apple revealed by genetic mapping of root bark percentage. *J Exp Bot*. 2016;67:1871–81.
32. Kenis K, Keulemans J. Study of tree architecture of apple (*Malus* × *Domestica* Borkh.) by QTL analysis of growth traits. *Mol Breed*. 2007;19:193–208.
33. Crossa J, Pérez-Rodríguez P, Cuevas J, Montesinos-López O, Jarquín D, de Los Campos G, et al. Genomic selection in plant breeding: methods, models, and perspectives. *Trends Plant Sci*. 2017;22:961–75.
34. Meuwissen TH, Hayes BJ, Goddard ME. Prediction of Total genetic value using genome-wide dense marker maps. *Genetics*. 2001;157:1819–29.
35. Rutkoski J, Benson J, Jia Y, Brown-Guedira G, Jannink J-L, Sorrells M. Evaluation of genomic prediction methods for fusarium head blight resistance in wheat. *Plant Genome*. 2012;5:51–61.
36. Lee J, Kim JM, Garrick DJ. Increasing the accuracy of genomic prediction in pure-bred Limousin beef cattle by including cross-bred Limousin data and accounting for an F94L variant in MSTN. *Anim Genet*. 2019;50:621–33.
37. Walter M, Roy S, Fisher BM, Mackle L, Amponsah NT, Curnow T, et al. How many conidia are required for wound infection of apple plants by *Neonectria ditissima*. *NZPP*. 2016;69:238–45.
38. de Mendiburu F, Yaseen M. *Agricolae: statistical procedures for agricultural research*. 2021. <https://CRAN.R-project.org/package=agricolae>. Accessed 1 Dec 2021.
39. Rodríguez-Álvarez MX, Boer MP, van Eeuwijk FA, Eilers PHC. Correcting for spatial heterogeneity in plant breeding experiments with P-splines. *Spat Stat*. 2018;23:52–71.
40. Bates D, Mächler M, Bolker B, Walker S. Fitting linear mixed-effects models using lme4. *J Stat Softw*. 2015;67:1–48.
41. Lamour K, Finley L. A strategy for recovering high quality genomic DNA from a large number of *Phytophthora* isolates. *Mycologia*. 2006;98:514–7.
42. Bianco L, Cestaro A, Sargent DJ, Banchi E, Derdak S, Di Guardo M, et al. Development and validation of a 20K single nucleotide polymorphism (SNP) whole genome genotyping Array for apple (*Malus* × *Domestica* Borkh). *Plos One*. 2014;9:e110377.
43. Laurens F, Aranzana MJ, Arus P, Bassi D, Bink M, Bonary J, et al. An integrated approach for increasing breeding efficiency in apple and peach in Europe. *Hortic Res*. 2018;5:11.
44. Vanderzande S, Howard NP, Cai L, Da Silva Linge C, Antanaviciute L, Bink MCAM, et al. High-quality, genome-wide SNP genotypic data for pedigreed germplasm of the diploid outbreeding species apple, peach, and sweet cherry through a common workflow. *Plos One*. 2019;14:e0210928.
45. Bink M, Uimari P, Sillanpää J, Janss G, Jansen C. Multiple QTL mapping in related plant populations via a pedigree-analysis approach. *Theor Appl Genet*. 2002;104:751–62.
46. Bink MCAM, Totir LR, ter Braak CJF, Winkler CR, Boer MP, Smith OS. QTL linkage analysis of connected populations using ancestral marker and pedigree information. *Theor Appl Genet*. 2012;124:1097–113.
47. Bink MCAM, Boer MP, ter Braak CJF, Jansen J, Voorrips RE, van de Weg WE. Bayesian analysis of complex traits in pedigreed plant populations. *Euphytica*. 2008;161:85–96.

48. Allard A, Bink MCAM, Martinez S, Kelner J-J, Legave J-M, di Guardo M, et al. Detecting QTLs and putative candidate genes involved in Budbreak and flowering time in an apple multiparental population. *J Exp Bot*. 2016;67:2875–88.
49. Endelman JB. Ridge regression and other kernels for genomic selection with R package rrBLUP. *Plant Genome J*. 2011;4:250.

Publisher's Note

Springer Nature remains neutral with regard to jurisdictional claims in published maps and institutional affiliations.

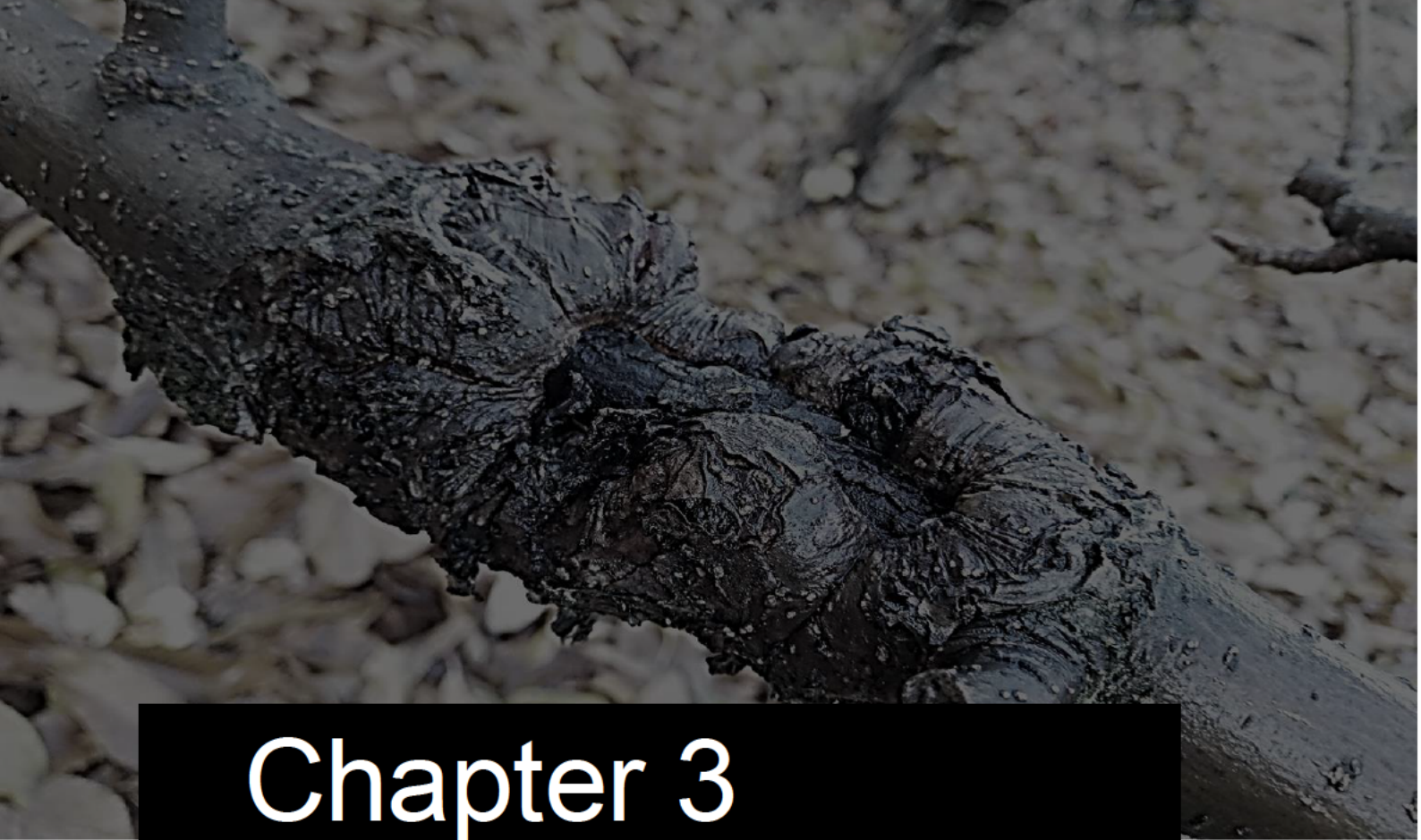
Ready to submit your research? Choose BMC and benefit from:

- fast, convenient online submission
- thorough peer review by experienced researchers in your field
- rapid publication on acceptance
- support for research data, including large and complex data types
- gold Open Access which fosters wider collaboration and increased citations
- maximum visibility for your research: over 100M website views per year

At BMC, research is always in progress.

Learn more biomedcentral.com/submissions





Chapter 3

Transcriptome analysis provide insights in resistance to European canker and reveal candidate resistance genes

This chapter describes the genetic response in apple to *Neonectria* infection through a transcriptome analysis and identifies candidate resistance genes within the QTL regions detailed in Chapter 2. This work was conducted to understand the type of molecular mechanisms that underly quantitative disease resistance to *N. ditissima* in *Malus*.

Transcriptome data from RNA sequencing of infected stems of 'Golden Delicious' and 'M9' was used to understand the global response to the pathogen. Additionally, this work aims to identify the genes underlying the QTL identified in Chapter 2. To this end, a comparative transcriptome analysis of full-sibling apple genotypes carrying resistant (QTL-R) and susceptible (QTL-S) alleles was conducted.

Transcriptome analysis provide insights in resistance to European canker and reveal candidate resistance genes

Amanda Karlström (1,2)

Antonio Gómez-Cortecero (1)

John Connell (1)

Charlotte F. Nellist (1)

Matthew Ordidge (2),

Jim M. Dunwell (2)

Richard J Harrison (3)

Amanda Karlström* (1,2), Amanda.Karlstrom@niab.com, ORCID: 0000-0002-2884-6759

Antonio Gómez-Cortecero (1), AGomezCortecero@gmail.com,

John Connell (1), John.Connell@niab.com,

Charlotte Florence Nellist (1), Charlotte.Nellist@niab.com, ORCID: 0000-0002-7453-3710

Matthew Ordidge (2), m.ordidge@reading.ac.uk, ORCID: 0000-0003-0115-5218

Jim M. Dunwell (2), j.m.dunwell@reading.ac.uk, ORCID: 0000-0003-2147-665X

Richard Jonathan Harrison (3), Richard.Harrison@wur.nl, ORCID: 0000-0002-3307-3519

*Corresponding author

(1) NIAB, Lawrence Weaver Rd, Cambridge, CB3 0LE, United Kingdom

(2) University of Reading, School of Agriculture, Policy and Development, RG6 7EU, Reading, United Kingdom

(3) Wageningen University and Research, 6708 PB, Wageningen, Netherlands

Abstract

The fungal pathogen *Neonectria ditissima* causes wood cankers on a wide range of dicotyledonous species and is a major disease threat to apple production globally. Despite the importance of this disease, the molecular basis of the quantitative resistance in *Malus* is largely unknown. A transcriptome analysis of RNA sequencing data from infected stems was used to assess the response of apple to a single isolate of *N. ditissima*. The analysis was performed on two partially tolerant cultivars; the scion variety 'Golden Delicious' and the rootstock cultivar 'M9'. Results show that >5,000 genes were differentially expressed in each of the two cultivars during fungal infection. Gene Ontology (GO), Kyoto Encyclopedia of Genes and Genome (KEGG) and protein family (PFAM) enrichment analyses of the differentially regulated genes suggest that secondary metabolism, hormone signalling, pathogen recognition, and metabolism of sugar and carbon are involved in the response to infection. Furthermore, we conducted a comparative transcriptome analysis of full-sibling apple genotypes carrying resistant (QTL-R) and susceptible (QTL-S) alleles at six resistance QTL to study the genetic mechanisms underlying quantitative resistance to this wood pathogen. The candidate gene search revealed differential expression of genes functioning in pathogen recognition, secondary metabolism, and detoxification within the QTL intervals. This study highlights the global shifts in expression patterns caused by European canker infection and identifies putative resistance genes which may play a role in quantitative resistance to *N. ditissima* in apple.

Introduction

European canker, caused by the fungal pathogen *Neonectria ditissima*, is a highly destructive disease in apple (*Malus x domestica*) growing regions, especially those with moderate temperatures and high precipitation (Weber, 2014). *N. ditissima* is foremost a wood pathogen, infecting through any type of wound on the branches or stem of the host, and thereafter spreading through the vascular system (Ghasemkhani, 2015). The fungus has a wide host range and is able to infect a large number of broad-leaved tree species (Walter et al., 2015).

A transcriptome study of the predicted secretome of *N. ditissima* during infection of an apple host has provided insight into the infection strategy of this pathogen (Gómez-Cortecero, 2019). The fungus was shown to express and potentially secrete a large number of carbohydrate-active enzymes (CAZymes) and had a high expression of glycoside hydrolase relatives which are involved in the degradation of polygalacturonan and xylan. Toxic secondary metabolites are important virulence factors for many fungal diseases with a necrotrophic lifestyle, and *N. ditissima* was shown to harbour a range of genes involved in secondary metabolism, a subset of which were highly expressed during infection (Gómez-Cortecero, 2019).

Host resistance to *N. ditissima* is an important component in the management of this pathogen, as cultural methods and fungicides offer little control to the establishment and spread of the disease. Despite this, there is limited information on the response of the host apple plants to infection nor is there information on the resistance mechanisms involved in limiting the spread of the disease. Reported sources of resistance to *N. ditissima* in *Malus* are all of quantitative nature (Bus et al., 2021; Bus et al., 2019; Gómez-Cortecero et al., 2016; Karlström et al., 2022; Skytte af Sättra et al., 2023). Multiple Quantitative Trait Loci (QTL) with small to moderate individual effects (4.3-19%) were shown to be involved in resistance to the disease in apple scion germplasm (Karlström et al., 2022). This suggests that the current resistance to European canker in apple is under polygenic control. The underlying molecular basis of Quantitative Disease Resistance (QDR) is poorly understood; by comparison the majority of described resistance (R) genes have been shown to belong to the nucleotide-binding site leucine-rich repeat (NLR) family (Araújo et al., 2019). QDR has been associated with genes performing a range of molecular functions, including kinases, WRKY-type transcription factors, zinc-finger proteins, lignin synthesis proteins, in addition to NLRs (Nelson et al., 2018). Plant membrane-bound receptors

with extracellular domains have also shown to play a central role in QDR in many plant-pathogen interactions as they are able to detect pathogen-derived ‘non-self’ patterns (Kaur et al., 2022). This type of immune receptors include a broad range of proteins, such as receptor-like kinases (RLKs), receptor-like proteins (RLPs), lysin motif (LysM)-containing receptors, lectin-containing receptors and wall-associated kinases (WAKs) (Stephens et al., 2022).

A study on the apple host response to *Valsa mali*, a necrotrophic fungal pathogen with a similar mode of infection and biology to *N. ditissima*, has shown that infection of *V. mali* triggers gene expression in pathways related to plant-pathogen interaction, plant hormone signal transduction, flavonoid biosynthesis, and phenylpropanoid biosynthesis (Xiaojie Liu et al., 2021). These biochemical pathways are known to play a vital role in how plants defend themselves towards pathogens (Kaur et al., 2022). Canker pathogens in poplar have been shown to induce similar host responses (Liao et al., 2014; Li et al., 2019), and we therefore hypothesise that apple trees infected with European canker will show a similar suite of responses.

In order to study the global gene expression patterns induced by *N. ditissima*, we investigated the transcriptomic response of one apple scion and one rootstock cultivar upon infection. The apple scion cultivar ‘Golden Delicious’ is partially tolerant to European canker (Garkava-Gustavsson et al., 2013; Karlström et al., 2022) whereas the rootstock ‘M9’ EMLA has a lower tolerance to the disease but is not completely susceptible (Bus et al., 2019; Karlström et al., 2022). To further elucidate the genes underlying QDR in the apple-*Neonectria* interaction we compared additional transcriptomes of 25 segregating progeny based on the presence/absence of specific single nucleotide polymorphism (SNP)-haplotypes at six genetic loci which have been linked to tolerance to European canker in earlier work (Karlström et al., 2022). The individuals in the studied full-sibbling family were derived from one of the crosses used by Karlstrom et al for QTL identification (‘EM Selection-4’ x ‘Gala’), Gala being an offspring of ‘Golden Delicious’ and therefore related through pedigree.

Materials and methods

Plant material

'Golden Delicious' and 'M9' EMLA were grafted onto 'M9' EMLA rootstocks at NIAB, East Malling. The trees were maintained in pots in an unheated greenhouse and irrigated weekly. Twelve replicates of each cultivar were propagated.

For the purpose of candidate gene identification, 25 progeny from a cross between 'EM-Selection 4' x 'Gala' as well as the two parents were grafted in six replicates on 'M9' EMLA rootstocks at NIAB, East Malling. The trees were kept in an unheated polytunnel and drip-irrigated for the full duration of the experiment. No trees showed symptoms of canker prior to the experiment.

Artificial inoculation with *Neonectria ditissima* and sampling

At the end of July, six months after grafting, the 'Golden Delicious' and 'M9' trees were moved to a chilled glasshouse four days prior to being inoculated. The order of plants in the glasshouse was randomised. The glasshouse conditions were the following: temperature 15-25°C, relative humidity $\geq 80\%$. Misting lines were installed under the benches with trees on top in order to maintain the humidity. These were equipped with 360° misting units spraying water for one minute at ten minute intervals. Three replicate trees of 'Golden Delicious' and 'M9' were inoculated with either a spore suspension or with a control consisting of water (suppl. Fig. 1).

The progeny trees were artificially infected in the unheated polytunnel in December, 11 months after grafting. Four replicate trees of each genotype were inoculated with *N. ditissima* spore suspension and two trees inoculated with a water control (suppl. Fig, 1).

Inoculations and the preparation of inoculum were performed as per Gomez-Cortecero et al. (2016). A single spore isolate of *N. ditissima*, Hg199, was used. Each tree was inoculated by removing two leaves and the corresponding axillary bud with a scalpel and thereafter adding the spore suspension/water to the wound with a pipette. Only the top infection-point was used for sequencing.

Samples from 'Golden Delicious' and 'M9' were collected at 25 days post-inoculation, by which time symptoms had appeared for all inoculated trees (Gomez-Cortecero, 2019). Progeny trees

were sampled four months post-inoculation, when most of the inoculated trees showed symptoms. The trees were at the same phenotypic disease stage in both experiments. Stem samples included transverse tissue sections from the cortex, phloem, cambium and xylem of each tree. Two samples were collected per inoculation point for 'Golden Delicious' and 'M9'; one sample was collected at approximately 0.5 cm distance from the leading edge of any developing canker lesion (P1), a second stem section was collected 0.5 cm from P1 (P2). Control plants and progeny trees were only sampled at 0.5 cm from the point of inoculation (suppl. Fig 1). All samples were taken apically in relation to the point of inoculation. Samples were flash frozen upon collection and stored at -80°C until RNA extraction.

RNA-extraction and transcriptome sequencing

The frozen stem samples were ground using DEPC-treated pestle and mortars in the presence of liquid nitrogen. Total RNA was isolated using Qiagen RNeasy Plant Mini Kit (Qiagen Inc., Valencia, CA) according to instructions from the manufacturer.

For 'Golden Delicious' and 'M9', two samples were sequenced for each inoculated tree: P1 and P2. One sample per tree was sequenced for progeny trees and control trees (P1). Sequencing was performed by Novogene (Novogene, Hong Kong and Cambridge) on Illumina HiSeq 4000. The presence of *N. ditissima* in the RNA of the P2 samples was confirmed by Reverse Transcriptase Polymerase Chain Reaction (RT-PCR) using specific primers of *N. ditissima* from the β -tubulin gene, Bt-fw135/Bt-rw284 as per (Ghasemkhani et al., 2016).

Processing of sequence data and genome alignment

Adaptor sequences and low-quality data were removed from sequencing reads using fastqc-mcf (Aronesty, 2013). RNA-seq data quality was evaluated using the quality control tool FastQC version 0.10.1 (Andrews, 2010). Quantification of the expression of transcripts was done using Salmon version 0.9.1 (Patro et al., 2017) using the 'Golden Delicious' transcriptome GDDH13 version 1.1. Salmon works by mapping RNA-seq data directly to a given transcriptome using a quasi-mapping approach (Srivastava et al., 2016) for a fast and accurate quantification of transcript-level abundance. Transcripts from 'Golden Delicious' and 'M9' were also aligned to a transcriptome of *N. ditissima* isolate Hg199 for quantification (Gomez-Cortecero, 2019).

Analysis of differentially expressed genes in ‘Golden Delicious’ and ‘M9’

Differential expression (DE) analysis was performed in R (R version 4.0.4) using packages edgeR (Robinson et al., 2010) and limma (version 3.52.1, Law et al., 2014; Phipson et al., 2016). Initially, transcripts with low expression in the experimental samples were removed from the dataset in edgeR. edgeR was also used to calculate normalisation factors. Differential expression analysis was conducted by using function voom in package limma. Voom transforms raw counts to \log_2 counts per million reads (CPM), incorporating the normalisation factors. P1 and P2 samples were compared separately to the controls due to a lack of independence between the samples from the same tree. Multidimensional scaling (MDS) plots were used to visually inspect the clustering of samples. A cultivar specific term was included in the contrasts to understand whether *N.ditissima* infection had the same effect on gene expression in both cultivars. The cultivar specific term was modelled as: (“Inoculated Golden Delicious” - “Control Golden Delicious”) - (“Inoculated M9” - “Control M9”). Thresholds of \log_2 Ratio $|\geq 1$ and a Benjamini-Hochberg (BH) adjusted p -value of ≤ 0.05 were used to determine if a gene was to be considered DE. Visualisations of expression data are shown as log fold change (LFC) in CPM. The gene functions shown in figures are from predicted genes in the apple genome GDDH13 version 1.1.

Functional annotation and enrichment analysis

Predicted genes in the GDDH1.1 genome were annotated with Gene Ontology (GO), Kyoto Encyclopedia of Genes and Genome (KEGG) and protein family (PFAM) terms. First, FASTA sequences for all genes were obtained from the Genome database for Rosaceae (Jung et al., 2019). The gene annotation was thereafter performed in eggNOG-mapper 2.1.7 (Cantalapiedra et al., 2021).

Gene set enrichment analysis of ‘Golden Delicious’ and ‘M9’ transcriptomes was performed in R, using package topGO (Alexa et al., 2016) for GO terms and clusterProfiler (Wu et al., 2021) for KEGG and PFAM terms. The list of background genes considered in the enrichment analyses was limited to genes that were expressed within the experiment. Terms with BH adjusted p -value of ≤ 0.05 were considered to be enriched. Only KEGG pathways that were represented in *M. x domestica* in the KEGG PATHWAY Database (Kanehisa & Goto, 2000) are presented.

Identification of candidate genes within resistance loci

Progeny from a cross between 'EM Selection-4' x 'Gala' were included in this study based on the presence/absence of specific SNP-haplotypes at six genetic loci which have been linked to tolerance to European canker (Karlström et al, 2022). Individuals with the resistance allele are denoted QTL-R while those lacking the allele are denoted QTL-S. The resistant haplotypes are as described in Karlström et al (2022). Two additional haplotypes were included in this study (on chr 8 and 16, Table 1). They did not have a significant effect on canker phenotypes in the full population used in the previous study but had a significant effect on disease spread in the family used for this study.

The DE analysis to identify candidate genes within resistance QTL was carried out as described above, with two exceptions: 1) a correlation factor was added to the linear model fit in limma-voom to allow for comparisons both within and between apple genotypes, 2) for each QTL two contrasts were defined: (*QTL-S Control plants*) - (*QTL-R Control plants*) and (*QTL-S Inoculated plants*) - (*QTL-R Inoculated plants*). Hence extracting one list of DEGs for non-infected plants and one list for plants inoculated with *N. ditissima*. The analysis did not differentiate between individuals with one or two copies of the resistance allele.

The DEGs for each QTL were reduced to only include transcripts with a genome position within the QTL interval. The physical position of the QTL regions were defined by the genome position of the boundary SNPs identified in Karlström et al (2022).

Independent validation of candidate genes was performed by examining whether they were DE in 'Golden Delicious' and 'M9' in a comparison between control and inoculated plants carried out in a separate experiment. 'Golden Delicious' was used as a parent for QTL discovery by Karlström et al (2022) and has at least one copy of each haplotype associated with the resistance QTL (Karlström et al., 2022), whereas the effect of the 'M9' SNP-haplotypes is unknown. InterPro (Paysan-Lafosse et al., 2023) was used to provide further information on putative gene function for validated genes.

Results

Transcriptome profiling of apple trees upon *N. ditissima* infection using RNA-Seq

We sequenced the transcriptome of two moderately canker tolerant apple cultivars ('Golden Delicious' and 'M9') during infection with *N. ditissima*, to study the host response to this pathogen. The average number of reads mapped to the 'Golden Delicious' genome were 48 and 49 million for infected and uninfected trees of 'Golden Delicious' and 46 and 51 million for infected and uninfected trees of 'M9', respectively. The number of genes which were expressed in any sample in the experiment was 36,802 (79% of the predicted genes in the genome). A transcript quantification of the number of genes mapping to *N. ditissima* showed a total of 33 million mapped reads in the proximal samples and 180,000 in the distal samples.

Full-sibling progeny segregating for resistance QTL to *N. ditissima* were also subject to transcriptome profiling, in order to identify candidate genes underlying the QTL. For the progeny samples, a mean library size of 18.5 Mb was obtained and 33,167 transcripts were retained after filtering out transcripts with low expression. A total of 146 samples were included in the final analysis after the removal of samples from infected trees that never developed symptoms and/or showed an unusual MDS clustering compared to other replicates of the same genotype.

Differentially expressed genes in 'Golden Delicious' and 'M9'

Venn diagrams with the number of differentially expressed genes (DEGs) for the proximal (P1) and distal (P2) sampling position are shown in Figure 1. 'Golden Delicious' had 5,180 DEGs compared to the control of the same variety at P1. The number of DEGs in 'M9' was 5,011. A comparison of DEGs at P1 indicated that 1742 unique genes were DE in 'Golden Delicious' and 1,501 transcripts were uniquely DE in 'M9' upon infection (Fig. 1). There was a significant cultivar specific direction of expression for 12 of the DEGs at P1, that is a gene where the direction of regulation is opposite between cultivars or a much larger change in one cultivar from the control.

A smaller number of genes were DE in P2. There were 2,149 DEGs in 'Golden Delicious', whereas the number of DEGs in 'M9' was smaller, only 913. There was no significant cultivar specific pattern in gene expression for the two varieties at P2.

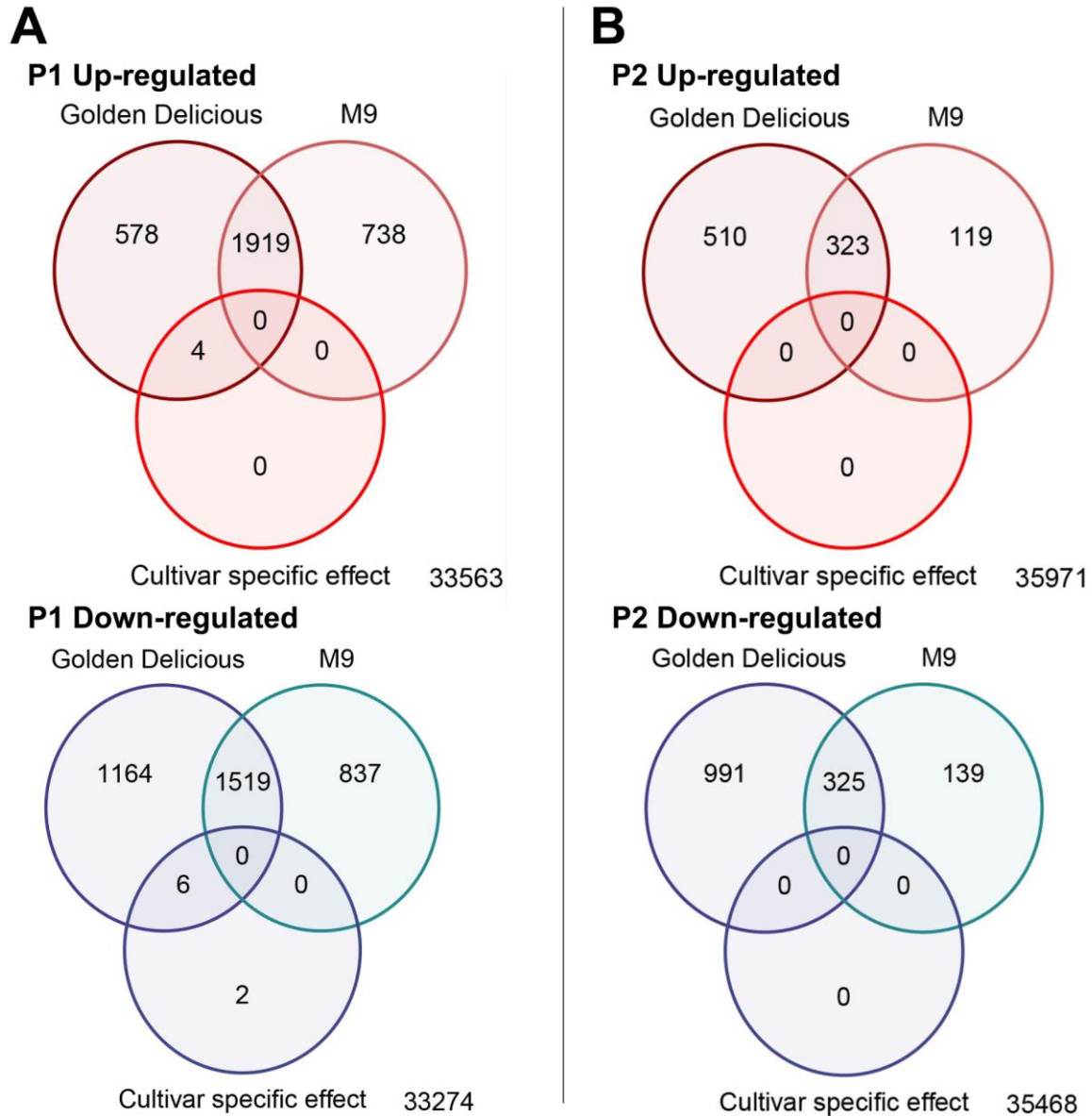


Figure 1. Apple (*Malus x domestica*) trees infected with *Neonectria ditissima* show differential gene expression compared to the control. Venn diagrams showing A) DEGs in tissue samples taken at 0.5 cm beyond the leading edge of symptomatic tissue (P1), B) DEGs in tissue samples taken at 1 cm beyond the leading edge of symptomatic tissue (P2). The number in the bottom-right corner of each venndiagram shows the number of expressed genes for which there was no significant difference between inoculated and control samples.

Gene ontology enrichment analysis

Out of the predicted genes expressed in this experiment 47% could be annotated with GO terms. The GO enrichment analysis identified key biological processes and molecular functions overrepresented among DEGs. The largest number of significantly enriched GO terms ($q \leq 0.05$) were found in 'M9' P1 with 73 terms enriched, whereas 57, 31 and 12 terms were enriched in 'Golden Delicious' P1, 'Golden Delicious' P2 and 'M9' P2, respectively. The 15 most significantly enriched GO terms for all four conditions are shown in Figure 2 (only 12 are shown for 'M9' P2). The full list of enriched terms is presented in Supplementary Table 1.

The three GO terms: 'response to wounding' (GO:0009611), 'response to drug' (GO:0042493), and 'glutathione metabolic process' (GO:0006749) were among the top five most significant groups in all conditions apart from 'Golden Delicious' P2. However, response to wounding and glutathione metabolism were also significantly enriched in 'Golden Delicious' P2 (Supplementary Table 1).

Several pathways related to sugar metabolism were significantly enriched in infected trees: fructose 1,6-bisphosphate metabolism (GO:0030388), sucrose biosynthesis (GO:0005986), fructose 6-phosphate metabolism (GO:0006002) gluconeogenesis (GO:0006094), fructose metabolism (GO:0006000). Out of these, the first three terms were significantly overrepresented in 'Golden Delicious' P1 and P2 as well as 'M9' P1. In contrast, gluconeogenesis and fructose metabolism were only overrepresented in 'Golden Delicious'.

KEGG pathway enrichment

A total of 28% of the predicted genes expressed in this experiment could be annotated with KEGG pathway terms. Significantly enriched ($q \leq 0.05$) KEGG terms are shown in Figure 3 and Supplementary Table 2. 'Golden Delicious' had 37 and 20 significantly enriched pathways at sampling position P1 and P2, respectively. In contrast, 'M9' had 37 and 11 significantly overrepresented KEGG terms at sampling position P1 and P2, respectively.

A number of significantly enriched KEGG categories are part of the biosynthesis of secondary metabolites (e.g phenylpropanoid (ko00940), flavonoid (ko00941) and stilbenoid, diarylheptanoid and gingerol biosynthesis (ko00945)) or metabolism of terpenoids and polyketides (e.g zeatin

(ko00908), monoterpenoid (ko00902) and sesquiterpenoid and triterpenoid biosynthesis (ko00909)).

Pathways within the processing of environmental information were significantly overrepresented in infected samples. The KEGG pathways ABC transporters (ko02010) and plant hormone signal transduction (ko04075) were significantly enriched in all four types of samples, whereas the Mitogen-activated protein kinase (MAPK) signalling pathway (ko04016) was only enriched at P1. Genes within plant-pathogen interaction (ko04626) were only significantly overrepresented in 'Golden Delicious' at P1.

Protein family enrichment

PFAM enrichment was conducted due to the low annotation rate of GO and KEGG terms. A total of 79% of the predicted genes expressed in the experiment could be annotated with a PFAM domain. Significantly enriched PFAM terms are shown in Supplementary Table 3 and the 20 protein families with the smallest q -value are shown in Figure 4. The number of overrepresented protein families were 103, 49, 111 and 34 for 'Golden Delicious' P1, 'Golden Delicious' P2, 'M9' P1 and 'M9' P2, respectively.

The most significant PFAM term in both P1 and P2 for 'Golden Delicious' was UDP-glycosyltransferase (UDPGT, abbreviated UGT), with 84 and 45 DEGs of 192 annotated genes, respectively. This term was also significantly enriched in both sampling positions of 'M9', where 73 and 23 genes were differentially expressed in P1 and P2, respectively.

Fructose-1,6-bisphosphatase (FBPase) had the largest percentage DEGs out of the total annotated genes in 'Golden Delicious' P1 (10 out of 12 genes) and P2 (10 out of 12 genes) and 'M9' P1 (8 out of 12 genes). However, this term was not enriched in 'M9' P2.

There was evidence of a significant overrepresentation of genes with a potential involvement in pathogen recognition and plant immunity. The plant pathogenesis-related (PR) protein family PR10/Bet v 1 was significantly enriched in all four conditions. Out of the 25 DEGs with PR10 motifs, 68% were predicted to belong to the major latex-like protein (MLP) subfamily, of which a majority were up-regulated upon infection. Genes containing domains specific to leucine rich repeats (LRR_4) and salt-stress and antifungal activity (Stress-antifung) were overrepresented in both cultivars at P1 but not at P2. Out of the 35 DEGs annotated 'Stress-antifung', 71 % were

predicted to be cysteine-rich RLKs. Among the 48 DEGs annotated with the protein family domain 'LRR_4', 23% were predicted to be leucine-rich RLKs (LRR-RLKs) and 38% leucine-rich repeat protein kinases. Genes containing a lysin motif (LysM), which are known to be involved in the recognition of fungal chitin, were significantly enriched in 'Golden Delicious' P1 ($q=0.027$) but not in any of the other sampling conditions. Twelve of the 35 genes annotated as LysM-containing were differentially expressed in 'Golden Delicious' at P1. The protein family B-lectins was significantly enriched in all conditions apart from 'M9' P2. Out of the 74 DEGs annotated as B-lectins, 58% were putative S-locus lectin protein kinases.

Several of the overrepresented protein domains (GST_C, GST_C_2, GST_N and GST_N_3) are associated with Glutathione S-transferases (GSTs).

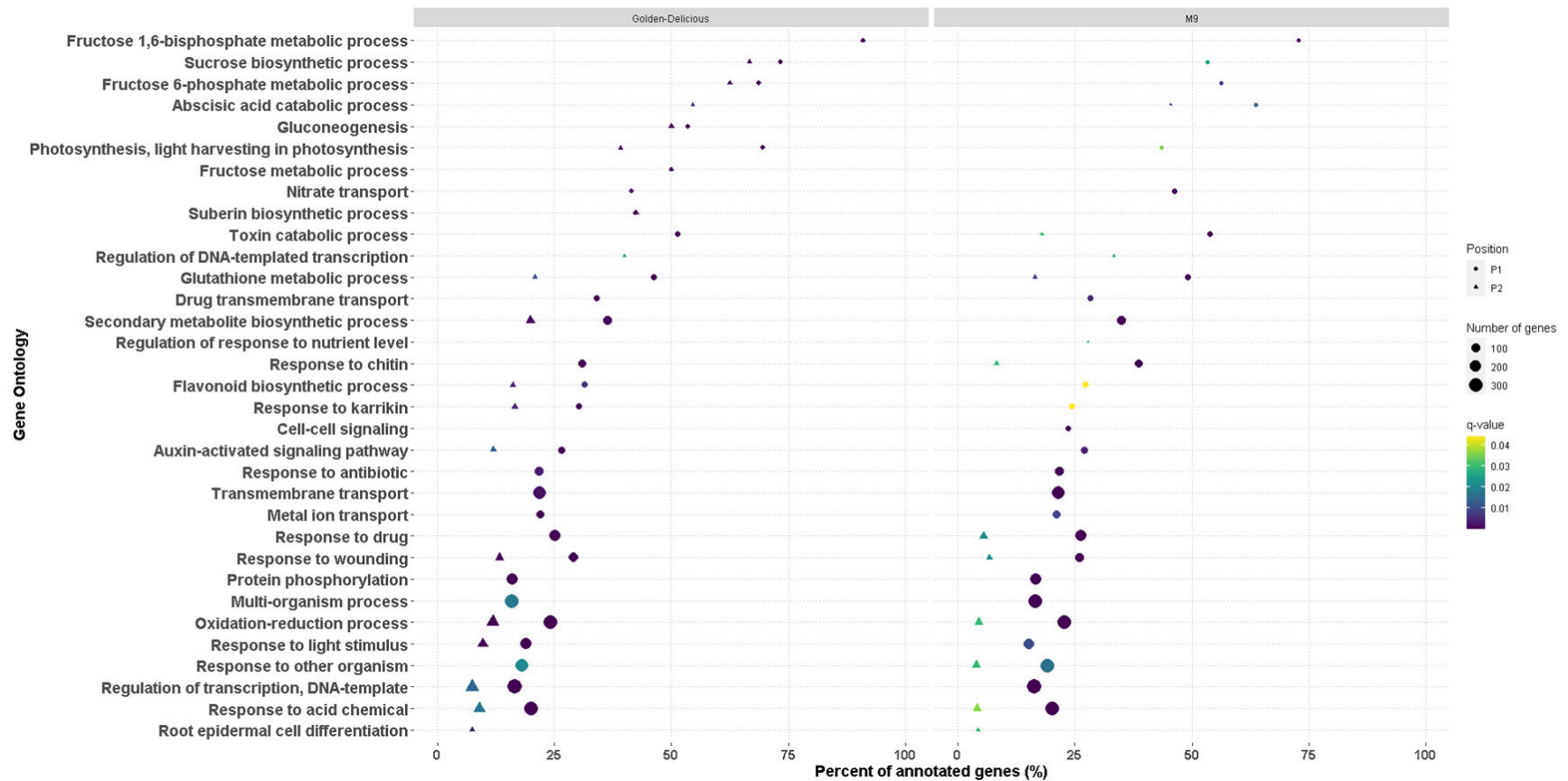


Figure 2. Dot plot showing significantly enriched GO terms. The top 15 GO terms with the smallest q -value from all four sampling conditions are plotted in order of percent annotated genes that are differentially expressed (only 12 terms were significant for 'M9' P2). The shape of the dots represents the sampling position in relation to the symptomatic tissue, size of dots represents the number of genes in the significant DE gene list associated with the GO term and dot colour signifies the q -value of the GO term.

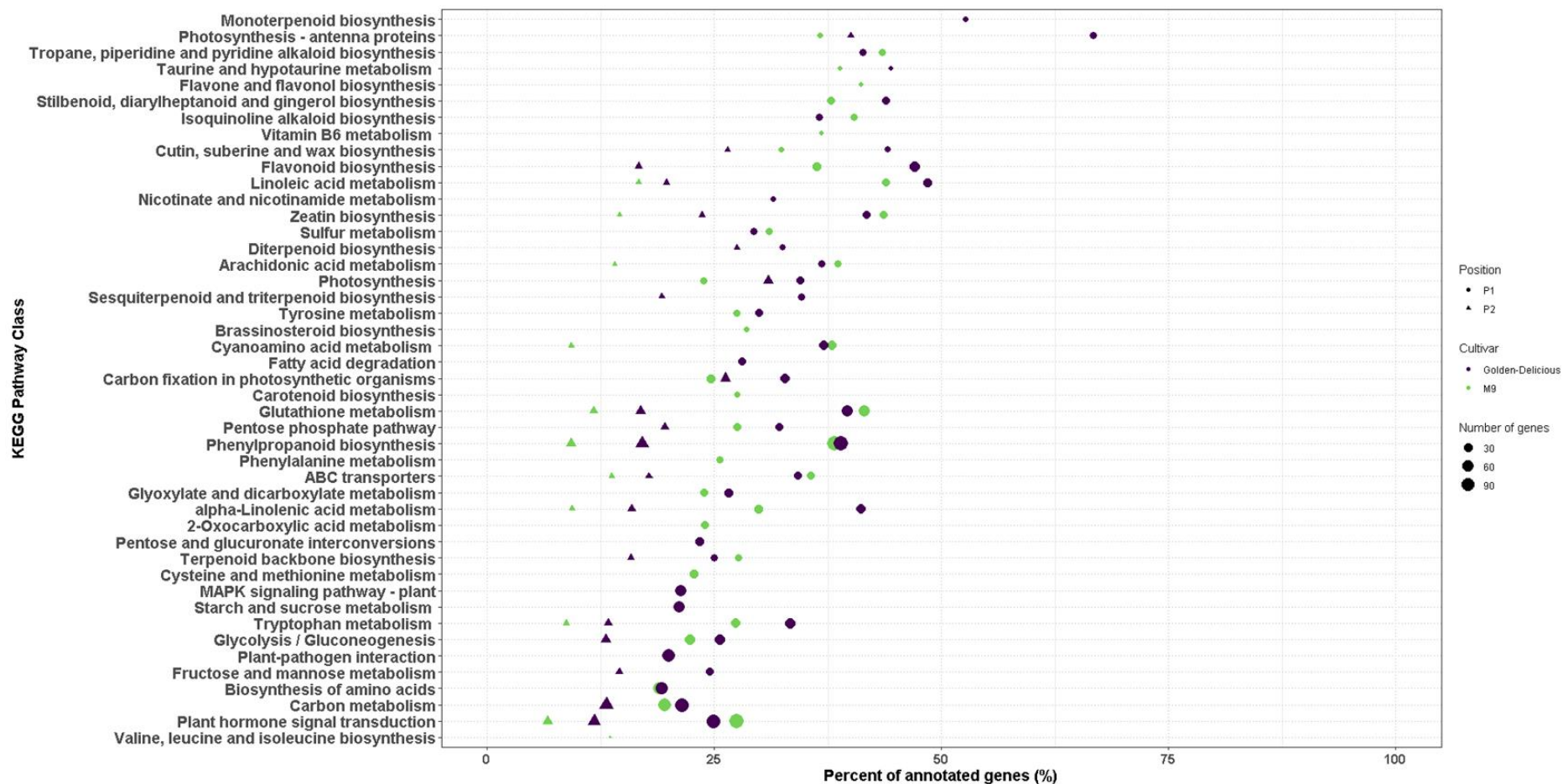


Figure 3. Dot plot showing significantly enriched KEGG terms. All significant KEGG terms from all four sampling conditions are plotted in order of percent annotated genes that are differentially expressed. The shape of the dots represents the sampling position in relation to the symptomatic tissue, dot colour signifies apple cultivar and the size of dots represents the number of genes in the significant DE gene list associated with the KEGG term.

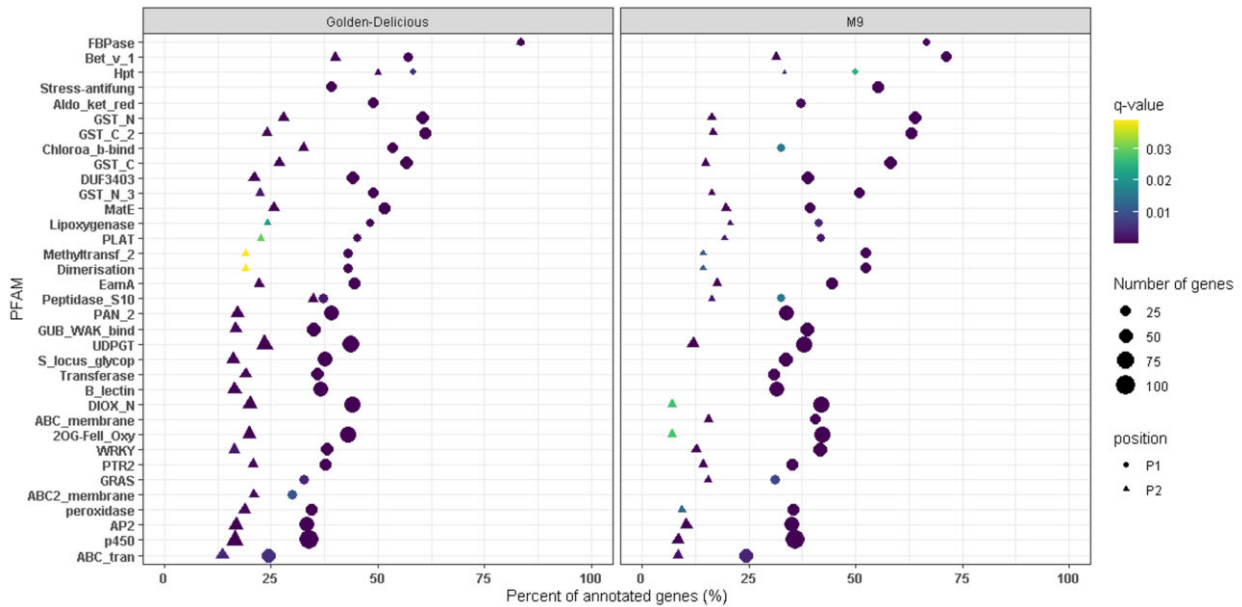


Figure 4. Dot plot showing significantly enriched PFAM terms. The top 20 most significant PFAM terms from all four sampling conditions are plotted in order of percent annotated genes that are differentially expressed. The shape of the dots represent the sampling position in relation to the symptomatic tissue and the size of dots represent the number of genes in the significant DE gene list associated with the PFAM term.

Secondary metabolites

The enrichment analyses indicated that a number of genes involved in secondary metabolism are differentially regulated upon infection with *N. ditissima*. Among DEGs associated with secondary metabolite biosynthesis (GO:0044550), approximately half were up-regulated (57 DEGs) and half down-regulated (64 DEGs) as a response to the pathogen infection (Figure 5A). In the KEGG enrichment analysis the phenylpropanoid pathway (ko00940) was the most statistically significant secondary metabolite pathway in all samples (Suppl. Table 2). A total of 61% of DEGs with a potential role in this pathway had an increased abundance as a response to infection with *N. ditissima* (Figure 5B). Out of the 148 DEGs annotated to the phenylpropanoid pathway 44 were predicted to be peroxidases, of which approximately half were up-regulated in the infected samples. Three domains associated with the multicopper containing oxidase protein family (Cu-oxidases) were significantly enriched in both cultivars at P1, but not at P2 (Supplementary Table 3). Two-thirds of the 90 DEGs annotated to these protein families were predicted to be laccases.

The GO term for suberin biosynthesis (GO:0010345) was significantly enriched at both sampling positions of 'Golden Delicious' but not in 'M9'. Suberin is a polymer found in specialised cells, e.g. the cork cells in bark (Bernards et al., 2004). At both positions 14 of 33 expressed genes annotated with the term were differentially expressed. All were downregulated.

Plant pathogen interaction

The fold-change expression of DEGs annotated with the KEGG term 'Plant Pathogen Interaction' (ko04626), a term that was only significantly enriched in 'Golden Delicious', are shown in Figure 6. The subset of 36 genes that were only DE in 'Golden Delicious' are shown in Figure 6B. Sixteen of these genes were up-regulated in 'Golden Delicious', as a result of the infection with *N. ditissima*, including a predicted CC-NBS-LRR class disease resistance protein which had an six-fold increase in expression in P1 compared to the control plants (*MD07G1251200*). A further 20 genes were only significantly down-regulated in 'Golden Delicious', among which were seven cyclic nucleotide gated channel proteins for which transcript abundances were reduced between 2.3 to 4.9 fold.

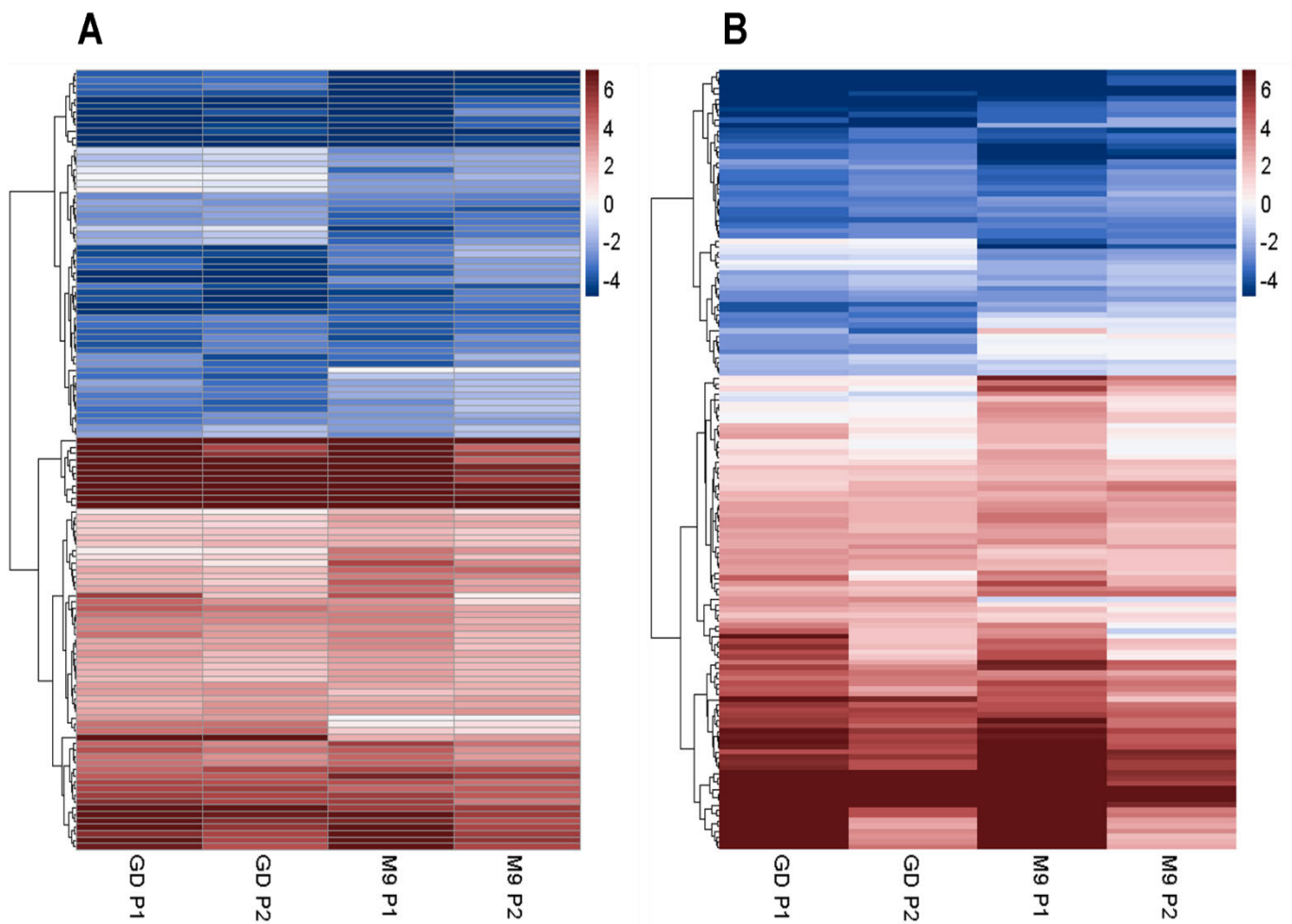


Figure 5. Heatmap and clustering of the average log₂ CPM fold change in expression for differentially expressed genes involved in A) secondary metabolite biosynthesis and B) the phenylpropanoid pathway. “GD P1” = ‘Golden Delicious’ sampling position P1, “GD P2”= ‘Golden Delicious’ sampling position P2, “M9 P1”= ‘M9’ sampling position P1, “M9 P2”= ‘M9’ sampling position P2. The dendrogram shows unsupervised hierarchical clustering of rows.

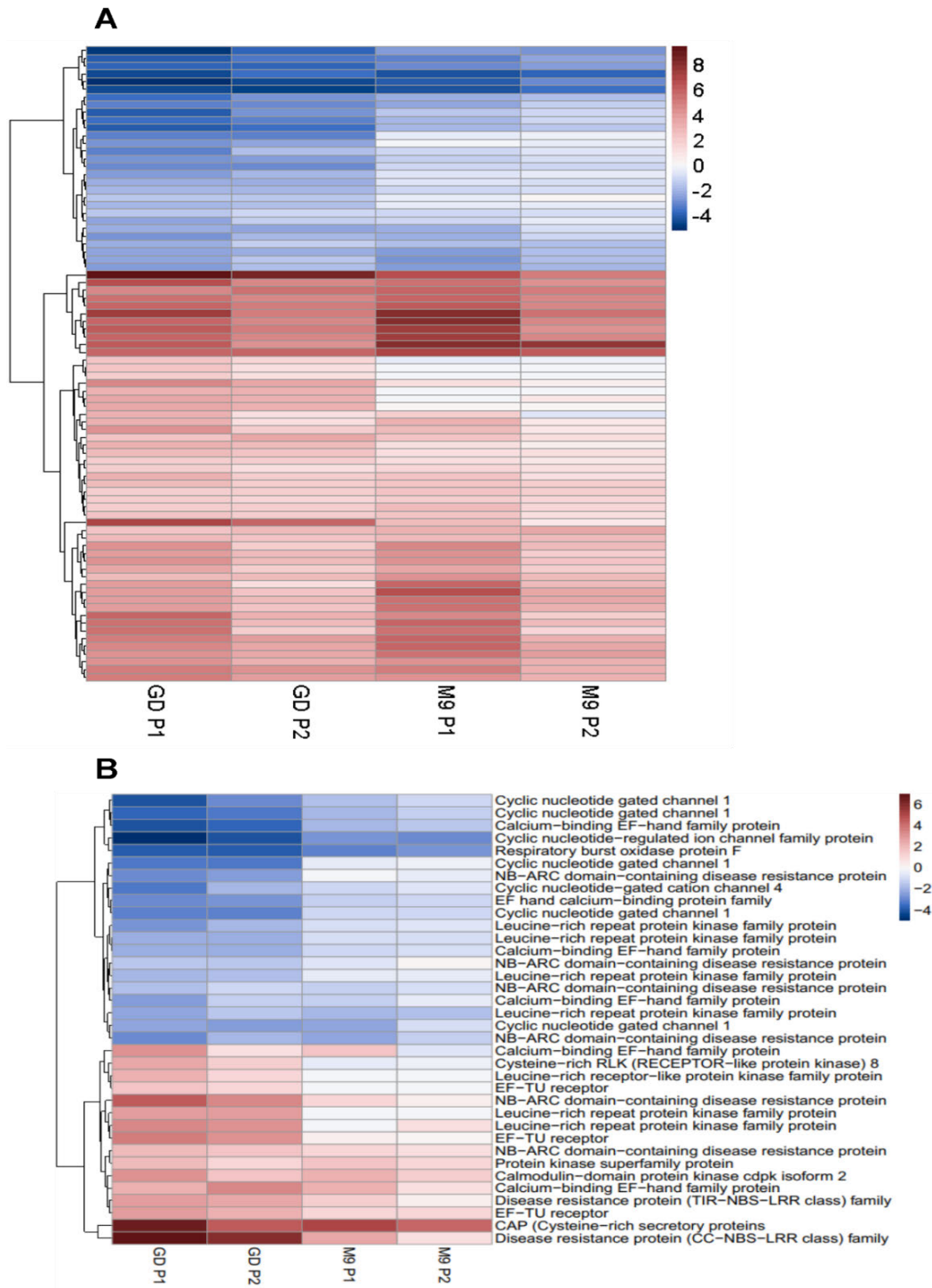


Figure 6. Heatmap and clustering of the average \log_2 CPM fold change in expression for plant-pathogen interaction associated genes (ko4626) for a) all differentially expressed (DE) genes and b) the subset of genes that are DE exclusively in 'Golden Delicious'. "GD P1" = 'Golden Delicious' sampling position P1, "GD P2" = 'Golden Delicious' sampling position P2, "M9 P1" = 'M9'

sampling position P1, “M9 P2”= ‘M9’ sampling position P2. The dendrogram shows unsupervised hierarchical clustering of rows.

Identification of candidate genes within resistance loci

Full-sib progeny from a cross between ‘EM-Selection 4’ x ‘Gala’ were grouped based on the presence/absence of resistance alleles at six QTL described in Karlström et al (2022, Table 1, Suppl. table 4). The number of known resistance alleles for the QTL are also shown for ‘Golden Delicious’ and ‘M9’. ‘Golden Delicious’ was one of the parents of the population used for QTL discovery in the study, whereas ‘M9’ was not included as a parent. The comparison of QTL-R and QTL-S transcriptomes was conducted for plants infected with *N. ditissima* (sampling position P1), but also for control plants in order to deduce whether the candidate genes constitutively differed in abundance between the two groups.

Table 2 shows a summary of the results from the DE analysis of the comparison of individuals with or without a resistance allele at each QTL. All DEGs within the QTL boundaries are shown in Supplementary table 5. Figure 5 further highlights the DEGs with positions within the QTL regions identified by Karlstrom et al (2022) that were also differentially expressed upon infection in ‘Golden Delicious’ or ‘M9’. To note is that constitutively expressed genes would not be expected to be validated in ‘Golden Delicious’ or ‘M9’ as their expression is expected to be the same in control and infected plants. Below follows a description of selected DEGs in comparisons of QTL-R and QTL-S trees, furthermore the presented transcripts were either: validated or had the same predicted gene function as a validated gene within the same QTL interval or had a predicted gene function as a disease resistance gene (Table 3, Fig. 5, Suppl. Table 6).

Table 1 QTL configuration for each genetic locus for the 27 apple genotypes that were included in the study as well as for ‘Golden Delicious’ and ‘M9’.

Chr	SNP haplotype associated with resistance	No. of individuals with resistance QTL-allele	No. of individuals with no resistance QTL-allele	Known resistance QTL-alleles in ‘Golden Delicious’	Known resistance QTL-alleles in ‘M9’
2	HB2-Gala-R	18	9	1	0
6	HB6-shared-R	23	4	2	0
8	HB8-shared-R /HB8-36	22	5	1	0
10	HB10-shared-R1	23	4	2	0
15	HB15-shared-R	18	9	1	0
16	HB16-38	10	17	1	0

Table 2 Summary of number of differentially expressed genes (DEGs) from the comparison of individuals with QTL-R or QTL-S allele for each of the six QTL

QTL	<i>All chromosomes</i>	<i>Within QTL interval</i>			
	Total no. of DEGs	Total no. of DEGs	DEGs in both control and infected plants	DEGs in only control plants	DEGs in only infected plants
2	432	63	29	7	27
6	116	17	6	1	10
8	294	23	0	2	21
10	83	18	5	4	9
15	172	50	21	4	25
16	149	24	7	8	9

DEGs within the QTL-region on chromosome 2

Among the DEGs within the QTL interval on chr 2, there were 14 putative WAKLs (containing the PFAM domains GUB_WAK_bind and Pkinase_Tyr; (Suppl. table 6, Liu et al., 2021). Seven of these were constitutively higher expressed in QTL-S plants (i.e DE in both control and infected plants). The other seven were significantly higher expressed in QTL-R trees, but only upon infection (Table 3). Five of the WAKLs could be validated in expression data from 'Golden Delicious' or 'M9' (i.e were DE in one of these cultivars in response to infection, Fig 7, Table 3).

A gene predicted to encode a zinc induced facilitator-like transporter (*MD02G1267000*) was DE in control plants, with QTL2-R having a 4.0 logFC compared to trees without the allele (Table 3). This gene could also be validated in "Golden Delicious" and 'M9', which had an increase in transcript abundance upon infection. The protein encoded by this gene was predicted to function as a membrane transport protein in the Major facilitator superfamily or function in multidrug resistance. One gene encoding a cytochrome P450 (CYP) enzyme was DE in infected trees, with QTL2-S having >1.5 logFC compared to QTL2-R (Fig. 7). It also had a significantly increased expression in 'M9' upon infection.

There were three DEGs putative NLRs within the QTL interval on chr 2; two NLRs with Toll/interleukin-1 receptor (TIR) domains (*MD02G1260200* and *MD02G1217100*) and one with a coiled coil (CC) domain (*MD02G1164500*). The latter was DE in both control and infected plants and had a >2.5 logFC in QTL2-R. None of the three genes could be validated in 'Golden Delicious' or 'M9'.

DEGs within the QTL-region on chromosome 6

The QTL interval on chr 6 had one putative UGT with logFC=3.7 in QTL6-R trees compared to QTL6-S. The gene, *MD06G1103300*, was DE in trees infected with *N. ditissima*. And was significantly up-regulated in 'Golden Delicious' upon infection.

One gene annotated as a nuclear RNA polymerase had a higher expression in QTL6-S plants compared to QTL6-R (Table 3). The gene, *MD06G1069800*, was DE in infected plants and was down-regulated in 'Golden Delicious' trees infected with *N. ditissima*.

DEGs within the QTL-region on chromosome 8

A putative Heavy metal associated isoprenylated plant protein (HIPP) (*MD08G1026800*) was significantly more abundant in infected QTL8-S trees compared to QTL8-R (Table 3). The gene had a significantly reduced expression in infected 'Golden Delicious' trees compared to the mock-inoculated 'Golden Delicious' trees. Furthermore, a gene predicted to encode a jasmonic acid carboxyl methyltransferase (JMT) *MD08G1027300* was DE in control plants, with QTL8-R having a larger number of transcripts compared to QTL8-S. The gene was significantly down-regulated upon infection in both 'Golden Delicious' and 'M9'.

Two genes with predicted functionality as a glutamate receptors (*MD08G1048600*) and a glutathione peroxidase (*MD08G1055100*) were DE in infected plants. Both were up-regulated in QTL8-R compared to trees without the resistance allele. Transcripts of these two genes were also significantly higher in infected trees of 'Golden Delicious' and 'M9' compared to the controls.

MD08G1064100, predicted to encode a heat shock transcription factor, was DE in trees inoculated with *N. ditissima*. The gene was up-regulated in QTL8-S trees compared to trees with the QTL8-R allele. Furthermore, the gene was significantly down-regulated in 'Golden Delicious' and 'M9' in response to infection.

There were three DEGs with functional annotations as disease resistance proteins within the QTL-interval; two NLRs with TIR domains (*MD08G1019600* and *MD08G1020000*) and one with a nucleotide-binding adaptor shared by APAF-1, R proteins, and CED-4 (NB-ARC) domain (*MD08G1042700*). All of them were DE in infected trees with a higher expression in trees with the QTL8-R allele. Neither could be validated in 'Golden Delicious' or 'M9'.

DEGs within the QTL-region on chromosome 10

A putative NAC-transcription factor had a significantly higher expression in QTL10-R individuals (Table 3). This transcript also had a significant increase in abundance in infected trees of 'M9' and 'Golden Delicious' compared to the non-inoculated control.

Three putative wall associated kinases (WAKs) were DE in the QTL interval on chr 10. *MD10G1250000* and *MD10G1251200* were constitutively higher expressed in QTL10-R, whereas

MD10G1250500 was also more abundant in QTL10-R but significantly so only in control plants (Table 3). None of the three WAKs could be validated in 'M9' or 'Golden Delicious' data.

An additional four genes predicted to encode protein subunits of a coatomer protein complex were DE in infected plants. All were more highly expressed in QTL10-S plants compared to QTL10-R. One of these genes (*MD10G1250100*) was significantly down-regulated in 'M9' upon infection with *N. ditissima*.

DEGs within the QTL-region on chromosome 15

There were five predicted disease resistance proteins within the QTL interval on chr 15, three with NB-ARC domains and two NLRs. None of the disease resistance proteins were DE in 'Golden Delicious' or 'M9'.

One predicted ATP-binding cassette (ABC) transporter was significantly DE in control plants, with a 1.3 logFC in QTL15-R compared to QTL15-S trees (Table 3). This gene was also significantly up-regulated in 'Golden Delicious' and 'M9' when infected with *N. ditissima*.

A predicted MYC/MYB transcription factor (*MD15G1077600*) was significantly more highly expressed in QTL15-S compared to QTL15-R in control plants, whereas no difference was found in infected trees. This transcript was significantly down-regulated in both 'Golden Delicious' and 'M9' as a response to infection.

DEGs within the QTL-region on chromosome 16

There were two putative AMP-dependent synthetases among the DEGs within the QTL region on chr 16 (*MD16G1112900* and *MD16G1113000*). Both were more highly expressed in QTL16-R plants compared to individuals without the resistance allele (logFC>2). However, *MD16G1113000* was significantly more highly expressed in both control and infected plants whereas *MD16G1112900* was only significantly DE in infected trees. The expression of *MD16G1112900* was significantly higher in infected trees of 'Golden Delicious' and 'M9' compared to control. InterProScan identified the protein encoded by both genes to show similarities to 4-Coumarate-CoA Ligases (4CL).

There were three DEGs within the interval functionally annotated as CYP enzymes. These genes were only significantly DE in control trees. Two of them, *MD16G1104200* and *MD16G1104300* were more highly expressed in QTL16-S compared to QTL16-R ($\log_{2}FC > 1.9$), whereas the opposite was true for *MD16G1116300* ($\log_{2}FC = 3.2$). The latter gene was significantly up-regulated in both 'Golden Delicious' and 'M9' as a response to infection.

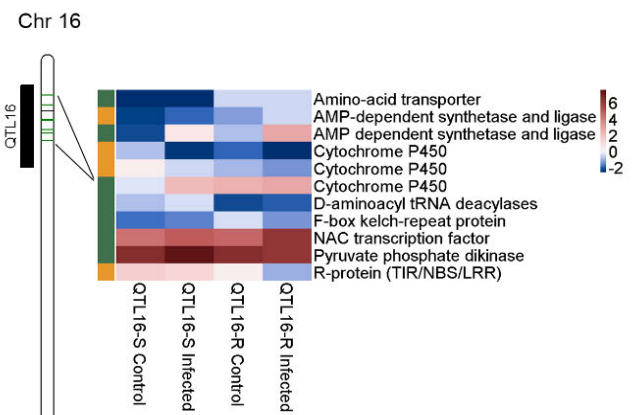
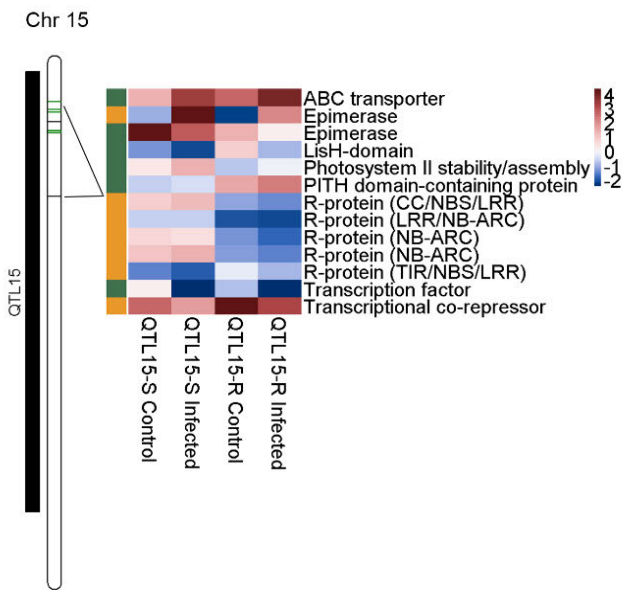
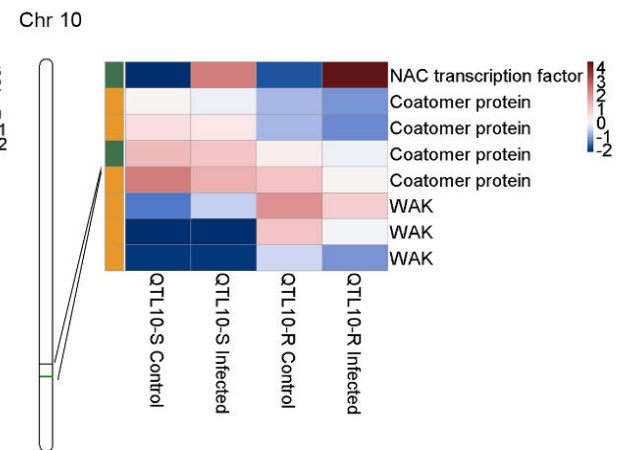
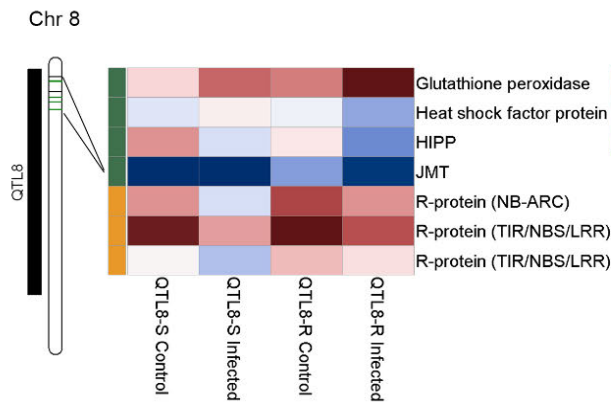
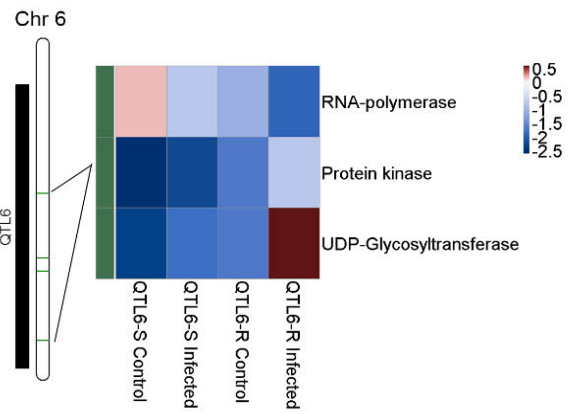
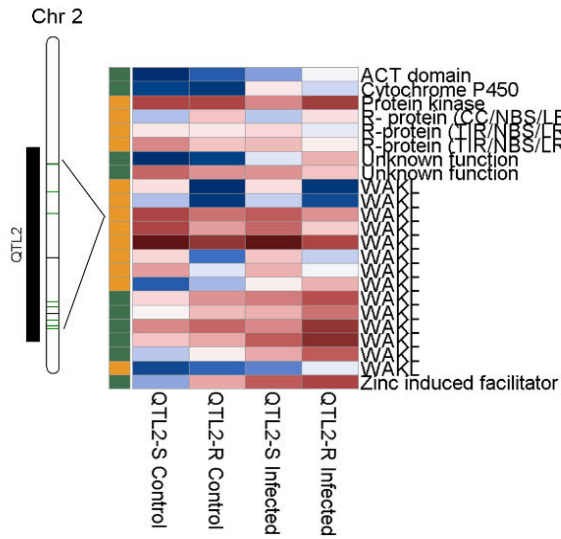


Figure 7. Heatmaps showing the average log₂ CPM expression for candidate genes within six genetic loci associated with resistance to *Neonectria ditissima*. The genes were identified as differentially expressed (DE) in an analysis comparing individuals with or without a resistance allele at each QTL. Transcripts marked in green were also DE in the apple cultivars 'Golden Delicious' or 'M9' in a separate experiment.

Table 3 DEGs of particular interest identified in comparisons of gene expression in apple genotypes with QTL-R vs QTL-S alleles. The table shows DEGs which are validated, had the same predicted gene function as a validated gene at the same QTL, or had a predicted gene function within disease resistance. For each gene it is also shown the log fold change (logFC) for QTL-S – QTL-R and whether the gene was DE in 'Golden Delicious' or 'M9'.

Gene ID GDDH13_v1.1	QTL	logFC Control	logFC Infected	Putative gene function	Sig. DE GD or M9
MD02G1188900	QTL2	N.S	-1.8	ACT domain	Yes
MD02G1200700	QTL2	N.S	1.5	Cytochrome P450	Yes
MD02G1164500	QTL2	-3.3	-2.6	Disease resistance protein (CC NBS LRR class)	No
MD02G1217100	QTL2	N.S	1.5	Disease resistance protein (TIR NBS LRR class)	No
MD02G1260200	QTL2	1.5	1.5	Disease resistance protein (TIR NBS LRR class)	No
MD02G1282000	QTL2	N.S	-1.4	Protein kinase	No
MD02G1276500	QTL2	N.S	1.1	Unknown function	Yes
MD02G1164900	QTL2	N.S	-2.7	Unknown function	Yes
MD02G1245800	QTL2	1.0	1.2	Wall associated kinase like (WAKL)	No
MD02G1246300	QTL2	1.0	1.4	Wall associated kinase like (WAKL)	No
MD02G1247400	QTL2	N.S	-1.9	Wall associated kinase like (WAKL)	No
MD02G1234300	QTL2	5.4	4.9	Wall associated kinase like (WAKL)	No
MD02G1234800	QTL2	3.2	2.6	Wall associated kinase like (WAKL)	No
MD02G1246100	QTL2	1.9	2.2	Wall associated kinase like (WAKL)	No

MD02G1246600	QTL2	4.0	2.4	Wall associated kinase like (WAKL)	No
MD02G1274600	QTL2	<i>N.S</i>	-2.0	Wall associated kinase like (WAKL)	No
MD02G1246700	QTL2	2.8	2.2	Wall associated kinase like (WAKL)	No
MD02G1249500	QTL2	<i>N.S</i>	-1.2	Wall associated kinase like (WAKL)	Yes
MD02G1273500	QTL2	<i>N.S</i>	-1.3	Wall associated kinase like (WAKL)	Yes
MD02G1273700	QTL2	<i>N.S</i>	-1.8	Wall associated kinase like (WAKL)	Yes
MD02G1249700	QTL2	<i>N.S</i>	-1.4	Wall associated kinase like (WAKL)	Yes
MD02G1254300	QTL2	<i>N.S</i>	-2.0	Wall associated kinase like (WAKL)	Yes
MD02G1267000	QTL2	-4.0	<i>N.S</i>	Zinc induced facilitator	Yes
MD06G1099100	QTL6	<i>N.S</i>	-1.1	ABC transporter	No
MD06G1116500	QTL6	<i>N.S</i>	-2.7	Protein kinase	Yes
MD06G1069800	QTL6	<i>N.S</i>	2.3	RNA-polymerase	Yes
MD06G1103300	QTL6	<i>N.S</i>	-3.8	UDP-Glycosyltransferase	Yes
MD08G1042700	QTL8	<i>N.S</i>	-2.5	Disease resistance protein (NB-ARC domain)	No
MD08G1019600	QTL8	<i>N.S</i>	-1.2	Disease resistance protein (TIR-NBS-LRR class)	No
MD08G1020000	QTL8	<i>N.S</i>	-1.8	Disease resistance protein (TIR-NBS-LRR class)	No
MD08G1055100	QTL8	<i>N.S</i>	-1.2	Glutathione peroxidase	Yes
MD08G1064100	QTL8	<i>N.S</i>	1.5	Heat shock factor protein	Yes
MD08G1026800	QTL8	<i>N.S</i>	1.6	Heavy metal associated isoprenylated plant protein (HIPP)	Yes
MD08G1027300	QTL8	-2.6	<i>N.S</i>	Jasmonic acid carboxyl methyltransferase (JMT)	Yes
MD10G1248600	QTL10	<i>N.S</i>	1.5	Coatomer protein	No
MD10G1248700	QTL10	<i>N.S</i>	2.5	Coatomer protein	No
MD10G1250100	QTL10	<i>N.S</i>	1.5	Coatomer protein	Yes
MD10G1251000	QTL10	<i>N.S</i>	1.6	Coatomer protein	No
MD10G1238200	QTL10	<i>N.S</i>	-2.5	NAC transcription factor	Yes
MD10G1250000	QTL10	-5.6	-3.4	Wall associated kinase (WAK)	No
MD10G1250500	QTL10	-2.9	<i>N.S</i>	Wall associated kinase (WAK)	No
MD10G1251200	QTL10	-4.9	-2.2	Wall associated kinase (WAK)	No
MD15G1102100	QTL15	-1.3	<i>N.S</i>	ABC transporter	Yes
MD15G1090400	QTL15	2.8	3.6	Disease resistance protein (CC NBS LRR class)	No
MD15G1090100	QTL15	2.7	2.9	Disease resistance protein (LRR and NB-ARC domains)	No
MD15G1090000	QTL15	3.2	3.5	Disease resistance protein (NB-ARC domain)	No
MD15G1090300	QTL15	3.5	4.2	Disease resistance protein (NB-ARC domain)	No

MD15G1179700	QTL15	<i>N.S</i>	-2.0	Disease resistance protein (TIR NBS LRR class)	No
MD15G1073400	QTL15	<i>N.S</i>	2.3	Epimerase	No
MD15G1073500	QTL15	4.1	3.5	Epimerase	Yes
MD15G1103500	QTL15	-3.1	-2.1	LisH-domain	Yes
MD15G1106700	QTL15	<i>N.S</i>	2.0	Photosystem II stability assembly factor	Yes
MD15G1061900	QTL15	-3.0	-3.5	PITH domain-containing protein	Yes
MD15G1077600	QTL15	1.4	<i>N.S</i>	Transcription factor	Yes
MD15G1103400	QTL15	-1.6	-1.4	LisH-domain	No
MD16G1112900	QTL16	<i>N.S</i>	-2.1	AMP dependent synthetase and ligase	Yes
MD16G1113000	QTL16	-2.3	-2.4	AMP-dependent synthetase and ligase	No
MD16G1104200	QTL16	2.0	<i>N.S</i>	Cytochrome P450	No
MD16G1104300	QTL16	2.0	<i>N.S</i>	Cytochrome P450	No
MD16G1116300	QTL16	-3.2	<i>N.S</i>	Cytochrome P450	Yes
MD16G1055500	QTL16	<i>N.S</i>	2.6	D-aminoacyl tRNA deacylases	Yes
MD16G1082200	QTL16	<i>N.S</i>	3.0	Disease resistance protein (TIR NBS LRR class)	No
MD16G1096400	QTL16	-2.5	<i>N.S</i>	F-box kelch-repeat protein	Yes
MD16G1125800	QTL16	<i>N.S</i>	-1.2	NAC transcription factor	Yes
MD16G1097800	QTL16	<i>N.S</i>	1.3	Pyruvate phosphate dikinase	Yes
MD16G1072500	QTL16	-4.1	-4.0	Transmembrane amino-acid transporter	Yes

Discussion

This study investigated the global expression profile of two apple cultivars, 'Golden Delicious' and 'M9', during infection by the canker pathogen *N. ditissima*. By employing a RNA-seq approach we were able to elucidate the potential mechanisms involved in resistance to European canker in cultivated apple. Furthermore, we utilised individuals from a full-sibling family of apple to study the genetic mechanisms underlying QDR to this wood pathogen.

Global trends in response to infection with *N. ditissima*

The transcriptome analysis revealed that a large number of genes (>5,000) were differentially regulated in each of the cultivars 'Golden Delicious' and 'M9' at approximately a month after infection with *N. ditissima*. Apple stem tissue was sampled at two distances from the canker lesion to compare expression profiles in cells adjacent to the symptomatic tissue as well as cells located at a further distance to the diseased tissue.

Overall, a similar number of genes were DE in the two apple cultivars at P1. However, there was a substantial proportion of unique DEGs in each cultivar at P1; 34% and 31% for 'Golden Delicious' and 'M9', respectively. This indicates that a subset of different genes were activated in each cultivar due to infection, suggesting different repertoires of resistance responses in the two moderately tolerant cultivars. The use of two cultivars with a larger difference in resistance to European canker may have facilitated the identification of expression patterns specific to resistant cultivars.

Whilst there were fewer DEGs at P2 the difference between cultivars was proportionally larger. This showed that a shift in expression appeared at a further distance from the point of infection in 'Golden Delicious' compared to 'M9', with approximately 2,000 versus 900 DEGs in the respective cultivar at P2. The wider differential response in 'Golden Delicious' to *N. ditissima* infection may be indicative of a more rapid and/or more systemic response to the pathogen in this cultivar compared to 'M9'.

The enrichment analyses for genes annotated with different functional classes show that a range of molecular processes are affected as a result of *N. ditissima* infection. The protein family analysis indicated an enrichment of genes involved in pathogen and chitin recognition, hormone

signalling, response and transport of toxins and xenobiotics, secondary metabolism as well as sugar and carbon metabolism. The results suggest that the host response to *N. ditissima* is mediated through a combination of pattern triggered immunity and effector triggered immunity (Jones & Dangl, 2006; Yuan et al., 2021). Pathogen recognition then activates hormone signalling and altered metabolism of sugars, carbon and secondary metabolites. The observed changes in genes associated with catabolism and transport of toxins and xenobiotics (e.g multidrug and toxic compound extrusion (MATE) family genes, GSTs) could either have a role in attenuating host induced oxidative stress and endogenous metabolites or the detoxification of toxins produced by the pathogen (Gullner et al., 2018; Shoji, 2014; Upadhyay et al., 2019). The percentage of genes that could be annotated with KEGG or GO terms was low (28 and 47%, respectively) which could potentially skew the enrichment analysis. However, the PFAM enrichment analysis described a similar picture and was based on a larger percentage of annotated genes (79%).

The responses observed here are similar to what has been observed during infection of *Valsa mali*, another fungal pathogen causing cankers in apple, including pathways related to phenylpropanoid biosynthesis, starch and sucrose metabolism, plant-hormone signal transduction and plant-pathogen interaction (Liu et al., 2021).

N. ditissima infection alters expression of genes involved in the phenylpropanoid pathway and lignification

The phenylpropanoid pathway is responsible for the biosynthesis of a wide array of secondary metabolites derived from the deamination of phenylalanine to cinnamic acid by phenylalanine ammonia-lyase (PAL) (Dixon et al., 2002). Cinnamic acid is then further converted in order to produce the plant cell wall components lignin and suberin as well as coumarins, flavonoids and stilbenes. DEGs associated with the phenylpropanoid pathway were identified in both cultivars and sampling positions in this experiment, with 61% of those identified showing an increased abundance after infection. A third of the DEGs annotated to the phenylpropanoid pathway were peroxidases. Moreover, 60 DEGs were predicted to be laccases. Although peroxidases and laccases perform various functions in plants, both are involved in the polymerization of monolignols to form lignin (Dong & Lin, 2021). A cell-wall degrading enzyme (CWDE) from *Botrytis cinerea* was shown to alter expression of peroxidases and genes in the phenylpropanoid pathway as well as increase lignin content in tomato (Yang et al., 2018). Furthermore, laccase

and peroxidase activity have been associated with altered lignification and resistance to plant pathogens for some time (Elfstrand et al., 2002; Hu et al., 2018; Soni et al., 2020; Yu et al., 2020). A further support for the importance of the phenylpropanoid pathway in apple tolerance to *N. ditissima* is the identification of two putative 4CL genes (*MD16G1112900* and *MD16G1113000*) within the QTL interval on chr 16. Both genes were significantly more highly expressed in apple progeny with the QTL16-R resistance allele. 4CL is a key enzyme in the beginning of the phenylpropanoid pathway, in which it catalyses the conversion of hydroxycinnamates into corresponding CoA esters for biosynthesis of flavonoids and lignin (Sun et al., 2013). The activity of 4CLs, and the subsequent accumulation of lignins have previously been linked to plant pathogen resistance in multiple crops (Alariqi et al., 2023; Dhokane et al., 2016; Li et al., 2021). Furthermore, two putative *CYP* genes were identified within the QTL regions on chr 2 and 16. CYPs belong to a large enzymatic gene family with important functions in the synthesis of secondary metabolites (Xu et al., 2015). Our results suggest that one of the responses in apple trees to *N. ditissima* infection is a shift in expression of phenylpropanoid pathway genes and altered lignin accumulation through peroxidase and laccase activity. However, further studies would be required to evaluate the relative importance of lignin biosynthesis and phenylpropanoids in quantitative disease resistance to European canker.

Pathogen interaction

The infection with *N. ditissima* altered the expression of a multitude of genes involved in pathogen recognition, including PRs, NLRs, RLKs, and genes with LysM-domains. Our results indicate that *N. ditissima* is recognised by the apple host by a combination of basal immunity and more specialised NLRs. Nevertheless, it is not clear whether the NLRs have a role in QDR or have been hijacked by the pathogen to function as susceptibility genes (Nelson et al., 2018).

We identified several candidate genes with a role in pathogen interaction within QTL that have already been associated with resistance to *N. ditissima* in scion apple germplasm (Karlstrom et al., 2022). Clusters of putative WAKs and WAKLs were identified in the QTL intervals on chr 10 and 2, respectively. WAKs are usually characterised by the three following domains; a serine/threonine kinase, an epidermal growth factor (EGF) and a galacturonan-binding (GUB) domain. Compared with WAK, WAKL usually lacks the extracellular EGF domain (Gou et al., 2023). *WAK/WAKL*-genes are a sub-family of RLKs that function in plant growth and stress-response and that in many cases acts as a positive regulator in plant immune response (Gou et al., 2023). Nevertheless there are examples of host-pathogen systems where WAKs have been

shown to negatively regulate host resistance (Delteil et al., 2016; Harkenrider et al., 2016; Liu et al., 2012). Furthermore, a genome-wide study of WAKs in apple showed these to be both positively and negatively regulated as a response to infection with *V. mali*, *Alternaria alternata* and *Pythium ultimum* (Zuo et al., 2018). There were three WAKs among the candidate genes within the QTL interval on chr 10. All of these had a significantly lower expression in trees with the resistant allele at QTL10. Furthermore, the gene was significantly down-regulated in 'M9' upon infection. A cluster of 14 putative WAKs were identified as candidates underlying the QTL on chr 2. Five of these WAKs (*MD02G1249500*, *MD02G1273500*, *MD02G1273700* and *MD02G1254300*) are particularly interesting as candidate genes as they were validated in the transcriptome data from 'Golden Delicious'/'M9 and more highly expressed in apple trees with the QTL2-R allele.

Several putative NLRs were DE in QTL regions on chr 2, 8, 15 and 16 when comparing individuals with or without a resistant allele at each QTL. However, the association of these genes to *N. ditissima* infection could not be confirmed in the transcriptome data from 'Golden Delicious' or 'M9'.

Putative genes underlying observed variation in tolerance to *N. ditissima*

Apple trees rely on quantitative resistance to combat infection with *N. ditissima*. We dissected seven QTL associated with QDR to European canker, in order to understand the mechanisms that underpin tolerance to this wood pathogen. In addition to the above mentioned roles of candidate genes in the phenylpropanoid pathway and pathogen interaction, genes with several other functions were identified. A putative *UGTs* were DE within the QTL interval on chr 6. The *UGT* gene family was also significantly enriched after canker infection in both 'Golden Delicious' and 'M9', and >38% of the genes annotated to this protein family were DE at the sampling positions closest to the pathogen lesion. *UGT* is a very large superfamily of enzymes in plants, which catalyse glycosidation. These enzymes have been linked to QDR in multiple species through the glycosylation of endogenous phytohormones, defensive compounds and other secondary metabolites but also by reducing the toxicity of pathogen derived xenobiotics (Gharabli et al., 2023). The *UGT* on chr 6, *MD06G1103300*, is particularly interesting as a candidate gene as it was strongly up-regulated in infected trees with the resistance allele on chr 6 (Fig. 5).

Transcription factors were identified as candidate genes within the QTL regions on chr 8 (heat shock transcription factor), 10, 15 and 16. This group of proteins are known to be important in the transcriptional reprogramming that occurs in response to pathogen infection (Amorim et al., 2017).

Among the candidate genes within the QTL interval on chr 8 was a putative HIPP encoding gene, which had a lower expression in QTL-R trees. HIPP genes have been described as targets of multiple necrotrophic pathogens (Cowan et al., 2018; Guo et al., 2018) and as susceptibility genes in nematode-plant interactions (Radakovic et al., 2018; Dutta et al., 2023). The most well-described HIPP in plant disease is probably *HIPP05* from *Oryza sativa*, also known as *Pi21*, which functions as a susceptibility factor in interactions with the necrotrophic pathogen *Magnaporthe oryzae*. Loss-of-function mutations of this gene results in field resistance to the pathogen (Fukuoka et al., 2009) – while overexpression in the non-host *Arabidopsis* has been shown to result in increased pathogenicity of *M. oryzae* on this species (Nakao et al., 2011)

This study used a transcriptome approach to identify candidate genes associated with multiple resistance QTL to European canker in apple. However, only a limited subset of the genes that were DE between QTL-R and QTL-S plants could be validated in expression data from ‘Golden Delicious’ or ‘M9’, despite the presence of resistance alleles for all QTL in ‘Golden Delicious’ (Table 1). There could be several reasons for this; 1) differences in timing of sampling of infected tissue between progeny and validation. The differences in number of DEGs between P1 and P2, as well as the differences between ‘Golden Delicious’ and ‘M9’ in their response at these two positions, shows that infection stage has a large influence on gene expression in the host. The progeny and validation were sampled at the same phenotypical stage and at the same distance from the active lesion. However, the response to different disease progression stages will vary between genotypes and even small variations may influence gene expression. 2) The validation was specific to genes which were differentially expressed upon infection by *N. ditissima* and would therefore miss constitutively expressed genes. 3) Differences between QTL-R and QTL-S are spurious and due to allelic variation but not related to the response to *N. ditissima*. This is however an unlikely explanation for genes which are only DE in infected trees.

In addition, the “true” genes underlying resistance QTL may not have been detected in this study. The DE-analysis compared the effect of single alleles on gene expression, ignoring the effects of background QTL. This could potentially hinder the identification of candidate genes if the QTL has a small effect on overall disease progression. The parents of the segregating progeny harboured

different haplotype alleles associated with resistance for QTL 8. However, the resistance genes underlying the two alleles were assumed to be the same. This assumption may be incorrect and there may indeed be different genetic variation underlying the resistance for each allele. Furthermore, the low representation of genotypes with no resistance allele for QTL6 and QTL8 may have resulted in a limited power to detect differences in transcript abundance for these QTL.

Despite above limitations we have identified a number of candidate genes associated with resistance loci to *N. ditissima*. Upon functional characterization, these can pave the way to developing highly canker resistant apple varieties.

References

- Alariqi, M., Ramadan, M., Wang, Q., Yang, Z., Hui, X., Nie, X., Ahmed, A., Chen, Q., Wang, Y., Zhu, L., Zhang, X., & Jin, S. (2023). Cotton 4-coumarate-CoA ligase 3 enhanced plant resistance to *Verticillium dahliae* by promoting jasmonic acid signaling-mediated vascular lignification and metabolic flux. *The Plant Journal*, *115*(1), 190–204. <https://doi.org/10.1111/tpj.16223>
- Alexa A., Rahnenführer J. (2016) topGO: Enrichment Analysis for Gene Ontology. R package version 2.24.0.
- Amorim, L. L., da Fonseca Dos Santos, R., Neto, J. P. B., Guida-Santos, M., Crovella, S., & Benko-Iseppon, A. M. (2017). Transcription factors involved in plant resistance to pathogens. *Current Protein Peptide Science*, *18*(4), 335-51.
- Andrews, S. (2010). FastQC: A Quality Control Tool for High Throughput Sequence Data [Online]. Available online at: <http://www.bioinformatics.babraham.ac.uk/projects/fastqc/>
- Araújo, A. C. de, Fonseca, F. C. D. A., Cotta, M. G., Alves, G. S. C., & Miller, R. N. G. (2019). Plant NLR receptor proteins and their potential in the development of durable genetic resistance to biotic stresses. *Biotechnology Research and Innovation*, *3*, 80–94. <https://doi.org/10.1016/j.biori.2020.01.002>
- Aronesty, E. (2013). Comparison of Sequencing Utility Programs. *The Open Bioinformatics Journal*, *7*(1), 1–8. <https://doi.org/10.2174/1875036201307010001>
- Bernards, M. A., Summerhurst, D. K., & Razem, F. A. (2004). Oxidases, peroxidases and hydrogen peroxide: The suberin connection. *Phytochemistry Reviews*, *3*(1–2), 113–126. <https://doi.org/10.1023/B:PHYT.0000047810.10706.46>
- Bus, V., Singla, G., Horner, M., Jesson, L., Walter, M., Kitson, B., López-Girona, E., Kirk, C., Gardiner, S., Chagné, D., & Volz, R. (2021). Preliminary genetic mapping of fire blight and European canker resistances in two apple breeding families. *Acta Horticulturae*, *1307*, 199–204. <https://doi.org/10.17660/ActaHortic.2021.1307.31>

- Bus, V. G. M., Scheper, R. W. A., Walter, M., Campbell, R. E., Kitson, B., Turner, L., Fisher, B. M., Johnston, S. L., Wu, C., Deng, C. H., Singla, G., Bowatte, D., Jesson, L. K., Hedderley, D. I., Volz, R. K., Chagné, D., & Gardiner, S. E. (2019). Genetic mapping of the European canker (*Neonectria ditissima*) resistance locus Rnd1 from Malus 'Robusta 5.' *Tree Genetics & Genomes*, 15(2), 25. <https://doi.org/10.1007/s11295-019-1332-y>
- Cantalapiedra, C. P., Hernández-Plaza, A., Letunic, I., Bork, P., & Huerta-Cepas, J. (2021). eggNOG-mapper v2: Functional Annotation, Orthology Assignments, and Domain Prediction at the Metagenomic Scale. *Molecular Biology and Evolution*, 38(12), 5825–5829. <https://doi.org/10.1093/molbev/msab293>
- Cowan, G. H., Roberts, A. G., Jones, S., Kumar, P., Kalyandurg, P. B., Gil, J. F., ... & Torrance, L. (2018). Potato mop-top virus co-opts the stress sensor *HIPP26* for long-distance movement. *Plant Physiology*, 176(3), 2052-2070.
- Delteil, A., Gobbato, E., Cayrol, B., Estevan, J., Michel-Romiti, C., Dievart, A., Kroj, T., & Morel, J. B. (2016). Several wall-associated kinases participate positively and negatively in basal defense against rice blast fungus. *BMC Plant Biology*, 16, 17. <https://doi.org/10.1186/s12870-016-0711-x>
- Dhokane, D., Karre, S., Kushalappa, A. C., & McCartney, C. (2016). Integrated Metabolo-Transcriptomics Reveals Fusarium Head Blight Candidate Resistance Genes in Wheat QTL-*Fhb2*. *Plos One*, 11(5), e0155851. <https://doi.org/10.1371/journal.pone.0155851>
- Dixon, R. A., Achnine, L., Kota, P., Liu, C.-J., Reddy, M. S. S., & Wang, L. (2002). The phenylpropanoid pathway and plant defence—a genomics perspective. *Molecular Plant Pathology*, 3(5), 371–390. <https://doi.org/10.1046/j.1364-3703.2002.00131.x>
- Dong, N.-Q., & Lin, H.-X. (2021). Contribution of phenylpropanoid metabolism to plant development and plant-environment interactions. *Journal of Integrative Plant Biology*, 63(1), 180–209. <https://doi.org/10.1111/jipb.13054>
- Dutta, T. K., Vashisth, N., Ray, S., Phani, V., Chinnusamy, V., & Sirohi, A. (2023). Functional analysis of a susceptibility gene (*HIPP27*) in the *Arabidopsis thaliana*-*Meloidogyne incognita* pathosystem by using a genome editing strategy. *BMC Plant Biology*, 23(1), 390.

- Elfstrand, M., Sitbon, F., Lapierre, C., Bottin, A., & von Arnold, S. (2002). Altered lignin structure and resistance to pathogens in *spi 2*-expressing tobacco plants. *Planta*, *214*(5), 708–716. <https://doi.org/10.1007/s00425-001-0681-5>
- Fukuoka, S., Saka, N., Koga, H., Ono, K., Shimizu, T., Ebana, K., ... & Yano, M. (2009). Loss of function of a proline-containing protein confers durable disease resistance in rice. *Science*, *325*(5943), 998-1001.
- Garkava-Gustavsson, L., Zborowska, A., Sehic, J., Rur, M., Nybom, H., Englund, J. E., Lateur, M., Van de Weg, E., & Holefors, A. (2013). Screening of apple cultivars for resistance to european canker, *Neonectria ditissima*. *Acta Horticulturae*, *976*, 529–536. <https://doi.org/10.17660/ActaHortic.2013.976.75>
- Gharabli, H., Della Gala, V., & Welner, D. H. (2023). The function of UDP-glycosyltransferases in plants and their possible use in crop protection. *Biotechnology Advances*, *67*, 108182. <https://doi.org/10.1016/j.biotechadv.2023.108182>
- Ghasemkhani, M., Holefors, A., Marttila, S., Dalman, K., Zborowska, A., Rur, M., Rees-George, J., Nybom, H., Everett, K. R., Scheper, R. W. A., & Garkava-Gustavsson, L. (2016). Real-time PCR for detection and quantification, and histological characterization of *Neonectria ditissima* in apple trees. *Trees*, *30*(4), 1111–1125. <https://doi.org/10.1007/s00468-015-1350-9>
- Ghasemkhani M. (2015) Resistance against fruit tree canker in apple, vol. 77. Sueciae: Doctoral thesis, Swedish University of Agricultural Sciences, Alnarp, Sweden / Acta Universitas Agriculturae, p. 64.
- Gómez-Cortecero, A., Saville, R. J., Scheper, R. W. A., Bowen, J. K., Agripino De Medeiros, H., Kingsnorth, J., Xu, X., & Harrison, R. J. (2016). Variation in Host and Pathogen in the *Neonectria/Malus* Interaction; toward an Understanding of the Genetic Basis of Resistance to European Canker. *Frontiers in Plant Science*, *7*, 1365. <https://doi.org/10.3389/fpls.2016.01365>
- Gómez-Cortecero, A. (2019). *The molecular basis of pathogenicity of Neonectria ditissima*. Doctoral thesis, University of Reading, Reading, United Kingdom.
- Guo, L., Cesari, S., de Guillen, K., Chalvon, V., Mammri, L., Ma, M., ... & Kroj, T. (2018). Specific recognition of two MAX effectors by integrated HMA domains in plant immune receptors

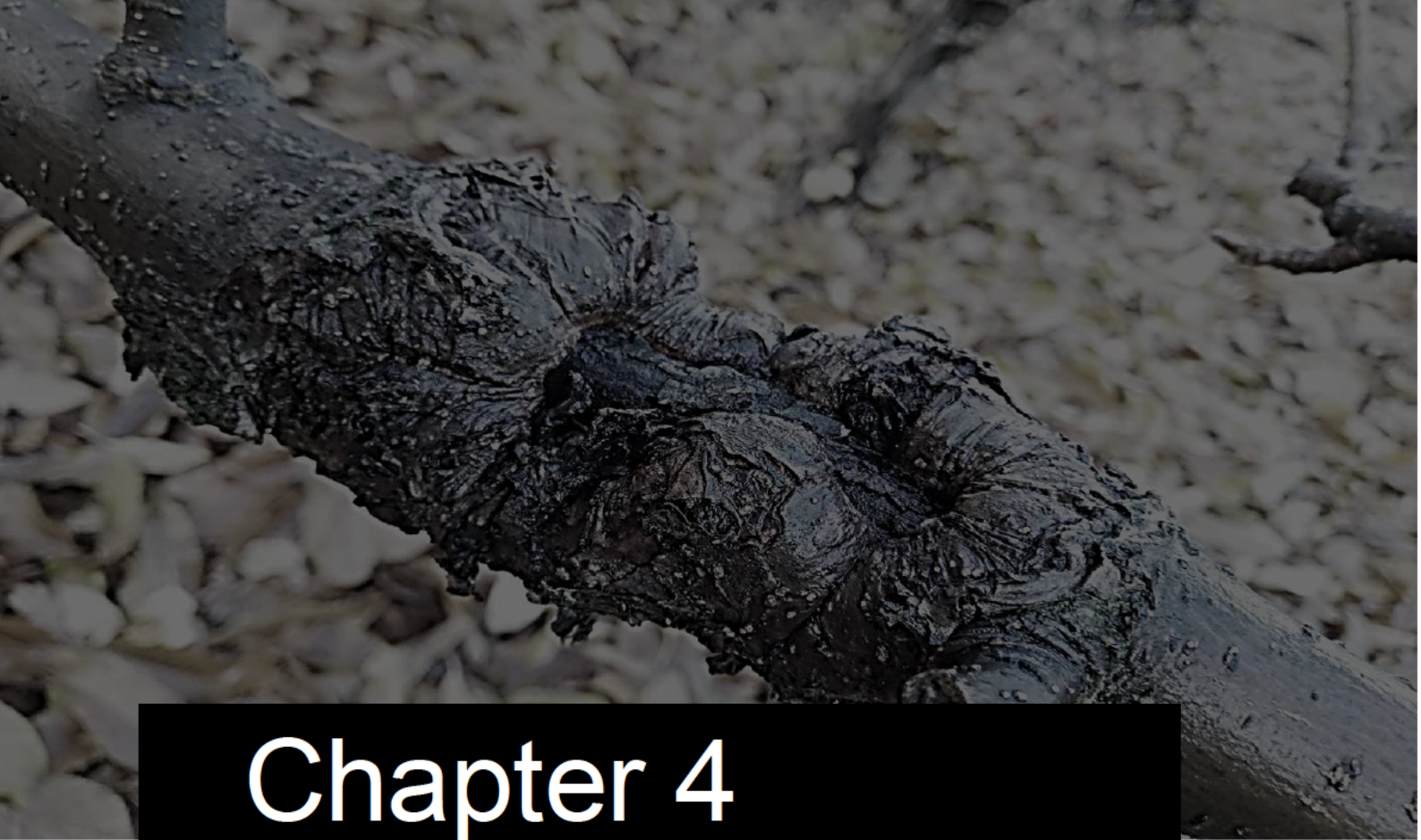
- involves distinct binding surfaces. *Proceedings of the National Academy of Sciences*, 115(45), 11637-11642.
- Gou, M., Balint-Kurti, P., Xu, M., & Yang, Q. (2023). Quantitative disease resistance: Multifaceted players in plant defense. *Journal of Integrative Plant Biology*, 65(2), 594–610. <https://doi.org/10.1111/jipb.13419>
- Gullner, G., Komives, T., Király, L., & Schröder, P. (2018). Glutathione S-Transferase Enzymes in Plant-Pathogen Interactions. *Frontiers in Plant Science*, 9, 1836. <https://doi.org/10.3389/fpls.2018.01836>
- Harkenrider, M., Sharma, R., De Vleeschauwer, D., Tsao, L., Zhang, X., Chern, M., Canlas, P., Zuo, S., & Ronald, P. C. (2016). Overexpression of Rice Wall-Associated Kinase 25 (*OsWAK25*) Alters Resistance to Bacterial and Fungal Pathogens. *Plos One*, 11(1), e0147310. <https://doi.org/10.1371/journal.pone.0147310>
- Hu, Q., Min, L., Yang, X., Jin, S., Zhang, L., Li, Y., Ma, Y., Qi, X., Li, D., Liu, H., Lindsey, K., Zhu, L., & Zhang, X. (2018). Laccase *GhLac1* Modulates Broad-Spectrum Biotic Stress Tolerance via Manipulating Phenylpropanoid Pathway and Jasmonic Acid Synthesis. *Plant Physiology*, 176(2), 1808–1823. <https://doi.org/10.1104/pp.17.01628>
- Jones, J. D. G., & Dangl, J. L. (2006). The plant immune system. *Nature*, 444(7117), 323–329. <https://doi.org/10.1038/nature05286>
- Jung, S., Lee, T., Cheng, C.-H., Buble, K., Zheng, P., Yu, J., Humann, J., Ficklin, S. P., Gasic, K., Scott, K., Frank, M., Ru, S., Hough, H., Evans, K., Peace, C., Olmstead, M., DeVetter, L. W., McFerson, J., Coe, M., ... Main, D. (2019). 15 years of GDR: New data and functionality in the Genome Database for Rosaceae. *Nucleic Acids Research*, 47(D1), D1137–D1145. <https://doi.org/10.1093/nar/gky1000>
- Kanehisa, M., & Goto, S. (2000). KEGG: Kyoto encyclopedia of genes and genomes. *Nucleic Acids Research*, 28(1), 27–30. <https://doi.org/10.1093/nar/28.1.27>
- Karlström, A., Gómez-Cortecero, A., Nellist, C. F., Ordidge, M., Dunwell, J. M., & Harrison, R. J. (2022). Identification of novel genetic regions associated with resistance to European canker in apple. *BMC Plant Biology*, 22(1), 452. <https://doi.org/10.1186/s12870-022-03833-0>

- Kaur, S., Samota, M. K., Choudhary, M., Choudhary, M., Pandey, A. K., Sharma, A., & Thakur, J. (2022). How do plants defend themselves against pathogens-Biochemical mechanisms and genetic interventions. *Physiology and Molecular Biology of Plants : An International Journal of Functional Plant Biology*, 28(2), 485–504. <https://doi.org/10.1007/s12298-022-01146-y>
- Law, C. W., Chen, Y., Shi, W., & Smyth, G. K. (2014). voom: Precision weights unlock linear model analysis tools for RNA-seq read counts. *Genome Biology*, 15(2), R29. <https://doi.org/10.1186/gb-2014-15-2-r29>
- Liao, W., Ji, L., Wang, J., Chen, Z., Ye, M., Ma, H., & An, X. (2014). Identification of glutathione S-transferase genes responding to pathogen infestation in *Populus tomentosa*. *Functional & Integrative Genomics*, 14(3), 517–529. <https://doi.org/10.1007/s10142-014-0379-y>
- Liu, Xiaojie, Li, X., Wen, X., Zhang, Y., Ding, Y., Zhang, Y., Gao, B., & Zhang, D. (2021). PacBio full-length transcriptome of wild apple (*Malus sieversii*) provides insights into canker disease dynamic response. *BMC Genomics*, 22(1), 52. <https://doi.org/10.1186/s12864-021-07366-y>
- Liu, Xintong, Wang, Z., Tian, Y., Zhang, S., Li, D., Dong, W., Zhang, C., & Zhang, Z. (2021). Characterization of wall-associated kinase/wall-associated kinase-like (WAK/WAKL) family in rose (*Rosa chinensis*) reveals the role of *RcWAK4* in *Botrytis* resistance. *BMC Plant Biology*, 21(1), 526. <https://doi.org/10.1186/s12870-021-03307-9>
- Liu, Z., Zhang, Z., Faris, J. D., Oliver, R. P., Syme, R., McDonald, M. C., McDonald, B. A., Solomon, P. S., Lu, S., Shelver, W. L., Xu, S., & Friesen, T. L. (2012). The cysteine rich necrotrophic effector SnTox1 produced by *Stagonospora nodorum* triggers susceptibility of wheat lines harboring Snn1. *PLoS Pathogens*, 8(1), e1002467. <https://doi.org/10.1371/journal.ppat.1002467>
- Li, Peiqin, Ruan, Z., Fei, Z., Yan, J., & Tang, G. (2021). Integrated Transcriptome and Metabolome Analysis Revealed That Flavonoid Biosynthesis May Dominate the Resistance of *Zanthoxylum bungeanum* against Stem Canker. *Journal of Agricultural and Food Chemistry*, 69(22), 6360–6378. <https://doi.org/10.1021/acs.jafc.1c00357>
- Li, Ping, Liu, W., Zhang, Y., Xing, J., Li, J., Feng, J., Su, X., & Zhao, J. (2019). Fungal canker pathogens trigger carbon starvation by inhibiting carbon metabolism in poplar stems. *Scientific Reports*, 9(1), 10111. <https://doi.org/10.1038/s41598-019-46635-5>

- Nakao, M., Nakamura, R., Kita, K., Inukai, R., & Ishikawa, A. (2011). Non-host resistance to penetration and hyphal growth of *Magnaporthe oryzae* in Arabidopsis. *Scientific reports*, 1(1), 171.
- Nelson, R., Wiesner-Hanks, T., Wisser, R., & Balint-Kurti, P. (2018). Navigating complexity to breed disease-resistant crops. *Nature Reviews. Genetics*, 19(1), 21–33. <https://doi.org/10.1038/nrg.2017.82>
- Patro, R., Duggal, G., Love, M. I., Irizarry, R. A., & Kingsford, C. (2017). Salmon provides fast and bias-aware quantification of transcript expression. *Nature Methods*, 14(4), 417–419. <https://doi.org/10.1038/nmeth.4197>
- Paysan-Lafosse, T., Blum, M., Chuguransky, S., Grego, T., Pinto, B. L., Salazar, G. A., Bileschi, M. L., Bork, P., Bridge, A., Colwell, L., Gough, J., Haft, D. H., Letunić, I., Marchler-Bauer, A., Mi, H., Natale, D. A., Orengo, C. A., Pandurangan, A. P., Rivoire, C., ... Bateman, A. (2023). InterPro in 2022. *Nucleic Acids Research*, 51(D1), D418–D427. <https://doi.org/10.1093/nar/gkac993>
- Phipson, B., Lee, S., Majewski, I. J., Alexander, W. S., & Smyth, G. K. (2016). Robust hyperparameter estimation protects against hypervariable genes and improves power to detect differential expression. *The Annals of Applied Statistics*, 10(2), 946–963. <https://doi.org/10.1214/16-AOAS920>
- Radakovic, Z. S., Anjam, M. S., Escobar, E., Chopra, D., Cabrera, J., Silva, A. C., ... & Siddique, S. (2018). Arabidopsis *HIPP27* is a host susceptibility gene for the beet cyst nematode *Heterodera schachtii*. *Molecular Plant Pathology*, 19(8), 1917-1928.
- Robinson, M. D., McCarthy, D. J., & Smyth, G. K. (2010). edgeR: a Bioconductor package for differential expression analysis of digital gene expression data. *Bioinformatics*, 26(1), 139–140. <https://doi.org/10.1093/bioinformatics/btp616>
- Shoji, T. (2014). ATP-binding cassette and multidrug and toxic compound extrusion transporters in plants: a common theme among diverse detoxification mechanisms. *International Review of Cell and Molecular Biology*, 309, 303–346. <https://doi.org/10.1016/B978-0-12-800255-1.00006-5>

- Skytte af Sättra, J., Odilbekov, F., Ingvarsson, P. K., van de Weg, E., & Garkava-Gustavsson, L. (2023). Parametric mapping of QTL for resistance to European canker in apple in 'Aroma' × 'Discovery.' *Tree Genetics & Genomes*, *19*(2), 12. <https://doi.org/10.1007/s11295-023-01587-w>
- Soni, N., Hegde, N., Dhariwal, A., & Kushalappa, A. C. (2020). Role of laccase gene in wheat NILs differing at QTL-Fhb1 for resistance against Fusarium head blight. *Plant Science*, *298*, 110574. <https://doi.org/10.1016/j.plantsci.2020.110574>
- Srivastava, A., Sarkar, H., Gupta, N., & Patro, R. (2016). RapMap: a rapid, sensitive and accurate tool for mapping RNA-seq reads to transcriptomes. *Bioinformatics*, *32*(12), i192–i200. <https://doi.org/10.1093/bioinformatics/btw277>
- Stephens, C., Hammond-Kosack, K. E., & Kanyuka, K. (2022). WAKsing plant immunity, waning diseases. *Journal of Experimental Botany*, *73*(1), 22–37. <https://doi.org/10.1093/jxb/erab422>
- Sun, H., Li, Y., Feng, S., Zou, W., Guo, K., Fan, C., Si, S., & Peng, L. (2013). Analysis of five rice 4-coumarate:coenzyme A ligase enzyme activity and stress response for potential roles in lignin and flavonoid biosynthesis in rice. *Biochemical and Biophysical Research Communications*, *430*(3), 1151–1156. <https://doi.org/10.1016/j.bbrc.2012.12.019>
- Upadhyay, N., Kar, D., Deepak Mahajan, B., Nanda, S., Rahiman, R., Panchakshari, N., Bhagavatula, L., & Datta, S. (2019). The multitasking abilities of MATE transporters in plants. *Journal of Experimental Botany*, *70*(18), 4643–4656. <https://doi.org/10.1093/jxb/erz246>
- Walter, M., Glaister, M. K., Clarke, N. R., Lutz, H. V., Eld, Z., & Amponsah, N. T. (2015). Are shelter belts potential inoculum sources for *Neonectria ditissima* apple tree infections? *New Zealand Plant Protection*, *240*(1975), 227–240.
- Weber, R. W. S. (2014). Biology and control of the apple canker fungus *Neonectria ditissima* (syn. *N. galligena*) from a Northwestern European perspective. *Erwerbs-Obstbau*, *56*(3), 95–107. <https://doi.org/10.1007/s10341-014-0210-x>
- Wu, T., Hu, E., Xu, S., Chen, M., Guo, P., Dai, Z., Feng, T., Zhou, L., Tang, W., Zhan, L., Fu, X., Liu, S., Bo, X., & Yu, G. (2021). clusterProfiler 4.0: A universal enrichment tool for interpreting

- omics data. *Innovation (Cambridge (Mass.))*, 2(3), 100141.
<https://doi.org/10.1016/j.xinn.2021.100141>
- Xu, J., Wang, X., & Guo, W. (2015). The cytochrome P450 superfamily: Key players in plant development and defense. *Journal of Integrative Agriculture*, 14(9), 1673–1686.
[https://doi.org/10.1016/S2095-3119\(14\)60980-1](https://doi.org/10.1016/S2095-3119(14)60980-1)
- Yang, C., Liang, Y., Qiu, D., Zeng, H., Yuan, J., & Yang, X. (2018). Lignin metabolism involves *Botrytis cinerea* BcGs1- induced defense response in tomato. *BMC Plant Biology*, 18(1), 103.
<https://doi.org/10.1186/s12870-018-1319-0>
- Yuan, M., Ngou, B. P. M., Ding, P., & Xin, X.-F. (2021). PTI-ETI crosstalk: an integrative view of plant immunity. *Current Opinion in Plant Biology*, 62, 102030.
<https://doi.org/10.1016/j.pbi.2021.102030>
- Yu, X., Gong, H., Cao, L., Hou, Y., & Qu, S. (2020). MicroRNA397b negatively regulates resistance of *Malus hupehensis* to *Botryosphaeria dothidea* by modulating *MhLAC7* involved in lignin biosynthesis. *Plant Science*, 292, 110390. <https://doi.org/10.1016/j.plantsci.2019.110390>
- Zuo, C., Liu, Y., Guo, Z., Mao, J., Chu, M., & Chen, B. (2018). Genome-wide annotation and expression responses to biotic stresses of the WALL-ASSOCIATED KINASE - RECEPTOR-LIKE KINASE (WAK-RLK) gene family in Apple (*Malus domestica*). *European Journal of Plant Pathology*, 153(3), 1–15. <https://doi.org/10.1007/s10658-018-1591-8>



Chapter 4

Quantitative trait loci associated with apple endophytes during pathogen infection

This chapter explores the feasibility to breed apple cultivars amenable to endophyte colonization and discusses the association of specific endophytic taxa with tolerance to *Neonectria ditissima*. The aim of this work is to identify genetic regions that promote host-microbial associations with *N. ditissima* suppressive endophytes. This information can be used to inform breeding of new cultivars with disease suppressive microbiomes and to facilitate the identification of genes that promote associations with beneficial microorganisms. The work is based on a previous publication by Papp-Rupar et al (2022), in which it was shown that apple genotype has a significant effect on the abundance of several bacterial and fungal endophyte taxa. The amplicon sequencing data from wood endophytes in the prior study was used together with SNP marker data to study QTL influencing the phyllosphere microbiome assembly.



OPEN ACCESS

EDITED BY

Pablo Velasco,
Biological Mission of Galicia, Spanish
National Research Council (CSIC), Spain

REVIEWED BY

Eric Morrison,
University of New Hampshire, United States
Bohra Amina Bahri,
University of Georgia, United States

*CORRESPONDENCE

Amanda Karlström
✉ Amanda.Karlstrom@niab.com

SPECIALTY SECTION

This article was submitted to
Plant Breeding,
a section of the journal
Frontiers in Plant Science

RECEIVED 27 September 2022

ACCEPTED 15 March 2023

PUBLISHED 28 March 2023

CITATION

Karlström A, Papp R, Rugar M, Passey TAJ,
Deakin G and Xu X (2023) Quantitative trait
loci associated with apple endophytes
during pathogen infection.
Front. Plant Sci. 14:1054914.
doi: 10.3389/fpls.2023.1054914

COPYRIGHT

© 2023 Karlström, Papp Rugar, Passey,
Deakin and Xu. This is an open access article
distributed under the terms of the [Creative
Commons Attribution License \(CC BY\)](#). The
use, distribution or reproduction in other
forums is permitted, provided the original
author(s) and the copyright owner(s) are
credited and that the original publication in
this journal is cited, in accordance with
accepted academic practice. No use,
distribution or reproduction is permitted
which does not comply with these terms.

Quantitative trait loci associated with apple endophytes during pathogen infection

Amanda Karlström*, Matevz Papp-Rugar, Tom A. J. Passey,
Greg Deakin and Xiangming Xu

NIAB East Malling, East Malling, United Kingdom

The plant phyllosphere is colonized by microbial communities that can influence the fitness and growth of their host, including the host's resilience to plant pathogens. There are multiple factors involved in shaping the assemblages of bacterial and fungal endophytes within the phyllosphere, including host genetics and environment. In this work, the role of host genetics in plant-microbiome assembly was studied in a full-sibling family of apple (*Malus x domestica*) trees infected with the fungal pathogen *Neonectria ditissima*. A Quantitative Trait Loci (QTL) analysis showed that there are multiple loci which influence the abundance of individual endophytic taxa, with the majority of QTL having a moderate to large effect (20–40%) on endophyte abundance. QTL regions on LG 1, 3, 4, 5, 10, 12, 13, 14 and 15 were shown to affect multiple taxa. Only a small proportion of the variation in overall taxonomic composition was affected by host genotype, with significant QTL hits for principal components explaining <8% and <7.4% of the total variance in bacterial and fungal composition, respectively. Four of the identified QTL colocalised with previously identified regions associated with tolerance to *Neonectria ditissima*. These results suggest that there is a genetic basis shaping apple endophyte composition and that microbe-host associations in apple could be tailored through breeding.

KEYWORDS

apple, microbiome, *Neonectria ditissima*, European canker, phyllosphere, *Malus x domestica*

Introduction

Neonectria ditissima is a fungal pathogen that causes wood cankers in apple and other broad-leaved trees (Weber, 2014; Saville et al., 2019) in most of the temperate areas of the world. A most damaging aspect of this disease is that latent infection established in nurseries can develop into main stem cankers post-planting, rapidly girdling the trees resulting in high tree mortality in young high intensity orchards. Given the withdrawal of several effective fungicides (e.g. carbendazim and copper-based products), host resistance is thus an important component in managing canker disease. Many modern apple varieties

are highly susceptible to *N. ditissima* (Gomez-Cortecero et al., 2016; Papp-Rupar et al., 2022). Since host resistance against *N. ditissima* is quantitative (Gomez-Cortecero et al., 2016; Bus et al., 2019), it may take a long time to breed apple cultivars with effective resistance against the pathogen. The effects of identified apple scion Quantitative Trait Loci (QTL) on disease resistance are low to moderate, with 4.3 to 19% of variance explained by a single QTL (Karlström et al., 2022).

Many bacterial and fungal endophytes can improve tolerance of host plants to abiotic and biotic stresses and enhance their growth (Khare et al., 2018; Omomowo and Babalola, 2019; Dini-Andreote, 2020). A number of apple endophytes at leaf scars, a major entry site of *N. ditissima*, are associated with host susceptibility to *N. ditissima* (Olivieri et al., 2021). Furthermore, specific endophytes from apple show *in-vitro* antagonistic effects against *N. ditissima* (Liu et al., 2020). Apple genotypes can significantly influence endophyte species richness and composition (Hirakue and Sugiyama, 2018; Liu et al., 2018; Liu et al., 2020) and cultivars with a higher degree of relatedness share similarities in endophyte community (Liu et al., 2018). In addition to cultivar, environment and apple tissue type can also considerably influence endophyte composition (Liu et al., 2020; Olivieri et al., 2021).

Apple endophyte composition could potentially be altered through specific agronomic practices or augmentation of specific endophyte strains with biocontrol ability to reduce susceptibility to *N. ditissima*. In breeding programmes, specific (desirable) endophytes may be included as a selection criterion to breed cultivars with disease suppressive endophyte composition. To adopt this second approach, we need to assess the magnitude of the heritability of endophyte communities and to exploit genetic markers for specific endophytic components.

In a previous paper (Papp-Rupar et al., 2022), we used F₁ progeny trees derived from a cross between two moderately canker tolerant cultivars in an experimental orchard to determine the variability and heritability of bacterial and fungal endophyte communities in apple leaf scars. We also estimated correlations of endophytes with canker development. The results showed that specific components of endophytes as well as individual fungal/bacterial taxa in leaf scars were partially controlled by host genotypes. The broad sense heritability for specific aspect of endophytic composition and individual bacterial/fungal groups ranged between 0.05 to 0.37.

This study further investigates the host-genetic factors associated with endophytes and uses the metabarcoding data set from our previous publication (Papp-Rupar et al., 2022) to identify genetic regions involved in shaping apple endophyte composition. Through this analysis we aim to understand the genetic architecture of the interaction between the apple host and the microbial communities contained within its wood. The genetic mapping can also provide tools, in the form of molecular markers, to tailor microbe-host associations through breeding. Traits (Principal Components [PC]) of endophytes or abundance of individual endophyte taxa) that showed significant genetic variability among F₁ progeny trees in the previous study were included in the QTL analysis in this study.

Materials and methods

Experimental design, canker assessment and endophyte profiling

Experimental materials and methods including orchard layout, canker inoculation, disease monitoring, profiling of fungal and bacterial endophytes, bioinformatic processing of amplicon sequences, and estimation of broad-sense heritability of endophytes were fully described in our previous publication (Papp-Rupar et al., 2022). The methodology is briefly described below to aid the understanding of this study.

A biparental cross between ‘Aroma’ x ‘Golden Delicious’ cultivars consisting of 56 genotypes including the two parents and 54 F₁ genotypes were grafted on M9 EMLA rootstock. Four replicate trees were grown in a randomised block design in an orchard at East Malling, Kent, UK. Five leaf scars were inoculated per tree (one per shoot) with *N. ditissima* Hg199 isolate. The length of canker lesions was measured at 5, 8 and 11 months post inoculation (mpi) and the average canker lesion size at every used in further analysis (Karlström et al., 2022). The trees were also assessed at 20 mpi for percent canopy area with healthy foliage (Healthy Tree Area, %HTA) and percent branches with canker (Cankered Branches, %CB).

The samples for endophyte analysis were taken by dissecting 12 freshly exposed leaf scars per tree according to Olivieri et al. (2021). Sampled leaf scars were taken from four healthy, one-year-old shoots per tree. DNA was extracted (DNeasy Plant Mini kit, Qiagen) and subjected to amplicon sequencing of ITS1 (ITS1-1F/ITS2; White et al., 1990; Gardes and Bruns, 1993) and 16S V5-V7 (799F/1193R, Chelius and Triplett, 2001; Bodenhausen et al., 2013) regions.

Amplicon sequence data were processed to produce OTU representative sequences and frequency tables with the UPARSE pipeline (Version 10.0) (Edgar, 2013), as previously described (Papp-Rupar et al., 2022). The lowest taxonomic rank with a confidence of $\geq 80\%$ has been used to describe the OTUs. The fungal and bacterial OTU abundance tables were normalised by the median-of-ratios (MR) method implemented in DESeq2 (Love et al., 2014).

Traits for QTL analysis

Variance in endophyte abundances attributed to the host genetic factor was statistically tested in the previous study (Papp-Rupar et al., 2022) by comparing a model with the genotypic component included with the model without (Chi square, df=1). Bacterial and fungal PCs and OTUs for which there was a significant host genotypic effect ($\alpha=0.05$) found in previously published research (Papp-Rupar et al., 2022) were included in the QTL analysis in this study, namely, bacteria: 7 PCs and 47 OTUs, fungi: 4 PCs and 22 OTUs. Associations between traits were evaluated using the native R-function `cor.test` with Pearson correlation using data from individual trees. All statistical

analyses were conducted in R (version 4.0.4; R Core Team, 2014). Average values across all four replicates were used for the QTL analysis.

Genotypic data for the apple biparental population and linkage map DNA from the biparental population and the two parental cultivars were extracted as per Karlström et al. (2022). The population was genotyped on the Illumina Infinium® 20k SNP array. Genotype assignment was performed in GenomeStudio Genotyping Module 2.0 (Illumina). SNP filtering was conducted in ASSisT, leaving 11,000 SNPs to be used for further analysis.

QTL analysis

The linkage map used for the analysis was produced in the OneMap package (Margarido et al., 2007). Markers were removed from the dataset if they had a distorted segregation, both parents were homozygous, or both parents had missing genotype data for the marker. To reduce the computational burden, markers with a pairwise recombination fraction of zero were collapsed into bins represented by the marker with the lower amount of missing data among those in the bin. A LOD score ≥ 3.0 and recombination fraction ≥ 0.50 were considered to indicate linkage between markers. Markers were ordered according to the iGL consensus linkage map (di Piero et al., 2016) whereas genetic distances between markers were calculated by OneMap using the Kosambi mapping function. The relationship between segregations of single markers and traits were analysed with a Kruskal-Wallis test (K-W) using the 'kruskal.test' function and the Benjamini-Hochberg method (Benjamini and Hochberg, 1995) was used to adjust p-values for false discovery rate. QTL positions of significant K-W markers were determined as their position on the linkage map produced in Onemap. The position of markers which had been removed in the binning process were given by a marker from within the same bin. The percentages of phenotypic variation (R^2) explained by QTLs were estimated in FullsibQTL. All significant QTL positions were included in the calculation of QTL effects for each phenotype.

Verification of the QTL mapping was performed through Composite Interval Mapping (CIM) in the FullsibQTL package as described previously (Gazaffi et al., 2014). A maximum of 10 cofactors were stipulated to locate QTLs. A random permutation test ($\alpha = 0.05$; $n = 1000$ replicates) in FullsibQTL was used to determine the critical Logarithm of Odds (LOD) score for declaring the presence of a true QTL.

Results

Trait data

The studied endophyte abundance traits showed normal distributions in the studied population. Distributions of trait data for each trait associated with a QTL is shown in Supplementary Figure 1. Mean values for the biparental population and the two parents is shown in Supplementary Table 2, 3. The correlation in

the abundance of endophyte and canker disease traits are shown in Supplementary Figure 2 to indicate the degree of correlation among these phenotypic traits. Further descriptions of trait data from the same experiment is detailed in Karlström et al. (2022) and Papp-Rupar et al. (2022) for disease and endophyte abundance results, respectively. Disease results for standard reference cultivars from the field experiment is detailed in Karlström et al. (2022).

Linkage map

The linkage map had 8,032 SNP markers, which were divided into 3,681 bins to produce the map. Markers were distributed along 9,685 cM with an average distance between markers of 2.56 cM (Supplementary Table 1). The ordering of markers was forced to follow the map positions in the iGL consensus map produced by di Piero et al. (2016). The linkage map from the Aroma x Golden Delicious population deviated substantially in size from the consensus map, as it was 8,418 cM longer and had a larger average distance between markers compared to the consensus map.

QTL analysis

Bacterial endophytes

There were significant QTLs associated with 21 of the 47 OTUs (Tables 1, 2; Supplementary Table 2). These significant QTL hits were distributed over 15 linkage groups (LGs) with the QTL position on seven LGs (LG1, 4, 5, 10, 12, 14, 15) associated with multiple bacterial OTUs (Figure 1). The seven PCs representing specific bacterial endophyte communities in apple leaf scars were associated with QTL hits on five LGs, four of which were present at positions that were supported by multiple phenotypes. The CIM analysis resulted in 37 significant hits across all bacterial abundance traits and LGs (Table 1), whereas 17 significant marker-trait associations were identified with the K-W test (Table 2). The QTL positions on LG 4, 5, 10, 12, 14 and 15 were supported by both the CIM and K-W test. Only SNP marker alleles of QTL detected with both methods are described below.

A QTL on LG4 was associated with PC17 and the abundance of five bacterial OTUs: Proteobacteria (OTU922), Microbacteriaceae (OTU462), *Kineococcus* (OTU5), *Nocardioidea* (OTU42) and *Deinococcus* (OTU135). The QTL position on LG4 of *Deinococcus* (OTU135) was supported by both the CIM and K-W test (Tables 1, 2; Figure 1). A lower relative abundance of this OTU segregated with the 'A'-allele of the SNP marker FB 0593780 (Figure 2), which was located in the centre of the QTL. The 'A'-allele was inherited from both parents and seemed to have a dominant effect on the *Deinococcus* abundance. The QTL effect for LG4, as estimated from the CIM analysis, ranged from 4.5% to 32.0% (with an average of 23.0%) depending on bacterial abundance trait (Table 1).

A QTL region on LG5 was associated with 16s PC2 and three OTUs: Rhodobacteraceae (OTU100), Deltaproteobacteria (OTU124) and Rhodospirillales (OTU3169) (Figure 1). The QTL position for Deltaproteobacteria OTU124 was supported by both the CIM and K-W test (Tables 1, 2). The 'A'-allele, inherited from

TABLE 1 Quantitative trait loci (QTL) composite interval mapping for abundance data of bacterial (16S) and fungal (ITS) endophytes in apple leaf scar tissues of a full-siblings mapping population of a 'Aroma' x 'Golden Delicious' cross.

Trait	Taxonomy (> 80% confidence)	LG	Position (cM)		Maximum LOD	Maximum LOD-score	R ² (%)	Correlation to canker severity (%HTA)
			Start	Finish				
16S								
OTU644	Actinobacteria	16	439	442	442	11	1	
OTU27	Aurantimonadaceae	13	358	370	365	12	27	
OTU38	Aureimonas							0.22
		10	28	33	32	10	26	
		14	21	32	26	11	22	
OTU128	Bacteria	10	111	122	120	13	36	
OTU950	Bacteria							-0.095
		1	326	334	332	14	34	
		17	57	63	62	12	19	
OTU52	Comamonadaceae	2	102	114	110	14	36	
		7	129	132	74	10	12	
		12	74	84	81	10	27	
OTU18	Deinococcus	10	573	581	581	10	6	
		15	0	5	5	10	25	
OTU135	Deinococcus							0.07
		4	513	519	516	11	29	
		10	115	124	120	11	22	
OTU124	Deltaproteobacteria	5	261	271	267	14	31	
		8	505	508	508	10	6	
OTU5	Kineococcus	4	332	340	340	9	4	
OTU53	Marmoricola	15	2	13	7	11	37	
OTU462	Microbacteriaceae	4	293	304	299	12	27	
		10	573	581	579	11	6	
OTU42	Nocardioides	4	394	397	399	9	26	
		6	179	186	179	11	23	
		13	153	162	156	10	16	
OTU922	Proteobacteria	4	292	304	304	15	32	
OTU85	Pseudokineococcus	3	367	376	374	11	13	
		6	421	432	429	11	26	
		15	229	240	232	11	27	
OTU100	Rhodobacteraceae	5	203	216	213	12	29	0.11
OTU3169	Rhodospirillales	5	286	295	290	9	24	
OTU84	Roseomonas	12	493	512	499	13	34	0.10
OTU8	Sphingomonas	10	253	266	262	16	50	0.23
OTU99	Terracoccus	1	326	334	332	14	36	
		16	86	100	93	12	20	

(Continued)

TABLE 1 Continued

Trait	Taxonomy (> 80% confidence)	LG	Position (cM)		Maximum LOD	Maximum LOD-score	R ² (%)	Correlation to canker severity (%HTA)
			Start	Finish				
OTU60	Williamsia	14	0	7	0	13	35	
PC16		8	63	75	71	13	35	
PC17		4	399	408	404	10	23	
PC7		14	0	1	0	10	36	0.26
ITS								
OTU143	Dothideomycetes	15	511	521	511	11	40	0.10
OTU35	Entyloma	3	436	440	438	11	44	-0.14
OTU50	Entyloma calendulae	14	19	25	25	12	35	-0.12
OTU12	Fungi	12	402	409	405	10	42	
OTU19	Fungi							-0.008
		6	531	546	536	13	27	
		15	402	412	402	12	15	
OTU40	Fungi	13	206	213	210	10	23	
OTU62	Phaeosphaeriaceae	15	197	200	199	10	3	
OTU26	Subplenodomus iridicola	1	321	324	322	13	19	0.003
OTU71	Taphrina							-0.05
		8	141	152	141	11	17	
		17	312	315	314	11	34	
OTU310	Taphrina	16	15	22	20	12	25	
OTU15	Tilletiopsis washingtonensis	3	544	561	549	11	30	
PC3								-0.19
		4	502	518	508	11	22	
		6	442	445	444	12	30	
PC11		5	0	13	4	10	7	
		10	0	59	9	17	20	

For traits with a significant correlation to canker severity, the Pearson correlation coefficient to % healthy tree area (%HTA) is shown.

'Golden Delicious', for the SNP FB 0614211 was associated with a lower abundance of the Deltaproteobacteria OTU124 (Figure 2). The CIM analysis estimated the effect of the QTL on LG5 in the range of 24.0 to 31.0% (Table 1).

One region in the top of LG10 was associated with five OTUs: *Sphingomonas* (OTU8), *Aureimonas* (OTU38), *Deinococcus* (OTU135), and two OTUs (OTU59 and OTU128) that could only be assigned to the bacteria kingdom with 80% confidence (Table 1). The CIM QTL position was supported by K-W test for three OTUs – OTU8, OTU38 and OTU135 (Table 2; Figure 1). The SNP marker FB 0726172 had a significant effect on these three traits and the 'B'-allele for this marker, inherited from 'Aroma', was associated with a higher abundance of the bacterial groups (Figure 2). A second QTL region, positioned at the bottom of LG10, was associated with the abundance of *Deinococcus* (OTU18) and Microbacteriaceae (OTU462). The effect of the QTL on LG10

was estimated to be in the range of 6.0% to 50.0%, with an average of 24.0% (Table 1).

Significant QTL hits were identified on LG12 for PC7 and three OTUs: *Aureimonas* (OTU38), Comamonadaceae (OTU52) and *Roseomonas* (OTU84). The QTL location on LG12 was supported by both the CIM and K-W test for *Roseomonas* OTU84 only. The 'A'-allele of the significant SNP marker FB 0140805 was inherited from 'Golden Delicious' and associated with a lower abundance of *Roseomonas* OTU84. Interestingly, the same allele was linked to higher relative abundance of the fungal OTU12, for which taxonomic rank below kingdom could not be assigned (Table 1; Figure 2). The CIM estimated that the QTL on LG12 for OTU52 and OTU84 accounted for 27.0% and 34.0% of the total phenotypic variation, respectively (Table 1).

OTU60 (*Williamsia*), OTU38 (*Aureimonas*) and PC7 were associated with QTLs positioned on LG14. The QTL on LG14

TABLE 2 Quantitative trait loci (QTL) identified from Kruskal-Wallis test for abundance data of bacterial (16s) and fungal (ITS) endophytes in apple leaf scar tissues of a full-sibling mapping population of 'Aroma' x 'Golden Delicious' cross.

Trait	Taxonomy (> 80% confidence)	LG	Position (cM)		Correlation to canker severity (%HTA)
			Start	Finish	
16s					
OTU38	Aureimonas				0.22
		6	3	57	
		10	32	366	
		12	120	544	
		14	26	26	
OTU59	Bacteria	10	32	169	0.13
OTU135	Deinococcus				0.07
		4	512	516	
		10	120	143	
OTU124	Deltaproteobacteria	5	156	291	
OTU53	Marmoricola	15	37	37	
OTU3169	Rhodospirillales	15	20	37	
OTU84	Roseomonas	12	440	514	0.10
OTU20	Sphingomonadaceae	15	37	37	
OTU8	Sphingomonas	10	32	386	0.23
PC2		5	255	291	
		15	37	37	
PC7					0.26
		12	116	518	
		14	8	47	
ITS					
OTU12	Fungi	12	74	544	

For traits with a significant correlation to canker severity, the Pearson correlation coefficient to % healthy tree area (%HTA) is shown.

were identified on LG1, 3, 4, 5, 6, 8, 10, 12, 14, 15, 16 and 17. The majority of QTL hits were identified by the CIM analysis, whereas only one significant QTL location on LG12 (for OTU12 – Fungi) was identified by the K-W test.

A significant QTL associated with OTU26 (*Subplenodomus iridicola*) was identified on LG1. The same QTL position was also associated with two bacterial OTUs (OTU950 and OTU99, Figure 1). The QTL on LG1 explained 19% of the variation in abundance of *Subplenodomus iridicola* OTU26. Two QTLs were identified on LG3 for OTU15 (*Tilletiopsis washingtonensis*) and OTU35 (*Entyloma*), with the respective estimated QTL effect of 30.0% and 44.0% (Table 1).

The QTL location on LG12 associated with OTU12 (Fungi) was identified with both the CIM and K-W analysis and had a effect size of 42% (Table 1). A single fungal OTU had a QTL hit on LG13 (OTU40, Fungi), this LG was also associated with the bacterial endophyte traits OTU42 (Nocardioides) and OTU27

(Aurantimonadaceae). However, different genetic positions were identified for each of the three QTL (Figure 1).

Three fungal OTUs had significant QTL hits on LG15, with the estimated effects in the range of 3.0% to 40.0%. These fungal OTUs associated with LG15 were OTU19 (Fungi), OTU62 (Phaeosphaeriaceae) and OTU143 (Dothideomycetes). The fungal endophyte QTL on LG15 do not overlap with the QTL associated with the bacterial endophyte traits.

Fungal PC3 had two QTL hits, one on LG4 which overlapped with QTL for the bacterial OTU135 (*Deinococcus*) and one on LG6. The QTL hits had estimated effect sizes of 22 and 30%, respectively (Table 1), and together account for over half of the genetic variation in this trait.

Canker phenotypes

There was no significant QTL associated with canker traits (lesion size, %HTA or %CB) from either CIM or K-W analysis.

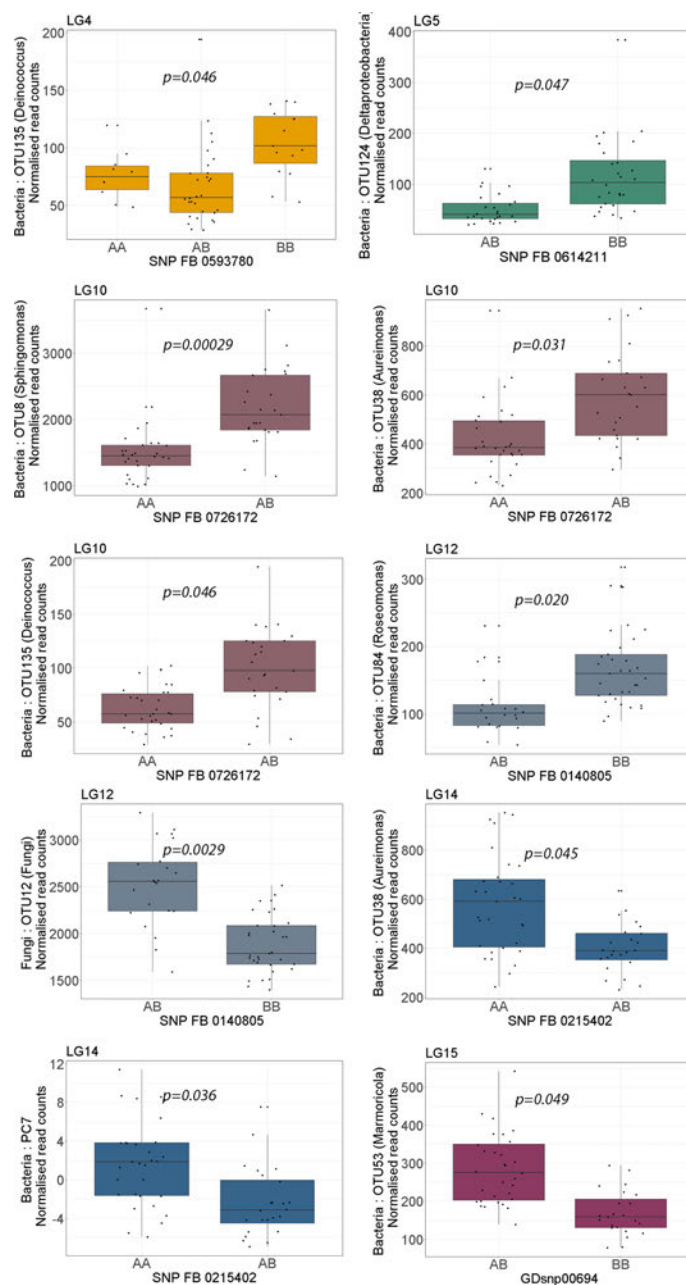


FIGURE 2

Boxplots showing the effect of phenotypic variation between SNP marker genotypes linked to QTLs for endophyte abundance. Kruskal Wallis test was used to determine the significant differences between the mean values of SNP genotypes. Graph colour indicates the respective linkage group (LG) of the QTL.

Association between QTL traits and severity of European canker

Significant correlations between endophyte abundance traits and European canker disease based on adjusted P-values were given in Papp-Rupar et al. (2022). Here we focused on the correlation between canker development and those microbial traits with significant QTLs identified. In addition, significance of correlations in this study was not adjusted as in the previous research. There was a significant correlation between OTU abundance/PC score and canker disease phenotypes for 11 of

the 27 bacterial traits for which significant QTL were identified (Tables 1 and 2). The bacterial endophytes belonging to OTU59 (Bacteria), OTU38 (*Aureimonas*), OTU135 (*Deinococcus*) and OTU8 (*Sphingomonas*) for which QTL regions positioned in the top of LG 10 were identified were positively correlated with % HTA (Tables 1, 2). i.e. higher abundance was present in the trees with higher % of healthy canopy). Similarly, bacterial endophyte traits that were associated with the QTL regions on LG 12 (*Roseomonas*-OTU84, *Aureimonas*-OTU38) and LG 14 (*Aureimonas*-OTU38, 16s-PC7) were positively correlated with %HTA (Tables 1, 2).

Discussion

A number of studies in maize, Arabidopsis, rye grass and lettuce have investigated the genetic control of endophytic community by the plant host (Horton et al., 2014; Faville et al., 2015; Wallace et al., 2018; Damerum et al., 2021). It has further been shown that specific genetic regions control the association between plants and beneficial microbes (Vidotti et al., 2019; Yassue et al., 2021; Brachi et al., 2022), and that there is variation in the phyllosphere microbiome between resistant and susceptible genotypes (Balint-Kurti et al., 2010; Ginnan et al., 2020; Xueliang et al., 2020). This is, however, the first study to investigate QTLs that potentially affect endophyte recruitment in woody tissues and their association with resistance to European canker.

QTL associated with bacterial and fungal endophytes

Previously we reported significant effect of apple host genotype on 20% of the 200 most abundant bacterial OTUs and 13% of the 100 most abundant fungal OTUs (Papp-Rupar et al., 2022). The current study found that the abundance data of approximately 40–60% of these OTUs could be associated with QTLs in the host. The failure to detect QTLs for a proportion of the OTUs influenced by host genotype could be due to the presence of small effect QTLs for which the size of the studied population was not sufficient to identify, or due to a lack of markers segregating with the causative variation in the genetic region of interest.

The majority of identified QTLs had a moderate-large effect on OTU abundance with R^2 -values in the range of 20–40%. This indicates the feasibility to breed cultivars with enhanced ability to harbour small number of specific endophytic taxa. The results from this study would need to be reproduced in additional sites and years as spatial and temporal variability is known to affect endophyte composition. It has been demonstrated that there is a large spatial variability in endophyte composition in above-ground plant tissues. For example, block within orchard and orchard site have significant effect on apple leaf scar community of the same apple genotypes (Olivieri et al., 2021). Differences in microclimatic conditions, management practice and the environmental inoculum (load and diversity) could be explain the observed differences. Site-specific soil factors, including pH, carbon content, and C:N ratio, were also found to affect endophyte community (Pacífico et al., 2019). Additionally, our unpublished data on apple leaf scar microbiomes sampled in spring and autumn suggests that both size and diversity of leaf scar communities change with season. Tree age has also been found to be an important factor affecting foliar endophytes (Yu et al., 2021). Taken together, the significance and effect size of QTLs identified here could be affected by the properties of local climatic conditions, soil properties, inoculum availability and tree age.

Sphingomonas (OTU8) was associated with a QTL on LG10 and positively correlated with %HTA in the present data, indicting a potential role in suppressing disease development or improving general plant health. We note that OTU8 abundance significantly correlated with canker traits in this study where a subset of 45 traits (with QTLs identified) were analysed, but not in the previous

research that used 300 most abundant traits (Papp-Rupar et al., 2022). Higher number of traits analysed in the previous research necessitated correction for multiple tests – thus a higher correlation is needed to achieve statistical significance. A different *Sphingomonas* OTU (OTU72) was found to correlate with %HTA in the previous research, however, no QTL was found associated with it in this study. Moreover, we recently showed that several abundant *Sphingomonas* OTUs had an overall higher relative abundance in several *N. ditissima* resistant apple cultivars than in susceptible cultivars when assessed three times over two growing seasons at two sites (Xu, unpublished). Specific *Sphingomonas* strains are known to promote plant growth (Pan et al., 2016; Luo et al., 2019). Furthermore, one seed-endophytic strain, *Sphingomonas melonis* ZJ26, is naturally enriched in specific rice cultivars and confers resistance against a bacterial pathogen (Matsumoto et al., 2021).

The relative abundance of *Sphingomonas* OTU8 was associated with a large effect QTL ($R^2 = 50\%$) and hence amenable to conventional breeding. The ‘B’ allele of the SNP marker FB 0726172, which is located within this QTL, was associated with a higher abundance of *Sphingomonas*. Thus, marker assisted breeding could be a feasible approach for manipulating the association of apple trees with this taxa, although the effect of this molecular marker would need to be confirmed in a wider range of germplasm.

Aureimonas (OTU38) was linked to QTL hits on LG10 and LG14, and positively correlated to tree health in plants inoculated with canker (%HTA). This genus has previously been found in increased abundance in the leaf phyllosphere of ash trees tolerant to the fungal disease ash dieback, *Hymenoscyphus fraxineus* (Ulrich et al., 2020). The inoculation of ash seedlings with *Aureimonas altamirensis* C2P003 had positive effect on the plant health and reduced ash dieback symptoms (Becker et al., 2022). Furthermore, a study has shown an isolate of *Aureimonas* to have antifungal activity towards rice blast, *Magnaporthe oryzae*. The two QTL identified in this study together accounted for 48% of the genetic variation of OTU abundance. Interestingly, the SNP allele inherited from ‘Aroma’ for FB 0726172 on LG10 was associated with a higher abundance of OTUs from *Sphingomonas*, *Aureimonas* as well as *Deinococcus*. The number of normalised read counts of these three bacterial groups were approximately double in ‘Aroma’ compared to ‘Golden Delicious’. Hence, this locus may have a role in promoting associations with multiple beneficial microbes and is of interest for further studies. *Sphingomonas* spp. and *Aureimonas* spp. would be good candidates to further explore in terms of effect on canker disease development as well as understanding the molecular mechanisms underlying the QTL identified in this study.

Only minor PCs were shown to be significantly affected by host genotype (Papp-Rupar et al., 2022). The variation in endophyte abundance attributed to PCs with significant QTL hits was <8% for bacterial and <7.4% for fungal PCs. Hence breeding may have limited scope to target changes in larger endophytic features/communities. This contrasts with studies of rhizosphere endophyte communities, where major PCs have been shown to be associated with host genotype (Deng et al., 2021; Oyserman et al., 2022). This could be due to a broader and more active interaction between roots and microbes (through root exudates and other

mechanisms) compared to the very specific interaction of particular strains in above-ground tissues (e.g. leaf-scars).

The linkage map used in our study based on the ‘Aroma’ x ‘Golden Delicious’ population was highly inflated compared to the iGL consensus map from which the marker orders were derived (di Pierro et al., 2016). This is likely due to a higher number of co-segregating markers in the biparental population as there is a limited number of recombination events compared to the multiple populations used to produce the consensus map (N’Diaye et al., 2017)

Co-localisation of endophyte QTL and genetic regions associated with susceptibility to European canker

Several QTL regions (on LG 5, 8, 15 and 16) associated with endophyte abundance and composition colocalize with previously identified QTLs for resistance to *N. ditissima* (Karlström et al., 2022). OTU3169 (*Rhodospirillales*) and the bacterial PC2 had two QTL hits colocalizing with canker QTLs (on LG5 and 15), whereas the other OTUs/PCs with overlapping hits were specific to one of the canker QTL regions. Only a subset of the endophyte QTL with significant correlation to canker traits had QTL hits that co-localised with previously reported resistance QTL (bacteria: OTU8, OTU38, OTU59, OTU100, OTU159, fungi: PC3, OTU19, OTU71, OTU143). However, the canker disease QTL reported by Karlström et al. (2022) had small to moderate effect sizes (4–19%). The effect sizes of QTL associated with the bacterial traits that were correlated with canker traits were comparably larger. It is therefore plausible that the population size used by Karlström et al. (2022) was not sufficient to identify some small effect QTL associated with canker disease traits, however, the biparental population used in this study was enough to detect endophyte QTL which had relatively larger effect sizes.

The mode of action of QTLs associated with endophyte abundance and *N. ditissima* resistance are so far unknown. Plant host factors that have been shown to affect the phyllosphere microbiome include plant immunity, signalling, cuticle formation and secondary metabolites (Kniskern et al., 2007; Vogel et al., 2016; Chen et al., 2020; Jacoby et al., 2021). Similar molecular functions may influence the abundance of specific endophytes as well as the ability to reduce *N. ditissima* spread within the plant. Indeed, genes that are differentially regulated in apple trees after *Neonectria* infection are involved in plant defences and cell wall modifications (Ghasemkhani, 2015). Further studies will be needed to fully decipher whether identified QTLs have a direct effect in shaping phyllosphere community, or whether the shift in microbial composition is due to microbe-*Neonectria* interactions or altered plant responses.

Data availability statement

The sequence data presented in the study are deposited in the European Nucleotide Archive (ENA), accession number:

PRJEB49633. The SNP data presented in the study are deposited European Variation Archive, accession number PRJEB54689. The linkage map, trait data for each genotype and SNP data can be found in a supplementary data file.

Author contributions

XX conceived the study. XX, AK, TP and MP-R designed, planned and carried out the experiment. GD performed OTU clustering and taxonomy assignment. AK produced the linkage map and carried out the QTL analysis. AK and XX wrote the manuscript. All authors discussed the results and commented on the manuscript. All authors contributed to the article and approved the submitted version.

Funding

This study received funding from the UK Biotechnology and Biological Science Research Council (BBSRC) and the industry organisations listed above. The funders were not involved in the study design, collection, analysis, interpretation of data, the writing of this article or the decision to submit it for publication. All authors declare no other competing interests. This work was supported by the UK Biotechnology and Biological Science Research Council (BBSRC) [grant number: BB/P007899/1 and BB/P000851/1] and several industry organisations (Agriculture and Horticulture Development Board [AHDB], Adrian Scripps Limited, Avalon Produce Limited, T&G Global, Frank P Matthews Limited, and Worldwide Fruit Limited).

Conflict of interest

The authors declare that the research was conducted in the absence of any commercial or financial relationships that could be construed as a potential conflict of interest.

This study received funding from the UK Biotechnology and Biological Science Research Council BBSRC and the industry organisations: Agriculture and Horticulture Development Board AHDB, Adrian Scripps Limited, Avalon Produce Limited, T&G Global, Frank P Matthews Limited, and Worldwide Fruit Limited. The funders were not involved in the study design, collection, analysis, interpretation of data, the writing of this article or the decision to submit it for publication.

Publisher’s note

All claims expressed in this article are solely those of the authors and do not necessarily represent those of their affiliated organizations, or those of the publisher, the editors and the reviewers. Any product that may be evaluated in this article, or claim that may be made by its manufacturer, is not guaranteed or endorsed by the publisher.

Supplementary material

The Supplementary Material for this article can be found online at: <https://www.frontiersin.org/articles/10.3389/fpls.2023.1054914/full#supplementary-material>

References

- Balint-Kurti, P., Simmons, S. J., Blum, J. E., Ballaré, C. L., and Stapleton, A. E. (2010). Maize leaf epiphytic bacteria diversity patterns are genetically correlated with resistance to fungal pathogen infection. *Mol. Plant-Microbe Interact.* 23 (4), 473–484. doi: 10.1094/MPMI-23-4-0473
- Becker, R., Ulrich, K., Behrendt, U., Schneek, V., and Ulrich, A. (2022). Genomic characterization of *aureimonas altamirensis* C2P003—a specific member of the microbiome of fraxinus excelsior trees tolerant to ash dieback. *Plants* 11, 3487. doi: 10.3390/plants11243487
- Benjamini, Y., and Hochberg, Y. (1995). Controlling the false discovery rate: a practical and powerful approach to multiple testing. *J. Roy Stat. Soc. B* 57, 289–300. doi: 10.1111/j.2517-6161.1995.tb02031.x
- Bodenhausen, N., Horton, M. W., and Bergelson, J. (2013). Bacterial communities associated with the leaves and the roots of *Arabidopsis thaliana*. *PLoS One* 8 (2), e56329. doi: 10.1371/journal.pone.0056329
- Brachi, B., Filiault, D., Whitehurst, H., Darne, P., Le Gars, P., Le Mentec, M., et al. (2022). Plant genetic effects on microbial hubs impact host fitness in repeated field trials. *Proc. Natl. Acad. Sci.* 119 (30), 2201285119. doi: 10.1073/pnas.2201285119
- Bus, V. G. M., Scheper, R. W. A., Walter, M., Campbell, R. E., Kitson, B., Turner, L., et al. (2019). Genetic mapping of the European canker (*Neonectria ditissima*) resistance locus *Rnd1* from *Malus robusta* 5'. *Tree Genet. Genomes* 15, 1–13. doi: 10.1007/s11295-019-1332-y
- Chelius, M. K., and Triplett, E. W. (2001). The diversity of archaea and bacteria in association with the roots of *Zea mays* L. *Microbial Ecol.* 41, 252–263. doi: 10.1007/s002480000087
- Chen, T., Nomura, K., Wang, X., Sohrabi, R., Xu, J., Yao, L., et al. (2020). A plant genetic network for preventing dysbiosis in the phyllosphere. *Nature* 580 (7805), 653–657. doi: 10.1038/s41586-020-2185-0
- Damerum, A., Arnold, E. C., Bernard, V., Smith, H. K., and Taylor, G. (2021). Good and bad lettuce leaf microbes? Unravelling the genetic architecture of the microbiome to inform plant breeding for enhanced food safety and reduced food waste. *bioRxiv*. doi: 10.1101/2021.08.06.455490
- Deng, S., Caddell, D. F., Xu, G., Dahlen, L., Washington, L., Yang, J., et al. (2021). Genome wide association study reveals plant loci controlling heritability of the rhizosphere microbiome. *ISME J.* 15 (11), 3181–3194. doi: 10.1038/s41396-021-00993-z
- Dini-Andreote, F. (2020). Endophytes: The second layer of plant defense. *Trends Plant Sci.* 25, 319–322. doi: 10.1016/j.tplants.2020.01.007
- di Pierro, E. A., Gianfranceschi, L., di Guardo, M., Koehorst-Van Putten, H. J., Kruijselbrink, J. W., Longhi, S., et al. (2016). A high-density, multi-parental SNP genetic map on apple validates a new mapping approach for outcrossing species. *Horticult Res.* 3, 1–13. doi: 10.1038/hortres.2016.57
- Edgar, R. C. (2013). UPARSE: highly accurate OTU sequences from microbial amplicon reads. *Nat. Methods* 10, 996–998. doi: 10.1038/nmeth.2604
- Faville, M. J., Briggs, L., Cao, M., Koulman, A., Jahufer, M. Z., Koolaard, J., et al. (2015). QTL analysis of host plant effects on fungal endophyte biomass and alkaloid expression in perennial ryegrass. *Mol. Breed.* 35 (8), 161. doi: 10.1007/s11032-015-0350-1
- Gardes, M., and Bruns, T. D. (1993). ITS primers with enhanced specificity for basidiomycetes-application to the identification of mycorrhizae and rusts. *Mol. Ecol.* 2 (2), 113–118. doi: 10.1111/j.1365-294X.1993.tb00005.x
- Gazaffi, R., Margarido, G. R. A., Pastina, M. M., Mollinari, M., and Garcia, A. A. F. (2014). A model for quantitative trait loci mapping, linkage phase, and segregation pattern estimation for a full-sib progeny. *Tree Genet. Genomes* 10, 791–801. doi: 10.1007/s11295-013-0664-2
- Ghasemkhani, M. (2015). Resistance against fruit tree canker in apple. doctoral thesis (Acta Universitatis Agriculturae Sueciae: Swedish University of Agricultural Sciences), 64. Available at: <https://res.slu.se/id/publ/77464>.
- Ginnan, N. A., Dang, T., Bodaghi, S., Ruegger, P. M., McCollum, G., England, G., et al. (2020). Disease-induced microbial shifts in citrus indicate microbiome-derived responses to huanglongbing across the disease severity spectrum. *Phytobiomes J.* 4 (4), 375–387. doi: 10.1094/PBIOMES-04-20-0027-R
- Gomez-Cortecero, A., Saville, R. J., Scheper, R. W. A., Bowen, J. K., de Medeiros, H. A., Kingsnorth, J., et al. (2016). Variation in host and pathogen in the *Neonectria/Malus* interactions; towards an understanding of the genetic basis of resistance to European canker. *Front. Plant Sci.* 7, 1365. doi: 10.3389/fpls.2016.01365
- Hirakue, A., and Sugiyama, S. (2018). Relationship between foliar endophytes and apple cultivar disease resistance in an organic orchard. *Biol. Control* 127, 139–144. doi: 10.1016/j.biocontrol.2018.09.007
- Horton, M. W., Bodenhausen, N., Beilsmith, K., Meng, D., Muegge, B. D., Subramanian, S., et al. (2014). Genome-wide association study of *Arabidopsis thaliana* leaf microbial community. *Nat. Commun.* 5 (1), 1–7. doi: 10.1038/ncomms6320
- Jacoby, R. P., Koprivova, A., and Kopriva, S. (2021). Pinpointing secondary metabolites that shape the composition and function of the plant microbiome. *J. Exp. Bot.* 72 (1), 57–69. doi: 10.1093/jxb/eraa424
- Karlström, A., Gómez-Cortecero, A., Nellist, C.F., Ordidge, M., Dunwell, J.M., Harrison, R.J., et al. (2022). Identification of novel genetic regions associated with resistance to European canker in apple. *BMC Plant Biol.* 22, 452. doi: 10.1186/s12870-022-03833-0
- Khare, E., Mishra, J., and Arora, N. K. (2018). Multifaceted interactions between endophytes and plant: Developments and prospects. *Front. Microbiol.* 9, 2732. doi: 10.3389/fmicb.2018.02732
- Kniskern, J. M., Traw, M. B., and Bergelson, J. (2007). Salicylic acid and jasmonic acid signaling defense pathways reduce natural bacterial diversity on *Arabidopsis thaliana*. *Mol. Plant-Microbe Interact.* 20 (12), 1512–1522. doi: 10.1094/MPMI-20-12-1512
- Liu, J., Abdelfattah, A., Norelli, J., Burchard, E., Schena, L., Droby, S., et al. (2018). Apple endophytic microbiota of different rootstock/scion combinations suggests a genotype-specific influence. *Microbiome* 6, 1–11. doi: 10.1186/s40168-018-0403-x
- Liu, J., Ridgway, H. J., and Jones, E. E. (2020). Apple endophyte community is shaped by tissue type, cultivar and site and has members with biocontrol potential against *Neonectria ditissima*. *J. Appl. Microbiol.* 128, 1735–1753. doi: 10.1111/jam.14587
- Love, M. I., Huber, W., and Anders, S. (2014). Moderated estimation of fold change and dispersion for RNA-seq data with DESeq2. *Genome Biol.* 15, 550. doi: 10.1186/s13059-014-0550-8
- Luo, Y., Wang, F., Huang, Y., Zhou, M., Gao, J., Yan, T., et al. (2019). Sphingomonas sp. Cra20 increases plant growth rate and alters rhizosphere microbial community structure of *Arabidopsis thaliana* under drought stress. *Front. Microbiol.* 10, 1221. doi: 10.3389/fmicb.2019.01221
- Margarido, G. R. A., Souza, A. P., and Garcia, A. A. F. (2007). OneMap: software for genetic mapping in outcrossing species. *Hereditas* 144, 78–79. doi: 10.1111/j.2007.0018-0661.02000.x
- Matsumoto, H., Fan, X., Wang, Y., Kusstatscher, P., Duan, J., Wu, S., et al. (2021). Bacterial seed endophyte shapes disease resistance in rice. *Nat. Plants* 7, 60–72. doi: 10.1038/s41477-020-00826-5
- N'Diaye, A., Haile, J. K., Fowler, D. B., Ammar, K., and Pozniak, C. J. (2017). Effect of co-segregating markers on high-density genetic maps and prediction of map expansion using machine learning algorithms. *Front. Plant Sci.* 8, 1434. doi: 10.3389/fpls.2017.01434
- Olivieri, L., Saville, R. J., Gange, A. C., and Xu, X. (2021). Apple endophyte community in relation to location, scion and rootstock genotypes and susceptibility to European canker. *FEMS Microbiol. Ecol.* 97, 131. doi: 10.1093/femsec/fiab131
- Omomowo, O. I., and Babalola, O. O. (2019). Bacterial and fungal endophytes: Tiny giants with immense beneficial potential for plant growth and sustainable agricultural productivity. *Microorganisms* 7, 481. doi: 10.3390/microorganisms7110481
- Oyserman, B. O., Flores, S. S., Griffioen, T., Pan, X., van der Wijk, E., Pronk, E., et al. (2022). Disentangling the genetic basis of rhizosphere microbiome assembly in tomato. *Nat. Commun.* 13, 3228. doi: 10.1038/s41467-022-30849-9
- Pacifico, D., Squartini, A., Crucitti, D., Barizza, E., Lo Schiavo, F., Muresu, R., et al. (2019). The role of the endophytic microbiome in the grapevine response to environmental triggers. *Front. Plant Sci.* 10, 1256. doi: 10.3389/fpls.2019.01256
- Pan, F., Meng, Q., Wang, Q., Luo, S., Chen, B., Khan, K. Y., et al. (2016). Endophytic bacterium *Sphingomonas* SaMR12 promotes cadmium accumulation by increasing glutathione biosynthesis in *Sedum alfredii* Hance. *Chemosphere* 154, 358–366. doi: 10.1016/j.chemosphere.2016.03.120
- Papp-Rupar, M., Karlstrom, A., Passey, T., Deakin, G., and Xu, X. (2022). The influence of host genotypes on the endophytes in the leaf scar tissues of apple trees and

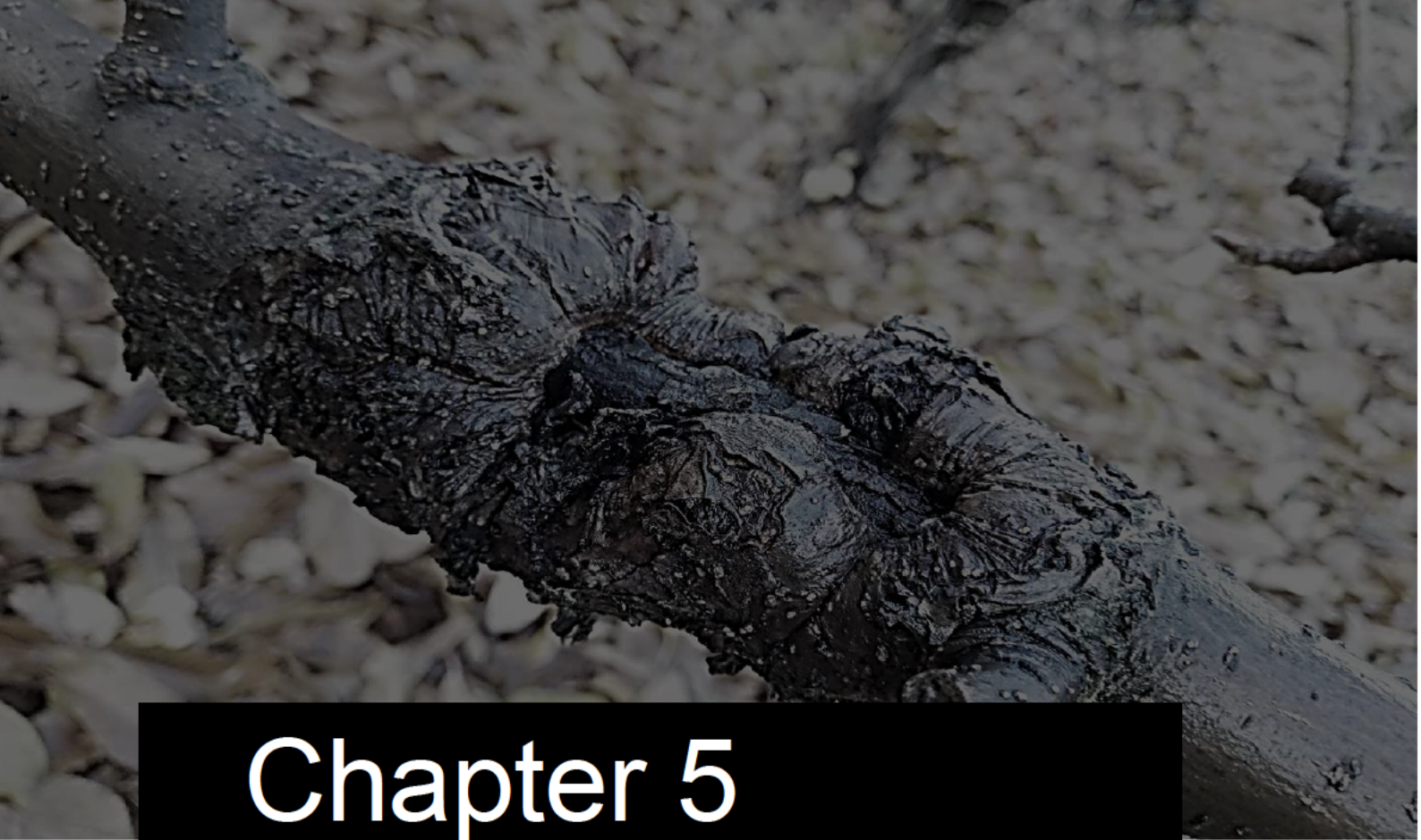
SUPPLEMENTARY FIGURE 1

Histograms of trait distributions in the biparental population.

SUPPLEMENTARY FIGURE 2

Correlation matrix of Pearson's correlation coefficient between bacterial (in grey) and fungal (black) abundance traits, and severity of canker disease (in yellow). This data originates from a previous publication by Papp Rupar et al. (2022).

- correlation of the endophytes with apple canker (*Neonectria ditissima*) development. *Phytobiomes* 6 (2), 127. doi: 10.1094/PBIOMES-10-21-0061-R
- R Core Team (2014). R: A language and environment for statistical computing. (Vienna, Austria: R Foundation for Statistical Computing). Available at: <http://www.R-project.org/>.
- Saville, R. J., Olivieri, L., Xu, X., and Fountain, M. (2019). "Fungal diseases of fruit: apple cankers in Europe," in *Integrated management of diseases and insect pests of tree fruit* (Cambridge: Burleigh Dodds Science Publishing), 59–83.
- Ulrich, K., Becker, R., Behrendt, U., Kube, M., and Ulrich, A. (2020). A comparative analysis of ash leaf-colonizing bacterial communities identifies putative antagonists of *hymenoscyphus fraxineus*. *Front. Microbiol.* 11, 966. doi: 10.3389/fmicb.2020.00966
- Vidotti, M. S., Lyra, D. H., Morosini, J. S., Granato, Í.S.C., Quecine, M. C., Azevedo, J. L. D., et al. (2019). Additive and heterozygous (dis) advantage GWAS models reveal candidate genes involved in the genotypic variation of maize hybrids to *azospirillum brasilense*. *PLoS One* 14 (9), 0222788. doi: 10.1371/journal.pone.0222788
- Vogel, C., Bodenhausen, N., Gruissem, W., and Vorholt, J. A. (2016). The *Arabidopsis* leaf transcriptome reveals distinct but also overlapping responses to colonization by phyllosphere commensals and pathogen infection with impact on plant health. *New Phytol.* 212 (1), 192–207. doi: 10.1111/nph.14036
- Wallace, J. G., Kremling, K. A., Kovar, L. L., and Buckler, E. S. (2018). Quantitative genetics of the maize leaf microbiome. *Phytobiomes J.* 2 (4), 208–224. doi: 10.1094/PBIOMES-02-18-0008-R
- Weber, R. W. S. W. S. (2014). Biology and control of the apple canker fungus *Neonectria ditissima* (syn. *N. galligena*) from a northwestern European perspective. *Erwerbs-Obstbau.* 56 (3), 95–107. doi: 10.1007/s10341-014-0210-x
- White, T. J., Bruns, T., Lee, S. J. W. T., and Taylor, J. (1990). Amplification and direct sequencing of fungal ribosomal RNA genes for phylogenetics. *PCR protocols: guide to Methods Appl.* 18 (1), 315–322. doi: 10.1016/B978-0-12-372180-8.50042-1
- Xueliang, T., Dan, X., Tingting, S., Songyu, Z., Ying, L., and Diandong, W. (2020). Plant resistance and leaf chemical characteristic jointly shape phyllosphere bacterial community. *World J. Microbiol. Biotechnol.* 36 (9), 1–12. doi: 10.1007/s11274-020-02908-0
- Yassue, R. M., Carvalho, H. F., Gevartosky, R., Sabadin, F., Souza, P. H., Bonatelli, M. L., et al. (2021). On the genetic architecture in a public tropical maize panel of the symbiosis between corn and plant growth-promoting bacteria aiming to improve plant resilience. *Mol. Breed.* 41, 63. doi: 10.1007/s11032-021-01257-6
- Yu, Z., Ding, H., Shen, K., Bu, F., Newcombe, G., Liu, H., et al. (2021). Foliar endophytes in trees varying greatly in age. *Eur. J. Plant Pathol.* 160, 375–384. doi: 10.1007/s10658-021-02250-7



Chapter 5

Discussion

Discussion

European canker is an economically damaging disease in many areas of apple production, as it results in high number of tree deaths in many modern cultivars. Numerous apple scion varieties with some degree of tolerance to *Neonectria ditissima* have been reported, yet the implementation of resistance breeding to this pathogen has been slow. Phenotyping-based breeding techniques are not optimal for the improvement of disease resistance to European canker as even resistant/tolerant accessions develop symptoms, which means that the phenotyping is destructive. The implementation of European canker phenotyping protocols is therefore only economically feasible in later stages of selection for most breeding programmes. Alternative phenotyping protocols, utilising detached shoots, have therefore been tested (Garkava-Gustavsson et al., 2016; Scheper et al., 2018). The results from this study show that the variation in tolerance in detached shoots only captures a subset of the resistance responses present in scion germplasm (Karlström et al., 2022). Such protocols are therefore not suitable for implementation in breeding programmes when selecting individuals with improved tolerance to European canker. Although host resistance to *N. ditissima* is essential, several factors have been shown to modulate tolerance to this pathogen (Berdeni et al., 2018; Vorster et al., 2021). It is therefore important to understand the components contributing to resistance and how these interact with the apple host.

The main objective of this work was to facilitate breeding and variety development of new apple cultivars with improved tolerance to *N. ditissima*. Marker assisted selection (MAS) for *N. ditissima* resistance would enable selection for this trait already at the seedling stage and thus improve the achieved genetic gain. To this end, Chapter 2 of this thesis reports of seven European canker resistance QTL segregating in a multiparental population of apple. This chapter also describes SNP-haplotypes segregating with the resistant allele for each QTL. Chapter 3 goes on to study the genetic response to *Neonectria* infection through a transcriptome analysis and identifies candidate resistance genes within the QTL regions detailed in the previous chapter. Chapter 4 of this thesis explores the feasibility to breed apple cultivars amenable to endophyte colonization and discusses the association of specific endophytic taxa with tolerance to canker.

1. The potential of improving resistance to *N. ditissima* in apple cultivars

Chapter 2 describes the identification of QTL on LG 2, 5, 6, 8, 10, 15 and 16. Similarly to the current study, Bus et al (2021) reported identifying European canker QTL on LG8 and LG16. The SNP markers reported by Bus et al lie within the QTL-interval identified in this study but are not included within the genomic regions spanned by the most significant haploblock. The biparental population used for QTL identification in the study by Bus et al featured 'Scired' ('Gala' x 'Splendour') x A045R14T055 ('Falstaff' x T31-12) as parents. Based on the pedigree of the biparental population as well as SNP haplotype data of the cultivars, it is likely that the QTL on LG8 and LG16 both originates from the same cultivar, namely 'Golden Delicious' ('Golden Delicious' -> 'Gala' for LG8 and 'Golden Delicious' -> 'Falstaff' for LG16). Skytte af Satra et al (2023) likewise studied resistance QTL to *N. ditissima* in a population derived from 'Aroma' x 'Discovery' and found QTL on LG8, LG15 and LG16. The identification of these QTL in multiple studies supports the presence of true QTL at these loci and indicates the feasibility of developing SNP marker tests to implement MAS for canker resistance. The SNP-haplotypes could also be used to characterise breeding parents to maximise the number of resistance loci segregating in families.

However, the reported QTL effects for individual loci were small-moderate in all three studies and multiple QTL would therefore need to be considered when breeding for resistance to European canker. Hence, it would perhaps be more efficient to use genome-wide selection methods that inadvertently take all QTL into account to gain improvement in resistance to *N. ditissima*. Thus, the accuracy of genomic prediction models for canker resistance, based on the multiparental population described in Chapter 2, are currently being validated in additional breeding populations (Karlstrom, unpublished).

Relying on the quantitative disease resistance described within this thesis for the development of the next generation of apple cultivars would diminish the risk of an emergence of resistance breaking *N. ditissima* isolates. Nevertheless, even cultivars like 'Golden Delicious', which has a total of nine resistance alleles at the identified QTL, develop disease symptoms. Adding to the problem is that European canker in moderately tolerant cultivars can be further exacerbated by stress factors such as waterlogging (Weber, 2014). It would therefore be worth exploring whether there are additional *Malus* germplasm harbouring resistance loci with large effects towards *N. ditissima* infection. The crab apple hybrid *Malus x hartwigii* has shown a similar level of European canker tolerance as *Malus* 'Robusta 5' in a field experiment (Karlstrom, unpublished) and could constitute an additional source of resistance.

New legislation in the UK (Precision Breeding Act, 2023) as well as proposed changes in EU legislation (EC regulation No 1829/2003) are likely to make tools such as genome-editing and transgene-free cis-genesis useful for commercial breeding in Europe. These technologies could be applied to expediate the introgression of large effect resistance genes to European canker, such as *Rnd1* from 'Robusta 5', but would be less advantageous for the multiple QTL of small effects that are present in apple scion germplasm. However, the gene/s underlying the *Rnd1* resistance locus is still unknown and further work is therefore required before these tools could be applicable to improve tolerance to European canker in apple.

The *Malus: Neonectria* interaction takes place in a non-sterile environment in the presence of a myriad of other microorganisms, which in other host-pathogen systems have been shown to affect disease outcomes (Griffiths et al., 2020; Liu et al., 2023; Romero et al., 2019). It is therefore possible that host resistance in apple could be augmented by associations with disease suppressing beneficial microorganisms. Papp-Rupar et al (2023) demonstrated that isolated endophytes may be effective as biocontrol agents towards *N. ditissima*. To ensure the efficacy of such biocontrol agents the inoculated host genotype needs to be taken into consideration. Plant growth promoting rhizobacteria (PGPR) are known to improve yields and reduce the susceptibility to disease of their plant hosts through an induced systemic resistance which results in a non-specific and broad-spectrum counter to pathogen-attack (Meena et al., 2020; Salwan et al., 2023; Samain et al., 2019). There are multiple commercial PGPR products available but their full potential are often not realised under field conditions as they are applied without consideration of plant genotype or optimal nutrient availability for successful inoculation (García de Salamone & Di Salvo, 2021). Chapter 4 of this thesis describes the genetic regions of apple that are associated with microbial abundance and species composition, with a focus on taxa that correlate with tree health during infection of *N. ditissima*. This initial work will pave the way for the characterization of alleles within the apple genome that promote the colonisation of endophytes that suppress *N. ditissima* infection. An example is the QTL on the top of LG10, which was associated with the abundance of *Sphingomonas* OTU8, *Aureimonas* OTU38 and *Deinococcus* OTU135, two of which are associated with tree health during canker infection. The QTL haplotype which favours associations with these three bacterial taxa is also present in the apple cultivars 'Jonathan', 'Idared', 'Fiesta', 'Jonamac' and 'M9'. To successfully exploit this QTL, it will need to be determined if indeed taxa belonging to *Sphingomonas* and *Aureimonas* are able to suppress *N. ditissima* infection and whether genotypes carrying the QTL haplotype consistently are more highly colonised by these endophytic bacteria. Once validated, the QTL could be used to determine biocontrol strategies for already existing cultivars and in the breeding of new cultivars amenable to inoculations with disease suppressive bacteria. Learning from the

experience of the role of the gut microbiome in human disease (Bai et al., 2023), it may be a better approach to consider microbial consortia to improve tolerance to *N. ditissima*, rather than relying on single microbial strains. It should be highlighted that the experiment described in Chapter 4 does not disentangle whether the observed endophyte abundance is due to host specific factors directly interacting with endophytes or a consequence of the interaction between resistant/susceptible hosts and *N. ditissima*. As an example of indirect plant pathogen effects on other microbiota, Seybold et al (2020) could show how infection with the fungal wheat pathogen *Zymoseptoria tritici* strongly altered leaf-associated bacteria in a resistant wheat cultivar but not in a susceptible one, correlating with induced defense responses in the resistant cultivar. A better understanding is therefore needed on the changes in phyllosphere microbiome because of *N. ditissima* infection microbiome in both tolerant and susceptible genotypes.

2. Understanding the resistance response to *Neonectria* infection

The results from Chapter 2 and 3 of this thesis highlight how a multitude of genes within several genetic regions contribute to the *Malus* response to *N. ditissima* infection. Chapter 3 describes how two moderately tolerant cultivars ('Golden Delicious' and 'M9') respond to infection by altered expression of a cascade of genes within pathogen recognition, secondary metabolism, hormone signalling, detoxification and metabolism of sugar and carbon. Furthermore, a transcriptomic approach is used to understand what type of host mechanisms govern the QTL identified in Chapter 2.

One of the identified QTL, on LG16, was only found in a late stage of *N. ditissima* infection within a field experiment (Karlstrom et al., 2022). The candidate gene search within this genetic region identified two putative 4-coumarate:coenzyme A ligases (4CL)s which were more highly expressed in apple genotypes with the resistant allele at this locus. 4CL genes can either be involved in biosynthesis of lignin and other phenylpropanoid derivatives or in the production of plant flavonoids (Chen et al., 2019). Interestingly, one of the most visual responses to *N. ditissima* infection in tolerant apple hosts is the development of a enforced border around the canker lesion (Weber, 2014). It is possible that host genotypes with a higher expression of 4CLs within this genetic region can deposit more lignin, thereby strengthening secondary cell walls and reducing the penetration by *N. ditissima*. To further study the effects of this locus on lignin or flavonoid synthesis, assays quantifying these compounds in germplasm with different QTL alleles would be needed.

Several of the candidate genes within the QTL regions had potential roles in pathogen recognition, including clusters of Wall associated kinase-like (WAKL) genes on chr 2 and wall

associated kinases (WAK) on chr 10. This type of receptors tends to interact with a broad-spectrum of pathogens (Stephens et al., 2022; Sun et al., 2020) which suggests that they could confer non-race specific resistance to *N. ditissima*. A QTL conferring an intermediate level of resistance towards multiple isolates of apple scab (*Venturia inaequalis*) has also been reported at the lower end of chromosome 2 (Bus et al., 2004; Calenge et al., 2004), while a putative disease resistance cluster with implications in resistance to fireblight (*Erwinia amylovora*), scab and powdery mildew (*Podosphaera leucotricha*) has been proposed to reside on chr 10 (Le Roux et al., 2010). These genetic regions lie approximately 1-2 Mbp and 16-28 Mbp from the WAKL and WAK gene clusters on chromosome 2 and 10, respectively (Calenge et al. 2004; Le Roux et al. 2012; Le Roux et al. 2010). It can therefore be hypothesised that the WAK/WAKL genes on chr 2 and 10 are involved in the interaction with multiple pathogens. There is an increasing amount of evidence showing that WAKs/WAKLs have an important role in plant pathogen interactions. Similarly to the case of *N. ditissima*, several of the described WAKs are involved in resistance towards hemibiotropic or necrotrophic Ascomycete fungi of the Dothideomycetes class (Stephens et al., 2022). Their roles in defense range from detecting effectors or other molecules indicating pathogen invasion to inducing callus deposition and lignin biosynthesis (Stephens et al., 2022).

Among the QTLs identified in Chapter 2, one located on LG15 had the largest estimated effect (>17% for later time-points). However, the position of this QTL on the linkage group was highly uncertain, with different phenotyping events indicating different positions. This could be explained by two QTL being present on the chromosome but there being insufficient number of progeny (and therefore insufficient recombination events) in the mapping population to clearly separate the two QTL. The genetic region at the top of chr 15 has been implicated in resistance to not only *N. ditissima* but also fire blight (*Erwinia amylovora*) (Desnoues et al., 2018; Thapa et al., 2021) and Valsa canker (*Valsa mali*) (Tan et al., 2017). Interestingly, the gene *MD15G1030400* which is located within the canker and fire blight QTL on chr 15, was among the differentially expressed (DE) genes upon fire blight infection (Thapa et al., 2021) but was also described in Chapter 3 as having a significantly higher expression in apple genotypes with a resistant allele at this locus. This gene unfortunately encodes an uncharacterized protein and does not have any domains of known function. Furthermore, 63 transcripts located within fire blight QTL regions were DE upon not only *Erwinia* infection (Silva et al., 2019) but also in 'Golden Delicious' or 'M9' when infected with *N. ditissima*. Eleven of these genes were putative RLKs, protein kinases or NLRs.

The results from this thesis suggest that some of the genetic regions involved in European canker resistance have a broad effect on pathogen interaction and may play a role in resistance to other apple diseases. However, it is feasible that a genetic loci can contribute to

disease resistance towards one pathogen whilst functioning as a susceptibility factor in another pathogen interaction as has been seen in wheat (Gruner et al., 2020). The role of the identified resistance genes in different apple diseases would therefore need to be further studied.

3. How do host factors affect endophytes in the phyllosphere?

The specific genetic mechanisms that influence the apple microbiome are still not known. Chapter 3 describes several genetic loci that are associated with the overall composition or abundance of multiple endophytes, yet the underlying genes are still elusive. Liu et al (2023) conducted one of few studies that describe the host mechanisms that control endophyte abundance. They showed that rice panicles with a reduced infection of rice smut (*Ustilaginoidea virens*) had a different composition of microbiota compared to diseased panicles. The disease-suppressive panicles also had higher levels of branched chain amino acids (BCAA), particularly leucine. The authors could show that microbial keystone taxa (belonging to *Aspergillus* and *Lactobacillus*) suppressed the gene expression of BCAA aminotransferase (*OsBCAT*) leading to an accumulation of BCAAs. The keystone microbes enhanced resistance to *U. virens* in *OsBCAT* wild-type plants but did not have a similar impact on *OsBCAT* mutants (Liu et al., 2023).

Like pathogens, endophytes also possess pathogen-like MAMPs that can be recognized by pattern recognition receptors (Zhan et al., 2022). A possible explanation for the variation in endophyte abundance between apple host genotypes could therefore be the presence/absence of receptors which perceive signals from non-pathogenic microbiota. In a genome wide association study (GWAS) of host effect on endophytes in *Arabidopsis*, Horton et al (2014) found that defense genes and kinases were enriched in regions with significant GWAS hits. The study further found genes associated with cell wall integrity (such as pectinases) and ABC transporters in loci that were associated with fungal community composition. A pectinesterase (*AT2G36710*) was found in the genetic region implicated in the abundance of an OTU assigned to *Sphingomonas* (Horton et al., 2014). Defense genes, receptor kinases, ABC-transporters and genes involved in cell-wall modifications were all among the groups of genes which were differentially expressed in apple trees during infection with *N. ditissima*, as described in Chapter 4 of this thesis. It is therefore plausible that the host response to *N. ditissima* has secondary effects on the colonization of endophytes in the phyllosphere.

Two of the QTL associated with tolerance to European canker, on chr 5 and 15, overlapped with QTL regions associated with changes in the abundance of multiple endophytes (Karlström et al., 2022, 2023). There could be multiple reasons for the overlap between these QTL; either the loci interact directly with the endophytes or there is a secondary effect of the resistance loci on non-pathogenic microbiota due to their influence on *N. ditissima* colonization of the phyllosphere. Further studies, characterising the genes underlying the QTL associated with endophyte abundance in apple, would need to be conducted to fully understand the interplay between the *Malus* host and its associated microbiota.

4. Concluding remarks

This work has contributed to improving the understanding of the disease triangle of European canker by studying host factors as well as the phyllosphere microbiotic interactions which potentially influence *N. ditissima* infection. However, there are still many areas of the European canker disease triangle which are poorly understood. Environmental factors have repeatedly been reported to have a large effect on disease outcomes in *N. ditissima* infection (Berdeni et al., 2018; Vorster et al., 2021; Weber, 2014; Weber & Børve, 2021), yet it is unknown how these affect the disease. Nitrogen fertilisation has been reported as a factor that increases the susceptibility of apple trees to canker infection (Vorster et al., 2021; Weber & Børve, 2021). However, these studies and observations have been made on susceptible cultivars and it is thus unclear whether the effects of nitrogen are host genotype specific. A better understanding of the role of environmental effects on *N. ditissima* infection could also help elucidate which factors trigger the switch from a latent endophytic-like lifestyle to a pathogenic one. Environmental factors that have been suggested to affect fungal lifestyle switches include; light, nutrient balance and salinity, but it is still largely unknown what causes the lifestyle switch in the majority of fungi (Bhunjun et al., 2023). *Colletotrichum tofieldiae* is a root-associated endophytic fungus that promotes plant growth in *Arabidopsis thaliana*, but a pathogenic isolate of this species (Ct3) has also been identified (Hiruma et al., 2023). Hiruma et al (2023) showed that Ct3 was able to cause pathogenesis under sufficient phosphate availability, but had reduced pathogenic ability in phosphate deficient conditions. Furthermore, the authors showed how disrupting genes involved in the biosynthesis of ABA and a sesquiterpene in the isolate Ct3 lead to a switch from pathogenic to a beneficial lifestyle (Hiruma et al., 2023). The study also showed how the *Arabidopsis* plant was able to suppress virulence of Ct3 at elevated temperatures. The study on *C. tofieldiae* gives an insight in the complexity of the parasitic–mutualistic continuum and how biotic factors such as nutrient availability and temperature can influence the fungal lifestyle.

Based on the results from Chapter 3, which shows that secondary metabolism plays an important role in the *Malus* response to *N. ditissima*, it would be of interest to study the metabolome of apple genotypes with contrasting levels of resistance during infection. Not least because secondary metabolites with antimicrobial properties may play an additional role in how the plant phyllosphere is shaped by host genotype.

References

- Bai, X., Huang, Z., Duraj-Thatte, A. M., Ebert, M. P., Zhang, F., Burgermeister, E., Liu, X., Scott, B. M., Li, G., & Zuo, T. (2023). Engineering the gut microbiome. *Nature Reviews Bioengineering*. <https://doi.org/10.1038/s44222-023-00072-2>
- Berdeni, D., Cotton, T. E. A., Daniell, T. J., Bidartondo, M. I., Cameron, D. D., & Evans, K. L. (2018). The Effects of Arbuscular Mycorrhizal Fungal Colonisation on Nutrient Status, Growth, Productivity, and Canker Resistance of Apple (*Malus pumila*). *Frontiers in Microbiology*, 9, 1461. <https://doi.org/10.3389/fmicb.2018.01461>
- Bhunjun, C. S., Phukhamsakda, C., Hyde, K. D., McKenzie, E. H. C., Saxena, R. K., & Li, Q. (2023). Do all fungi have ancestors with endophytic lifestyles? *Fungal Diversity*. <https://doi.org/10.1007/s13225-023-00516-5>
- Bus, V., Singla, G., Horner, M., Jesson, L., Walter, M., Kitson, B., López-Girona, E., Kirk, C., Gardiner, S., Chagné, D., & Volz, R. (2021). Preliminary genetic mapping of fire blight and European canker resistances in two apple breeding families. *Acta Horticulturae*, 1307, 199–204. <https://doi.org/10.17660/ActaHortic.2021.1307.31>
- Bus, V., van de Weg, W. E., Durel, C. E., Gessler, C., Calenge, F., Parisi, L., Rikkerink, E., Gardiner, S., Patocchi, A., Meulenbroek, M., Schouten, H., & Laurens, F. (2004). Delineation of a scab resistance gene cluster on linkage group 2 of apple. *Acta Horticulturae*, 663, 57–62. <https://doi.org/10.17660/ActaHortic.2004.663.3>
- Calenge, F., Faure, A., Goerre, M., Gebhardt, C., Van de Weg, W. E., Parisi, L., & Durel, C. E. (2004). Quantitative Trait Loci (QTL) Analysis Reveals Both Broad-Spectrum and Isolate-Specific QTL for Scab Resistance in an Apple Progeny Challenged with Eight Isolates of *Venturia inaequalis*. *Phytopathology*, 94(4), 370–379. <https://doi.org/10.1094/PHYTO.2004.94.4.370>

- Chen, X., Wang, H., Li, X., Ma, K., Zhan, Y., & Zeng, F. (2019). Molecular cloning and functional analysis of 4-Coumarate:CoA ligase 4 (4CL-like 1) from *Fraxinus mandshurica* and its role in abiotic stress tolerance and cell wall synthesis. *BMC Plant Biology*, *19*(1), 231. <https://doi.org/10.1186/s12870-019-1812-0>
- Desmedt, W., Vanholme, B., & Kyndt, T. (2021). Plant defense priming in the field: a review. In *Recent highlights in the discovery and optimization of crop protection products* (pp. 87–124). Elsevier. <https://doi.org/10.1016/B978-0-12-821035-2.00045-0>
- Desnoues, E., Norelli, J. L., Aldwinckle, H. S., Wisniewski, M. E., Evans, K. M., Malnoy, M., & Khan, A. (2018). Identification of Novel Strain-Specific and Environment-Dependent Minor QTLs Linked to Fire Blight Resistance in Apples. *Plant Molecular Biology Reporter / ISPMB*, *36*(2), 247–256. <https://doi.org/10.1007/s11105-018-1076-0>
- EC Regulation No 1829/2003, *Regulation (EC) No 1829/2003 of the European Parliament and of the Council of 22 September 2003 on genetically modified food and feed* <https://eur-lex.europa.eu/legal-content/EN/TXT/?uri=CELEX%3A32003R1829&qid=1690190306030> (European Parliament, Council of the European Union, 2003).
- García de Salamone, I. E., & Di Salvo, L. P. (2021). Interactions between plant genotypes and PGPR are a challenge for crop breeding and improvement inoculation responses. In R. Soni, D. C. Suyal, P. Bhargava, & R. Goel (Eds.), *Microbiological activity for soil and plant health management* (pp. 331–349). Springer Singapore. https://doi.org/10.1007/978-981-16-2922-8_14
- Garkava-Gustavsson, L., Ghasemkhani, M., Zborowska, A., Englund, J. E., Lateur, M., & van de Weg, E. (2016). Approaches for evaluation of resistance to European canker (*Neonectria ditissima*) in apple. *Acta Horticulturae*, *1127*, 75–82. <https://doi.org/10.17660/ActaHortic.2016.1127.14>
- Griffiths, S. M., Galambao, M., Rowntree, J., Goodhead, I., Hall, J., O'Brien, D., Atkinson, N., & Antwis, R. E. (2020). Complex associations between cross-kingdom microbial endophytes and host genotype in ash dieback disease dynamics. *The Journal of Ecology*, *108*(1), 291–309. <https://doi.org/10.1111/1365-2745.13302>
- Gruner, K., Esser, T., Acevedo-Garcia, J., Freh, M., Habig, M., Strugala, R., Stukenbrock, E., Schaffrath, U., & Panstruga, R. (2020). Evidence for Allele-Specific Levels of

Enhanced Susceptibility of Wheat mlo Mutants to the Hemibiotrophic Fungal Pathogen *Magnaporthe oryzae* pv. *Triticum*. *Genes*, 11(5). <https://doi.org/10.3390/genes11050517>

Hiruma, K., Aoki, S., Takino, J., Higa, T., Utami, Y. D., Shiina, A., Okamoto, M., Nakamura, M., Kawamura, N., Ohmori, Y., Sugita, R., Tanoi, K., Sato, T., Oikawa, H., Minami, A., Iwasaki, W., & Saijo, Y. (2023). A fungal sesquiterpene biosynthesis gene cluster critical for mutualist-pathogen transition in *Colletotrichum tofieldiae*. *Nature Communications*, 14(1), 5288. <https://doi.org/10.1038/s41467-023-40867-w>

Horton, M. W., Bodenhausen, N., Beilsmith, K., Meng, D., Muegge, B. D., Subramanian, S., Vetter, M. M., Vilhjálmsson, B. J., Nordborg, M., Gordon, J. I., & Bergelson, J. (2014). Genome-wide association study of *Arabidopsis thaliana* leaf microbial community. *Nature Communications*, 5, 5320. <https://doi.org/10.1038/ncomms6320>

Karlström, A., Gómez-Cortecero, A., Nellist, C. F., Ordidge, M., Dunwell, J. M., & Harrison, R. J. (2022). Identification of novel genetic regions associated with resistance to European canker in apple. *BMC Plant Biology*, 22(1), 452. <https://doi.org/10.1186/s12870-022-03833-0>

Karlström, A., Papp-Rupar, M., Passey, T. A. J., Deakin, G., & Xu, X. (2023). Quantitative trait loci associated with apple endophytes during pathogen infection. *Frontiers in Plant Science*, 14, 1054914. <https://doi.org/10.3389/fpls.2023.1054914>

Le Roux, P. M. F., Khan, M. A., Broggini, G. A. L., Duffy, B., Gessler, C., & Patocchi, A. (2010). Mapping of quantitative trait loci for fire blight resistance in the apple cultivars “Florina” and “Nova Easygro”. *Genome*, 53(9), 710–722. <https://doi.org/10.1139/g10-047>

Liu, X., Matsumoto, H., Lv, T., Zhan, C., Fang, H., Pan, Q., Xu, H., Fan, X., Chu, T., Chen, S., Qiao, K., Ma, Y., Sun, L., Wang, Q., & Wang, M. (2023). Phyllosphere microbiome induces host metabolic defence against rice false-smut disease. *Nature Microbiology*, 8(8), 1419–1433. <https://doi.org/10.1038/s41564-023-01379-x>

Meena, M., Swapnil, P., Divyanshu, K., Kumar, S., Harish, Tripathi, Y. N., Zehra, A., Marwal, A., & Upadhyay, R. S. (2020). PGPR-mediated induction of systemic resistance and physiochemical alterations in plants against the pathogens: Current perspectives. *Journal of Basic Microbiology*, 60(10), 828–861. <https://doi.org/10.1002/jobm.202000370>

Papp-Rupar, M., Olivieri, L., Saville, R., Passey, T., Kingsnorth, J., Fagg, G., McLean, H., & Xu, X. (2023). From Endophyte Community Analysis to Field Application: Control of Apple

Canker (*Neonectria ditissima*) with *Epicoccum nigrum* B14-1. *Agriculture*, 13(4), 809.
<https://doi.org/10.3390/agriculture13040809>

Precision Breeding Act, c. 6.

https://www.legislation.gov.uk/ukpga/2023/6/pdfs/ukpga_20230006_en.pdf

Romero, F. M., Rossi, F. R., Gárriz, A., Carrasco, P., & Ruíz, O. A. (2019). A Bacterial Endophyte from Apoplast Fluids Protects Canola Plants from Different Phytopathogens via Antibiosis and Induction of Host Resistance. *Phytopathology*, 109(3), 375–383.
<https://doi.org/10.1094/PHYTO-07-18-0262-R>

Salwan, R., Sharma, M., Sharma, A., & Sharma, V. (2023). Insights into plant beneficial microorganism-triggered induced systemic resistance. *Plant Stress*, 7, 100140.
<https://doi.org/10.1016/j.stress.2023.100140>

Samain, E., Aussenac, T., & Selim, S. (2019). The Effect of Plant Genotype, Growth Stage, and *Mycosphaerella graminicola* Strains on the Efficiency and Durability of Wheat-Induced Resistance by *Paenibacillus* sp. Strain B2. *Frontiers in Plant Science*, 10, 587.
<https://doi.org/10.3389/fpls.2019.00587>

Scheper, R. W. A., Fisher, B. M., Taylor, T., & Hedderley, D. I. (2018). Detached shoot treatments cannot replace whole-tree assays when phenotyping for apple resistance to *Neonectria ditissima*. *New Zealand Plant Protection*, 71, 151–157.
<https://doi.org/10.30843/nzpp.2018.71.137>

Seybold, H., Demetrowitsch, T. J., Hassani, M. A., Szymczak, S., Reim, E., Haueisen, J., Lübbers, L., Rühlemann, M., Franke, A., Schwarz, K., & Stukenbrock, E. H. (2020). A fungal pathogen induces systemic susceptibility and systemic shifts in wheat metabolome and microbiome composition. *Nature Communications*, 11(1), 1910.
<https://doi.org/10.1038/s41467-020-15633-x>

Silva, K. J. P., Singh, J., Bednarek, R., Fei, Z., & Khan, A. (2019). Differential gene regulatory pathways and co-expression networks associated with fire blight infection in apple (*Malus × domestica*). *Horticulture Research*, 6, 35. <https://doi.org/10.1038/s41438-019-0120-z>

Skytte af Sättra, J., Odilbekov, F., Ingvarsson, P. K., van de Weg, E., & Garkava-Gustavsson, L. (2023). Parametric mapping of QTL for resistance to European canker in

- apple in 'Aroma' × 'Discovery.' *Tree Genetics & Genomes*, 19(2), 12.
<https://doi.org/10.1007/s11295-023-01587-w>
- Stephens, C., Hammond-Kosack, K. E., & Kanyuka, K. (2022). WAKsing plant immunity, waning diseases. *Journal of Experimental Botany*, 73(1), 22–37.
<https://doi.org/10.1093/jxb/erab422>
- Tan, Y., Shen, F., Chen, R., Wang, Y., Wu, T., Li, T., Xu, X., Han, Z., & Zhang, X. (2017). Candidate genes associated with resistance to Valsa canker identified via quantitative trait loci in apple. *Journal of Phytopathology*, 165(11–12), 848–857.
<https://doi.org/10.1111/jph.12658>
- Thapa, R., Singh, J., Gutierrez, B., Arro, J., & Khan, A. (2021). Genome-wide association mapping identifies novel loci underlying fire blight resistance in apple. *The Plant Genome*, 14(2), e20087. <https://doi.org/10.1002/tpg2.20087>
- Vorster, L., Butler, R. C., Turner, L., Patrick, E., Campbell, R. E., Orchard, S., & Walter, M. (2021). The effect of nitrogen source and quantity on disease expression of *Neonectria ditissima* in apple. *New Zealand Plant Protection*, 74(2S), S20–S33.
<https://doi.org/10.30843/nzpp.2021.74.11748>
- Weber, R W S. (2014). Biology and control of the apple canker fungus *Neonectria ditissima* (syn. *N. galligena*) from a Northwestern European perspective. *Erwerbs-Obstbau*, 56(3), 95–107. <https://doi.org/10.1007/s10341-014-0210-x>
- Weber, Roland W. S., & Børve, J. (2021). Infection biology as the basis of integrated control of apple canker (*Neonectria ditissima*) in Northern Europe. *CABI Agriculture and Bioscience*, 2(1), 5. <https://doi.org/10.1186/s43170-021-00024-z>
- Zhan, C., Matsumoto, H., Liu, Y., & Wang, M. (2022). Pathways to engineering the phyllosphere microbiome for sustainable crop production. *Nature Food*, 3(12), 997–1004.
<https://doi.org/10.1038/s43016-022-00636-2>

Supplementary data - Chapter 2

All supplementary data for this chapter can be found in its original format in Karlstrom et al (2022, <https://doi.org/10.1186/s12870-022-03833-0>)

Supplementary Table 1 Mean and standard error for European canker phenotypes for families included in the multiparental population used in this study

Family ID	Parent 1	Parent 2	Family size	Field 5 mpi		Field 8 mpi		Field 11 mpi		Field 20 mpi - % HTA		Field 20 mpi - % CB		Field 20 mpi - CI		Shoot		Potted tree		No. of branches	
				Mean	Standard Error	Mean	Standard Error	Mean	Standard Error	Mean	Standard Error	Mean	Standard Error	Mean	Standard Error	Mean	Standard Error	Mean	Standard Error	Mean	Standard Error
MDX 051	Gala	-	69	29.5	0.8	91.9	2.9	188.1	6.7	54.0	3.2	79.5	2.2	1.3	0.0	41.3	13.7	91.7	45.0	17.5	0.4
MDX 054	Aroma	Golden Delicious	62	24.6	0.5	87.6	2.1	171.3	5.0	77.0	1.9	71.6	2.1	1.4	0.0	31.9	11.7	64.5	23.6	15.7	0.4
MDX 060	EM-Selection-2	EM-Selection-3	65	33.4	0.8	125.1	3.8	221.5	7.1	40.0	2.9	90.3	1.6	1.3	0.0	41.5	13.4	74.8	32.4	16.2	0.3
MDX 061	EM-Selection-4	Gala	60	29.1	0.6	98.7	2.4	198.3	5.0	50.0	3.2	89.9	1.5	1.3	0.0	37.6	13.4	67.5	24.7	16.3	0.4
MDX 063	EM-Selection-1	Golden Delicious	61	24.2	0.5	88.0	2.5	147.9	3.8	75.5	2.4	70.9	2.2	1.4	0.0	32.6	10.6	67.9	25.8	16.5	0.4

Supplementary Table 2 Broad sense heritability for resistance to European apple canker for a multiparental population phenotyped in different experiments and at different time-points within experiment

Phenotype	H²
Field 5 mpi	0.58
Field 8 mpi	0.65
Field 11 mpi	0.54
Field 20 mpi: % Healthy Tree Area (HTA)	0.76
Field 20 mpi: % Cankered Branches (CB)	0.63
Field 20 mpi: Canker Index (CI)	0.37
Shoots	0.16
Potted trees	0.46

Supplementary Table 3 Summary of the selected haploblocks within each of the QTL-regions associated with resistance to European apple canker

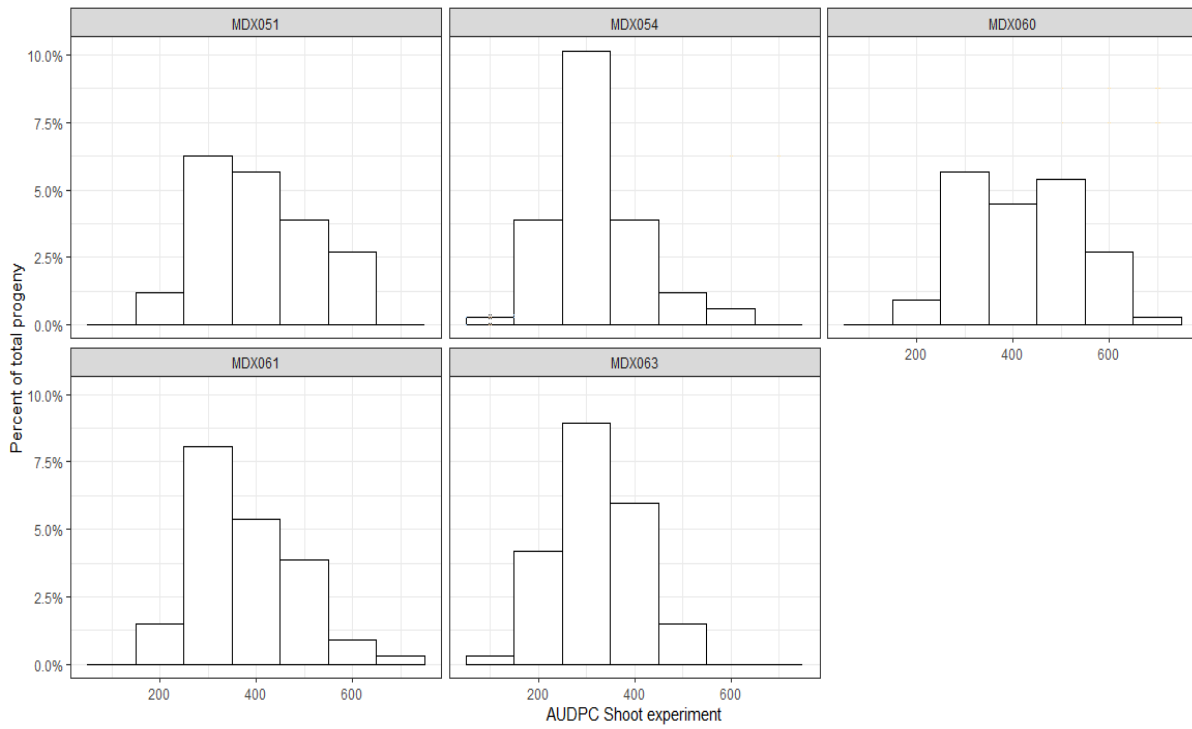
Hapl obloc k	LG	Sta rt	En d	No. of haplot ypes	No. of markers	Start marker	End marker	Segregating parents	Resistant haplotypes
HB2	2	57	66	9	58	RosBREEDSNP_SNP_TG_29 827721_Lg2_MDP0000556302 _MAF30_MDP0000556302_ex on1	SNP_F B_0961 817	Gala, Golden Delicious, Aroma, EM-Selection-2	HB2-Gala-R, HB2- Aroma-R, HB2-GD- R
HB5	5	28	43	10	78	SNP_FB_0609815	SNP_F B_0622 222	Golden Delicious, Aroma, EM-Selection-3	HB5-Aroma-R, HB5-GD-R, HB5- Sel3-R
HB6	6	12	14	6	9	SNP_FB_1080093	SNP_F B_0410 474	Gala, EM-Selection-2, EM-Selection-4	HB6-shared-R
HB8	8	15	29	19	61	SNP_FB_0736339	SNP_F B_0746 401	Golden Delicious, Gala, EM-Selection-3	HB8-shared-R, HB8-GD-R
HB10	10	47	56	10	35	SNP_FB_0037831	SNP_F B_0041 082	Gala, EM-Selection-1, EM-Selection-3, EM- Selection-4	HB10-shared-R1, HB10-shared-R2
HB15	15	38	38	6	5	SNP_FB_0271888	SNP_F B_1072 204	Golden Delicious, EM- Selection-2, EM- Selection-4	HB15-shared-R1, HB15-shared-R2
HB16	16	9	19	9	42	SNP_FB_0918148	SNP_F B_1074 919	Golden Delicious, Aroma, EM-Selection-1	HB16-GD-R, HB16- Sel1-R, HB16- Aroma-R

Supplementary table 4 is too large to reproduce in this format. Please refer to the supplementary data in Karlstrom et al (2022, <https://doi.org/10.1186/s12870-022-03833-0>) to see this table.

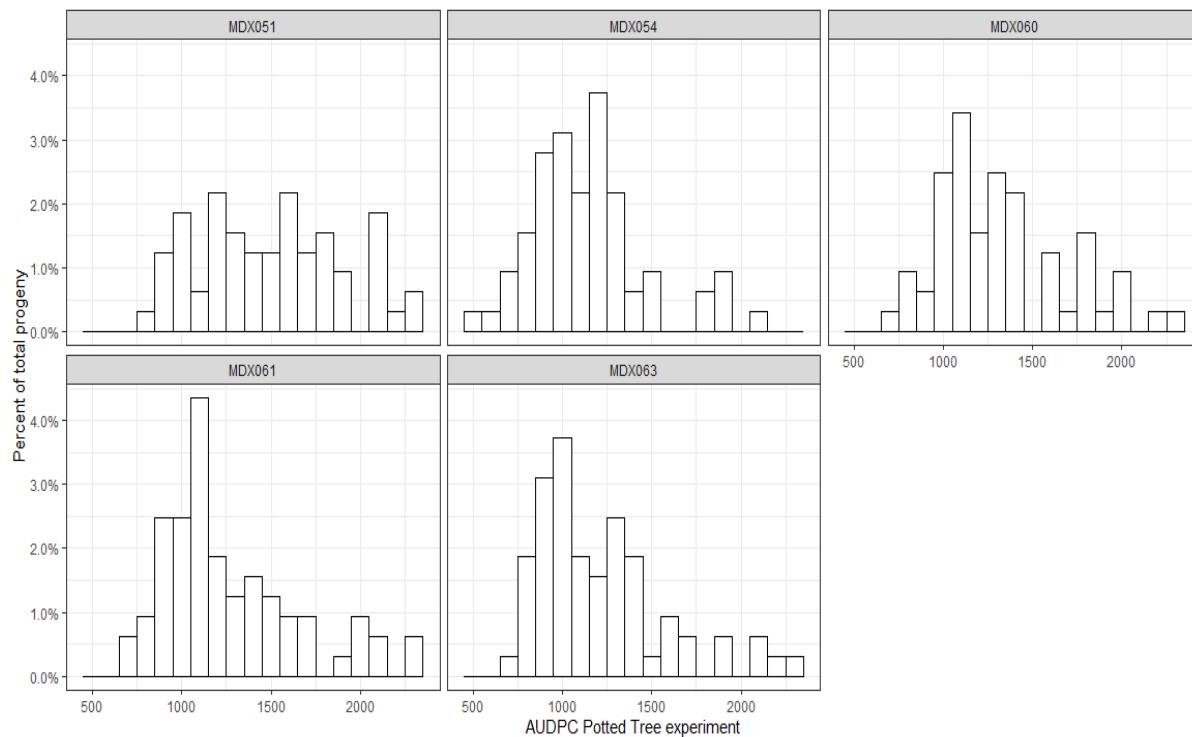
Supplementary Table 5 Mean, standard error and significance of haploblock alleles in validation experiment

Haplotype	Parental origin	No. of copies haplotype	Potted tree				Shoot			
			Mean AUDPC	Standard Error	Est. variance due to haplotype	p-value	Mean AUDPC	Standard Error	Est. variance due to haplotype (%)	p-value
HB2										
HB2-shared-S2	Golden Delicious, M9	0	913	39	-	n.s	730	39	5.38	0.02
		1	964	35			776	30		
		2	1024	52			889	59		
HB2-GD-R	Golden Delicious	0	1015	34	-	n.s	817	39	-	n.s
		1	907	31			759	28		
HB2-shared-S1	M9	0	946	40	-	n.s	836	35	4.51	0.047
		1	955	29			745	30		
								9.89		
HB5			47				62			
HB5-GD-R	Golden Delicious	1	978	37	-	n.s	810	33	-	n.s
HB5-shared-S	Golden Delicious	1	931	31			748	32		
HB5-M9-1	M9	1	960	36	-	n.s	774	38	-	n.s
HB5-M9-2	M9	1	946	30			780	29		
HB6										
HB6-shared-VS	M9	1	962	33	-	n.s	754	30	-	n.s
HB6-M9-1	M9	1	963	31			810	31		
HB6-shared-R	Golden Delicious	Parent homozygous								
HB8										
HB8-GD-R	Golden Delicious	1	931	31	-	0.058	766	32	-	n.s
HB8-shared-S	Golden Delicious	1	1025	38			788	34		

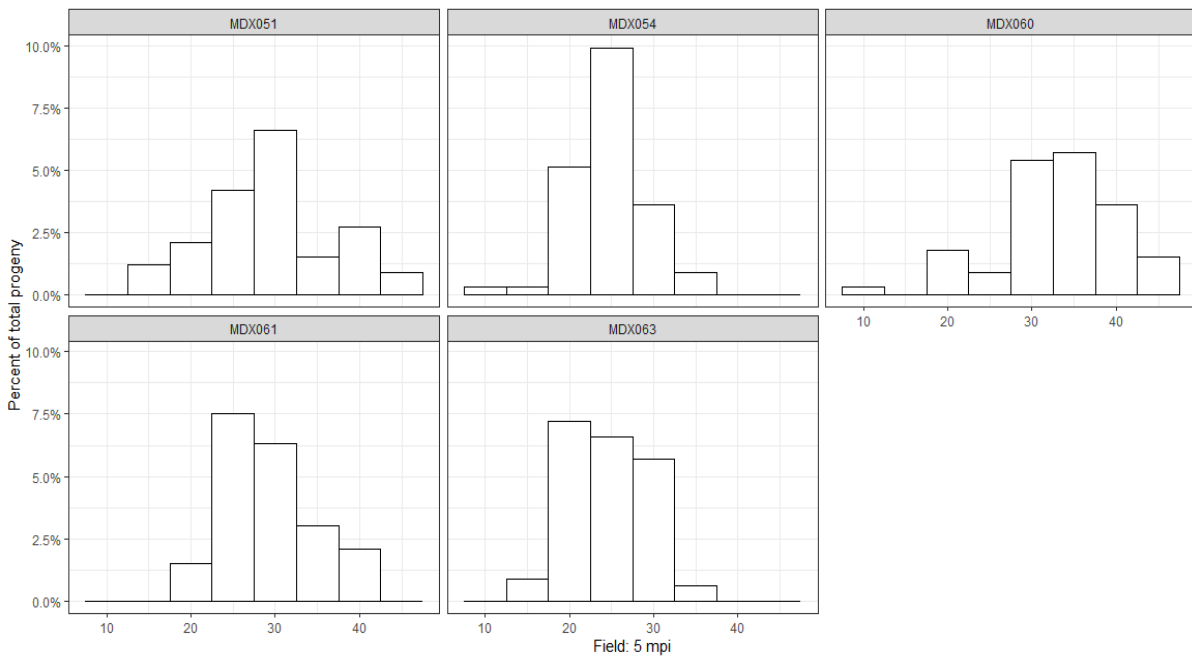
HB8-M9-1	M9	1	949	44	-	n.s	801	49	-	n.s
HB8-M9-2	M9	1	966	28			774	25		
HB10										
HB10-shared-R1	Golden Delicious	1	943	34	-	n.s	820	34	-	n.s
HB10-GD	Golden Delicious	1	974	31			758	29		
HB10-M9-1	M9	1	975	33	-	n.s	780	33	-	n.s
HB10-M9-2	M9	1	950	33			784	29		
HB15										
HB15-shared-S2	Golden Delicious, M9	0	938	49	-	n.s	791	41	-	n.s
		1	933	29			794	34		
		2	1032	47			756	39		
HB15-shared-R	Golden Delicious	0	987	32	-	n.s	789	32	-	n.s
		1	935	32			779	30		
HB15-M9	M9	0	987	32	-	n.s	762	29	-	n.s
		1	933	31			811	33		
HB16										
HB16-shared-S	Golden Delicious	1	971	34	-	n.s	855	34	4.97	0.01
HB16-GD-MR	Golden Delicious	1	943	33			737	31		
HB16-M9-1	M9	1	988	29	-	n.s	763	29	-	n.s
HB16-M9-2	M9	1	920	36			803	34		
All progeny			970				782			
			94				22			



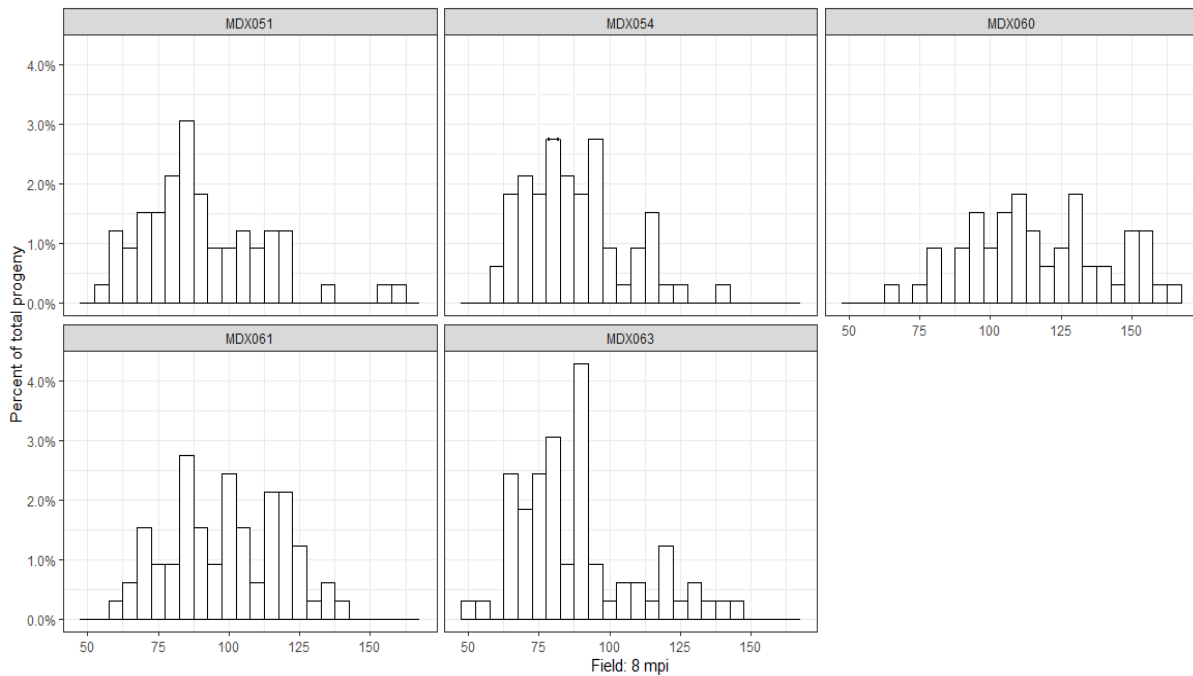
Supplementary figure 1A. Phenotypic distribution of Area Under Disease Progression Curve (AUDPC) in response to European canker in the shoot experiment. Distribution shown by family.



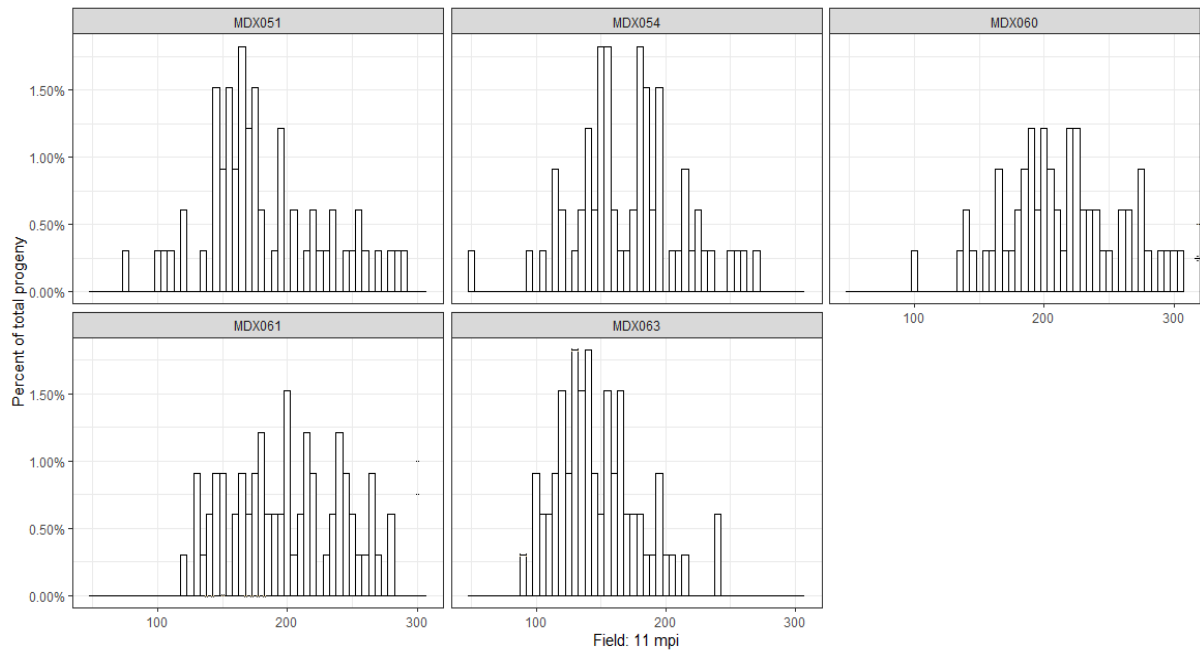
Supplementary figure 1B. Phenotypic distributions of Area Under Disease Progression Curve (AUDPC) in response to European canker in the potted tree experiment. Distribution shown by family.



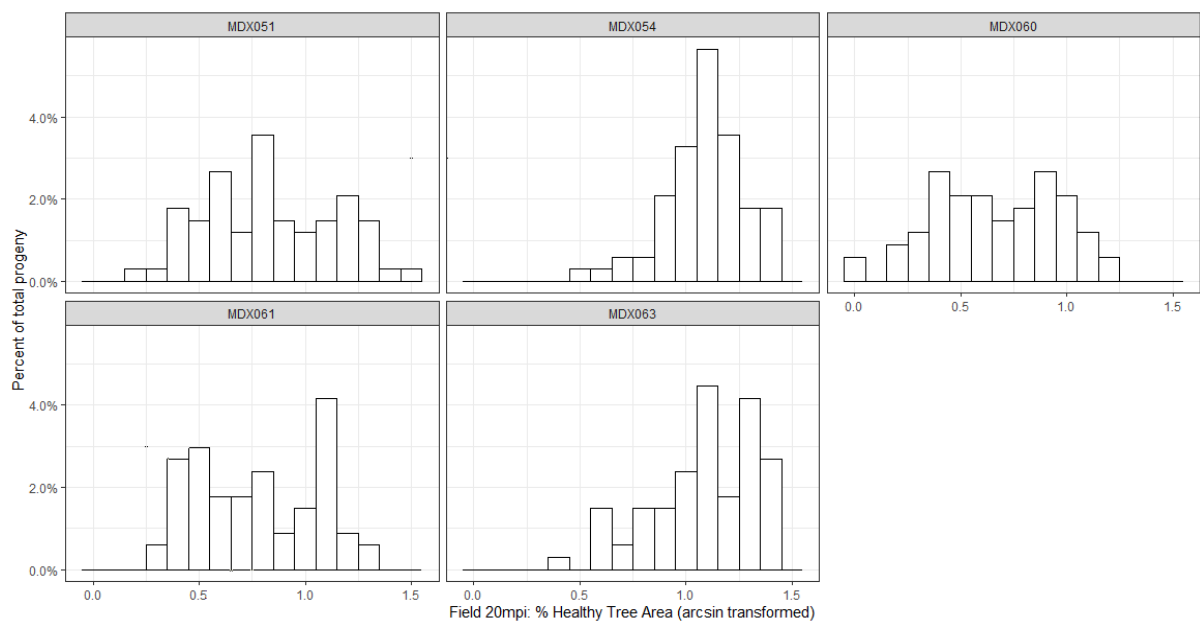
Supplementary figure 1C. Phenotypic distributions of lesion length (in mm) after infection with European canker in Field 5 months post inoculation. Distribution shown by family.



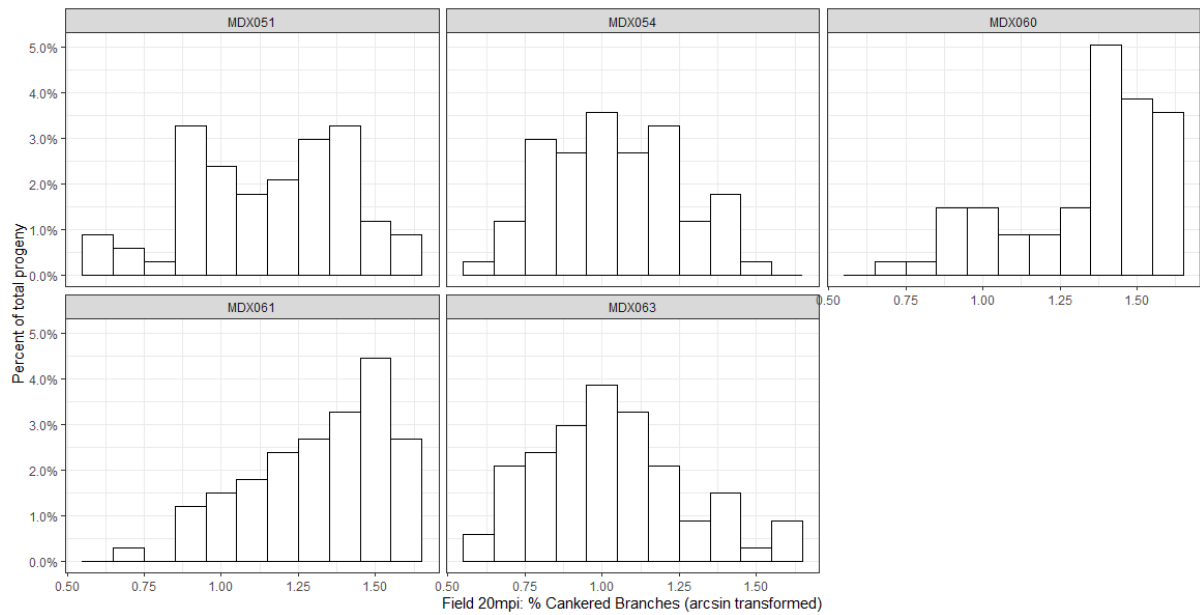
Supplementary figure 1D. Phenotypic distributions of lesion length (in mm) after infection with European canker in Field 8 months post inoculation. Distribution shown by family.



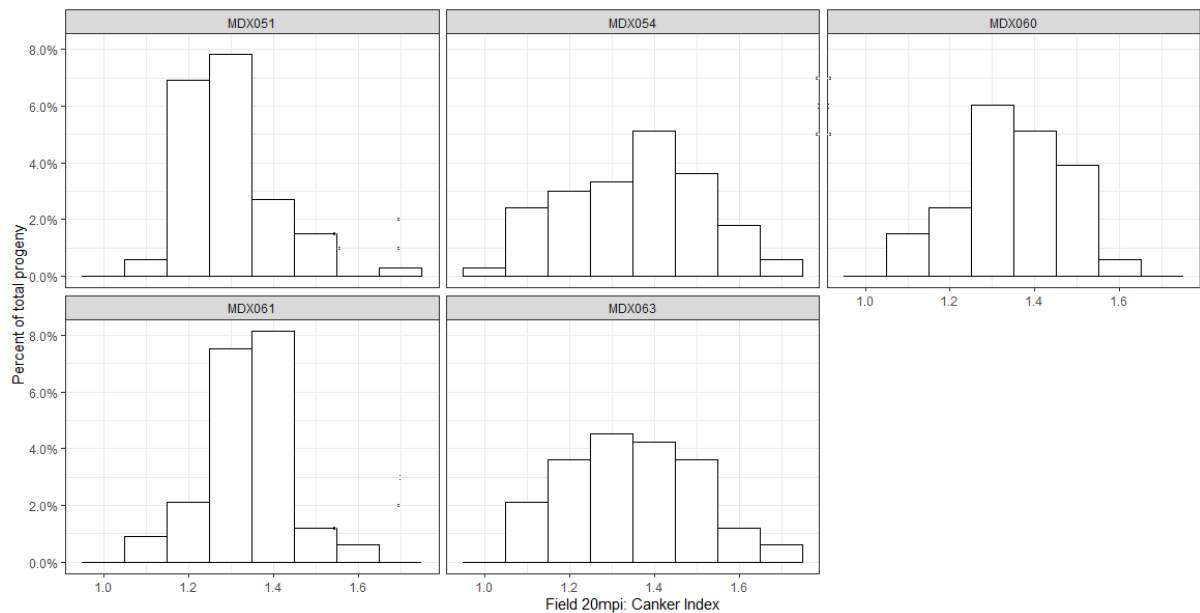
Supplementary figure 1E. Phenotypic distributions of lesion length (in mm) after infection with European canker in Field 11 months post inoculation. Distribution shown by family.



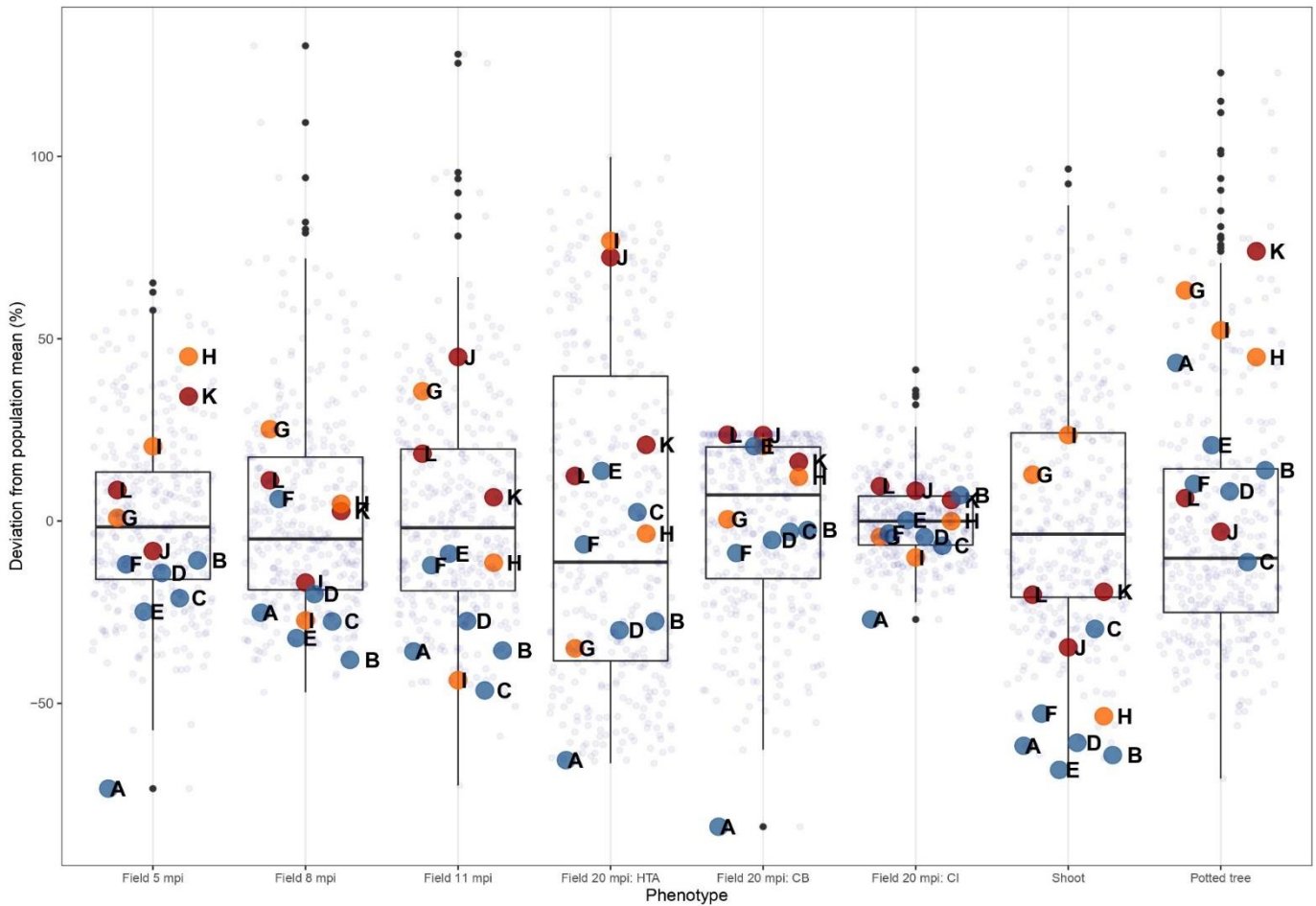
Supplementary figure 1F. Phenotypic distributions of arcsin transformed data for susceptibility to European canker in Field 20 months post inoculation: % Healthy Tree Area. Distribution shown by family.



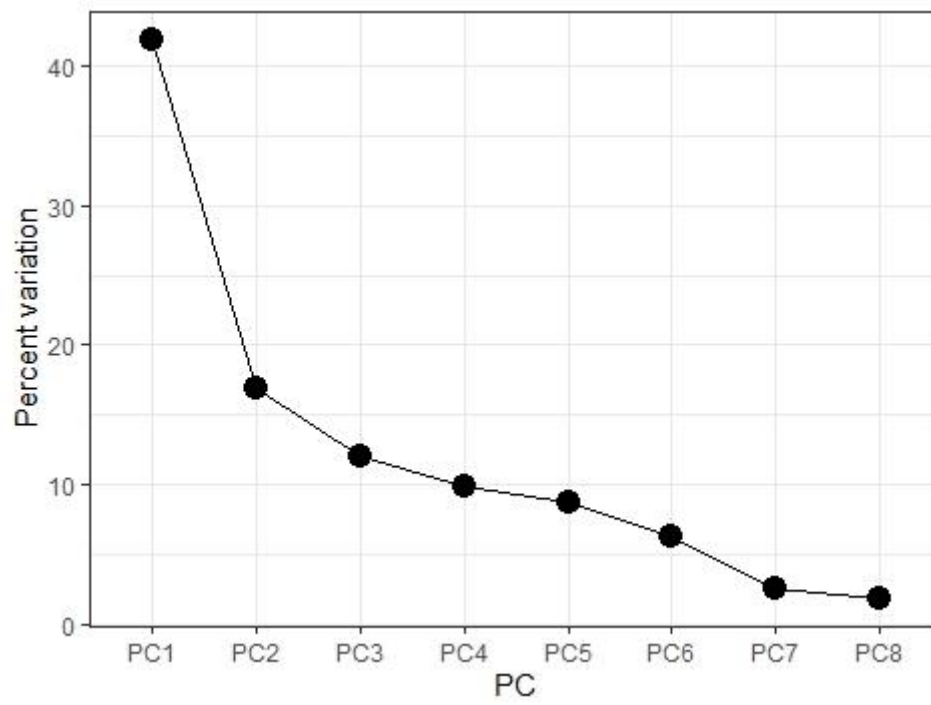
Supplementary figure 1G. Phenotypic distributions of arcsin transformed data for susceptibility to European canker in Field 20 months post inoculation: % Cankered Branches. Distribution shown by family.



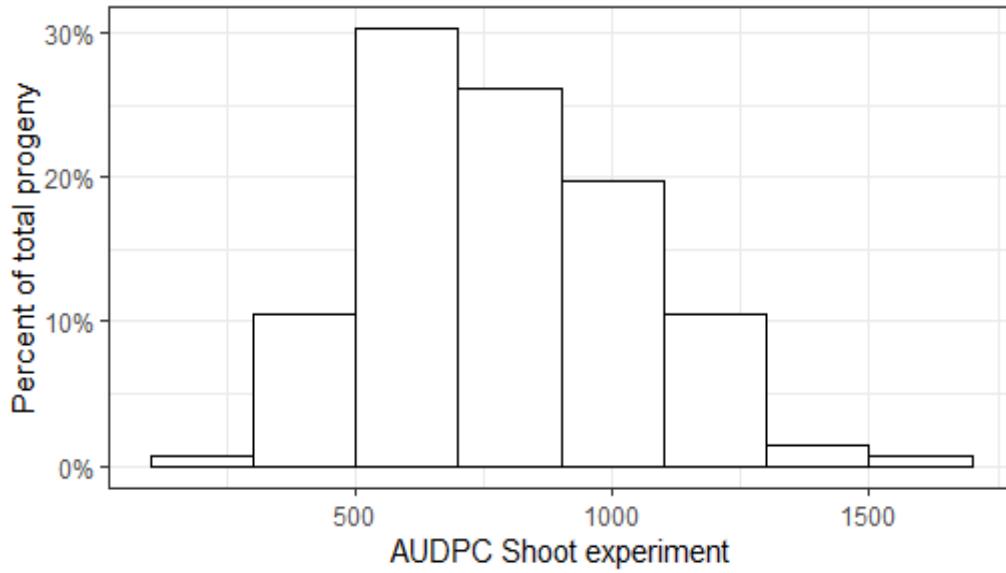
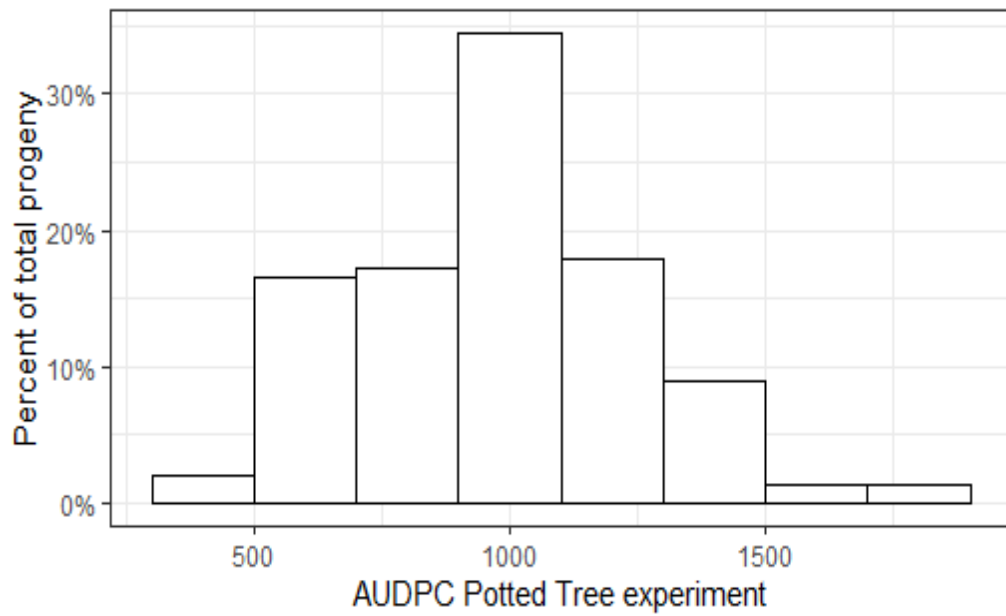
Supplementary figure 1H. Phenotypic distributions data for susceptibility to European canker in Field 20 months post inoculation: Canker Index. Distribution shown by family.



Supplementary figure 2. Best Linear Unbiased Estimates (BLUEs) of the multiparental population for each European canker phenotype. The data are shown as percent deviation from population mean, without the removal of outliers. Parents and standards are highlighted in colour, where the codes A-L refer to (A) seedling of *Malus robusta*, (B) Santana, (C) Jonathan, (D) Golden Delicious, (E) Elstar, (F) EM-Selection-1, (G) Aroma, (H), EM-Selection-2, (I) Cox Orange Pippin, (J) EM-Selection-4, (K) Gala, (L) EM-Selection-4. The inverse of %HTA is shown.



Supplementary figure 3. Scree plot from the principal component analysis (PCA) of the European canker phenotype data.



Supplementary figure 4. Phenotypic distributions for progeny of 'Golden Delicious' x 'M9' for susceptibility to European canker in a potted tree and a shoot experiment.

Supplementary data -Chapter 3

Supplementary Table 1 The table shows significantly enriched Gene Ontology (GO) terms from the enrichment analysis of differentially expressed genes in 'Golden Delicious' and 'M9' upon infection with *Neonectria ditissima*

Variety	Position	GO.ID	Term	Annotated	Significant	Expected	BH- adjusted p-value (q-value)
M9	P1	GO:0046345	Abscisic acid catabolic process	11	7	1.57	0.015516
M9	P1	GO:0006084	acetyl-CoA metabolic process	20	10	2.85	0.003998
M9	P1	GO:0003333	amino acid transmembrane transport	92	26	13.1	0.004896
M9	P1	GO:0017001	antibiotic catabolic process	31	12	4.42	0.036407
M9	P1	GO:0009734	Auxin-activated signaling pathway	193	52	27.49	0.003998
M9	P1	GO:0010268	brassinosteroid homeostasis	60	21	8.55	0.004896
M9	P1	GO:0016131	brassinosteroid metabolic process	68	22	9.68	0.008649
M9	P1	GO:0019722	calcium-mediated signaling	65	23	9.26	0.002998
M9	P1	GO:0009056	catabolic process	1645	252	234.29	0.035362
M9	P1	GO:0007166	cell surface receptor signaling pathway	387	83	55.12	0.000873
M9	P1	GO:0007267	Cell-cell signaling	85	20	12.11	0.000472
M9	P1	GO:0042219	cellular modified amino acid catabolic p...	10	6	1.42	0.048054
M9	P1	GO:0010588	cotyledon vascular tissue pattern format...	20	9	2.85	0.044331
M9	P1	GO:0009823	cytokinin catabolic process	10	6	1.42	0.048054
M9	P1	GO:0050832	defense response to fungus	432	91	61.53	0.011518
M9	P1	GO:0050982	detection of mechanical stimulus	20	9	2.85	0.044331
M9	P1	GO:0042938	dipeptide transport	10	6	1.42	0.048054
M9	P1	GO:0015752	D-ribose transmembrane transport	11	7	1.57	0.015516
M9	P1	GO:0006855	Drug transmembrane transport	123	35	17.52	0.003998
M9	P1	GO:0015753	D-xylose transmembrane transport	11	7	1.57	0.015516
M9	P1	GO:0009873	ethylene-activated signaling pathway	136	27	19.37	0.016547
M9	P1	GO:0009813	Flavonoid biosynthetic process	124	34	17.66	0.044331
M9	P1	GO:0030388	Fructose 1,6-bisphosphate metabolic process	11	8	1.57	0.003036
M9	P1	GO:0006002	Fructose 6-phosphate metabolic process	16	9	2.28	0.008649
M9	P1	GO:0009740	gibberellic acid mediated signaling path...	91	28	12.96	0.006845
M9	P1	GO:0006749	Glutathione metabolic process	67	33	9.54	6.27E-09

M9	P1	GO:0015793	glycerol transport	12	7	1.71	0.027914
M9	P1	GO:1901657	glycosyl compound metabolic process	191	47	27.2	0.005519
M9	P1	GO:0042446	hormone biosynthetic process	266	66	37.89	0.039957
M9	P1	GO:0042445	hormone metabolic process	401	116	57.11	0.004896
M9	P1	GO:0042538	hyperosmotic salinity response	72	23	10.25	0.008649
M9	P1	GO:0009694	jasmonic acid metabolic process	60	22	8.55	0.027707
M9	P1	GO:0015797	mannitol transport	11	7	1.57	0.015516
M9	P1	GO:0030001	Metal ion transport	378	80	53.84	0.008649
M9	P1	GO:0051704	Multi-organism process	1955	324	278.44	3.68E-05
M9	P1	GO:0015798	myo-inositol transport	12	7	1.71	0.027914
M9	P1	GO:0045926	negative regulation of growth	77	23	10.97	0.030919
M9	P1	GO:0015706	Nitrate transport	41	19	5.84	0.000193
M9	P1	GO:0035672	oligopeptide transmembrane transport	21	10	2.99	0.016547
M9	P1	GO:0055114	Oxidation-reduction process	1303	295	185.58	2.02E-12
M9	P1	GO:0010233	phloem transport	28	12	3.99	0.015516
M9	P1	GO:0009768	Photosynthesis, light harvesting in photosynthesis	23	10	3.28	0.035362
M9	P1	GO:0009773	photosynthetic electron transport in pho...	17	10	2.42	0.003514
M9	P1	GO:0010023	proanthocyanidin biosynthetic process	16	8	2.28	0.039
M9	P1	GO:0006468	Protein phosphorylation	1147	191	163.36	8.82E-05
M9	P1	GO:2000280	regulation of root development	139	27	19.8	0.015516
M9	P1	GO:0006355	Regulation of transcription, DNA-template	2210	361	314.76	6.26E-07
M9	P1	GO:0009737	response to abscisic acid	754	139	107.39	0.007613
M9	P1	GO:0001101	Response to acid chemical	1521	305	216.63	3.75E-06
M9	P1	GO:0072347	response to anesthetic	14	9	1.99	0.003514
M9	P1	GO:0046677	Response to antibiotic	410	89	58.39	1.32E-05
M9	P1	GO:0009617	response to bacterium	696	115	99.13	0.029156
M9	P1	GO:0009741	response to brassinosteroid	176	42	25.07	0.015516
M9	P1	GO:0010037	response to carbon dioxide	14	9	1.99	0.003514
M9	P1	GO:0010200	Response to chitin	207	80	29.48	8.1E-15
M9	P1	GO:0042493	Response to drug	783	206	111.52	1.1E-14
M9	P1	GO:0009725	response to hormone	2122	433	302.23	0.004896
M9	P1	GO:0009753	response to jasmonic acid	326	82	46.43	0.005519
M9	P1	GO:0080167	Response to karrikin	139	34	19.8	0.044331

M9	P1	GO:0009416	Response to light stimulus	928	141	132.17	0.010119
M9	P1	GO:0051707	Response to other organism	1549	295	220.62	0.016547
M9	P1	GO:0009751	response to salicylic acid	279	58	39.74	0.003018
M9	P1	GO:1902074	response to salt	35	14	4.98	0.01285
M9	P1	GO:0009611	Response to wounding	385	100	54.83	6.27E-09
M9	P1	GO:0009696	salicylic acid metabolic process	52	16	7.41	0.000548
M9	P1	GO:0044550	Secondary metabolite biosynthetic process	292	102	41.59	5.34E-07
M9	P1	GO:0015795	sorbitol transport	11	7	1.57	0.015516
M9	P1	GO:0005986	Sucrose biosynthetic process	15	8	2.14	0.025757
M9	P1	GO:0009407	Toxin catabolic process	39	21	5.55	3.04E-06
M9	P1	GO:0007178	transmembrane receptor protein serine/th...	248	53	35.32	0.018739
M9	P1	GO:0055085	Transmembrane transport	1229	264	175.04	5.34E-05
M9	P1	GO:0042939	tripeptide transport	13	7	1.85	0.044331
M9	P1	GO:0006722	triterpenoid metabolic process	37	19	5.27	0.003514
GD	P1	GO:0055114	Oxidation-reduction process	1303	313	186.52	4.72E-16
GD	P1	GO:0009611	Response to wounding	385	112	55.11	1.11E-13
GD	P1	GO:0042493	Response to drug	783	197	112.08	1.35E-08
GD	P1	GO:0006355	Regulation of transcription, DNA-template	2210	365	316.36	1.1E-07
GD	P1	GO:0006749	Glutathione metabolic process	67	31	9.59	2.29E-07
GD	P1	GO:0010200	Response to chitin	207	64	29.63	3.6E-07
GD	P1	GO:0009768	Photosynthesis, light harvesting in photosynthesis	23	16	3.29	1.3E-06
GD	P1	GO:0044550	Secondary metabolite biosynthetic process	292	106	41.8	1.6E-06
GD	P1	GO:0006855	Drug transmembrane transport	123	42	17.61	8.99E-06
GD	P1	GO:0009416	Response to light stimulus	928	175	132.84	1.04E-05
GD	P1	GO:0030388	Fructose 1,6-bisphosphate metabolic process	11	10	1.57	1.04E-05
GD	P1	GO:0009734	Auxin-activated signaling pathway	193	51	27.63	1.07E-05
GD	P1	GO:0009407	Toxin catabolic process	39	20	5.58	1.38E-05
GD	P1	GO:0030001	Metal ion transport	378	83	54.11	1.66E-05
GD	P1	GO:0001101	Response to acid chemical	1521	304	217.73	5.85E-05
GD	P1	GO:0005986	Sucrose biosynthetic process	15	11	2.15	8.22E-05
GD	P1	GO:0009753	response to jasmonic acid	326	79	46.67	0.000131
GD	P1	GO:0006468	Protein phosphorylation	1147	183	164.19	0.000178
GD	P1	GO:0080167	Response to karrikin	139	42	19.9	0.000186

GD	P1	GO:0006002	Fructose 6-phosphate metabolic process	16	11	2.29	0.000186
GD	P1	GO:0006094	Gluconeogenesis	28	15	4.01	0.000193
GD	P1	GO:0003333	amino acid transmembrane transport	92	31	13.17	0.000552
GD	P1	GO:0043090	amino acid import	10	8	1.43	0.00088
GD	P1	GO:0009056	catabolic process	1645	237	235.48	0.000956
GD	P1	GO:1901657	glycosyl compound metabolic process	191	46	27.34	0.001754
GD	P1	GO:0055085	Transmembrane transport	1229	268	175.93	0.001946
GD	P1	GO:0015706	Nitrate transport	41	17	5.87	0.002499
GD	P1	GO:0009773	photosynthetic electron transport in pho...	17	10	2.43	0.003132
GD	P1	GO:0046677	Response to antibiotic	410	89	58.69	0.003373
GD	P1	GO:0009695	jasmonic acid biosynthetic process	51	19	7.3	0.00461
GD	P1	GO:0009813	Flavonoid biosynthetic process	124	39	17.75	0.005549
GD	P1	GO:0019722	calcium-mediated signaling	65	22	9.3	0.006114
GD	P1	GO:0009740	gibberellic acid mediated signaling path...	91	29	13.03	0.00744
GD	P1	GO:0007166	cell surface receptor signaling pathway	387	69	55.4	0.00744
GD	P1	GO:0010345	Suberin biosynthetic process	33	14	4.72	0.007806
GD	P1	GO:0042446	hormone biosynthetic process	266	67	38.08	0.008245
GD	P1	GO:0009718	anthocyanin-containing compound biosynth...	46	18	6.58	0.010939
GD	P1	GO:0006000	Fructose metabolic process	20	10	2.86	0.014202
GD	P1	GO:0017001	antibiotic catabolic process	31	13	4.44	0.014703
GD	P1	GO:0009751	response to salicylic acid	279	59	39.94	0.016454
GD	P1	GO:0080144	amino acid homeostasis	17	9	2.43	0.016454
GD	P1	GO:0060918	auxin transport	144	29	20.61	0.018332
GD	P1	GO:0046916	cellular transition metal ion homeostasi...	83	17	11.88	0.018332
GD	P1	GO:0051704	Multi-organism process	1955	311	279.85	0.018332
GD	P1	GO:0010088	phloem development	32	13	4.58	0.018332
GD	P1	GO:0009809	lignin biosynthetic process	74	26	10.59	0.018332
GD	P1	GO:0051707	Response to other organism	1549	279	221.74	0.020812
GD	P1	GO:0062197	cellular response to chemical stress	210	40	30.06	0.021784
GD	P1	GO:0010089	xylem development	73	20	10.45	0.026158
GD	P1	GO:0009694	jasmonic acid metabolic process	60	25	8.59	0.031706
GD	P1	GO:0098869	cellular oxidant detoxification	139	35	19.9	0.031746
GD	P1	GO:0016131	brassinosteroid metabolic process	68	20	9.73	0.032433

GD	P1	GO:0009624	response to nematode	126	32	18.04	0.044549
GD	P1	GO:0046688	response to copper ion	31	12	4.44	0.044973
GD	P1	GO:0042737	drug catabolic process	62	19	8.88	0.044973
GD	P1	GO:0009820	alkaloid metabolic process	16	8	2.29	0.044973
GD	P1	GO:0010023	proanthocyanidin biosynthetic process	16	8	2.29	0.044973
M9	P2	GO:0006749	Glutathione metabolic process	67	11	1.85	0.006746
M9	P2	GO:0046345	Abscisic acid catabolic process	11	5	0.3	0.010625
M9	P2	GO:0042493	Response to drug	783	43	21.6	0.021081
M9	P2	GO:0009611	Response to wounding	385	26	10.62	0.021081
M9	P2	GO:0043620	Regulation of DNA-templated transcription	15	5	0.41	0.02496
M9	P2	GO:0010200	Response to chitin	207	17	5.71	0.029682
M9	P2	GO:0010053	Root epidermal cell differentiation	161	7	4.44	0.029682
M9	P2	GO:0009407	Toxin catabolic process	39	7	1.08	0.029682
M9	P2	GO:0051707	Response to other organism	1549	61	42.74	0.029682
M9	P2	GO:0055114	Oxidation-reduction process	1303	58	35.95	0.029682
M9	P2	GO:0032107	Regulation of response to nutrient level	18	5	0.5	0.030357
M9	P2	GO:0001101	Response to acid chemical	1521	62	41.97	0.036541
GD	P2	GO:0046345	Abscisic acid catabolic process	11	6	0.7	0.004947
GD	P2	GO:0009734	Auxin-activated signaling pathway	193	23	12.2	0.013653
GD	P2	GO:0042335	cuticle development	40	10	2.53	0.018889
GD	P2	GO:0009813	Flavonoid biosynthetic process	124	20	7.84	0.004578
GD	P2	GO:0030388	Fructose 1,6-bisphosphate metabolic process	11	10	0.7	3.37E-08
GD	P2	GO:0006002	Fructose 6-phosphate metabolic process	16	10	1.01	3.09E-06
GD	P2	GO:0006000	Fructose metabolic process	20	10	1.26	3.75E-05
GD	P2	GO:0009740	gibberellic acid mediated signaling path...	91	16	5.75	0.043523
GD	P2	GO:0009686	gibberellin biosynthetic process	66	12	4.17	0.043523
GD	P2	GO:0006094	Gluconeogenesis	28	14	1.77	4.38E-07
GD	P2	GO:0006749	Glutathione metabolic process	67	14	4.23	0.011007
GD	P2	GO:0015706	nitrate transport	41	11	2.59	0.006957
GD	P2	GO:0055114	Oxidation-reduction process	1303	154	82.35	8.1E-07
GD	P2	GO:0009768	Photosynthesis, light harvesting in photosynthesis	23	9	1.45	0.001717
GD	P2	GO:0009767	photosynthetic electron transport chain	56	16	3.54	0.01827
GD	P2	GO:0009773	photosynthetic electron transport in pho...	17	7	1.07	0.008245
GD	P2	GO:0019253	reductive pentose-phosphate cycle	11	5	0.7	0.038382

GD	P2	GO:1901957	regulation of cutin biosynthetic process	13	6	0.82	0.012311
GD	P2	GO:0043620	Regulation of DNA-templated transcription	15	6	0.95	0.023736
GD	P2	GO:0006355	Regulation of transcription, DNA-template	2210	163	139.67	0.014259
GD	P2	GO:0001101	Response to acid chemical	1521	136	96.12	0.017598
GD	P2	GO:0080167	Response to karrikin	139	23	8.78	0.004578
GD	P2	GO:0009416	Response to light stimulus	928	90	58.65	0.000024
GD	P2	GO:0009611	Response to wounding	385	51	24.33	1.25E-05
GD	P2	GO:0010053	Root epidermal cell differentiation	161	12	10.17	0.004578
GD	P2	GO:0044550	Secondary metabolite biosynthetic process	292	58	18.45	0.001012
GD	P2	GO:0016125	sterol metabolic process	92	17	5.81	0.01946
GD	P2	GO:0010345	Suberin biosynthetic process	33	14	2.09	2.63E-06
GD	P2	GO:0005986	Sucrose biosynthetic process	15	10	0.95	1.86E-06
GD	P2	GO:0006722	triterpenoid metabolic process	37	12	2.34	0.008245
GD	P2	GO:0006833	water transport	65	16	4.11	0.038382

Supplementary Table 2 The table shows significantly enriched Kyoto encyclopaedia of genes and genomes (KEGG) terms from the enrichment analysis of differentially expressed genes in 'Golden Delicious' and 'M9' upon infection with *Neonectria ditissima*

Variety	Pos.	ID	GeneRatio	BgRatio	BH-adj. p-value (q-value)	pathway	Class
GD	P1	ko02010	25/1483	73/10405	0.000112	ABC transporters	Environmental Information Processing; Membrane transport
GD	P1	ko00592	44/1483	107/10405	2.17E-10	alpha-Linolenic acid metabolism	Metabolism; Lipid metabolism
GD	P1	ko00590	21/1483	57/10405	0.000139	Arachidonic acid metabolism	Metabolism; Lipid metabolism
GD	P1	ko01230	77/1483	401/10405	0.012122	Biosynthesis of amino acids	Biosynthesis of amino acids
GD	P1	ko00710	40/1483	122/10405	1.9E-06	Carbon fixation in photosynthetic organisms	Metabolism; Energy metabolism
GD	P1	ko01200	93/1483	435/10405	0.000178	Carbon metabolism	Carbon metabolism
GD	P1	ko00703	15/1483	34/10405	0.000178	Cutin, suberine and wax biosynthesis	Metabolism; Lipid metabolism
GD	P1	ko00460	40/1483	108/10405	4.74E-08	Cyanoamino acid metabolism	Metabolism; Metabolism of other amino acids
GD	P1	ko00904	13/1483	40/10405	0.01063	Diterpenoid biosynthesis	Metabolism; Metabolism of terpenoids and polyketides
GD	P1	ko00701	23/1483	82/10405	0.003668	Fatty acid degradation	Metabolism; Lipid metabolism
GD	P1	ko00941	48/1483	102/10405	7.77E-14	Flavonoid biosynthesis	Metabolism; Biosynthesis of other secondary metabolites
GD	P1	ko00051	27/1483	110/10405	0.01063	Fructose and mannose metabolism	Metabolism; Carbohydrate metabolism
GD	P1	ko00480	61/1483	154/10405	2E-13	Glutathione metabolism	Metabolism; Metabolism of other amino acids
GD	P1	ko00100	55/1483	215/10405	6.19E-05	Glycolysis / Gluconeogenesis	Metabolism; Carbohydrate metabolism
GD	P1	ko00630	30/1483	113/10405	0.002047	Glyoxylate and dicarboxylate metabolism	Metabolism; Carbohydrate metabolism
GD	P1	ko00950	19/1483	52/10405	0.000361	Isoquinoline alkaloid biosynthesis	Metabolism; Biosynthesis of other secondary metabolites
GD	P1	ko00591	32/1483	66/10405	6.91E-10	Linoleic acid metabolism	Metabolism; Lipid metabolism
GD	P1	ko04016	60/1483	281/10405	0.003155	MAPK signaling pathway - plant	Environmental Information Processing; Signal transduction

GD	P	ko00902	10/1483	19/10405	0.000565	Monoterpenoid biosynthesis	Metabolism; Metabolism of terpenoids and polyketides
GD	P	ko00760	11/1483	35/10405	0.025759	Nicotinate and nicotinamide metabolism	Metabolism; Metabolism of cofactors and vitamins
GD	P	ko00040	32/1483	137/10405	0.01063	Pentose and glucuronate interconversions	Metabolism; Carbohydrate metabolism
GD	P	ko00030	28/1483	87/10405	0.000128	Pentose phosphate pathway	Metabolism; Carbohydrate metabolism
GD	P	ko00940	114/1483	293/10405	8.06E-24	Phenylpropanoid biosynthesis	Metabolism; Biosynthesis of other secondary metabolites
GD	P	ko00195	29/1483	84/10405	2.45E-05	Photosynthesis	Metabolism; Energy metabolism
GD	P	ko00196	20/1483	30/10405	1.55E-09	Photosynthesis - antenna proteins	Metabolism; Energy metabolism
GD	P	ko04075	97/1483	390/10405	1.51E-07	Plant hormone signal transduction	Environmental Information Processing; Signal transduction
GD	P	ko04626	82/1483	410/10405	0.003207	Plant-pathogen interaction	Organismal Systems; Environmental adaptation
GD	P	ko00909	18/1483	52/10405	0.001052	Sesquiterpenoid and triterpenoid biosynthesis	Metabolism; Metabolism of terpenoids and polyketides
GD	P	ko00500	56/1483	265/10405	0.005618	Starch and sucrose metabolism	Metabolism; Carbohydrate metabolism
GD	P	ko00945	29/1483	66/10405	7.22E-08	Stilbenoid, diarylheptanoid and gingerol biosynthesis	Metabolism; Biosynthesis of other secondary metabolites
GD	P	ko00920	17/1483	58/10405	0.009238	Sulfur metabolism	Metabolism; Energy metabolism
GD	P	ko00430	8/1483	18/10405	0.00808	Taurine and hypotaurine metabolism	Metabolism; Metabolism of other amino acids
GD	P	ko00900	19/1483	76/10405	0.029362	Terpenoid backbone biosynthesis	Metabolism; Metabolism of terpenoids and polyketides
GD	P	ko00960	19/1483	46/10405	6.19E-05	Tropane, piperidine and pyridine alkaloid biosynthesis	Metabolism; Biosynthesis of other secondary metabolites
GD	P	ko00380	50/1483	150/10405	4.17E-08	Tryptophan metabolism	Metabolism; Amino acid metabolism
GD	P	ko00350	24/1483	80/10405	0.001161	Tyrosine metabolism	Metabolism; Amino acid metabolism
GD	P	ko00908	23/1483	55/10405	6.4E-06	Zeatin biosynthesis	Metabolism; Metabolism of terpenoids and polyketides
GD	P	ko00195	26/652	84/10405	4.45E-10	Photosynthesis	Metabolism; Energy metabolism
GD	P	ko00710	32/652	122/10405	4.45E-10	Carbon fixation in photosynthetic organisms	Metabolism; Energy metabolism
GD	P	ko00940	50/652	293/10405	3.53E-09	Phenylpropanoid biosynthesis	Metabolism; Biosynthesis of other secondary metabolites

GD	P	ko01200	57/652	435/10405	2.46E-06	Carbon metabolism	Carbon metabolism
GD	P	ko00196	12/652	30/10405	3.14E-06	Photosynthesis - antenna proteins	Metabolism; Energy metabolism
GD	P	ko00480	26/652	154/10405	7.02E-05	Glutathione metabolism	Metabolism; Metabolism of other amino acids
GD	P	ko00030	17/652	87/10405	0.000363	Pentose phosphate pathway	Metabolism; Carbohydrate metabolism
GD	P	ko00904	11/652	40/10405	0.000363	Diterpenoid biosynthesis	Metabolism; Metabolism of terpenoids and polyketides
GD	P	ko04075	46/652	390/10405	0.000363	Plant hormone signal transduction	Environmental Information Processing; Signal transduction
GD	P	ko00908	13/652	55/10405	0.000375	Zeatin biosynthesis	Metabolism; Metabolism of terpenoids and polyketides
GD	P	ko00010	28/652	215/10405	0.002156	Glycolysis / Gluconeogenesis	Metabolism; Carbohydrate metabolism
GD	P	ko00073	9/652	34/10405	0.002156	Cutin, suberine and wax biosynthesis	Metabolism; Lipid metabolism
GD	P	ko00591	13/652	66/10405	0.002156	Linoleic acid metabolism	Metabolism; Lipid metabolism
GD	P	ko00941	17/652	102/10405	0.002156	Flavonoid biosynthesis	Metabolism; Biosynthesis of other secondary metabolites
GD	P	ko00592	17/652	107/10405	0.003589	alpha-Linolenic acid metabolism	Metabolism; Lipid metabolism
GD	P	ko02010	13/652	73/10405	0.005564	ABC transporters	Environmental Information Processing; Membrane transport
GD	P	ko000380	20/652	150/10405	0.009987	Tryptophan metabolism	Metabolism; Amino acid metabolism
GD	P	ko00909	10/652	52/10405	0.011152	Sesquiterpenoid and triterpenoid biosynthesis	Metabolism; Metabolism of terpenoids and polyketides
GD	P	ko00051	16/652	110/10405	0.011286	Fructose and mannose metabolism	Metabolism; Carbohydrate metabolism
GD	P	ko00900	12/652	76/10405	0.019829	Terpenoid backbone biosynthesis	Metabolism; Metabolism of terpenoids and polyketides
M9	P	ko00940	112/1441	293/10405	1.13E-23	Phenylpropanoid biosynthesis	Metabolism; Biosynthesis of other secondary metabolites
M9	P	ko00480	64/1441	154/10405	7.14E-16	Glutathione metabolism	Metabolism; Metabolism of other amino acids
M9	P	ko04075	107/1441	390/10405	1.61E-11	Plant hormone signal transduction	Environmental Information Processing; Signal transduction
M9	P	ko00460	41/1441	108/10405	7.41E-09	Cyanoamino acid metabolism	Metabolism; Metabolism of other amino acids
M9	P	ko00591	29/1441	66/10405	5.13E-08	Linoleic acid metabolism	Metabolism; Lipid metabolism

M9	P	ko00941	37/1441	102/10405	1.81E-07	Flavonoid biosynthesis	Metabolism; Biosynthesis of other secondary metabolites
M9	P	ko00908	24/1441	55/10405	1.02E-06	Zeatin biosynthesis	Metabolism; Metabolism of terpenoids and polyketides
M9	P	ko00960	20/1441	46/10405	1.05E-05	Tropene, piperidine and pyridine alkaloid biosynthesis	Metabolism; Biosynthesis of other secondary metabolites
M9	P	ko00945	25/1441	66/10405	1.07E-05	Stilbenoid, diarylheptanoid and gingerol biosynthesis	Metabolism; Biosynthesis of other secondary metabolites
M9	P	ko00950	21/1441	52/10405	2.23E-05	Isoquinoline alkaloid biosynthesis	Metabolism; Biosynthesis of other secondary metabolites
M9	P	ko02010	26/1441	73/10405	2.35E-05	ABC transporters	Environmental Information Processing; Membrane transport
M9	P	ko00590	22/1441	57/10405	2.71E-05	Arachidonic acid metabolism	Metabolism; Lipid metabolism
M9	P	ko00380	41/1441	150/10405	7.44E-05	Tryptophan metabolism	Metabolism; Amino acid metabolism
M9	P	ko00592	32/1441	107/10405	9.38E-05	alpha-Linolenic acid metabolism	Metabolism; Lipid metabolism
M9	P	ko00902	10/1441	19/10405	0.00046	Monoterpenoid biosynthesis	Metabolism; Metabolism of terpenoids and polyketides
M9	P	ko00909	18/1441	52/10405	0.000778	Sesquiterpenoid and triterpenoid biosynthesis	Metabolism; Metabolism of terpenoids and polyketides
M9	P	ko04016	60/1441	281/10405	0.001921	MAPK signaling pathway - plant	Environmental Information Processing; Signal transduction
M9	P	ko00010	48/1441	215/10405	0.002381	Glycolysis / Gluconeogenesis	Metabolism; Carbohydrate metabolism
M9	P	ko01200	85/1441	435/10405	0.0026	Carbon metabolism	Carbon metabolism
M9	P	ko00030	24/1441	87/10405	0.002806	Pentose phosphate pathway	Metabolism; Carbohydrate metabolism
M9	P	ko00920	18/1441	58/10405	0.002905	Sulfur metabolism	Metabolism; Energy metabolism
M9	P	ko00350	22/1441	80/10405	0.004726	Tyrosine metabolism	Metabolism; Amino acid metabolism
M9	P	ko00710	30/1441	122/10405	0.004821	Carbon fixation in photosynthetic organisms	Metabolism; Energy metabolism
M9	P	ko00900	21/1441	76/10405	0.005502	Terpenoid backbone biosynthesis	Metabolism; Metabolism of terpenoids and polyketides
M9	P	ko00270	36/1441	158/10405	0.006846	Cysteine and methionine metabolism	Metabolism; Amino acid metabolism
M9	P	ko00196	11/1441	30/10405	0.006846	Photosynthesis - antenna proteins	Metabolism; Energy metabolism
M9	P	ko01230	76/1441	401/10405	0.010033	Biosynthesis of amino acids	Biosynthesis of amino acids

M9	P 1	ko0 036 0	22/1 441	86/1 0405	0.011479	Phenylalanine metabolism	Metabolism; Amino acid metabolism
M9	P 1	ko0 063 0	27/1 441	113/ 1040 5	0.011573	Glyoxylate and dicarboxylate metabolism	Metabolism; Carbohydrate metabolism
M9	P 1	ko0 121 0	25/1 441	104/ 1040 5	0.014722	2-Oxocarboxylic acid metabolism	2-Oxocarboxylic acid metabolism
M9	P 1	ko0 090 6	16/1 441	58/1 0405	0.017518	Carotenoid biosynthesis	Metabolism; Metabolism of terpenoids and polyketides
M9	P 1	ko0 007 3	11/14 41	34/1 0405	0.018258	Cutin, suberine and wax biosynthesis	Metabolism; Lipid metabolism
M9	P 1	ko0 094 4	7/14 41	17/1 0405	0.019993	Flavone and flavonol biosynthesis	Metabolism; Biosynthesis of other secondary metabolites
M9	P 1	ko0 043 0	7/14 41	18/1 0405	0.028024	Taurine and hypotaurine metabolism	Metabolism; Metabolism of other amino acids
M9	P 1	ko0 019 5	20/1 441	84/1 0405	0.032961	Photosynthesis	Metabolism; Energy metabolism
M9	P 1	ko0 090 5	12/1 441	42/1 0405	0.032961	Brassinosteroid biosynthesis	Metabolism; Metabolism of terpenoids and polyketides
M9	P 1	ko0 075 0	7/14 41	19/1 0405	0.036024	Vitamin B6 metabolism	Metabolism; Metabolism of cofactors and vitamins
M9	P 2	ko0 029 0	5/26 5	37/1 0405	0.020021	Valine, leucine and isoleucine biosynthesis	Metabolism; Amino acid metabolism
M9	P 2	ko0 038 0	13/2 65	150/ 1040 5	0.00132	Tryptophan metabolism	Metabolism; Amino acid metabolism
M9	P 2	ko0 046 0	10/2 65	108/ 1040 5	0.004121	Cyanoamino acid metabolism	Metabolism; Metabolism of other amino acids
M9	P 2	ko0 048 0	18/2 65	154/ 1040 5	2.94E-06	Glutathione metabolism	Metabolism; Metabolism of other amino acids
M9	P 2	ko0 059 0	8/26 5	57/1 0405	0.001075	Arachidonic acid metabolism	Metabolism; Lipid metabolism
M9	P 2	ko0 059 1	11/26 5	66/1 0405	0.00002	Linoleic acid metabolism	Metabolism; Lipid metabolism
M9	P 2	ko0 059 2	10/2 65	107/ 1040 5	0.004006	alpha-Linolenic acid metabolism	Metabolism; Lipid metabolism
M9	P 2	ko0 090 8	8/26 5	55/1 0405	0.000931	Zeatin biosynthesis	Metabolism; Metabolism of terpenoids and polyketides
M9	P 2	ko0 094 0	27/2 65	293/ 1040 5	4.66E-07	Phenylpropanoid biosynthesis	Metabolism; Biosynthesis of other secondary metabolites
M9	P 2	ko0 201 0	10/2 65	73/1 0405	0.000265	ABC transporters	Environmental Information Processing; Membrane transport
M9	P 2	ko0 407 5	26/2 65	390/ 1040 5	0.000147	Plant hormone signal transduction	Environmental Information Processing; Signal transduction

Supplementary Table 3 The table shows significantly enriched protein family domains (PFAM) from the enrichment analysis of differentially expressed genes in 'Golden Delicious' and 'M9' upon infection with *Neonectria ditissima*

Variety	position	ID	GeneRatio	BgRatio	BH-adjusted p-value (q-value)	Count
GD	P1	Auxin_canalis	6/4279	10/28785	0.010196	6
GD	P1	Chalcone	6/4279	10/28785	0.010196	6
GD	P1	PH_2	6/4279	10/28785	0.010196	6
GD	P1	DUF3774	6/4279	11/28785	0.017036	6
GD	P1	GST_C_3	6/4279	11/28785	0.017036	6
GD	P1	PPO1_DWL	6/4279	11/28785	0.017036	6
GD	P1	PPO1_KFDV	6/4279	11/28785	0.017036	6
GD	P1	Tyrosinase	6/4279	11/28785	0.017036	6
GD	P1	DUF617	6/4279	12/28785	0.027295	6
GD	P1	Glycolytic	7/4279	11/28785	0.002848	7
GD	P1	Hpt	7/4279	12/28785	0.005304	7
GD	P1	BBE	7/4279	14/28785	0.014915	7
GD	P1	SE	8/4279	13/28785	0.001499	8
GD	P1	DUF1645	8/4279	14/28785	0.002848	8
GD	P1	Pec_lyase_C	8/4279	19/28785	0.024124	8
GD	P1	PFK	8/4279	20/28785	0.033394	8
GD	P1	GH3	9/4279	12/28785	8.69E-05	9
GD	P1	SEO_C	10/4279	15/28785	0.000118	10
GD	P1	SEO_N	10/4279	15/28785	0.000118	10
GD	P1	Oxidored_FMN	10/4279	17/28785	0.000462	10
GD	P1	PDDEXK_6	10/4279	21/28785	0.003389	10
GD	P1	AAA_assoc	10/4279	23/28785	0.00763	10
GD	P1	Methyltransf_7	10/4279	24/28785	0.010385	10
GD	P1	PP2	10/4279	27/28785	0.024124	10
GD	P1	MIP	10/4279	29/28785	0.03945	10
GD	P1	TCP	11/4279	29/28785	0.014386	11
GD	P1	ABC_trans_N	11/4279	31/28785	0.023316	11
GD	P1	PDR_assoc	11/4279	31/28785	0.023316	11
GD	P1	LysM	12/4279	35/28785	0.02211	12
GD	P1	FAD_binding_4	12/4279	37/28785	0.033451	12
GD	P1	FBPase	10/4279	12/28785	6.58E-06	10
GD	P1	p450	101/4279	297/28785	1.65E-14	101
GD	P1	Cupin_1	13/4279	32/28785	0.00333	13
GD	P1	Glyco_hydro_28	13/4279	41/28785	0.030668	13
GD	P1	zf-C2H2_6	13/4279	42/28785	0.036939	13
GD	P1	GMC_oxred_C	14/4279	23/28785	1.27E-05	14
GD	P1	GMC_oxred_N	14/4279	23/28785	1.27E-05	14
GD	P1	Lipoxygenase	14/4279	29/28785	0.000283	14
GD	P1	PLAT	14/4279	31/28785	0.000611	14

GD	P1	LOB	14/4279	41/28785	0.012251	14
GD	P1	Thaumatococcus	15/4279	34/28785	0.000474	15
GD	P1	ANF_receptor	15/4279	36/28785	0.000965	15
GD	P1	Lig_chan	15/4279	36/28785	0.000965	15
GD	P1	SBP_bac_3	15/4279	36/28785	0.000965	15
GD	P1	Peptidase_S10	16/4279	43/28785	0.002539	16
GD	P1	Glutaredoxin	16/4279	49/28785	0.010385	16
GD	P1	Dimerisation	18/4279	42/28785	0.000171	18
GD	P1	Methyltransf_2	18/4279	42/28785	0.000171	18
GD	P1	Glyco_hydro_1	18/4279	44/28785	0.000322	18
GD	P1	EF-hand_6	18/4279	66/28785	0.037417	18
GD	P1	Abhydrolase_3	19/4279	41/28785	3.12E-05	19
GD	P1	Usp	19/4279	57/28785	0.003389	19
GD	P1	GRAS	19/4279	58/28785	0.004216	19
GD	P1	TAXi_C	19/4279	62/28785	0.009953	19
GD	P1	TAXi_N	19/4279	63/28785	0.011203	19
GD	P1	Bet_v_1	20/4279	35/28785	2.94E-07	20
GD	P1	AUX_IAA	20/4279	62/28785	0.00386	20
GD	P1	ABC2_membrane	20/4279	67/28785	0.010196	20
GD	P1	AMP-binding_C	21/4279	52/28785	0.000116	21
GD	P1	Stress-antifung	22/4279	56/28785	0.000117	22
GD	P1	Chloroa_b-bind	23/4279	43/28785	1.54E-07	23
GD	P1	ABC_membrane	23/4279	64/28785	0.000322	23
GD	P1	GST_N_3	24/4279	49/28785	5.27E-07	24
GD	P1	AMP-binding	24/4279	66/28785	0.000187	24
GD	P1	Cu-oxidase	24/4279	70/28785	0.000474	24
GD	P1	Cu-oxidase_2	24/4279	70/28785	0.000474	24
GD	P1	Cu-oxidase_3	24/4279	70/28785	0.000474	24
GD	P1	Aldo_ket_red	25/4279	51/28785	2.94E-07	25
GD	P1	LEA_2	26/4279	68/28785	3.67E-05	26
GD	P1	adh_short_C2	26/4279	70/28785	6.71E-05	26
GD	P1	EF-hand_7	27/4279	107/28785	0.02211	27
GD	P1	EamA	28/4279	63/28785	5.27E-07	28
GD	P1	PTR2	29/4279	77/28785	1.65E-05	29
GD	P1	PGG	29/4279	80/28785	3.59E-05	29
GD	P1	ADH_N	29/4279	94/28785	0.000714	29
GD	P1	Lipase_GDSL	29/4279	97/28785	0.001234	29
GD	P1	Aa_trans	31/4279	77/28785	1.50E-06	31
GD	P1	adh_short	31/4279	85/28785	1.65E-05	31
GD	P1	ADH_zinc_N	32/4279	100/28785	0.000173	32
GD	P1	EF-hand_5	32/4279	132/28785	0.020079	32
GD	P1	GST_C_2	33/4279	54/28785	7.35E-13	33
GD	P1	peroxidase	33/4279	96/28785	3.09E-05	33
GD	P1	MatE	34/4279	66/28785	2.08E-10	34
GD	P1	HMA	35/4279	104/28785	2.75E-05	35
GD	P1	Abhydrolase_1	35/4279	129/28785	0.002147	35
GD	P1	Transferase	36/4279	100/28785	3.75E-06	36
GD	P1	LRR_4	36/4279	160/28785	0.037181	36

GD	P1	GST_N	37/4279	61/28785	3.48E-14	37
GD	P1	EF-hand_1	37/4279	124/28785	0.000216	37
GD	P1	GST_C	38/4279	67/28785	2.61E-13	38
GD	P1	DUF3403	42/4279	95/28785	3.53E-10	42
GD	P1	WRKY	42/4279	110/28785	7.23E-08	42
GD	P1	Ank_2	42/4279	191/28785	0.032035	42
GD	P1	ABC_tran	43/4279	177/28785	0.005304	43
GD	P1	GUB_WAK_bind	46/4279	132/28785	2.94E-07	46
GD	P1	S_locus_glycop	54/4279	143/28785	7.08E-10	54
GD	P1	AP2	58/4279	173/28785	2.81E-08	58
GD	P1	PAN_2	60/4279	153/28785	1.16E-11	60
GD	P1	B_lectin	60/4279	164/28785	3.09E-10	60
GD	P1	2OG-Fell_Oxy	67/4279	156/28785	4.99E-15	67
GD	P1	DIOX_N	68/4279	155/28785	1.11E-15	68
GD	P1	Myb_DNA-binding	77/4279	344/28785	0.001234	77
GD	P1	UDPGT	84/4279	192/28785	3.27E-19	84
GD	P2	FBPase	10/1808	12/28785	1.26E-08	10
GD	P2	Usp	10/1808	57/28785	0.029857	10
M9	P1	Cytokin-bind	6/4196	10/28785	0.008722	6
M9	P1	TPP_enzyme_M	6/4196	10/28785	0.008722	6
M9	P1	FAF	6/4196	11/28785	0.015634	6
GD	P2	GST_N_3	11/1808	49/28785	0.002842	11
M9	P1	Hpt	6/4196	12/28785	0.025297	6
M9	P1	EXS	6/4196	13/28785	0.036425	6
M9	P1	STAS	6/4196	13/28785	0.036425	6
M9	P1	Sulfate_transp	6/4196	13/28785	0.036425	6
M9	P1	PPO1_DWL	7/4196	11/28785	0.002847	7
GD	P2	GST_C_2	13/1808	54/28785	0.000564	13
M9	P1	PPO1_KFDV	7/4196	11/28785	0.002847	7
GD	P2	Bet_v_1	14/1808	35/28785	7.19E-07	14
GD	P2	Chloroa_b-bind	14/1808	43/28785	9.01E-06	14
GD	P2	EamA	14/1808	63/28785	0.000608	14
GD	P2	ABC2_membrane	14/1808	67/28785	0.001044	14
M9	P1	TPP_enzyme_C	7/4196	11/28785	0.002847	7
GD	P2	Peptidase_S10	15/1808	43/28785	1.63E-06	15
M9	P1	TPP_enzyme_N	7/4196	11/28785	0.002847	7
GD	P2	PTR2	16/1808	77/28785	0.000522	16
GD	P2	PGG	16/1808	80/28785	0.00061	16
GD	P2	GST_N	17/1808	61/28785	6.59E-06	17
GD	P2	MatE	17/1808	66/28785	1.87E-05	17
GD	P2	Abhydrolase_1	17/1808	129/28785	0.031244	17
GD	P2	GST_C	18/1808	67/28785	5.91E-06	18
GD	P2	peroxidase	18/1808	96/28785	0.000605	18
GD	P2	Lipase_GDSL	18/1808	97/28785	0.000608	18
GD	P2	WRKY	18/1808	110/28785	0.002729	18
M9	P1	Tyrosinase	7/4196	11/28785	0.002847	7
GD	P2	Transferase	19/1808	100/28785	0.000374	19
GD	P2	DUF3403	20/1808	95/28785	5.25E-05	20

GD	P2	GUB_WAK_bind	22/1808	132/28785	0.000598	22
GD	P2	S_locus_glycop	23/1808	143/28785	0.000608	23
M9	P1	DUF617	7/4196	12/28785	0.005118	7
GD	P2	ABC_tran	24/1808	177/28785	0.004585	24
M9	P1	GH3	7/4196	12/28785	0.005118	7
GD	P2	PAN_2	26/1808	153/28785	0.000107	26
GD	P2	B_lectin	27/1808	164/28785	0.000122	27
GD	P2	AP2	29/1808	173/28785	4.65E-05	29
M9	P1	DUF1645	7/4196	14/28785	0.013026	7
GD	P2	2OG-Fell_Oxy	31/1808	156/28785	7.19E-07	31
GD	P2	DIOX_N	31/1808	155/28785	7.19E-07	31
GD	P2	Chalcone	4/1808	10/28785	0.028145	4
GD	P2	Glycolytic	4/1808	11/28785	0.035642	4
M9	P1	Chal_sti_synt_C	7/4196	17/28785	0.037568	7
M9	P1	Chal_sti_synt_N	7/4196	17/28785	0.037568	7
M9	P1	DUF3475	7/4196	17/28785	0.037568	7
GD	P2	Myb_DNA-binding	41/1808	344/28785	0.001091	41
M9	P1	DUF668	7/4196	17/28785	0.037568	7
M9	P1	FBPase	8/4196	12/28785	0.000853	8
M9	P1	SE	8/4196	13/28785	0.001638	8
M9	P1	Zein-binding	8/4196	19/28785	0.021701	8
M9	P1	Oxidored_FMN	9/4196	17/28785	0.00276	9
M9	P1	ADH_N_2	9/4196	20/28785	0.008634	9
M9	P1	Glyco_hydro_18	9/4196	20/28785	0.008634	9
M9	P1	PDDEXK_6	9/4196	21/28785	0.011917	9
M9	P1	Dynamamin_M	9/4196	24/28785	0.028922	9
M9	P1	GED	9/4196	24/28785	0.028922	9
M9	P1	Cip_N	10/4196	24/28785	0.008722	10
M9	P1	Dirigent	11/4196	33/28785	0.032148	11
M9	P1	Lipoxygenase	12/4196	29/28785	0.003936	12
M9	P1	FAD_binding_4	12/4196	37/28785	0.028922	12
M9	P1	HSF_DNA-bind	12/4196	37/28785	0.028922	12
M9	P2	GST_N	10/768	61/28785	0.000163	10
M9	P2	ABC_membrane	10/768	64/28785	0.000204	10
M9	P2	GST_C	10/768	67/28785	0.000282	10
M9	P1	GMC_oxred_C	13/4196	23/28785	6.62E-05	13
M9	P2	Bet_v_1	11/768	35/28785	3.03E-07	11
M9	P2	EamA	11/768	63/28785	4.53E-05	11
M9	P2	PTR2	11/768	77/28785	0.000195	11
M9	P2	DIOX_N	11/768	155/28785	0.02733	11
M9	P2	2OG-Fell_Oxy	11/768	156/28785	0.027843	11
M9	P1	GMC_oxred_N	13/4196	23/28785	6.62E-05	13
M9	P1	PLAT	13/4196	31/28785	0.002451	13
M9	P1	Cupin_1	13/4196	32/28785	0.003124	13
M9	P1	ANF_receptor	13/4196	36/28785	0.008634	13
M9	P1	Lig_chan	13/4196	36/28785	0.008634	13
M9	P1	SBP_bac_3	13/4196	36/28785	0.008634	13
M9	P1	LOB	13/4196	41/28785	0.026489	13

M9	P1	DUF4228	13/4196	43/28785	0.036724	13
M9	P1	Thaumatococcus	14/4196	34/28785	0.001813	14
M9	P2	MatE	13/768	66/28785	1.67E-06	13
M9	P1	DPBB_1	14/4196	38/28785	0.005139	14
M9	P1	WAK_assoc	14/4196	38/28785	0.005139	14
M9	P1	zf-C2H2_6	14/4196	42/28785	0.012753	14
M9	P1	Chloroalba_bind	14/4196	43/28785	0.015634	14
M9	P1	Peptidase_S10	14/4196	43/28785	0.015634	14
M9	P1	Abhydrolase_3	15/4196	41/28785	0.003936	15
M9	P2	WRKY	14/768	110/28785	5.81E-05	14
M9	P1	zf-Dof	15/4196	44/28785	0.008121	15
M9	P1	PMEI	15/4196	48/28785	0.01725	15
M9	P1	Glyco_hydro_1	17/4196	44/28785	0.001116	17
M9	P2	ABC_tran	15/768	177/28785	0.00165	15
M9	P1	TAXi_C	17/4196	62/28785	0.036344	17
M9	P1	Glyco_hydro_17	17/4196	63/28785	0.03884	17
M9	P1	TAXi_N	17/4196	63/28785	0.03884	17
M9	P1	Cu_bind_like	18/4196	49/28785	0.001363	18
M9	P1	GRAS	18/4196	58/28785	0.008634	18
M9	P1	Aldo_ket_red	19/4196	51/28785	0.000817	19
M9	P2	AP2	18/768	173/28785	4.66E-05	18
M9	P1	MFS_1	19/4196	68/28785	0.020691	19
M9	P1	PA	19/4196	68/28785	0.020691	19
M9	P1	Dimerisation	22/4196	42/28785	3.18E-07	22
M9	P1	Methyltransf_2	22/4196	42/28785	3.18E-07	22
M9	P1	AMP-binding_C	22/4196	52/28785	2.74E-05	22
M9	P1	Cu-oxidase	23/4196	70/28785	0.001229	23
M9	P1	Cu-oxidase_2	23/4196	70/28785	0.001229	23
M9	P1	Cu-oxidase_3	23/4196	70/28785	0.001229	23
M9	P1	PGG	23/4196	80/28785	0.006936	23
M9	P1	ADH_N	23/4196	94/28785	0.039479	23
M9	P1	Inhibitor_I9	24/4196	68/28785	0.000282	24
M9	P2	UDPGT	23/768	192/28785	3.04E-07	23
M9	P1	Lipase_GDSL	24/4196	97/28785	0.032977	24
M9	P1	Bet_v_1	25/4196	35/28785	3.42E-12	25
M9	P1	GST_N_3	25/4196	49/28785	8.30E-08	25
M9	P1	AUX_IAA	25/4196	62/28785	1.68E-05	25
M9	P1	AMP-binding	25/4196	66/28785	5.30E-05	25
M9	P1	Peptidase_S8	25/4196	68/28785	8.73E-05	25
M9	P1	Sugar_tr	25/4196	94/28785	0.012067	25
M9	P1	ABC_membrane	26/4196	64/28785	8.97E-06	26
M9	P2	p450	25/768	297/28785	3.57E-05	25
M9	P1	MatE	26/4196	66/28785	1.68E-05	26
M9	P1	LEA_2	26/4196	68/28785	3.05E-05	26
M9	P1	adh_short_C2	26/4196	70/28785	5.30E-05	26
M9	P1	adh_short	26/4196	85/28785	0.00163	26
M9	P1	PTR2	27/4196	77/28785	0.000102	27
M9	P1	Abhydrolase_6	27/4196	95/28785	0.003619	27

M9	P1	EamA	28/4196	63/28785	3.51E-07	28
M9	P1	Aa_trans	28/4196	77/28785	3.80E-05	28
M9	P1	HMA	28/4196	104/28785	0.006498	28
M9	P1	Stress-antifung	31/4196	56/28785	8.83E-11	31
M9	P2	Glyco_hydro_19	3/768	11/28785	0.026256	3
M9	P1	ADH_zinc_N	31/4196	100/28785	0.000349	31
M9	P1	Transferase	31/4196	100/28785	0.000349	31
M9	P1	EF-hand_1	33/4196	124/28785	0.003434	33
M9	P1	GST_C_2	34/4196	54/28785	4.89E-14	34
M9	P1	peroxidase	34/4196	96/28785	8.28E-06	34
M9	P1	DUF3403	37/4196	95/28785	1.87E-07	37
M9	P1	GST_N	39/4196	61/28785	4.69E-16	39
M9	P1	GST_C	39/4196	67/28785	2.00E-14	39
M9	P1	Abhydrolase_1	39/4196	129/28785	7.51E-05	39
M9	P1	LRR_4	40/4196	160/28785	0.003534	40
M9	P2	Hpt	4/768	12/28785	0.003161	4
M9	P2	GAF	4/768	19/28785	0.015588	4
M9	P2	AAA_assoc	4/768	23/28785	0.02733	4
M9	P1	HLH	40/4196	169/28785	0.008634	40
M9	P1	Ank_2	41/4196	191/28785	0.036425	41
M9	P1	ABC_tran	43/4196	177/28785	0.003936	43
M9	P1	WRKY	46/4196	110/28785	2.12E-10	46
M9	P1	S_locus_glycop	48/4196	143/28785	3.18E-07	48
M9	P1	GUB_WAK_bind	51/4196	132/28785	4.49E-10	51
M9	P2	HisKA	5/768	31/28785	0.0146	5
M9	P2	Thaumatocin	5/768	34/28785	0.019989	5
M9	P2	HALZ	5/768	37/28785	0.02733	5
M9	P2	Abhydrolase_3	5/768	41/28785	0.038043	5
M9	P1	PAN_2	52/4196	153/28785	6.06E-08	52
M9	P1	B_lectin	52/4196	164/28785	5.81E-07	52
M9	P1	AP2	61/4196	173/28785	4.49E-10	61
M9	P2	Lipoxygenase	6/768	29/28785	0.001779	6
GD	P2	UDPGT	45/1808	192/28785	4.28E-12	45
GD	P2	p450	49/1808	297/28785	8.22E-08	49
GD	P2	GH3	5/1808	12/28785	0.007586	5
GD	P2	PUNUT	5/1808	14/28785	0.015771	5
GD	P2	CCT_2	5/1808	18/28785	0.039051	5
M9	P2	PLAT	6/768	31/28785	0.002343	6
M9	P2	Dimerisation	6/768	42/28785	0.011155	6
M9	P2	Methyltransf_2	6/768	42/28785	0.011155	6
M9	P2	Glyco_hydro_1	6/768	44/28785	0.012798	6
GD	P2	Hpt	6/1808	12/28785	0.000741	6
GD	P2	PsbP	6/1808	20/28785	0.014783	6
GD	P2	Glyco_hydro_9	6/1808	24/28785	0.031244	6
GD	P2	SQHop_cyclase_C	6/1808	24/28785	0.031244	6
GD	P2	SQHop_cyclase_N	6/1808	24/28785	0.031244	6
M9	P2	Glutaredoxin	6/768	49/28785	0.019756	6
M9	P1	DIOX_N	65/4196	155/28785	1.72E-14	65

M9	P1	2OG-Fell_Oxy	66/4196	156/28785	7.80E-15	66
M9	P1	Myb_DNA-binding	69/4196	344/28785	0.021366	69
M9	P1	UDPGT	73/4196	192/28785	7.75E-14	73
M9	P2	Peptidase_S10	7/768	43/28785	0.002201	7
GD	P2	Lipoxygenase	7/1808	29/28785	0.021535	7
GD	P2	MIP	7/1808	29/28785	0.021535	7
GD	P2	PLAT	7/1808	31/28785	0.029857	7
M9	P1	p450	107/4196	297/28785	1.45E-17	107
GD	P2	HALZ	8/1808	37/28785	0.021535	8
GD	P2	Dimerisation	8/1808	42/28785	0.039051	8
GD	P2	Methyltransf_2	8/1808	42/28785	0.039051	8
M9	P2	GST_N_3	8/768	49/28785	0.000868	8
M9	P2	Aa_trans	8/768	77/28785	0.012798	8
GD	P2	Thaumatococin	9/1808	34/28785	0.002842	9
GD	P2	Abhydrolase_3	9/1808	41/28785	0.011593	9
M9	P2	GST_C_2	9/768	54/28785	0.000283	9
M9	P2	GRAS	9/768	58/28785	0.000476	9
M9	P2	peroxidase	9/768	96/28785	0.012798	9

Supplementary Table 4 Description of the genome positions of the Quantitative trait loci (QTL) used in this study and the Single nucleotide polymorphisms (SNPs) haplotypes used to define the QTL-R al

Physical positions of QTL interval in GDDH13_v1.1			SNP haplotype within QTL interval used to characterise QTL-R alleles			
QTL	Start	End	Haplotype ID	SNP sequence		Described in Karlstrom et al (2022)
2	12184811	34586192	HB2-Gala-R	CGAAAAGAGGAGGACGGGAAGAGAAAACCACAGGAGCCGCAAAAAAGAGGGAACGAAG		Yes
6	4582999	36511754	HB6-shared-R	GGAAACAGA		Yes
8	644719	25701079	HB8-shared-R	AGCGGGGCAAGAAAAGGAGGAGAGAGGGAAAAAGGGAGAGGGGAAGAAGCAAGGAGAAGGG		Yes
8	-	-	HB8-36	CAAAGGGCAGAGAGGAGGGAGAGGAAGAAAAAGGGAGAGGGGAAGAAAACAGGGAGGAA		No
10	32739747	35052353	HB10-shared-R1	AAGAGCAGCCGCGGGACAACAGGAGAAACGCAGAG		Yes
15	1009852	47481793	HB15-shared-R	AAAAG		Yes
16	2811437	12155950	HB16-38	GAGGACCGAGAAACGAGGAGAGGAAGAACAAGAAAAGAAAA		No

Supplementary table 5 All differentially expressed (DE) genes within the quantitative trait loci (QTL) intervals in comparisons of gene expression in apple genotypes with QTL-R vs QTL-S alleles.

Gene ID GDDH13_ v1.1	QTL	Treat ment	Chromo some	logF C (QTL- S - QTL- R)	adj.P. Val	start	end	stra nd	Predicted gene function from GDDH13_v1.1
MD02G12 74400	QTL 2	Inocu lated	Chr02	1.183 198	0.028 637	32891 923	32895 562	-	3'-5'-exoribonuclease family protein
MD02G11 88900	QTL 2	Inocu lated	Chr02	- 1.829 55	0.044 457	17257 096	17261 825	-	ACT domain repeat 1
MD02G11 93600	QTL 2	Inocu lated	Chr02	- 1.610 87	0.039 697	18430 092	18431 221	+	ankyrin repeat family protein
MD02G12 54000	QTL 2	Contro l	Chr02	1.581 599	1.66E -11	30559 213	30563 052	+	ATP-dependent caseinolytic (Clp) protease/crotonase family protein
MD02G12 54000	QTL 2	Inocu lated	Chr02	1.133 449	3.53E -08	30559 213	30563 052	+	ATP-dependent caseinolytic (Clp) protease/crotonase family protein
MD02G11 91200	QTL 2	Contro l	Chr02	2.291 769	0.034 811	17766 777	17767 178	-	Branched-chain amino acid aminotransferase 2
MD02G11 91200	QTL 2	Inocu lated	Chr02	2.298 364	3.13E -05	17766 777	17767 178	-	Branched-chain amino acid aminotransferase 2
MD02G12 75700	QTL 2	Inocu lated	Chr02	- 1.250 07	0.042 905	33001 665	33003 718	+	cyclin family
MD02G12 00700	QTL 2	Inocu lated	Chr02	1.524 994	0.020 184	19804 842	19806 865	-	cytochrome P450
MD02G11 64500	QTL 2	Contro l	Chr02	- 3.329 84	0.023 329	14047 028	14047 783	+	Disease resistance protein (CC-NBS-LRR class) family
MD02G11 64500	QTL 2	Inocu lated	Chr02	- 2.631 93	0.008 751	14047 028	14047 783	+	Disease resistance protein (CC-NBS-LRR class) family
MD02G12 60200	QTL 2	Contro l	Chr02	1.521 796	0.026 122	31366 383	31368 219	-	disease resistance protein (TIR-NBS-LRR class)
MD02G12 60200	QTL 2	Inocu lated	Chr02	1.524 321	0.008 221	31366 383	31368 219	-	disease resistance protein (TIR-NBS-LRR class)
MD02G12 17100	QTL 2	Inocu lated	Chr02	1.505 535	0.039 697	24885 788	24887 962	-	Disease resistance protein (TIR-NBS-LRR class) family
MD02G12 42000	QTL 2	Inocu lated	Chr02	- 3.036 69	9.62E -08	29215 858	29220 262	+	Glycosyl hydrolase family protein
MD02G12 59900	QTL 2	Inocu lated	Chr02	1.585 712	0.001 406	31354 108	31354 434	+	Glycosyl hydrolase family protein
MD02G12 65300	QTL 2	Inocu lated	Chr02	- 1.019 67	0.047 493	31954 554	31959 766	+	Integrase-type DNA- binding superfamily protein
MD02G12 11800	QTL 2	Contro l	Chr02	3.847 031	5.18E -08	22663 038	22667 000	+	Leucine carboxyl methyltransferase
MD02G12 12000	QTL 2	Contro l	Chr02	3.301 918	4.16E -07	22674 090	22675 639	+	Leucine carboxyl methyltransferase
MD02G12 12000	QTL 2	Inocu lated	Chr02	2.883 225	2.19E -08	22674 090	22675 639	+	Leucine carboxyl methyltransferase

MD02G12 11800	QTL 2	Inoculated	Chr02	3.177 513	9.62E -08	22663 038	22667 000	+	Leucine carboxyl methyltransferase
MD02G12 24000	QTL 2	Control	Chr02	- 4.267 35	2.61E -05	26257 974	26261 351	+	Leucine-rich repeat protein kinase family protein
MD02G12 24000	QTL 2	Inoculated	Chr02	- 2.210 71	0.016 221	26257 974	26261 351	+	Leucine-rich repeat protein kinase family protein
MD02G12 87700	QTL 2	Control	Chr02	- 5.808 68	1.72E -26	34448 213	34449 189	+	Major facilitator superfamily protein
MD02G12 87800	QTL 2	Control	Chr02	- 4.663 09	3.42E -21	34449 192	34449 651	+	Major facilitator superfamily protein
MD02G12 87700	QTL 2	Inoculated	Chr02	- 5.219 78	1.1E- 32	34448 213	34449 189	+	Major facilitator superfamily protein
MD02G12 87800	QTL 2	Inoculated	Chr02	- 4.183 83	1.86E -26	34449 192	34449 651	+	Major facilitator superfamily protein
MD02G12 81700	QTL 2	Control	Chr02	2.212 713	1.34E -06	33752 118	33754 572	+	Mitochondrial transcription termination factor family protein
MD02G12 80700	QTL 2	Control	Chr02	- 1.838 7	0.001 057	33685 861	33687 174	+	Mitochondrial transcription termination factor family protein
MD02G12 79900	QTL 2	Control	Chr02	1.162 574	0.001 686	33607 596	33609 815	-	Mitochondrial transcription termination factor family protein
MD02G12 79500	QTL 2	Control	Chr02	1.893 556	0.007 942	33598 447	33599 563	-	Mitochondrial transcription termination factor family protein
MD02G12 80700	QTL 2	Inoculated	Chr02	- 2.591 91	7.17E -12	33685 861	33687 174	+	Mitochondrial transcription termination factor family protein
MD02G12 81700	QTL 2	Inoculated	Chr02	2.057 712	9.85E -09	33752 118	33754 572	+	Mitochondrial transcription termination factor family protein
MD02G12 79500	QTL 2	Inoculated	Chr02	1.832 791	0.000 286	33598 447	33599 563	-	Mitochondrial transcription termination factor family protein
MD02G12 44200	QTL 2	Control	Chr02	- 4.897 54	1.11E -37	29423 664	29425 298	-	NA
MD02G12 53200	QTL 2	Control	Chr02	- 2.273 5	4.28E -07	30484 780	30496 056	+	NA
MD02G12 40200	QTL 2	Control	Chr02	- 2.055 52	2.61E -05	28881 999	28883 594	+	NA
MD02G12 52200	QTL 2	Control	Chr02	1.291 196	5.22E -05	30394 460	30395 968	+	NA
MD02G12 50100	QTL 2	Control	Chr02	1.640 393	0.003 864	30120 368	30130 828	+	NA
MD02G12 77300	QTL 2	Control	Chr02	- 1.957 12	0.007 009	33306 979	33309 640	-	NA
MD02G12 52700	QTL 2	Control	Chr02	1.152 953	0.015 023	30445 992	30455 756	+	NA

MD02G12 57500	QTL 2	Contro l	Chr02	1.333 978	0.032 232	31015 139	31015 775	-	NA
MD02G11 96000	QTL 2	Contro l	Chr02	1.475 803	0.037 693	18822 031	18826 542	+	NA
MD02G12 86000	QTL 2	Contro l	Chr02	2.399 464	0.039 15	34292 354	34293 479	-	NA
MD02G12 44200	QTL 2	Inocul ated	Chr02	- 6.027 39	4.12E -62	29423 664	29425 298	-	NA
MD02G12 40200	QTL 2	Inocul ated	Chr02	- 3.048 13	1.43E -17	28881 999	28883 594	+	NA
MD02G12 53200	QTL 2	Inocul ated	Chr02	- 3.052 25	9.85E -18	30484 780	30496 056	+	NA
MD02G12 77300	QTL 2	Inocul ated	Chr02	- 2.840 52	2.21E -10	33306 979	33309 640	-	NA
MD02G12 76500	QTL 2	Inocul ated	Chr02	1.146 027	4.84E -07	33156 107	33159 245	+	NA
MD02G12 51700	QTL 2	Inocul ated	Chr02	- 1.808 1	2.18E -06	30324 295	30326 194	+	NA
MD02G11 54000	QTL 2	Inocul ated	Chr02	1.815 211	0.000 208	12758 887	12759 986	+	NA
MD02G12 57500	QTL 2	Inocul ated	Chr02	1.250 852	0.007 414	31015 139	31015 775	-	NA
MD02G11 64900	QTL 2	Inocul ated	Chr02	- 2.660 14	0.026 517	14087 651	14088 683	+	NA
MD02G12 86000	QTL 2	Inocul ated	Chr02	1.908 182	0.028 415	34292 354	34293 479	-	NA
MD02G12 63800	QTL 2	Contro l	Chr02	1.600 235	0.023 329	31782 818	31783 779	-	NAD(P)-linked oxidoreductase superfamily protein
MD02G12 63800	QTL 2	Inocul ated	Chr02	1.638 686	0.000 984	31782 818	31783 779	-	NAD(P)-linked oxidoreductase superfamily protein
MD02G12 38800	QTL 2	Contro l	Chr02	2.447 223	8.86E -06	28663 740	28665 471	-	Plant invertase/pectin methyltransferase inhibitor superfamily
MD02G12 38800	QTL 2	Inocul ated	Chr02	1.471 823	0.001 965	28663 740	28665 471	-	Plant invertase/pectin methyltransferase inhibitor superfamily
MD02G12 45800	QTL 2	Contro l	Chr02	1.029 726	0.000 366	29632 119	29634 729	+	PR5-like receptor kinase
MD02G12 46300	QTL 2	Contro l	Chr02	1.036 987	0.000 735	29660 249	29663 265	+	PR5-like receptor kinase
MD02G12 46300	QTL 2	Inocul ated	Chr02	1.405 806	2.06E -11	29660 249	29663 265	+	PR5-like receptor kinase
MD02G12 45800	QTL 2	Inocul ated	Chr02	1.230 883	9.21E -08	29632 119	29634 729	+	PR5-like receptor kinase
MD02G12 49500	QTL 2	Inocul ated	Chr02	- 1.161 33	0.013 881	30018 589	30021 247	-	PR5-like receptor kinase
MD02G12 47400	QTL 2	Inocul ated	Chr02	- 1.871 29	0.025 006	29761 547	29764 406	+	PR5-like receptor kinase
MD02G12 34300	QTL 2	Contro l	Chr02	5.413 78	2E-23	28091 239	28093 716	-	Protein kinase superfamily protein
MD02G12 34800	QTL 2	Contro l	Chr02	3.182 281	4.14E -08	28122 762	28125 276	-	Protein kinase superfamily protein
MD02G12 46600	QTL 2	Contro l	Chr02	3.956 846	2.44E -06	29691 118	29693 273	-	Protein kinase superfamily protein
MD02G12 46100	QTL 2	Contro l	Chr02	1.885 733	0.028 482	29647 020	29649 432	-	Protein kinase superfamily protein

MD02G12 34300	QTL 2	Inoculated	Chr02	4.894 487	1.52E -28	28091 239	28093 716	-	Protein kinase superfamily protein
MD02G12 34800	QTL 2	Inoculated	Chr02	2.608 994	2.43E -09	28122 762	28125 276	-	Protein kinase superfamily protein
MD02G12 54300	QTL 2	Inoculated	Chr02	- 1,984 13	9.52E -07	30585 393	30587 315	+	Protein kinase superfamily protein
MD02G12 74600	QTL 2	Inoculated	Chr02	- 1,984 57	0.000 354	32912 603	32914 929	+	Protein kinase superfamily protein
MD02G12 46600	QTL 2	Inoculated	Chr02	2.379 9	0.000 414	29691 118	29693 273	-	Protein kinase superfamily protein
MD02G12 46100	QTL 2	Inoculated	Chr02	2.204 048	0.000 949	29647 020	29649 432	-	Protein kinase superfamily protein
MD02G12 73700	QTL 2	Inoculated	Chr02	- 1,826 18	0.003 242	32825 037	32827 458	+	Protein kinase superfamily protein
MD02G12 73500	QTL 2	Inoculated	Chr02	- 1,252 48	0.006 915	32809 319	32811 838	-	Protein kinase superfamily protein
MD02G12 82000	QTL 2	Inoculated	Chr02	- 1,432 94	8.36E -06	33793 481	33808 000	+	protein kinases
MD02G12 40300	QTL 2	Control	Chr02	- 1,522 7	5.78E -05	28884 256	28885 593	-	Protein of unknown function
MD02G12 40300	QTL 2	Inoculated	Chr02	- 2,100 22	1.13E -13	28884 256	28885 593	-	Protein of unknown function
MD02G12 52300	QTL 2	Inoculated	Chr02	- 1,249 17	3.05E -09	30403 739	30406 081	+	Protein of unknown function
MD02G12 33500	QTL 2	Inoculated	Chr02	- 1,824 76	3.25E -05	27973 532	27988 072	+	Protein of unknown function
MD02G12 46700	QTL 2	Control	Chr02	2.839 29	0.002 786	29693 596	29694 447	+	RING/U-box superfamily protein
MD02G12 49700	QTL 2	Inoculated	Chr02	- 1,388 32	0.000 714	30037 327	30038 109	-	RING/U-box superfamily protein
MD02G12 46700	QTL 2	Inoculated	Chr02	2.155 775	0.005 954	29693 596	29694 447	+	RING/U-box superfamily protein
MD02G12 34500	QTL 2	Control	Chr02	- 3,818 12	4.97E -11	28113 753	28115 479	-	RNA polymerase Rpb7 N-terminal domain- containing protein
MD02G12 34500	QTL 2	Inoculated	Chr02	- 2,177 19	1.45E -05	28113 753	28115 479	-	RNA polymerase Rpb7 N-terminal domain- containing protein
MD02G11 90700	QTL 2	Inoculated	Chr02	- 2,088 01	0.019 325	17607 791	17609 979	-	sugar transporter 1
MD02G12 34600	QTL 2	Control	Chr02	- 3,165 21	2.38E -10	28115 481	28115 951	-	Tetratricopeptide repeat (TPR)-like superfamily protein
MD02G12 68500	QTL 2	Inoculated	Chr02	- 2,736 86	3.73E -15	32328 557	32330 968	+	ubiquitin-specific protease 12
MD02G12 48100	QTL 2	Inoculated	Chr02	- 2,402 43	0.004 215	29872 966	29874 339	+	UDP- Glycosyltransferase superfamily protein
MD02G12 48200	QTL 2	Inoculated	Chr02	- 2,253 43	0.041 831	29895 232	29896 752	+	UDP- Glycosyltransferase superfamily protein
MD02G12 67000	QTL 2	Control	Chr02	- 4,044 9	1.33E -05	32130 971	32136 524	+	zinc induced facilitator- like 1

MD06G10 74600	QTL 6	Contro l	Chr06	3.099 462	0.046 324	18630 173	18630 616	+	Calcium-binding EF-hand family protein
MD06G10 74600	QTL 6	Inocul ated	Chr06	2.686 598	0.020 025	18630 173	18630 616	+	Calcium-binding EF-hand family protein
MD06G11 16500	QTL 6	Inocul ated	Chr06	- 2,656 28	0.003 586	25565 461	25567 528	+	calmodulin-binding receptor-like cytoplasmic kinase 2
MD06G11 02500	QTL 6	Contro l	Chr06	- 3,480 19	0.000 809	23954 696	23957 493	-	Gag-Pol-related retrotransposon family protein
MD06G11 02500	QTL 6	Inocul ated	Chr06	- 2,928 5	4.18E -05	23954 696	23957 493	-	Gag-Pol-related retrotransposon family protein
MD06G10 99100	QTL 6	Inocul ated	Chr06	- 1,086 09	0.007 176	23536 308	23544 020	-	multidrug resistance-associated protein 14
MD06G10 64100	QTL 6	Contro l	Chr06	- 4,292 73	2.23E -06	13074 250	13077 332	+	NA
MD06G10 64100	QTL 6	Inocul ated	Chr06	- 4,123 56	3.08E -10	13074 250	13077 332	+	NA
MD06G11 20500	QTL 6	Inocul ated	Chr06	1,167 779	0.008 212	26081 728	26084 625	+	NA
MD06G11 03800	QTL 6	Inocul ated	Chr06	1,484 09	0.017 44	24179 552	24181 582	+	NAD(P)-binding Rossmann-fold superfamily protein
MD06G11 96900	QTL 6	Inocul ated	Chr06	- 1,816 64	0.026 087	33117 482	33120 005	-	NEP-interacting protein 2
MD06G10 69800	QTL 6	Inocul ated	Chr06	2,272 739	0.008 226	16777 376	16792 830	+	nuclear RNA polymerase D1A
MD06G11 16000	QTL 6	Inocul ated	Chr06	- 3,348 24	0.000 203	25491 474	25494 258	+	Protein kinase superfamily protein
MD06G11 07200	QTL 6	Contro l	Chr06	- 4,176 79	0.000 145	24688 790	24691 604	+	Protein of unknown function
MD06G11 07200	QTL 6	Inocul ated	Chr06	- 3,832 2	1.26E -06	24688 790	24691 604	+	Protein of unknown function
MD06G10 51400	QTL 6	Contro l	Chr06	- 2,467 05	0.005 224	71067 08	71116 14	+	Radical SAM superfamily protein
MD06G10 51400	QTL 6	Inocul ated	Chr06	- 2,229 52	0.001 47	71067 08	71116 14	+	Radical SAM superfamily protein
MD06G10 65300	QTL 6	Contro l	Chr06	- 2,929 05	0.000 362	13524 250	13525 760	+	Translation elongation factor EFG/EF2 protein
MD06G10 65300	QTL 6	Inocul ated	Chr06	- 2,529 5	4.71E -05	13524 250	13525 760	+	Translation elongation factor EFG/EF2 protein
MD06G10 65100	QTL 6	Inocul ated	Chr06	- 1,684 12	0.043 507	13522 014	13523 508	+	Translation elongation factor EFG/EF2 protein
MD06G10 65200	QTL 6	Inocul ated	Chr06	- 1,768 97	0.044 592	13523 560	13524 248	+	Translation elongation factor EFG/EF2 protein
MD06G11 03300	QTL 6	Inocul ated	Chr06	- 3,770 52	0.016 833	24105 009	24106 484	+	UDP-Glycosyltransferase superfamily protein
MD06G10 69100	QTL 6	Contro l	Chr06	2,742 601	0.049 703	16609 737	16612 809	-	YTH family protein
MD08G10 85600	QTL 8	Inocul ated	Chr08	2,318 76	0.029 699	71048 81	71197 75	+	calcium ATPase 2

MD08G10 22200	QTL 8	Control	Chr08	2.907 541	0.011 941	16110 15	16149 22	-	DEA(D/H)-box RNA helicase family protein
MD08G10 20000	QTL 8	Inoculated	Chr08	- 1.763 61	0.013 589	14629 30	14638 25	+	Disease resistance protein (TIR-NBS-LRR class) family
MD08G10 19600	QTL 8	Inoculated	Chr08	- 1.173 02	0.047 104	14489 12	14506 81	+	Disease resistance protein (TIR-NBS-LRR class) family
MD08G10 55100	QTL 8	Inoculated	Chr08	- 1.191 11	0.017 854	43030 47	43069 11	-	glutathione peroxidase 7
MD08G10 65500	QTL 8	Inoculated	Chr08	1.991 997	0.028 652	52294 70	52302 97	-	Granulin repeat cysteine protease family protein
MD08G10 64100	QTL 8	Inoculated	Chr08	1.507 411	0.041 618	51083 73	51102 67	+	heat shock transcription factor A2
MD08G10 26800	QTL 8	Inoculated	Chr08	1.600 757	0.009 609	19615 27	19630 48	-	Heavy metal transport/detoxification superfamily protein
MD08G10 27300	QTL 8	Control	Chr08	- 2.596 82	0.049 755	19908 69	19919 81	+	jasmonic acid carboxyl methyltransferase
MD08G10 55000	QTL 8	Inoculated	Chr08	2.434 892	0.000 172	42986 37	43016 10	-	Major facilitator superfamily protein
MD08G10 76200	QTL 8	Inoculated	Chr08	1.687 316	0.036 52	62113 77	62129 72	+	myb domain protein 84
MD08G10 20200	QTL 8	Inoculated	Chr08	- 1.772 23	0.003 662	14644 72	14654 75	+	NA
MD08G10 18800	QTL 8	Inoculated	Chr08	- 1.554 97	0.011 038	14245 37	14249 43	+	NA
MD08G10 20100	QTL 8	Inoculated	Chr08	- 1.790 95	0.020 73	14638 27	14644 41	-	NA
MD08G10 20500	QTL 8	Inoculated	Chr08	- 1.419 47	0.030 11	14773 14	14784 07	+	NA
MD08G10 42700	QTL 8	Inoculated	Chr08	- 2.457 35	0.015 826	31396 25	31439 87	+	NB-ARC domain- containing disease resistance protein
MD08G10 29500	QTL 8	Inoculated	Chr08	- 1.179 31	0.035 069	21332 69	21353 97	-	NmrA-like negative transcriptional regulator family protein
MD08G10 55500	QTL 8	Inoculated	Chr08	1.704 596	0.007 034	43141 52	43146 19	+	Pentatricopeptide repeat (PPR-like) superfamily protein
MD08G10 33500	QTL 8	Inoculated	Chr08	1.085 083	0.010 238	23723 60	23764 19	-	Protein of unknown function
MD08G10 09100	QTL 8	Inoculated	Chr08	2.050 426	0.019 224	67483 5	67619 9	-	Protein of unknown function (DUF677)
MD08G10 45000	QTL 8	Inoculated	Chr08	2.973 644	0.001 784	34146 19	34161 70	+	RING/U-box superfamily protein
MD08G10 82700	QTL 8	Inoculated	Chr08	1.266 69	0.041 351	68612 26	68645 53	+	Transducin/WD40 repeat-like superfamily protein
MD08G10 21400	QTL 8	Inoculated	Chr08	1.072 139	0.000 849	15392 41	15449 23	-	vacuolar proton ATPase A3
MD10G12 36400	QTL 10	Inoculated	Chr10	- 1.307 97	0.003 131	33296 860	33300 848	+	Argonaute family protein
MD10G12 48700	QTL 10	Inoculated	Chr10	2.527 028	0.000 217	34185 523	34185 885	-	Coatomer
MD10G12 50100	QTL 10	Inoculated	Chr10	1.521 246	0.005 444	34279 938	34281 142	-	Coatomer
MD10G12 51000	QTL 10	Inoculated	Chr10	1.640 318	0.006 117	34333 685	34336 855	-	Coatomer

MD10G12 48600	QTL 10	Inoculated	Chr10	1.481 317	0.013 51	34181 803	34182 537	-	Coatomer
MD10G12 55600	QTL 10	Control	Chr10	- 2.387 07	0.000 177	35019 412	35020 191	+	NA
MD10G12 48900	QTL 10	Control	Chr10	- 2.128 72	0.001 239	34201 188	34201 740	-	NA
MD10G12 55600	QTL 10	Inoculated	Chr10	- 2.686 63	4.09E -08	35019 412	35020 191	+	NA
MD10G12 48900	QTL 10	Inoculated	Chr10	- 1.748 67	0.000 401	34201 188	34201 740	-	NA
MD10G12 49400	QTL 10	Inoculated	Chr10	1.656 692	0.001 408	34212 396	34212 596	-	NA
MD10G12 55800	QTL 10	Inoculated	Chr10	- 1.702 36	0.006 868	35040 261	35040 983	-	NA
MD10G12 38200	QTL 10	Inoculated	Chr10	- 2.518 45	0.000 401	33437 479	33439 002	+	NAC domain containing protein 42
MD10G12 43100	QTL 10	Control	Chr10	- 1.177 2	1.03E -07	33786 047	33789 092	+	NAD(P)-binding Rossmann-fold superfamily protein
MD10G12 32900	QTL 10	Control	Chr10	- 2.985 32	8.49E -07	32922 604	32924 393	+	Pentatricopeptide repeat (PPR-like) superfamily protein
MD10G12 32900	QTL 10	Inoculated	Chr10	- 1.909 99	0.000 348	32922 604	32924 393	+	Pentatricopeptide repeat (PPR-like) superfamily protein
MD10G12 32000	QTL 10	Inoculated	Chr10	1.123 223	0.005 628	32837 566	32838 844	-	peroxisome 1
MD10G12 34400	QTL 10	Control	Chr10	- 3.840 04	8.52E -05	33056 980	33058 304	-	phloem protein 2-A10
MD10G12 48400	QTL 10	Control	Chr10	2.363 009	0.033 53	34136 665	34138 362	+	Protein of unknown function (DUF630)
MD10G12 50000	QTL 10	Control	Chr10	- 5.616 92	5.72E -09	34277 262	34278 350	+	wall associated kinase 5
MD10G12 50000	QTL 10	Inoculated	Chr10	- 3.398 73	3.22E -05	34277 262	34278 350	+	wall associated kinase 5
MD10G12 51200	QTL 10	Control	Chr10	- 4.909 06	1.31E -07	34454 093	34459 942	+	wall-associated kinase 2
MD10G12 50500	QTL 10	Control	Chr10	- 2.880 25	0.000 131	34297 043	34304 303	+	wall-associated kinase 2
MD10G12 51200	QTL 10	Inoculated	Chr10	- 2.184 62	0.016 179	34454 093	34459 942	+	wall-associated kinase 2
MD15G11 02100	QTL 15	Control	Chr15	- 1.283 53	0.008 86	72302 66	72335 35	+	ABC1 family protein
MD15G11 49200	QTL 15	Inoculated	Chr15	1.010 1	3.37E -05	11031 548	11032 305	-	Calcium-binding EF- hand family protein
MD15G11 28000	QTL 15	Inoculated	Chr15	1.434 6	0.016 389	92619 72	92665 93	+	Calcium-dependent lipid-binding (CaLB domain) family protein
MD15G11 09800	QTL 15	Inoculated	Chr15	- 1.811 09	0.049 976	76904 73	76939 06	-	Core-2/I-branching beta-1
MD15G10 75200	QTL 15	Inoculated	Chr15	- 1.257 98	0.007 555	51258 77	51285 07	+	Cyclin A3

MD15G11 56200	QTL 15	Inoculated	Chr15	- 3,671 73	2.21E -08	11600 506	11604 057	+	cysteine-rich RLK (RECEPTOR-like protein kinase) 16
MD15G10 90400	QTL 15	Control	Chr15	2.846 891	1.4E- 06	62779 99	62793 00	+	Disease resistance protein (CC-NBS-LRR class) family
MD15G10 90400	QTL 15	Inoculated	Chr15	3.618 436	6.89E -16	62779 99	62793 00	+	Disease resistance protein (CC-NBS-LRR class) family
MD15G11 79700	QTL 15	Inoculated	Chr15	- 1,976 13	0.012 736	14171 177	14173 488	+	Disease resistance protein (TIR-NBS-LRR class) family
MD15G10 59500	QTL 15	Inoculated	Chr15	2.167 329	6.15E -05	39668 98	39698 38	-	glutamate receptor 2.7
MD15G10 59200	QTL 15	Inoculated	Chr15	1.851 046	0.004 194	39528 18	39571 23	-	glutamate receptor 2.8
MD15G11 56300	QTL 15	Control	Chr15	2.596 563	0.004 129	11612 837	11615 954	+	Glycosyl hydrolase family protein with chitinase insertion domain
MD15G11 56300	QTL 15	Inoculated	Chr15	1.754 251	0.015 617	11612 837	11615 954	+	Glycosyl hydrolase family protein with chitinase insertion domain
MD15G10 74900	QTL 15	Inoculated	Chr15	3.067 052	1.48E -06	51019 27	51051 42	+	Leucine-rich repeat protein kinase family protein
MD15G12 40200	QTL 15	Inoculated	Chr15	1.077 009	0.031 177	19773 752	19780 706	+	Leucine-rich repeat transmembrane protein kinase
MD15G11 03400	QTL 15	Control	Chr15	- 1,610 61	0.000 178	72940 69	72969 15	-	LisH dimerisation motif
MD15G11 03500	QTL 15	Control	Chr15	- 3,080 33	0.000 17	72969 17	72974 94	-	LisH dimerisation motif
MD15G11 03400	QTL 15	Inoculated	Chr15	- 1,367 17	0.001 72	72940 69	72969 15	-	LisH dimerisation motif
MD15G11 03500	QTL 15	Inoculated	Chr15	- 2,120 95	0.004 267	72969 17	72974 94	-	LisH dimerisation motif
MD15G10 90100	QTL 15	Control	Chr15	2.715 92	5.46E -06	62706 74	62712 37	+	LRR and NB-ARC domains-containing disease resistance protein
MD15G10 90100	QTL 15	Inoculated	Chr15	2.877 241	5.6E- 11	62706 74	62712 37	+	LRR and NB-ARC domains-containing disease resistance protein
MD15G10 76200	QTL 15	Control	Chr15	2.500 812	0.000 703	51790 22	51823 73	+	MRG family protein
MD15G10 76200	QTL 15	Inoculated	Chr15	1.925 539	0.000 876	51790 22	51823 73	+	MRG family protein
MD15G11 12000	QTL 15	Control	Chr15	2.728 576	2.54E -05	78584 55	78594 92	-	NA
MD15G11 11500	QTL 15	Control	Chr15	1.523 576	5.14E -05	77936 48	77949 80	+	NA
MD15G11 11900	QTL 15	Control	Chr15	2.895 712	9.06E -05	78578 56	78584 52	-	NA
MD15G10 61900	QTL 15	Control	Chr15	- 2,988 71	0.004 34	41497 08	41505 01	-	NA
MD15G11 11700	QTL 15	Control	Chr15	2.369 97	0.007 039	78544 28	78551 45	-	NA
MD15G10 77600	QTL 15	Control	Chr15	1.441 889	0.009 577	52984 69	52994 47	+	NA

MD15G11 10900	QTL 15	Contro l	Chr15	2.216 545	0.015 25	77470 45	77484 21	-	NA
MD15G11 11000	QTL 15	Contro l	Chr15	2.148 362	0.017 377	77484 24	77494 58	-	NA
MD15G10 61900	QTL 15	Inocul ated	Chr15	- 3,539 9	8.66E -08	41497 08	41505 01	-	NA
MD15G11 11500	QTL 15	Inocul ated	Chr15	1.360 283	4.69E -06	77936 48	77949 80	+	NA
MD15G11 11900	QTL 15	Inocul ated	Chr15	2.636 637	4.88E -06	78578 56	78584 52	-	NA
MD15G11 11600	QTL 15	Inocul ated	Chr15	2.468 851	7.36E -06	78210 52	78235 68	+	NA
MD15G11 12000	QTL 15	Inocul ated	Chr15	2.292 259	7.66E -06	78584 55	78594 92	-	NA
MD15G10 86300	QTL 15	Inocul ated	Chr15	1.802 791	6.15E -05	59862 88	59881 27	+	NA
MD15G11 11000	QTL 15	Inocul ated	Chr15	2.179 68	0.000 713	77484 24	77494 58	-	NA
MD15G11 11700	QTL 15	Inocul ated	Chr15	2.027 607	0.001 271	78544 28	78551 45	-	NA
MD15G11 10900	QTL 15	Inocul ated	Chr15	1.851 413	0.006 444	77470 45	77484 21	-	NA
MD15G11 09700	QTL 15	Inocul ated	Chr15	1.021 338	0.013 442	76743 55	76789 62	+	NA
MD15G10 39400	QTL 15	Inocul ated	Chr15	2.044 114	0.015 284	27593 39	27623 82	+	NA
MD15G11 70200	QTL 15	Inocul ated	Chr15	- 1,211 78	0.028 854	13116 849	13118 596	-	NA
MD15G12 52900	QTL 15	Inocul ated	Chr15	1.840 054	0.044 944	21343 042	21347 913	+	NA
MD15G10 73500	QTL 15	Contro l	Chr15	4.125 588	4.8E- 06	50056 05	50072 09	+	NAD(P)-binding Rossmann-fold superfamily protein
MD15G10 73500	QTL 15	Inocul ated	Chr15	3.512 971	1.96E -05	50056 05	50072 09	+	NAD(P)-binding Rossmann-fold superfamily protein
MD15G10 73400	QTL 15	Inocul ated	Chr15	2.344 368	2.23E -05	49875 21	49888 34	-	NAD(P)-binding Rossmann-fold superfamily protein
MD15G10 67900	QTL 15	Contro l	Chr15	2.417 352	0.000 119	47120 79	47152 13	-	NADH-ubiquinone oxidoreductase-related
MD15G10 67900	QTL 15	Inocul ated	Chr15	1.671 319	0.016 817	47120 79	47152 13	-	NADH-ubiquinone oxidoreductase-related
MD15G10 90300	QTL 15	Contro l	Chr15	3.518 021	1.27E -07	62767 68	62779 97	+	NB-ARC domain- containing disease resistance protein
MD15G10 90000	QTL 15	Contro l	Chr15	3.238 931	1.13E -06	62693 79	62706 72	+	NB-ARC domain- containing disease resistance protein
MD15G10 90300	QTL 15	Inocul ated	Chr15	4.218 329	2.54E -16	62767 68	62779 97	+	NB-ARC domain- containing disease resistance protein
MD15G10 90000	QTL 15	Inocul ated	Chr15	3.544 775	3.06E -12	62693 79	62706 72	+	NB-ARC domain- containing disease resistance protein
MD15G11 03300	QTL 15	Contro l	Chr15	1.003 932	0.000 677	72910 41	72933 94	-	N-terminal nucleophile aminohydrolases (Ntn hydrolases) superfamily protein
MD15G10 84600	QTL 15	Inocul ated	Chr15	- 1,072 43	1.13E -05	58436 65	58460 47	-	origin recognition complex second largest subunit 2
MD15G11 06700	QTL 15	Inocul ated	Chr15	2.040 272	3.33E -05	74758 02	74776 94	+	photosystem II stability/assembly factor

MD15G11 37100	QTL 15	Contro l	Chr15	- 2.870 94	0.000 677	10044 558	10046 946	-	Probable cysteine desulfurase
MD15G11 37100	QTL 15	Inocul ated	Chr15	- 2.465 04	3.67E -05	10044 558	10046 946	-	Probable cysteine desulfurase
MD15G10 30400	QTL 15	Contro l	Chr15	- 2.439 2	0.008 184	18752 77	18793 57	+	Protein of unknown function
MD15G10 61800	QTL 15	Inocul ated	Chr15	- 1.164 09	0.000 55	41477 01	41496 94	+	Protein of unknown function
MD15G10 30400	QTL 15	Inocul ated	Chr15	- 1.891 37	0.023 793	18752 77	18793 57	+	Protein of unknown function
MD15G11 56700	QTL 15	Contro l	Chr15	2.173 591	0.034 462	11625 763	11628 805	+	receptor kinase 2
MD15G11 56700	QTL 15	Inocul ated	Chr15	2.634 103	4.84E -06	11625 763	11628 805	+	receptor kinase 2
MD15G11 57000	QTL 15	Inocul ated	Chr15	2.438 644	0.000 149	11661 076	11664 251	+	receptor kinase 2
MD15G11 46000	QTL 15	Inocul ated	Chr15	- 1.738 1	8.38E -05	10866 873	10868 368	+	Ribosomal protein L2 family
MD15G10 93400	QTL 15	Inocul ated	Chr15	1.605 304	0.000 842	64668 94	64681 20	+	RNI-like superfamily protein
MD15G11 11800	QTL 15	Inocul ated	Chr15	2.079 926	0.000 642	78551 47	78578 54	-	SHK1 binding protein 1
MD15G11 51100	QTL 15	Inocul ated	Chr15	- 1.346 2	0.002 104	11137 796	11138 709	-	SKP1 interacting partner 1
MD15G11 67400	QTL 15	Contro l	Chr15	- 2.007 35	0.011 745	12668 627	12670 640	-	Telomere-associated protein RIF1
MD15G11 47000	QTL 15	Contro l	Chr15	- 1.703 4	0.000 258	10920 300	10923 980	+	Thioesterase/thiol ester dehydrase-isomerase superfamily protein
MD15G11 47000	QTL 15	Inocul ated	Chr15	- 1.862 66	8.66E -08	10920 300	10923 980	+	Thioesterase/thiol ester dehydrase-isomerase superfamily protein
MD16G11 14800	QTL 16	Contro l	Chr16	- 3.214 85	4.25E -10	81461 11	81464 22	+	51 kDa subunit of complex I
MD16G11 14800	QTL 16	Inocul ated	Chr16	- 3.236 25	2.86E -15	81461 11	81464 22	+	51 kDa subunit of complex I
MD16G11 05600	QTL 16	Contro l	Chr16	2.724 198	0.007 623	73939 10	73989 21	-	ABC transporter family protein
MD16G11 05600	QTL 16	Inocul ated	Chr16	2.035 191	0.029 3	73939 10	73989 21	-	ABC transporter family protein
MD16G11 13000	QTL 16	Contro l	Chr16	- 2.310 3	0.007 02	79103 14	79128 25	+	AMP-dependent synthetase and ligase family protein
MD16G11 13000	QTL 16	Inocul ated	Chr16	- 2.407 48	7.25E -06	79103 14	79128 25	+	AMP-dependent synthetase and ligase family protein
MD16G11 12900	QTL 16	Inocul ated	Chr16	- 2.077 41	0.027 94	78972 78	79001 24	+	AMP-dependent synthetase and ligase family protein
MD16G11 16300	QTL 16	Contro l	Chr16	- 3.224 58	1.32E -05	82578 22	82587 75	-	cytochrome P450
MD16G11 04200	QTL 16	Contro l	Chr16	2.036 036	0.000 565	73056 85	73062 91	+	cytochrome P450
MD16G11 04300	QTL 16	Contro l	Chr16	1.963 103	0.020 162	73062 93	73077 96	+	cytochrome P450

MD16G10 55500	QTL 16	Inocul ated	Chr16	2.558 452	0.004 974	39145 85	39228 63	-	D-aminoacyl-tRNA deacylases
MD16G10 82200	QTL 16	Inocul ated	Chr16	3.018 096	4.28E -08	57728 71	57744 50	-	disease resistance protein (TIR-NBS-LRR class)
MD16G10 68800	QTL 16	Contro l	Chr16	- 1.287 16	5.19E -11	48584 49	48599 99	-	FKBP-like peptidyl- prolyl cis-trans isomerase family protein
MD16G10 96400	QTL 16	Contro l	Chr16	- 2.488 27	0.010 267	67032 49	67043 91	+	Kelch repeat- containing F-box family protein
MD16G11 02700	QTL 16	Contro l	Chr16	3.047 97	5.89E -08	71800 41	71851 52	-	MATE efflux family protein
MD16G11 17800	QTL 16	Contro l	Chr16	2.169 22	0.006 167	83783 77	83795 71	+	NA
MD16G11 03800	QTL 16	Inocul ated	Chr16	- 1.913 31	0.001 036	72616 04	72621 98	+	NA
MD16G11 40000	QTL 16	Inocul ated	Chr16	1.655 447	0.006 082	10765 486	10768 588	+	NA
MD16G10 82400	QTL 16	Inocul ated	Chr16	1.487 805	0.023 504	57767 16	57833 25	+	NA
MD16G11 17800	QTL 16	Inocul ated	Chr16	1.495 228	0.030 142	83783 77	83795 71	+	NA
MD16G11 25800	QTL 16	Inocul ated	Chr16	- 1.228 27	1.27E -07	91277 88	91297 66	+	NAC domain containing protein 83
MD16G10 85700	QTL 16	Contro l	Chr16	- 2.315 64	0.031 881	59940 62	59960 80	+	peptidase M20/M25/M40 family protein
MD16G11 24900	QTL 16	Contro l	Chr16	1.096 315	0.012 651	90592 78	90623 71	-	P-loop containing nucleoside triphosphate hydrolases superfamily protein
MD16G11 27600	QTL 16	Contro l	Chr16	- 3.558 61	5.86E -09	93017 96	93061 19	+	Protein of unknown function
MD16G11 27600	QTL 16	Inocul ated	Chr16	- 3.610 74	1.86E -12	93017 96	93061 19	+	Protein of unknown function
MD16G10 97800	QTL 16	Inocul ated	Chr16	1.293 888	0.000 301	68340 77	68446 89	+	Pyruvate phosphate dikinase
MD16G11 32900	QTL 16	Inocul ated	Chr16	- 1.195 51	0.035 97	10170 785	10175 095	+	TRAF-like family protein
MD16G10 72500	QTL 16	Contro l	Chr16	- 4.071 19	1.63E -23	50811 23	50832 87	-	Transmembrane amino acid transporter family protein
MD16G10 72500	QTL 16	Inocul ated	Chr16	- 3.994 95	1.12E -30	50811 23	50832 87	-	Transmembrane amino acid transporter family protein
MD16G10 82300	QTL 16	Contro l	Chr16	2.245 35	0.010 267	57746 98	57767 14	-	transmembrane receptors
MD16G10 82300	QTL 16	Inocul ated	Chr16	3.065 166	4.64E -06	57746 98	57767 14	-	transmembrane receptors

Supplementary table 6 DEGs of particular interest identified in comparisons of gene expression in apple genotypes with QTL-R vs QTL-S alleles. The table shows DEGs which are validated, had the same predicted gene function as a validated gene at the same quantitative trait loci (QTL), or had a predicted gene function within disease resistance. For each gene the genome position, predicted gene functions and protein family domains are also shown.

Gene ID GDDH13_v1.1	Resistance QTL	Chromosome	Pred. gene function GDDH13_v1.1	start	end	strand	Pred. gene function eggNOG	PFAMs
MD02G1164500	QTL2	Chr02	Disease-resistance-protein-(CC-NBS-LRR-class)	140 470 28	140 477 83	+	disease resistance	NB-ARC,RPW8
MD02G1217100	QTL2	Chr02	Disease-resistance-protein-(TIR-NBS-LRR-class)	248 857 88	248 879 62	-	TMV resistance protein N-like	LRR_8,NB-ARC,TIR
MD02G1260200	QTL2	Chr02	Disease-resistance-protein-(TIR-NBS-LRR-class)	313 663 83	313 682 19	-	RESISTANCE protein	LRR_3,LRR_8,NB-ARC,TIR
MD02G1245800	QTL2	Chr02	PR5-like-receptor-kinase	296 321 19	296 347 29	+	receptor-like protein kinase	GUB_WAK_bind,Pkinase,Pkinase_Tyr
MD02G1246300	QTL2	Chr02	PR5-like-receptor-kinase	296 602 49	296 632 65	+	receptor-like protein kinase	GUB_WAK_bind,Pkinase,Pkinase_Tyr
MD02G1247400	QTL2	Chr02	PR5-like-receptor-kinase	297 615 47	297 644 06	+	receptor-like	GUB_WAK_bind,Pkinase,Pkinase_Tyr

MD02G12 34300	QTL2	Chr02	Protein-kinase	280 912 39	280 937 16	-	protein kinase receptor- like protein kinase	GUB_WAK_bind,Pkinase,Pkinase_Tyr
MD02G12 34800	QTL2	Chr02	Protein-kinase	281 227 62	281 252 76	-	receptor- like protein kinase	GUB_WAK_bind,Pkinase,Pkinase_Tyr
MD02G12 46100	QTL2	Chr02	Protein-kinase	296 470 20	296 494 32	-	receptor- like protein kinase	GUB_WAK_bind,Pkinase,Pkinase_Tyr
MD02G12 46600	QTL2	Chr02	Protein-kinase	296 911 18	296 932 73	-	receptor- like protein kinase	GUB_WAK_bind,Pkinase,Pkinase_Tyr
MD02G12 74600	QTL2	Chr02	Protein-kinase	329 126 03	329 149 29	+	receptor- like protein kinase	GUB_WAK_bind,Pkinase,Pkinase_Tyr
MD02G12 82000	QTL2	Chr02	Protein-kinase	337 934 81	338 080 00	+	E3 ubiquitin -protein ligase	Ank_2,Ank_4,Pkinase,zf-C3HC4,zf-RING_2,zf-RING_5
MD02G12 46700	QTL2	Chr02	RING/U-box	296 935 96	296 944 47	+	receptor- like protein kinase	GUB_WAK_bind,Pkinase,Pkinase_Tyr
MD02G11 88900	QTL2	Chr02	ACT-domain-repeat-1	172 570 96	172 618 25	-	ACT domain	ACT,ACT_6

MD02G12 76500	QTL2	Chr02	Not annotated	331 561 07	331 592 45	+	Not annotated	Not annotated
MD02G12 00700	QTL2	Chr02	Cytochrome-P450	198 048 42	198 068 65	-	Cytochrome p450	p450
MD02G11 64900	QTL2	Chr02	Membrane-bound-protein- predicted-to-be-embedded-in-the- membrane*	140 876 51	140 886 83	+	Not annotated	Not annotated
MD02G12 49500	QTL2	Chr02	PR5-like-receptor-kinase	300 185 89	300 212 47	-	receptor- like protein kinase	GUB_WAK_bind,Pkinase,Pkinase_Tyr
MD02G12 73500	QTL2	Chr02	Protein-kinase	328 093 19	328 118 38	-	receptor- like protein kinase	GUB_WAK_bind,Pkinase,Pkinase_Tyr
MD02G12 73700	QTL2	Chr02	Protein-kinase	328 250 37	328 274 58	+	receptor- like protein kinase	GUB_WAK_bind,Pkinase,Pkinase_Tyr
MD02G12 49700	QTL2	Chr02	RING/U-box	300 373 27	300 381 09	-	receptor- like protein kinase	GUB_WAK_bind,Pkinase,Pkinase_Tyr
MD02G12 67000	QTL2	Chr02	Zinc-induced-facilitator-like-1	321 309 71	321 365 24	+	Protein ZINC INDUCED	MFS_1
MD02G12 54300	QTL2	Chr02	Protein-kinase	305 853 93	305 873 15	+	receptor- like protein kinase	GUB_WAK_bind,Pkinase,Pkinase_Tyr

MD06G11 16500	QTL6	Chr06	Calmodulin-binding-receptor-like- cytoplasmic-kinase-2	255 654 61	255 675 28	+	Belongs to the protein kinase superfa mily	PPR,Pkinase,Pkinase_Tyr
MD06G10 69800	QTL6	Chr06	Nuclear-RNA-polymerase-D1A	167 773 76	167 928 30	+	DNA- depende nt RNA polymer ase catalyzes the transcrip tion of DNA into RNA using the four ribonucl eoside triphosp hates as substrate s	DUF3223, RNA_pol_Rpb1_1, RNA_pol_Rpb1_2, RN A_pol_Rpb1_3, RNA_pol_Rpb1_4, RNA_pol_Rpb1 _5
MD06G11 03300	QTL6	Chr06	UDP-Glycosyltransferase	241 050 09	241 064 84	+	Belongs to the UDP- glycosylt ransferas e family	UDPGT

MD08G10 42700	QTL8	Chr08	Disease-resistance-protein-(NB-ARC-domain)	313 962 5	314 398 7	+	disease resistance protein	LRR_8,NB-ARC
MD08G10 19600	QTL8	Chr08	Disease-resistance-protein-(TIR-NBS-LRR-class)	144 891 2	145 068 1	+	Not annotated	Not annotated
MD08G10 20000	QTL8	Chr08	Disease-resistance-protein-(TIR-NBS-LRR-class)	146 293 0	146 382 5	+	Not annotated	Not annotated
MD08G10 55100	QTL8	Chr08	Glutathione-peroxidase-7	430 304 7	430 691 1	-	Belongs to the glutathio ne peroxida se family	GSHPx
MD08G10 64100	QTL8	Chr08	Heat-shock-transcription-factor-A2	510 837 3	511 026 7	+	Heat shock factor protein	HSF_DNA-bind
MD08G10 26800	QTL8	Chr08	Heavy-metal- transport/detoxification	196 152 7	196 304 8	-	Phospho rylates Ins(1,3,4, 5,6)P5 at position 2 to form Ins(1,2,3, 4,5,6)P6 (InsP6 or phytate)	HMA,Ins_P5_2-kin
MD08G10 27300	QTL8	Chr08	Jasmonic-acid-carboxyl- methyltransferase	199 086 9	199 198 1	+	Jasmona te	Methyltransf_7

MD15G10 90400	QTL15	Chr15	Disease-resistance-protein-(CC-NBS-LRR-class)	627 799 9	627 930 0	+	Not annotated	Not annotated
MD15G10 90100	QTL15	Chr15	Disease-resistance-protein-(LRR-and-NB-ARC-domains)	627 067 4	627 123 7	+	disease resistance	LRR_8,NB-ARC
MD15G10 90000	QTL15	Chr15	Disease-resistance-protein-(NB-ARC-domain)	626 937 9	627 067 2	+	disease resistance	LRR_8,NB-ARC
MD15G10 90300	QTL15	Chr15	Disease-resistance-protein-(NB-ARC-domain)	627 676 8	627 799 7	+	disease resistance	LRR_8,NB-ARC
MD15G11 79700	QTL15	Chr15	Disease-resistance-protein-(TIR-NBS-LRR-class)	141 711 77	141 734 88	+	TMV resistance protein N-like	NB-ARC,TIR
MD15G11 03400	QTL15	Chr15	LisH-dimerisation-motif	729 406 9	729 691 5	-	transcriptional co-repressor	LisH,WD40
MD15G10 73400	QTL15	Chr15	NAD(P)-binding-Rossmann-fold	498 752 1	498 883 4	-	3-oxo-Delta(4,5)-steroid 5-beta-reductase-like	Epimerase
MD15G11 02100	QTL15	Chr15	ABC1	723 026 6	723 353 5	+	domain-containing protein	ABC1,Beta-lactamase,WaaY
MD15G11 03500	QTL15	Chr15	LisH-dimerisation-motif	729 691 7	729 749 4	-	Not annotated	Not annotated

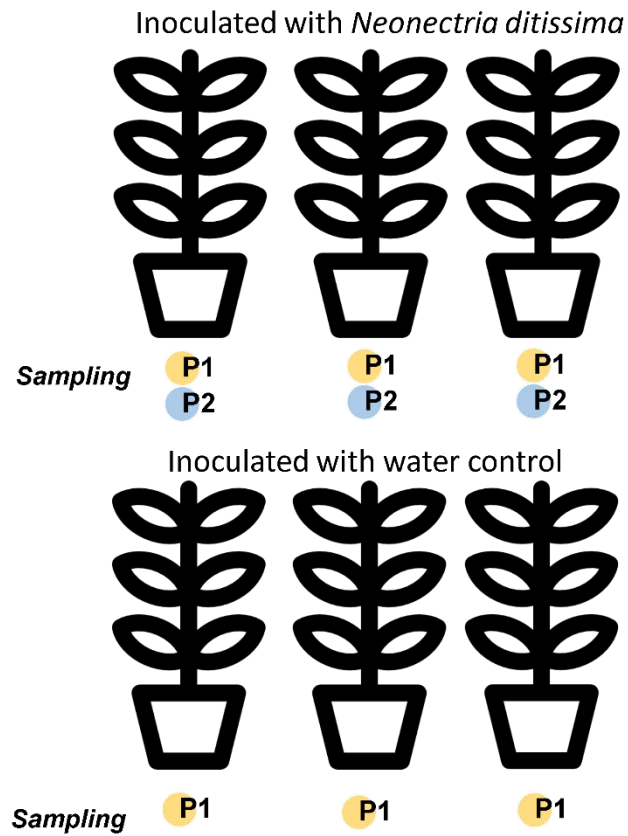
MD15G10 73500	QTL15	Chr15	NAD(P)-binding-Rossmann-fold	500 560 5	500 720 9	+	3-oxo-Delta(4,5)-steroid 5-beta-reductase-like	Epimerase
MD15G10 61900	QTL15	Chr15	Not annotated	414 970 8	415 050 1	-	PITH domain-containing protein 1-like	PITH
MD15G11 06700	QTL15	Chr15	Photosystem-II-stability/assembly-factor	747 580 2	747 769 4	+	Photosystem II stability assembly factor HCF136	PSII_BNR
MD15G10 77600	QTL15	Chr15	Transcription-factor-MYC/MYB-related*	529 846 9	529 944 7	+	bHLH-MYC and R2R3-MYB transcription factors N-terminal	bHLH-MYC_N
MD16G11 13000	QTL16	Chr16	AMP-dependent-synthetase-and-ligase	791 031 4	791 282 5	+	AMP-binding enzyme	AMP-binding,AMP-binding_C
MD16G11 04200	QTL16	Chr16	Cytochrome-P450	730 568 5	730 629 1	+	Cytochrome p450	p450

MD16G11 04300	QTL16	Chr16	Cytochrome-P450	730 629 3	730 779 6	+	Cytochrome p450	p450
MD16G10 82200	QTL16	Chr16	disease-resistance-protein-(TIR-NBS-LRR-class)	577 287 1	577 445 0	-	Belongs to the disease resistance NB-LRR family	LRR_8,NB-ARC,TIR
MD16G11 12900	QTL16	Chr16	AMP-dependent-synthetase-and-ligase	789 727 8	790 012 4	+	AMP-binding enzyme	AMP-binding,AMP-binding_C
MD16G11 16300	QTL16	Chr16	Cytochrome-P450	825 782 2	825 877 5	-	Belongs to the cytochrome P450 family	p450
MD16G10 55500	QTL16	Chr16	D-aminoacyl-tRNA-deacylases	391 458 5	392 286 3	-	D-aminoacyl-tRNA deacylase-like	tRNA_deacylase
MD16G10 96400	QTL16	Chr16	Kelch-repeat-containing-F-box	670 324 9	670 439 1	+	F-box kelch-repeat protein	F-box,Kelch_1,Kelch_6
MD16G11 25800	QTL16	Chr16	NAC-domain-containing-protein-83	912 778 8	912 976 6	+	NAC transcription factor	NAM
MD16G10 97800	QTL16	Chr16	Pyruvate-phosphate-dikinase	683 407 7	684 468 9	+	Alpha-glucan	PPDK_N

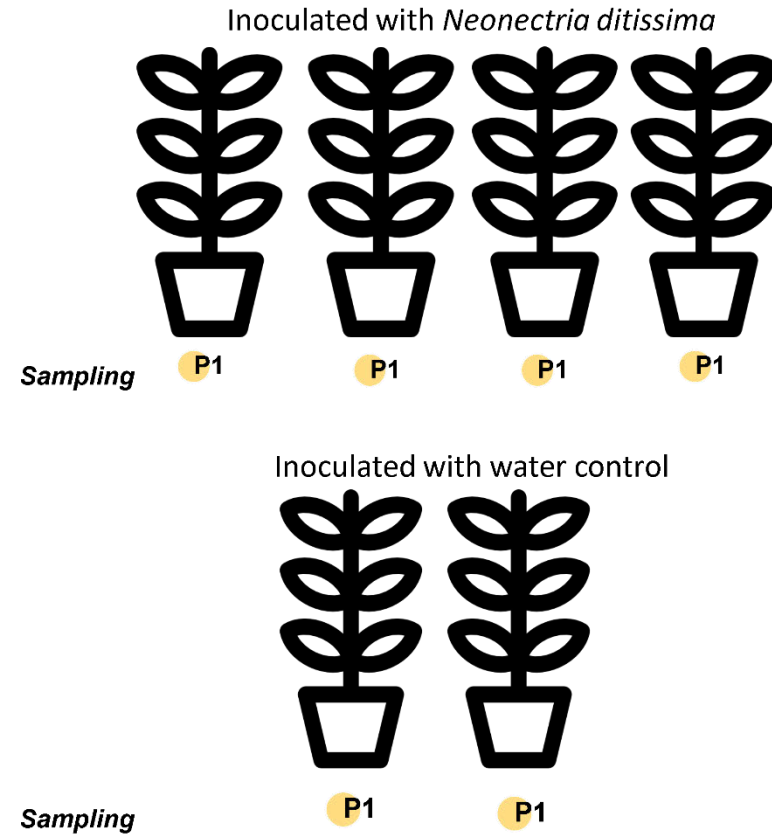
MD16G10 72500	QTL16	Chr16	Transmembrane-amino-acid-transporter	508 112 3	508 328 7	-	water dikinase Vacuolar amino acid transport er 1-like	Aa_trans
MD10G12 48600	QTL10	Chr10	Coatomer	341 818 03	341 825 37	-	Coatome r	COPI_C,Coatomer_WDAD,WD40
MD10G12 48700	QTL10	Chr10	Coatomer	341 855 23	341 858 85	-	Not annotate d	-
MD10G12 50100	QTL10	Chr10	Coatomer	342 799 38	342 811 42	-	Coatome r	COPI_C,Coatomer_WDAD,WD40
MD10G12 51000	QTL10	Chr10	Coatomer	343 336 85	343 368 55	-	Coatome r	COPI_C,Coatomer_WDAD,WD40
MD10G12 38200	QTL10	Chr10	NAC domain containing protein 42	334 374 79	334 390 02	+	Transcrip tion factor JUNGBR UNNEN 1-like	NAM
MD10G12 50000	QTL10	Chr10	wall associated kinase 5	342 772 62	342 783 50	+	Wall- associate d receptor kinase	EGF_CA,GUB_WAK_bind,Pkinase,Pkinase_Tyr,WA K
MD10G12 50500	QTL10	Chr10	wall-associated kinase 2	342 970 43	343 043 03	+	Wall- associate d	EGF_CA,GUB_WAK_bind,Pkinase,Pkinase_Tyr,WA K

MD10G12 51200	QTL10	Chr10	wall-associated kinase 2	344 540 93	344 599 42	+	receptor kinase Wall- associate d receptor kinase	EGF_CA,GUB_WAK_bind,Pkinase,Pkinase_Tyr,WA K
------------------	-------	-------	--------------------------	------------------	------------------	---	---	---

A Experiment with 'Golden Delicious' and 'M9'



B Experiment with full-sibling progeny derived from a cross between 'Gala' x EM-Selection-4



Supplementary figure 1. Overview of the experimental units and sampling procedure used for transcriptome sequencing in experiment **A** ('Golden Delicious' and 'M9') and **B** (full sibling family). Samples were collected at position **P1** (0.5 cm from disease lesion) or **P2** (1 cm from disease lesion). Each plant represents a biological replicate.

Supplementary data- Chapter 4

All supplementary data for this chapter can be found in its original format in Karlstrom et al (2023, <https://doi.org/10.3389/fpls.2023.1054914>). The publication in chapter 4 is based on OTU sequence data published in Papp-Rupar et al (2022, <https://doi.org/10.1094/PBIOMES-10-21-0061-R>), which is reproduced in its whole on page 7 of the supplementary data.

Supplementary table 1. Details of linkage map used for QTL analyses, showing total length of each linkage group (LG) and the average distance of markers on each linkage group

Linkage group	Total length (cM)	Average distance between markers (cM)
LG1	333.75	1.97
LG2	712.75	2.80
LG3	636.65	2.80
LG4	515.59	2.54
LG5	745.22	2.99
LG6	549.01	2.97
LG7	638.26	2.42
LG8	507.74	2.51
LG9	480.57	2.49
LG10	580.73	2.58
LG11	825.97	3.05
LG12	805.71	2.64
LG13	399.78	2.18
LG14	466.92	2.64
LG15	638.46	2.28
LG16	442.4	2.67
LG17	406.28	2.05

Supplementary table 2. Description of phenotypes from 16s sequencing

16s Phenotype	Minimum	Maximum	Mean	Correlation to canker phenotypes				
				Aroma mean value	Golden Delicious mean value	Associated with QTL	Significantly correlated to %HTA	Significantly correlated to %CB
PC2	-15.07	20.35	0.16	11.46	-7.08	*		
PC7	-6.95	11.38	-0.05	3.88	0.44	*	*	*
PC8	-6.00	6.91	0.18	-2.54	2.04		*	
PC13	-5.15	4.66	0.01	0.26	-1.70		*	
PC16	-4.88	6.29	0.00	-2.23	-4.88	*		
PC17	-4.79	4.20	-0.03	-1.13	1.82	*		
PC26	-4.45	3.28	-0.28	-1.97	0.48			
OTU100	36.27	181.59	97.49	118.53	40.82	*	*	
OTU105	47.89	173.37	100.13	71.46	64.00			
OTU114	25.81	144.92	72.61	51.18	49.45		*	
OTU123	26.00	166.45	82.91	130.50	50.69			
OTU124	20.41	204.45	79.96	110.51	24.16	*		
OTU126	30.20	157.94	75.14	39.18	99.79			
OTU128	41.53	177.52	102.28	177.52	113.16	*	*	
OTU13	851.40	2018.00	1293.90	865.93	1434.61			
OTU135	28.88	140.65	76.95	112.64	43.77	*	*	
OTU149	32.82	153.38	79.16	51.50	61.31			
OTU16	591.80	1973.00	1242.60	856.24	834.42			
OTU170	52.16	165.89	103.99	88.78	119.21		*	*
OTU18	519.50	1946.00	1155.10	662.72	912.58	*		
OTU20	322.30	1950.50	923.20	338.32	1028.20	*		
OTU2048	33.61	114.35	73.79	49.45	56.98			
OTU2625	43.91	132.47	86.68	64.48	89.64			
OTU27	384.40	1105.70	662.80	430.90	477.01	*		
OTU3	2849.00	6000.00	4294.00	3397.77	4476.59			
OTU30	355.60	1296.20	723.10	454.14	597.93			
OTU3169	30.90	146.76	78.05	45.54	89.75	*		
OTU37	221.60	1006.50	525.80	371.13	569.75			

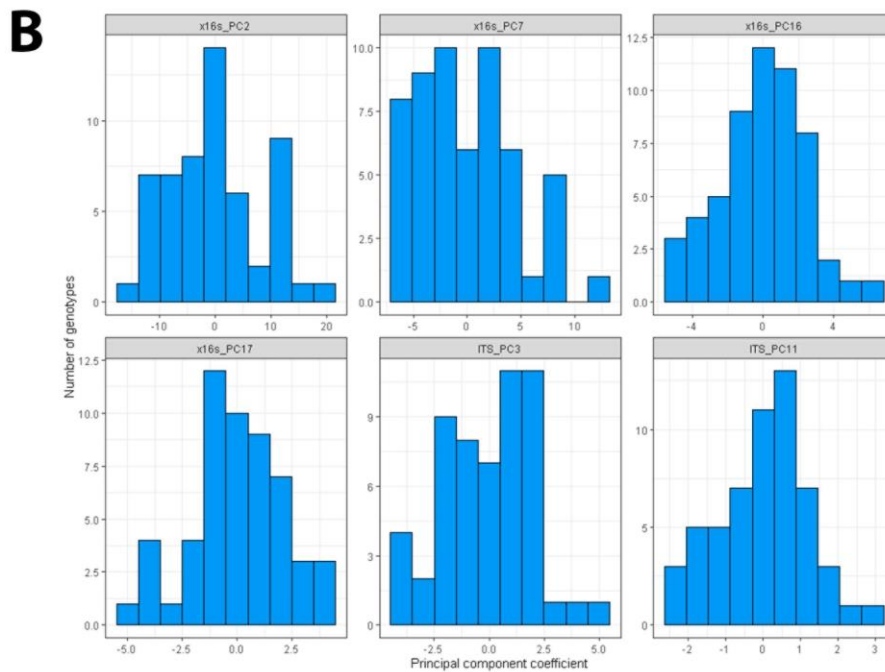
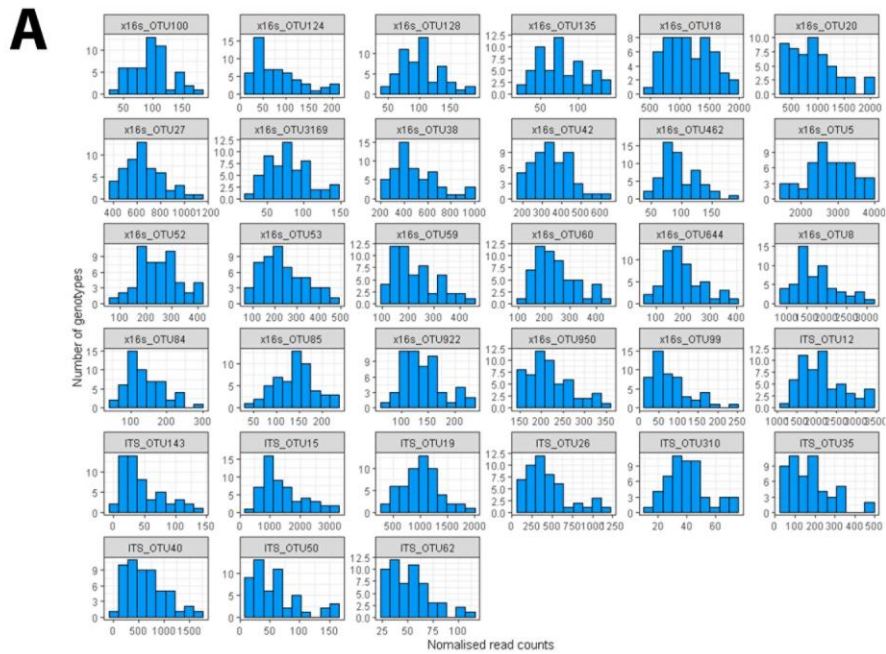
OTU38	229.70	951.60	497.00		688.60	355.93	*	*	
OTU383	100.40	253.10	168.30		171.90	252.17		*	*
OTU42	176.60	611.50	350.50		246.15	346.02	*		
OTU46	167.60	455.90	280.90		193.50	372.68			
OTU462	46.07	184.23	95.34		55.38	109.86	*		
OTU47	147.80	578.90	325.30		302.59	147.79		*	
OTU49	142.50	601.50	332.40		368.24	218.63			
OTU5	1636.00	3949.00	2795.00		2227.27	2732.64	*	*	
OTU504	75.53	235.30	134.86		228.34	117.75			
OTU52	88.56	418.79	248.76		116.13	152.97	*		
OTU53	77.22	462.21	235.59		79.52	328.34	*		
OTU57	75.89	428.91	194.68		144.62	97.15			
OTU59	109.10	439.20	224.70		293.69	135.51	*	*	
OTU60	106.70	436.30	243.40		224.99	138.02	*		
OTU644	59.92	376.68	193.67		176.65	133.09	*		
OTU68	76.62	354.12	191.20		271.64	109.07			
OTU7	639.70	3211.10	1851.00		953.35	925.75			
OTU73	88.36	365.55	193.67		183.25	88.36		*	
OTU8	988.20	3115.60	1740.10		2689.64	1406.67	*	*	
OTU813	47.96	188.36	111.17		199.60	117.33			
OTU84	53.37	288.14	138.42		145.64	98.07	*	*	
OTU85	47.67	232.55	140.57		57.54	183.29	*	*	
OTU89	21.50	314.47	104.89		150.75	40.79			
OTU922	68.77	226.69	138.57		106.81	142.08	*		
OTU950	142.60	339.20	218.80		261.44	324.17	*	*	*
OTU99	12.97	229.52	79.39		44.97	32.74	*		

Supplementary table 3. Description of phenotypes from ITS sequencing

Correlation to canker phenotypes

ITS phenotype	Minimum	Maximum	Mean	Aroma mean value	Golden Delicious mean value	Associated with QTL	Significantly correlated to %HTA (p=0.05)	Significantly correlated to %CB (p=0.05)
PC1	-3.60	3.67	-0.01	2.82	1.04			
PC3	-4.32	4.63	-0.06	1.03	7.07	*	*	*
PC11	-2.59	2.67	0.01	0.92	-0.21	*		
PC12	-2.64	3.28	0.00	0.56	-2.13			
OTU12	1276.00	3420.00	2150.00	1515.76	3066.93	*		
OTU1226	3.08	103.67	34.38	7.13	29.85			
OTU143	5.20	141.98	44.51	110.50	11.64	*	*	
OTU15	315.90	3142.20	1397.40	3029.91	4843.66	*		
OTU16	1175.00	3847.00	2235.00	1471.45	2167.59		*	
OTU17	282.50	3109.80	1542.60	2364.30	907.49		*	
OTU19	296.10	1871.20	1028.30	738.03	1026.73	*	*	
OTU20	200.50	1617.10	836.60	849.04	1338.80		*	
OTU21	403.60	1030.30	680.50	684.91	644.92		*	*
OTU26	85.29	1137.59	439.37	1584.06	337.00	*	*	
OTU29	165.40	751.30	397.80	610.61	329.50		*	*
OTU310	13.96	73.29	40.30	46.86	46.14	*		
OTU3360	857.40	2085.30	1377.20	857.40	1336.67			
OTU35	41.98	467.90	173.01	160.19	308.50	*	*	*
OTU40	72.06	1757.43	629.90	205.61	762.50	*		
OTU4179	13.39	102.48	46.12	146.47	212.51			
OTU50	12.53	154.77	57.29	55.91	92.18	*	*	*
OTU57	8.77	200.10	68.90	56.59	8.77			
OTU62	24.00	107.62	51.86	44.74	32.43	*		
OTU71	23.76	110.72	57.30	44.59	59.93	*	*	

OTU73	9.62	70.06	32.44	42.40	17.82		*	
OTU76	6.61	83.45	28.53	21.10	11.88			



Supplementary figure 1. Histograms showing endophyte trait distributions based on individuals in a biparental apple population originating from a cross between 'Aroma' x 'Golden Delicious'. The traits shown are A) endophyte abundance for individual OTUs and B) principal components (PCs) from a PC analysis of endophyte abundance traits.



RESEARCH

e-Xtra*

The Influence of Host Genotypes on the Endophytes in the Leaf Scar Tissues of Apple Trees and Correlation of the Endophytes with Apple Canker (*Neonectria ditissima*) Development

Matevz Papp-Rupar, Amanda Karlstrom, Thomas Passey, Greg Deakin, and Xiangming Xu[†]

NIAB EMR, New Road, East Malling, West Malling, Kent, ME19 6BJ, U.K.

Accepted for publication 7 February 2022.

ABSTRACT

Bacterial and fungal endophytes may help their host in terms of improved tolerance to abiotic and biotic stresses and enhanced growth. European apple canker, caused by *Neonectria ditissima*, is widespread in apple-growing regions. Infection by *N. ditissima* occurs through artificial or natural wounds, including leaf scars, picking wounds, and pruning cuts. Using F₁ progeny trees in an experimental orchard derived from a cross between a canker-susceptible genotype and a canker-tolerant or -resistant genotype, we assessed both bacterial and fungal endophyte communities in apple leaf scars, and determined correlations of endophytes with canker development. All trees were artificially inoculated with an *N. ditissima* isolate postplanting. Specific components of apple endophytes as well as a number of individual fungal or bacterial groups in leaf scars were

partially genetically controlled by host genotypes. Several bacterial groups were significantly correlated with canker-related traits, mostly positively associated with canker tolerance. A few fungal groups may facilitate canker development whereas others may compete with canker. However, most of these microbial groups could not be identified to the species level with confidence; even for those groups which could be assigned to the species level, there is insufficient knowledge about their ecological characteristics in relation to plants. The present results may be used to inform further research using biocontrol to manage *N. ditissima* and breeding for resistance.

Keywords: apple endophytes, crop, European apple canker, heritability, leaf scars, *Neonectria ditissima*, plant pathology

Many bacterial and fungal endophytes inhabit plant tissues without causing any adverse effect and may benefit their host in terms of improved tolerance to abiotic and biotic stresses (e.g., pests and pathogens) and enhanced growth (Dini-Andreote 2020; Khare et al. 2018; Omomowo and Babalola 2019). Due to increasing public concern about using pesticides, increased incidence of pesticide resistance, and decreasing numbers of commercial pesticides available (primarily due to regulation), there is an urgent need to exploit

beneficial microorganisms, including endophytes, and microbial-derived compounds for disease management.

Neonectria ditissima is a fungal pathogen that causes wood cankers in apple and other broad-leaved trees (Saville and Olivieri 2019; Weber 2014). Canker is widespread in apple-growing regions in most of the temperate areas of the world. *N. ditissima* infects trees through artificial or natural wounds; most frequently, through leaf scars, wounds caused by picking fruit, and pruning cuts. A most damaging phase of this disease is that latent infection established in nurseries can develop rapidly on the main stem postplanting, killing young trees. Due to withdrawal of several effective fungicides (e.g., carbendazim and copper-based products), current chemical control strategies only have a limited effect on the establishment and spread of *N. ditissima*. Thus, host resistance is an important component in managing canker disease. Unfortunately, many modern apple varieties are derived from a narrow genetic background with a high susceptibility to apple canker (Gómez-Cortecero et al. 2016). High-density orchards further exacerbate this problem because canker lesions on the main stem can easily girdle and subsequently kill small trees postplanting in such an orchard. Host resistance against *N. ditissima* is of a quantitative nature (Bus et al. 2019; Gómez-Cortecero et al. 2016). Therefore, it may take a long time to breed apple cultivars with effective

[†]Corresponding author: X. Xu; xiangming.xu@niab.com

Funding: This work was supported by the U.K. Biotechnology and Biological Science Research Council (grant number BB/P007899/1 and BB/P000851/1) and several industry organizations: the Agriculture and Horticulture Development Board, Adrian Scripps Limited, Avalon Produce Limited, ENZA (T&G global subsidiary), Frank P Matthews Limited, and Worldwide Fruit Limited.

*The e-Xtra logo stands for “electronic extra” and indicates that supplementary figures are published online.

The author(s) declare no conflict of interest.

This article is in the public domain and not copyrightable. It may be freely reprinted with customary crediting of the source. The American Phytopathological Society, 2022.

resistance against the pathogen given the nature of perennial trees and quantitative resistance.

There is evidence of host-genotypic effects on endophyte communities in apple (Hirakue and Sugiyama 2018; Liu et al. 2018, 2020), influencing both species richness and composition. Although the endophytic microbe composition was only studied in a limited number of apple cultivars, the results indicate that cultivars with a higher degree of relatedness also share similarities in endophyte community (Liu et al. 2018). Apple resistance to leaf pathogens appears to correlate more with fungal endophytes than bacterial endophytes (Hirakue and Sugiyama 2018). In addition to cultivar, specific location and apple tissue type can also considerably influence endophyte composition (Liu et al. 2020; Olivieri et al. 2021a).

It has been demonstrated recently that a number of apple endophytes at leaf scars were associated with the host susceptibility to *N. ditissima* (Olivieri et al. 2021a). Specific endophytes from apple showed in vitro antagonistic effects against *N. ditissima* (Liu et al. 2020). Thus, manipulating apple endophyte communities may be a viable approach to manage canker disease. Apple endophyte composition could be altered through specific agronomic practices or augmented application of specific endophyte strains with biocontrol ability to improve host resistance or tolerance against *N. ditissima*. Another approach would be to include specific (desirable) endophytes as a selection criterion in breeding programs to breed cultivars with desirable endophyte composition or the ability to recruit these specific microbes for disease suppression or tolerance. To adopt this second approach, we need to assess the magnitude of the heritability of endophyte communities with respect to overall communities as well as specific endophytes. Such knowledge of the host genetic component of endophytes is lacking because the current research has been focusing on the determination of differences in endophytes between genotypes.

In this study, we estimated the broad-sense heritability of endophyte communities as well as individual endophytes in apple leaf scars, an important entry site for *N. ditissima*. Progeny derived from a cross between two genotypes (one canker-susceptible cultivar and the other a canker-tolerant cultivar) were evaluated under field conditions. Bacterial and fungal endophytes at the leaf scar tissues were profiled with amplicon sequencing and correlated with canker development. All sequences have been deposited in the European Nucleotide Archive under project reference PRJEB49633.

MATERIALS AND METHODS

Field design and layout. A cross between cultivars ‘Aroma’ and ‘Golden Delicious’ was made in 2015. Canker resistance is not well understood yet but it is quantitative in nature. The two parents were selected based on empirical evidence as well as limited lab artificial-inoculation data (Gómez-Cortecero et al. 2016), which classified the two parents as moderately susceptible and highly resistant or tolerant, respectively, to *N. ditissima*. All 70 F₁ genotypes in the family, including the parents, were grafted onto M9 EMLA rootstocks in January 2017 at East Malling, United Kingdom. The plants were maintained in pots in polytunnels until October 2017, when they were planted in a randomized block design in an orchard. There were four blocks, with one tree per genotype in each block.

Inoculation with *N. ditissima*. The trees were artificially inoculated with a single isolate of *N. ditissima* (Hg199) at leaf scars in November 2018 in order to eliminate the issue of inoculum heterogeneity in the orchard. Because the research objective was to compare resistance and susceptibility of genotypes to *N. ditissima*, we decided to eliminate the issue of field inoculum heterogeneity via artificial inoculation from complicating data interpretation.

The inoculum was prepared according to a published protocol (Gómez-Cortecero et al. 2016). Five artificial leaf scars were inoculated per tree, and each leaf scar (pseudoreplicate) was positioned on a separate branch. A droplet of 6 µl of spore suspension (10⁵ macroconidia/ml) was pipetted onto each artificial leaf scar wound, then covered with petroleum jelly (Vaseline) immediately after absorption. The petroleum jelly was removed 2 weeks after inoculation.

Each inoculated leaf scar was marked to allow repeated measurements over time. Canker lesion development was measured with a digital caliper at three time-points: 5, 8, and 11 months postinoculation (mpi). A final assessment was conducted at 20 mpi on the percent branch area with foliage, percent branches with cankers, and number of cankers. Average number of cankers per branch was then calculated for each tree.

Sampling leaf scars, DNA extraction, and sequencing.

Many trees died of canker before leaf scars were sampled in autumn 2019 before leaf fall. Only those genotypes with a minimum of three surviving trees were sampled. In total, we sampled 216 trees, including the two parents and 54 F₁ genotypes. Leaf scars were sampled for characterization of endophytes in leaf scar tissues, following a published protocol (Olivieri et al. 2021a). Briefly, sampling and subsequent sample processing consisted of the following steps. Four 20-cm-long, healthy (i.e., free of any disease symptoms on all leaf scars), 1-year-old extension shoots were sampled randomly from each tree, not including those inoculated shoots (because those already became 2-year-old shoots). Our previous study showed that *N. ditissima* is unlikely to be systemic but usually is confined within the vicinity of canker lesions (Olivieri et al. 2021b). Thus, *N. ditissima* is not expected to be present in these healthy leaf scars because new infections of leaf scars usually take place after leaf fall in autumn. Three to four freshly exposed leaf scars were sampled from each of the four shoots and pooled into one sample for a single tree. Samples were freeze dried and dry weight was recorded before homogenization with a Geno/Grinder 2010 (SPEX CertiPrep) for 2 min at 1,500 rpm using 2-ml tubes and two 5-mm steel ball bearings. Sterile 0.1 M phosphate-buffered saline (PBS) buffer was added to the homogenized samples at a 1:5 ratio (dry weight [milligrams]/volume [microliters]). DNA was extracted from 120 µl of PBS resuspended homogenate with the DNeasy Plant mini kit (Qiagen) according to the manufacturer’s protocol. Pure DNA was eluted from the spin columns in two steps, each using 50 µl of molecular-grade water and 1 min of incubation before spinning at 14,000 × g. The purity and quantity of extracted DNA was assessed with NanoDrop1000 (Thermo Fisher Scientific). DNA extraction of samples was repeated if their concentration did not exceed 10 ng/µl. The samples were shipped on ice to Novogene UK (Cambridge, U.K.) where PCR amplification, library prep, and metabarcoding sequencing was done. The target regions were internal transcribed spacer (ITS)1-1F (ITS1-1F-F: 5'-CTTGGTCATTTAGAGGAAGTAA-3', ITS1-1F-R: 5'-GCTGCGTTCCTTCATCGATGC-3') and 16S V5-V7 (799F: 5'-AACMGGATTAGATACCCCKG-3', 1193R: 5'-ACGTCATCCCCACCTTCC-3'). To reduce untargeted amplification of plant mitochondrial and plastid DNA with the 16S amplicon, we used mPNA (5'-ggc aagtgttcttcgga-3') and pPNA (5'-ggctcaaccttgacag-3') oligo blockers (PNA Bio) at 200 nM final concentration. Samples were sequenced on Illumina NovaSeq platform in the 250-nucleotide paired-end mode.

We estimated fungal and bacterial community sizes with quantitative PCR (qPCR). Briefly, a pooled sample was prepared combining 2 µl of extracted DNA from each sample. Calibration curve (six steps, 10-fold serial dilutions) was prepared using the pooled sample, aliquoted, and stored at -20°C. Each block of samples was

run on a separate 384-well plate in at least two dilutions (5× and 20×), each dilution in duplicate. The standard curve was run in triplicate alongside samples and a nontemplate control on each plate. Reactions (10 µl each) were performed with SsoAdvanced Universal SYBR Green Supermix (Bio-Rad) and 2 µl of template DNA. The same primers as in the metabarcoding sequencing were used (ITS1-1f and 16S V5-V7) at a final concentration of 100 nM. PNA primers (mPNA and pPNA) at 200 nM final concentration were used in combination with 16S V5-V7 to prevent amplification of mitochondrial and chloroplast contaminants. The cycling protocol was denaturation for 5 min at 94°C and 40 cycles of 60 s at 94°C, 10 s at 75°C, 30 s at 55°C, and 60 s at 72°C, followed by melt curve analysis.

Community size in terms of ITS or 16S copy number was estimated using a calibration curve for each plate separately. First, we calculated the efficiency of amplification for each sample and standard curve on each plate separately [$E = 10^{(-1/\text{slope})}$]. Efficiency of calibration curves and samples were set to 100% by correcting their raw quantification cycle (Cq) values with their respective efficiency using the following formula: $Cq_c = \log_2(E^{Cq})$. The corrected Cq (Cq_c) value of a sample was used to calculate its theoretical copy number present in each sample using the efficiency corrected calibration curve equation: $C = (Cq_c - I_c)/S_c$, where C represents estimated log₁₀ copy number of ITS or 16S in the sample, Cq_c represents efficiency corrected Cq value of the sample, and I_c and S_c represent intercept and slope, respectively, of the efficiency corrected calibration curve.

The samples with efficiency below 0.8 and above 1.2 were repeated at lower DNA dilution (10× and 40× or 20× and 100×) to minimize the effect of PCR inhibitors. Samples that failed the efficacy threshold were removed from further analysis. The mean of four technical repeats on each sample was used.

Sequencing processing and taxonomy assignment. Paired-end amplicon sequence data were processed to produce operational taxonomic unit (OTU) representative sequences and frequency tables. Read pairs containing incorrect bases in primer regions or less than 250 bases in both pairs were discarded. Remaining read pairs were merged with a maximum difference in overlap of 5% with the UPARSE pipeline (version 10.0) (Edgar 2013). Merged reads of < 250 and 400 bp for ITS and 16S, respectively, were discarded. All remaining (unfiltered) reads were retained. Unfiltered reads were then filtered for quality, with a maximum expected error threshold of 0.5 per sequence (Edgar and Flyvbjerg 2015). Forward and reverse primers were removed from both filtered and unfiltered datasets. Filtered reads were dereplicated and singletons were discarded; then, representative OTUs at 97% similarity were constructed with the UPARSE pipeline. UPARSE also removes suspected chimeral sequences. Then, the unfiltered reads were aligned the OTU representative sequences at the level of 97% similarity to produce OTU frequency tables. Finally, the SINTAX algorithm (https://www.drive5.com/usearch/manual/sintax_algo.html) was used to assign taxonomic ranks to the OTU representative sequences with the Unite V8.3 (2021-05-10) fungal database (Köljalg et al. 2013) and the RDP training set 18 bacterial database (Cole et al. 2014). OTUs which were identified as chloroplast and mitochondria were then removed before statistical analysis.

Statistical data analysis. Only the most abundant OTUs that accounted for 99.0% of the total counts were retained for statistical data analysis. Rare taxa were excluded from statistical analysis for several reasons. First, the present objective was to assess the extent of differences between genotypes. However, genotypes would unlikely differ in the relative abundance of rare taxa (given their low counts). For the same reason, correlation of these rare taxa with canker variables also would not be expected to be significant.

Second, these rare taxa had very little effect on the main characteristics of microbiome composition, represented by principal components (PCs). Finally, the abundance of these rare taxa is more prone to sequencing errors than for the other taxa.

Before statistical analysis, the fungal and bacterial OTU tables were normalized by two methods: by the qPCR values of the generic ITS or 16S primers, or by the median-of-ratios (MR) method implemented in DESeq2 (Love et al. 2014). The former normalization incorporates the amount of microbial biomass between samples, estimated as the total number of DNA copies per sample, as well as relative proportion of individual OTUs within a sample. The latter only considers the relative proportions of individual OTUs within a sample. The MR method was used because of (i) nonsignificant differences between genotypes in qPCR values of 16S and ITS and (ii) large variability in qPCR values between replicates within each genotype.

Both α- and β-diversity indices were calculated. The former measures within-sample diversity in term of the number of species present and their corresponding abundance, whereas the latter measures between-sample diversity. Two α-diversity indices (Shannon and Simpson) were calculated with the R vegan 2.3-1 package (Dixon 2003). The ranks of α-diversity indices were subjected to analysis of variance to assess the differences between the two parents and between progeny genotypes via a permutation test for statistical significance. The β-diversity indices were calculated as Bray-Curtis indices, then subjected to permutational multivariate analysis of variance between parents and between progeny genotypes with a permutation test based on pseudo-F ratios (implemented as the Adonis function in the vegan package).

The main objective of the present study was to determine whether there is significant genetic variability among F₁ progeny genotypes. This was achieved by a random effect model in which the total variability among F₁ genotypes was partitioned into environmental (V_E = between blocks + residual) and genetic (V_G = between F₁ genotypes) variability. The significance of genetic variability (component) was statistically tested by comparisons of two nest models with a χ² test with one degree of freedom: one with the genotypic component included and the other without. The broad-sense heritability was then estimated as V_G/(V_E + V_G).

These variance components were estimated with the lmer function in the lme4 package (Bates et al. 2015). For each normalized set of counts data, two types of data were used for estimation of the genetic components: PC scores, representing the overall microbial composition, and the normalized counts data of those OTUs with highest count values (Table 1). Before PC analysis, the normalized counts data were logarithm transformed on the natural base, then standardized. Similarly, normalized OTU count values were logarithm transformed on the natural base before analysis. The random effect model was fitted to the data with the R lme4

TABLE 1
Number of the principal components (PCs) and operational taxonomic units (OTUs) with the highest counts for inclusion in estimation of differences between F₁ genotypes and correlation with canker variables

Group	Quantitative PCR normalized		Median of ratio normalized	
	PCs	OTUs	PCs	OTUs
Fungi (internal transcribed spacer)	30	100	80	100
Bacteria (16S)	30	200	50	200

package (Bates et al. 2015). Within the analysis of each data type (PC or OTU), the Benjamini-Hochberg (BH) adjustment (Benjamini and Hochberg 1995) was applied to correct for the false discovery rate associated with multiple testing. Statistical significance was determined at the 5% level (BH adjusted). In addition to the estimation of broad-sense heritability, correlation (both Pearson and Spearman) of canker-related variables with PC scores and normalized OTU counts were calculated.

All statistical analyses were carried out in R 4.0.3 (R Core Development Team 2019).

RESULTS

Overall sequencing, OTU generating, and qPCR results.

Fungi. In total, there were 4,268 fungal OTUs, most of which had few reads. The top 6 and 34 most abundant OTUs accounted for over 50 and 90% of the total reads, respectively (Fig. 1A). The top 206 OTUs accounted for 99.0% of total reads and were included in subsequent analysis.

The number of reads assigned to OTUs in each sample ranged from 51,780 to 134,300, with a median of 117,676; the number of reads for each OTU ranged from 1,706 to 4,289,841, with a median of 7,532. The top two were both identified as *Filobasidium* spp.: *F. wieringae* and *F. chernovii*, accounting for 18.0 and 12.0% of the total reads, respectively. The OTUs with the third and fourth most reads were both identified as *Vishniacozyma* spp., jointly accounting for 13.0% of the total reads. Of the 206 fungal OTUs, only 137, 118, 104, 79, 60, and 34 could be assigned to the taxonomic rank of phylum, class, order, family, genus, and species, respectively, with >80% confidence. Basidiomycota and Ascomycota accounted for 59.3 and 15.8%, respectively, of the total reads, whereas 24.9% of the reads could not be assigned to a phylum with >80% confidence and, hence, were designated as unknown (Fig. 2A).

For 13 of the 216 samples (54 F_1 genotypes and the two parents), we failed to obtain reliable qPCR ITS values. Of the remaining samples, there were large variabilities in the ITS qPCR values among replicates within a given genotype (Fig. 3A); genotypes did not differ significantly in the ITS qPCR values.

Bacteria. One sample failed to generate sequences. In total, there were 3,639 bacterial OTUs; the top 51 and 583 most abundant OTUs accounted for >50 and 90% of the total reads, respectively (Fig. 1B). Only the top 1,694 OTUs were included in subsequent analysis because all others jointly accounted for <1.0% of the total reads.

Of the 1,694 OTUs, the number of reads for each OTU ranged from 490 to 1,034,106, with a median of 2,654. The number of reads assigned to OTUs in each sample ranged from 14,180 to 127,718, with a median of 110,064. The top two OTUs by abundance were *Shingomonas* sp. (4.6%) and *Methylobacterium* sp. (4.2%). Of the 1,694 bacterial OTUs, only 1,341, 1,091, 809, 605, and 388 could be assigned to the taxonomic rank of phylum, class, order, family, and genus, respectively, with >80% confidence. *Proteobacteria* and *Actinobacteria* accounted for 54.9 and 24.5% of the total reads, respectively, whereas 9.0% of the reads could not be assigned to a phylum (Fig. 2B).

Of the 216 samples, we failed to obtain reliable qPCR 16S values for 14 samples. For eight samples, qPCR data for both fungi and bacteria were not available. As for fungi, there were large variabilities in the 16S qPCR values among replicates within a given genotype (Fig. 3B), and genotypes did not differ significantly in the 16S qPCR values. However, there were significant ($P < 0.001$) differences in the 16S qPCR values among the four blocks.

Microbial diversity indices. **Fungi.** For both the qPCR- and MR-normalized data, there were no significant differences in both Simpson and Shannon indices among the 54 F_1 genotypes. However, the blocks differed significantly ($P < 0.001$) in the two indices. For the qPCR-normalized data, F_1 genotypes did not differ in Bray-Curtis indices but differed ($P < 0.001$) in the indices for the MR-normalized data, accounting for approximately 25% of the total variability in the indices. The two parents did not differ in all indices for either normalized data set.

Bacteria. For both the qPCR- and MR-normalized data, 54 F_1 genotypes did not differ significantly in either Simpson or Shannon indices, and the blocks differed ($P < 0.001$) in the two indices. For the qPCR-normalized data, neither F_1 genotypes nor the two parents differed in Bray-Curtis indices. In contrast, F_1 genotypes ($P < 0.001$) as well as the two parents ($P < 0.05$) differed in Bray-Curtis indices for the MR-normalized data.

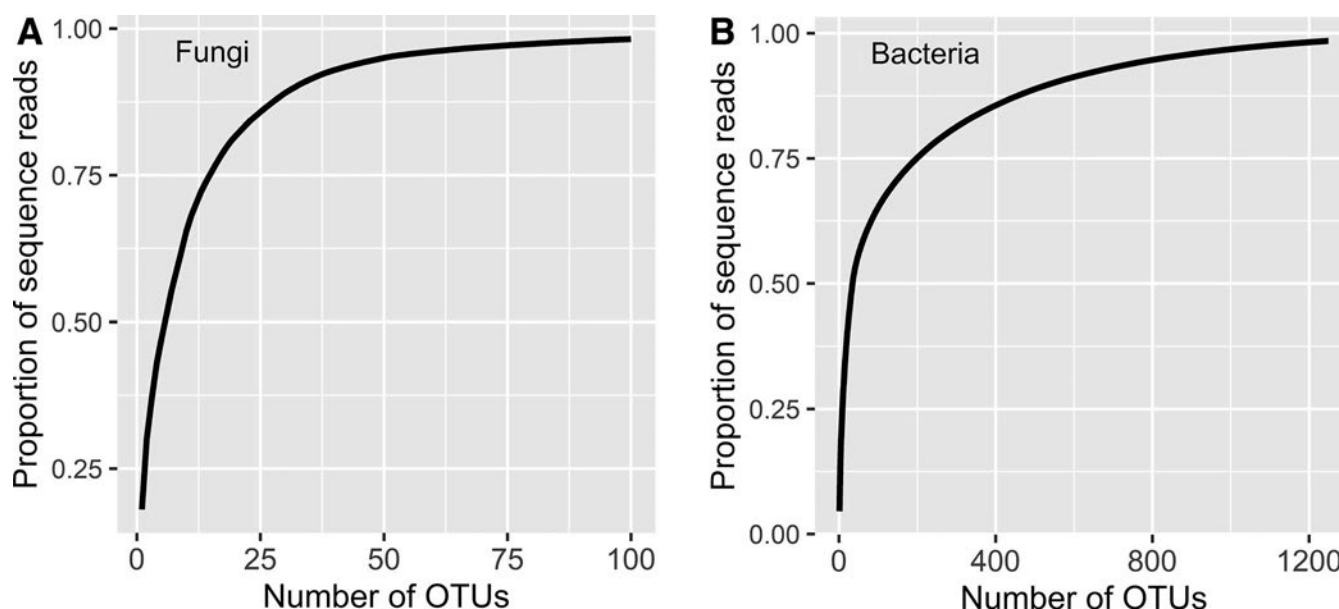


Fig. 1. Proportion of the cumulative sequence reads plotted against the number of **A**, fungal and **B**, bacterial operational taxonomic units (OTUs), where the OTUs were sorted in the descending order with respect to the number of their sequence reads.

Genetic components of PC scores. The summary of results for PC scores is shown in Table 2.

Fungi. For the qPCR-normalized data, the first two PCs explained approximately 50.9 and 4.0% of the total variability (Supplementary Fig. S1A). F₁ genotypes differed ($P < 0.001$) for PC5, with the corresponding estimated heritability value of 27.5%. For the MR-normalized data, the first two PCs explained only approximately

9.3 and 7.4% of the total variability (Supplementary Fig. S1B). F₁ genotypes differed for PC1, PC4, P9, PC12, P17, and P44, with corresponding heritability estimates of 5.5, 33.7, 20.8, 23.4, 19.4, and 21.9%.

Bacteria. For the qPCR-normalized data, the first two PCs explained approximately 45.3 and 3.8% of the total variability (Supplementary Fig. S2A). Only for 2 (PC3 and PC8) of the top 30 PCs

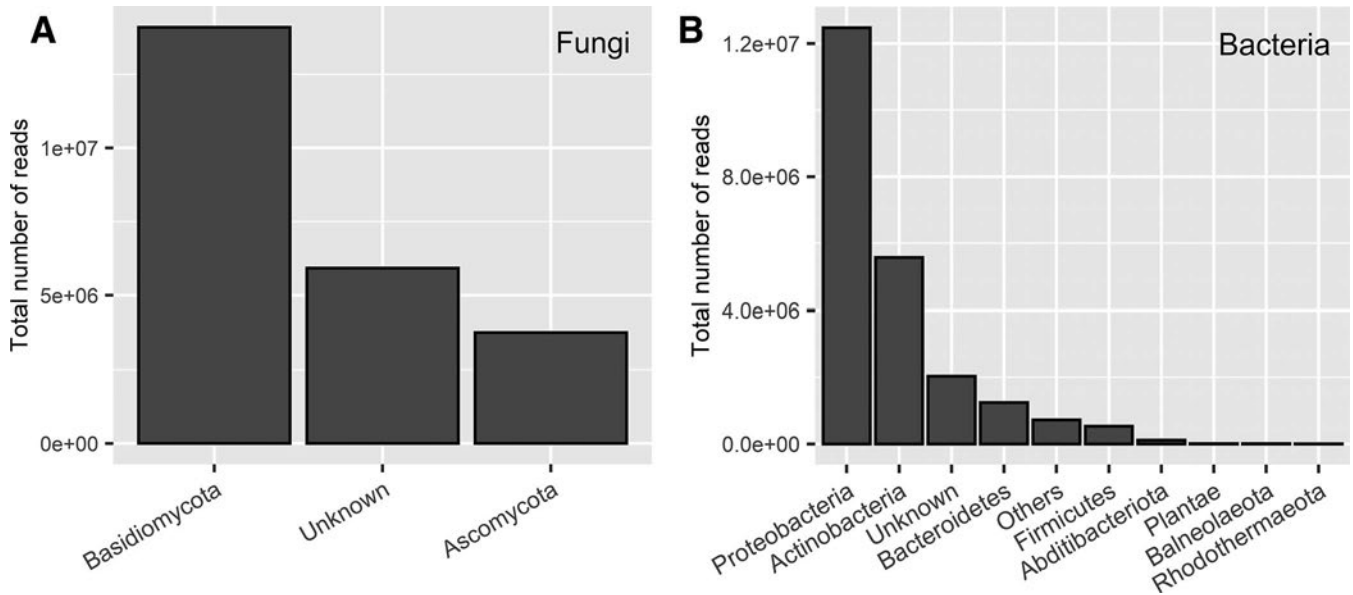


Fig. 2. Histogram of the number of the **A**, internal transcribed spacer and **B**, 16S sequences that were assigned to the phylum at the 80% confidence level; the “Unknown” group consists of those operational taxonomic units that cannot be assigned to a unique phylum.

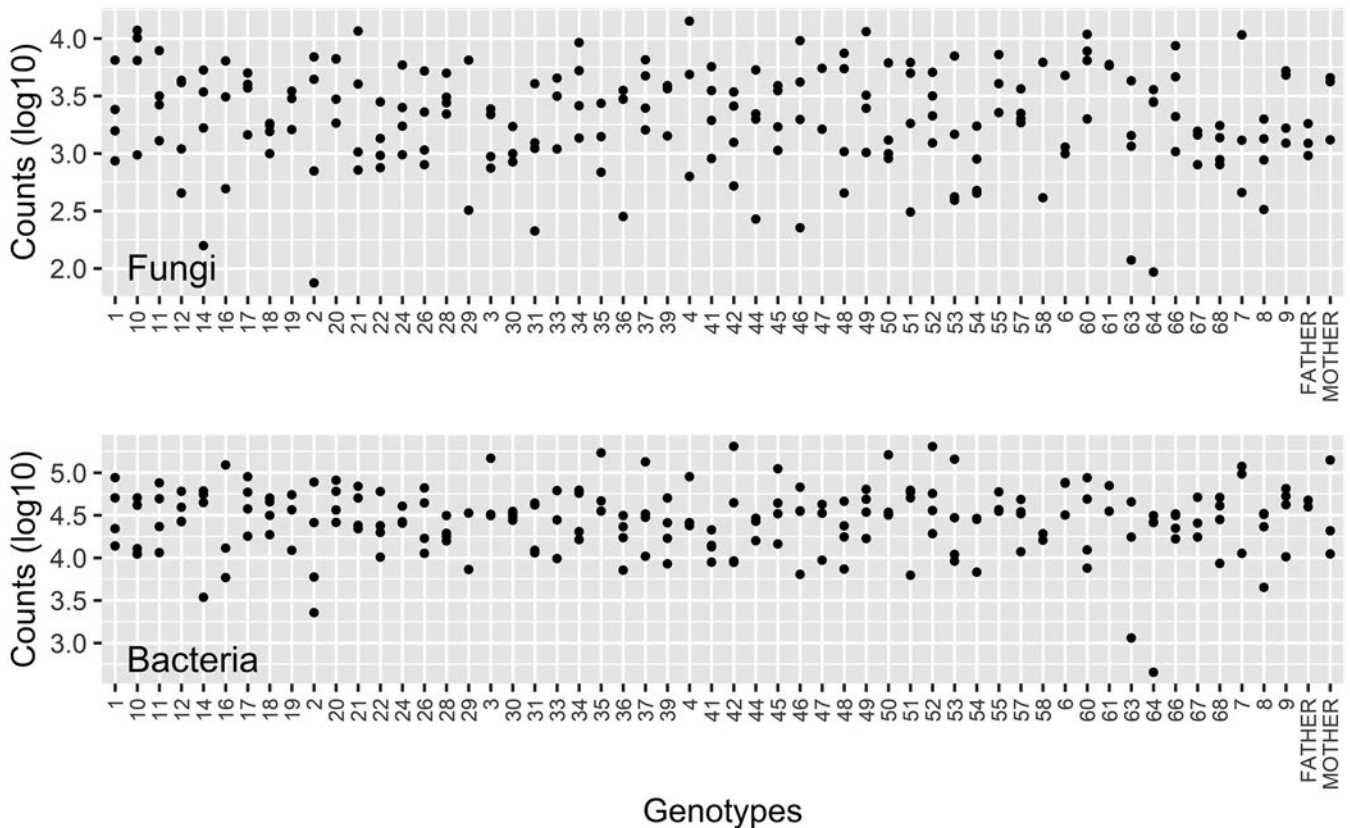


Fig. 3. Quantitative PCR results of both the internal transcribed spacer and 16S of endophytes in apple leaf scar tissues of individual trees of F₁ and parental genotypes. The cross was between cultivars Aroma and Golden Delicious.

did the 54 F₁ genotypes differ significantly ($P < 0.05$), with estimated heritability of 29.5 and 30.0%, respectively. For the MR-normalized data, the first two PCs explained only approximately 9.2 and 8.0% of the total variability (Supplementary Fig. S2B). For 7 (PC2, PC7, PC8, PC16, PC17, and PC26) of the top 50 PCs, F₁ genotypes differed significantly ($P < 0.05$), with heritability estimates ranging from 14.5% (PC13) to 33.2% (PC7).

Genetic components of individual OTUs. The summary of results for individual OTUs is shown in Table 2.

Fungi. For the qPCR-normalized data, F₁ genotypes did not differ significantly in any of the top 100 OTUs. For the MR-normalized data, F₁ genotypes differed ($P < 0.05$) for 24 of the top 100 OTUs (Fig. 4A; Table 3). Only 7 of the 24 OTUs could be assigned to the

species level; 2 of these OTUs were both identified as *Tilletiopsis washingtonensis*. The estimate of broad-sense heritability ranged from 10.2 to 34.7%, with an average of 18.5%.

Bacteria. For the qPCR-normalized data, F₁ genotypes differed significantly in only 1 of the top 200 OTUs (OTU89, *Roseomonas* sp.), with an estimated broad-sense heritability of 27.9%. For the MR-normalized data, F₁ genotypes differed significantly for 47 of the top 200 OTUs (Fig. 4B; Table 4). The estimate of broad-sense heritability ranged from 8.1 to 37.3%, with an average of 18.5%. These 47 OTUs also included OTU89; indeed, there were other OTUs from *Roseomonas* spp.

Canker development. Average canker size over the first three measurements (month 5, 8, and 11) ranged from 4.6 to 23.5 cm,

Variables	Quantitative PCR normalized				Median of ratio normalized			
	Fungi		Bacteria		Fungi		Bacteria	
	PCs	OTUs	PCs	OTUs	PCs	OTUs	PCs	OTUs
Genetic variance	1	0	2	1	6	24	7	47
Correlation								
Individual based								
Canker size	0 (0)	0 (0)	0 (0)	0 (0)	0 (0)	0 (0)	1 (0)	0 (0)
Canopy	1 (1)	2 (0)	1 (1)	0 (0)	1 (1)	7 (7)	1 (1)	6 (0)
Shoots cankered (%)	0 (0)	0 (0)	0 (0)	0 (0)	0 (0)	0 (0)	0 (0)	0 (0)
Family based								
Canker size	1 (1)	0 (2)	0 (0)	2 (2)	1 (1)	2 (2)	2 (2)	0 (0)
Canopy	1 (0)	5 (0)	0 (0)	0 (0)	1 (0)	8 (6)	1 (0)	4 (10)
Shoots cankered (%)	1 (0)	0 (0)	0 (0)	0 (0)	0 (0)	1 (0)	0 (0)	0 (0)

^a Values, shown as x (y), indicate the x and y number of significant Pearson and Spearman correlations, respectively.

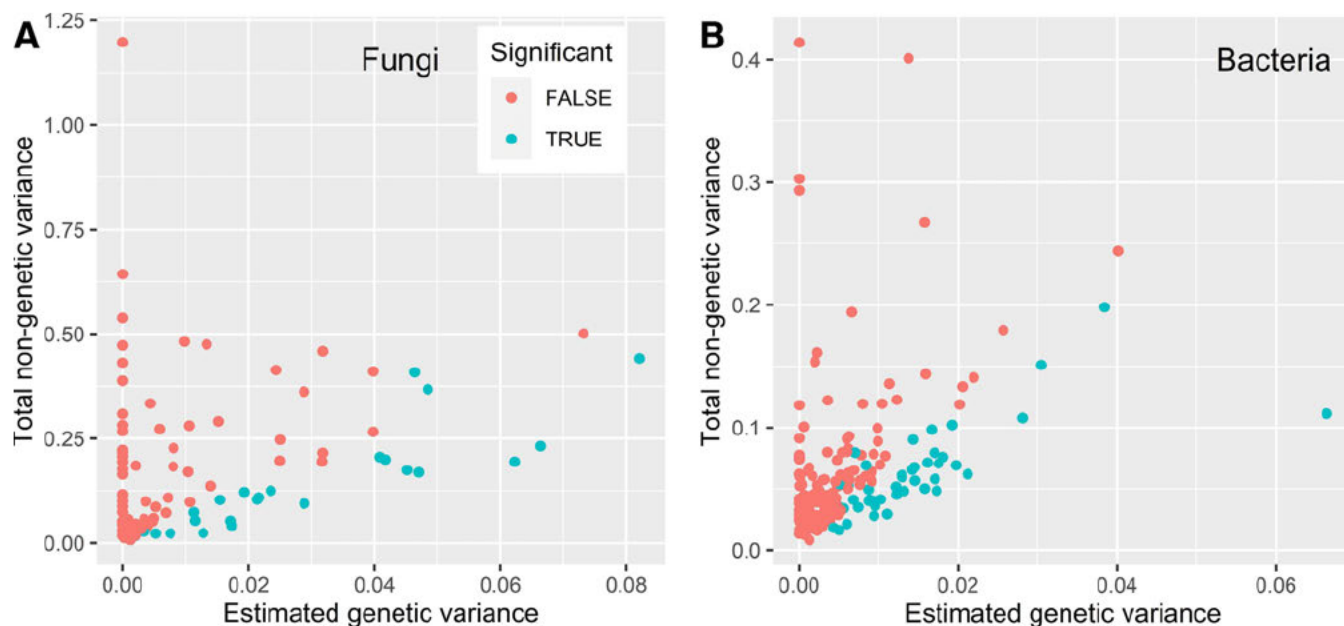


Fig. 4. Estimated genetic variance plotted against the total environmental variance for the top **A**, 100 fungal and **B**, 200 bacterial operational taxonomic units based on the median of ratio normalized counts data. The point color indicates whether the genetic variance is statistically significant or not.

with an average of 11.1 cm (Fig. 5A). In month 20, 35 trees had cankers in all shoots (Fig. 5C). The two parents did not differ in any of the three canker measurements. In contrast, F₁ genotypes differed significantly in average canker size ($P < 0.05$) and canopy coverage (Fig. 5B) and percent shoots with canker in month 20 ($P < 0.001$). The broad-sense heritability was 13.1, 23.8, and 31.9% for average canker size, percent canopy coverage, and percent shoots with canker at 20 mpi, respectively.

Correlation of microbial variables with canker variables. The summary of correlation results is shown in Table 2, with detailed correlation results given in Tables 5 and 6.

Fungi. Among the top 30 fungal PCs of the qPCR-normalized data, only PC5 scores were correlated with percent canopy coverage in month 20 based on the individual tree data. At the F₁ genotypic level, PC5 scores were correlated with percent canopy coverage in month 20, PC7 with canker size, and PC23 with percent shoots cankered. For the MR-normalized data, of the top 80 PCs, only PC4 scores were correlated with percent canopy coverage based on individual trees whereas, based on F₁ genotypic means, PC3 and P9 were correlated with percent canopy coverage and canker size, respectively.

In total, there were 42 significant correlations of canker variables with 16 fungal OTUs; 33 of these 42 cases were for the MR-normalized data. In 26 of the 42 cases, correlation was at the level of F₁ genotypic means. In 35, 6, and 1 cases, it involved percent canopy coverage, average canker size, and percent shoots with cankers, respectively. Among these 42 significant correlations,

25 and 17 were of the Pearson and Spearman type, respectively. Correlation coefficient ranged from -0.56 to 0.51. The magnitude of correlation was greater for genotypic means (from -0.56 to 0.51) than for individual trees (from -0.30 to 0.26) (Table 5). For several OTUs, the observed correlation was inconsistent; namely, different signs between qPCR- and MR-normalized data (e.g., OTU69) (Table 5), or between individual and genotypic levels (e.g., OTU49) (Table 5), or between Pearson and Spearman correlations (e.g., OTU1896) (Table 5). Nevertheless, several OTUs had consistent correlation patterns, including a group from *Entyloma* sp. (OTU35) and *Pseudoophiobolus rosae* (OTU57) (Table 5).

Bacteria. Among the top 30 PCs of the qPCR-normalized data, both Pearson and Spearman correlations of PC11 with percent canopy coverage were significant based on individual trees ($r = -0.24, -0.32$). For the MR-normalized data, PC7 was correlated with percent canopy coverage on individual trees (Pearson: -0.24, and Spearman: -0.26) (Fig. 6), whereas PC29 was correlated with average canker size (Pearson: 0.27). At the F₁ genotypic level, both PC6 and PC10 were correlated with average canker size ($r = -0.50, 0.47$) and PC7 with percent canopy coverage (Pearson: -0.44) (Fig. 6).

In total, there were 24 significant correlations of canker variables with 16 bacterial OTUs; 20 of these 24 cases were for the MR-normalized data (Table 6), all with percent canopy cover. All four correlations of qPCR-normalized data were with canker size. In 18 of these 24 cases, correlation was at the F₁ genotypic level. Half of the correlation was of the Pearson type. Correlation

TABLE 3
Summary of those fungal operational taxonomic units (OTUs) within the top 100 highest counts in the median of ratio normalized counts for which the genetic differences between F₁ genotypes were statistically significant

OTU	Taxonomy (>80% confidence)	Total reads (%)	Heritability (%)
OTU29	Ascomycota	0.37	17.57
OTU3360	Basidiomycota	1.30	11.00
OTU143	Dothideomycetes	0.05	21.76
OTU35	<i>Entyloma</i>	0.19	17.26
OTU50	<i>Entyloma calendulae</i>	0.07	24.21
OTU12	Fungi	1.97	24.43
OTU1226	Fungi	0.04	11.64
OTU147	Fungi	0.07	15.67
OTU19	Fungi	0.94	24.31
OTU40	Fungi	0.65	10.20
OTU73	<i>Leptospora</i>	0.03	17.04
OTU17	<i>Neosetophoma</i>	1.51	15.79
OTU20	Phaeosphaeriaceae	0.83	23.39
OTU62	Phaeosphaeriaceae	0.05	13.31
OTU76	Pleosporales	0.04	16.57
OTU57	<i>Pseudoophiobolus rosae</i>	0.08	22.26
OTU21	<i>Sporobolomyces roseus</i>	0.62	18.66
OTU26	<i>Subplenodomus iridicola</i>	0.49	20.57
OTU24	<i>Symmetrospora</i>	0.71	10.20
OTU310	<i>Taphrina</i>	0.04	29.12
OTU71	<i>Taphrina</i>	0.05	13.02
OTU16	<i>Taphrina carpini</i>	2.04	34.73
OTU15	<i>Tilletiopsis washingtonensis</i>	1.40	16.54
OTU4179	<i>T. washingtonensis</i>	0.05	13.68

TABLE 4
Summary of those bacterial operational taxonomic units (OTUs) within the 200 highest counts (median of ratio normalized) for which the genetic differences between F₁ genotypes were statistically significant

OTU	Taxonomy (>80% confidence)	Total reads (%)	Heritability (%)
OTU68	<i>Acetobacteraceae</i>	0.18	17.87
OTU16	<i>Actinobacteria</i>	1.21	8.61
OTU644	<i>Actinobacteria</i>	0.19	26.27
OTU383	<i>Alphaproteobacteria</i>	0.16	23.45
OTU105	<i>Arthrobacter</i>	0.10	21.01
OTU27	<i>Aurantimonadaceae</i>	0.67	10.49
OTU38	<i>Aureimonas</i>	0.48	21.04
OTU128	<i>Bacteria</i>	0.10	14.91
OTU59	<i>Bacteria</i>	0.22	19.06
OTU813	<i>Bacteria</i>	0.11	17.52
OTU950	<i>Bacteria</i>	0.21	18.97
OTU52	<i>Comamonadaceae</i>	0.26	13.76
OTU135	<i>Deinococcus</i>	0.08	25.53
OTU18	<i>Deinococcus</i>	1.15	19.88
OTU124	<i>Deltaproteobacteria</i>	0.08	16.79
OTU170	<i>Dyadobacter</i>	0.10	17.86
OTU57	<i>Enterococcus</i>	0.20	17.64
OTU46	<i>Erythrobacteraceae</i>	0.28	12.13
OTU2048	<i>Firmicutes</i>	0.07	19.93
OTU5	<i>Kineococcus</i>	2.74	14.17
OTU53	<i>Marmoricola</i>	0.23	14.46
OTU13	<i>Methylobacteriaceae</i>	1.28	12.11
OTU3	<i>Methylobacterium</i>	4.27	9.34
OTU462	<i>Microbacteriaceae</i>	0.09	17.65
OTU504	<i>Microbacteriaceae</i>	0.13	14.23
OTU37	<i>Nakamurellales</i>	0.54	17.83
OTU123	<i>Nocardioides</i>	0.09	18.42
OTU42	<i>Nocardioides</i>	0.35	10.78
OTU7	<i>Novosphingobium</i>	1.86	22.73
OTU2625	<i>Proteobacteria</i>	0.09	21.81
OTU73	<i>Proteobacteria</i>	0.19	21.27
OTU922	<i>Proteobacteria</i>	0.14	25.14
OTU85	<i>Pseudokineococcus</i>	0.14	20.44
OTU100	<i>Rhodobacteraceae</i>	0.10	17.66
OTU30	<i>Rhodococcus</i>	0.70	8.12
OTU3169	<i>Rhodospirillales</i>	0.08	23.89
OTU126	<i>Roseomonas</i>	0.08	22.19
OTU47	<i>Roseomonas</i>	0.32	21.44
OTU84	<i>Roseomonas</i>	0.14	17.45
OTU89	<i>Roseomonas</i>	0.13	37.34
OTU20	<i>Sphingomonadaceae</i>	0.93	20.67
OTU114	<i>Sphingomonas</i>	0.08	15.86
OTU149	<i>Sphingomonas</i>	0.08	19.25
OTU8	<i>Sphingomonas</i>	1.76	18.97
OTU49	<i>Spirosoma</i>	0.32	27.32
OTU99	<i>Terracoccus</i>	0.10	16.25
OTU60	<i>Williamsia</i>	0.24	19.93

coefficients ranged from -0.54 to 0.51 , and were greater for genotypic means (from -0.54 to 0.51) than for individual trees (from 0.22 to 0.25) (Table 6). For the qPCR-normalized data, only two OTUs (*Pseudokineococcus* sp. and order *Propionibacteriales*) were significantly correlated with average canker size at the genotypic level (Table 6). For the MR-normalized data, several OTUs had multiple high and consistent correlations with canopy size, including *Actinobacteria* (OTU93), *Armatimonadetes_gp5* (OTU107), *Sphingomonas* (OTU72), and *Dyadobacter* (OTU170) (Table 6).

DISCUSSION

The present study showed that specific components of apple endophytes as well as some individual fungal or bacterial groups in tissues around leaf scars in autumn are partially controlled genetically by host genotypes in an F₁ segregating population. Furthermore, there are specific microbial groups that are significantly correlated with canker-related plant traits. However, such correlations are often inconsistent for a given microbial group in terms of whether it is based on individual trees or genotypes or whether it is based on the Pearson or Spearman correlation.

Sequence data were normalized by two methods, qPCR data of generic 16S or ITS primers and MR. In general, genotypic differences were less profound for the qPCR-normalized data than for the MR-normalized data. Moreover, there were far more cases of significant correlations of endophytes with canker-related variables for the MR-normalized data than for the qPCR-normalized data. In theory, qPCR-normalized data should provide more informative data than the MR-normalized data. Although there were often a couple of magnitude differences in qPCR values between trees, F₁ genotypes did not differ significantly in the qPCR values. We also observed a large variability in PCR efficiencies between samples (data not shown) and, hence, repeated qPCR was necessary for many samples. Our experience suggested that conducting qPCR analysis of fungal and bacterial DNA extracted from woody tissues with generic 16S and ITS primers is more problematic than other types of samples such as rhizosphere soils. Nevertheless, qPCR is valuable for pathogen diagnosis such as confirming latent infection of *N. ditissima* in leaf scar tissues (Olivieri et al. 2021b). Further studies are needed to improve quantification of overall microbial biomass in plant (particularly woody) tissues. As an alternative to the qPCR method, each sample may be spiked with a known amount of a synthetic DNA fragment to estimate absolute abundance (Tkacz et al. 2018).

The present study showed that the overall plant genetic component was similar for bacterial and fungal endophytes. For many microbial groups, albeit still a small proportion of the entire microbiome, the variability among F₁ offspring is greater than random variability, indicating existence of host genetic control. There is a significant host genetic component in several PCs, which are jointly determined by many microbial groups. There have been many reports demonstrating that plant genotypes differ in their phytobiomes associated with the rhizosphere, endosphere, and phyllosphere (Liu et al. 2020; Olivieri et al. 2021a; Peiffer et al. 2013; Wagner et al. 2016, 2020; Wei et al. 2019). We found significant host genetic components affecting specific endophyte components of apple leaf scars, represented by PCs, often with a moderate level of genetic variance relative to the environmental variance. However, these microbial components are only a minor proportion of the entire endophytes in the leaf scar tissues, which can be seen from the small number of PCs or OTUs with significant host genetic components. Similarly, maize inbred lines differed significantly in their rhizosphere microbiome but the heritability level was low and the genetic relationship among the inbred lines was not

correlated with the diversity characteristics of the rhizosphere microbiome (Peiffer et al. 2013). The present research is based on an F₁ population from a specific cross, hence representing genetic variance between the two specific parental genotypes only. The overall low heritability of the phytobiome may be due to strong environmental effects (Clouse and Wagner 2021), including spatial

and temporal variation. For instance, we recently demonstrated that, although cultivars differed in their endophytes in leaf scars, orchard locations accounted for much greater variability in endophyte composition (Olivieri et al. 2021a). Plants are only able to recruit those microbial organisms present at a specific site with the recruitment outcome, likely depending on frequencies of available taxa. This

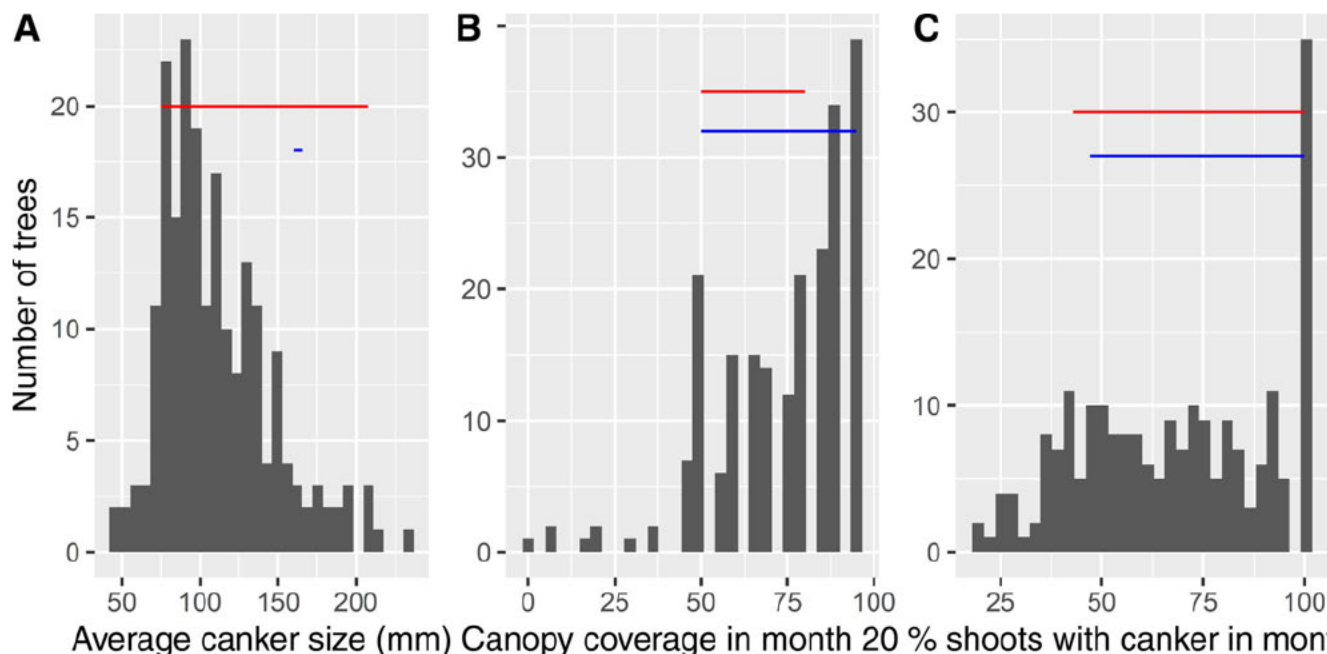


Fig. 5. Histogram of three canker variables assessed on individual trees. **A**, Average canker size measured 5, 8, and 11 months postinoculation; **B**, percent canopy cover; and **C**, percent shoots with cankers assessed 20 months postinoculation. Blue and red lines indicate the range of values for the female and male parents, respectively.

TABLE 5

Significant Pearson and Spearman (in parentheses) correlation coefficients of canker size, canopy cover and percent shoots with canker 20 months postinoculation with fungal operational taxonomic units (OTUs), with the highest counts based on individual trees or F₁ genotypic means

OTU ID	Taxonomy	Quantitative PCR normalized data			Median of ratio normalized data			
		Individual	Genotypic		Individual	Genotypic		
		Canopy	Canker size	Canopy	Canopy	Canker size	Canopy	Shoots (%)
OTU143	Dothideomycetes	-	-	-0.43	-	-	-	-
OTU35	<i>Entyloma</i>	-	(-0.47)	-	-	-0.50 (-0.55)	-	-
OTU59	Exobasidiomycetes	-	-	-	-	-	-0.45 (-0.42)	-
OTU36	Fungi	-0.25	-	-	-0.29 (-0.27)	-	-	-
OTU43	Fungi	-	(-0.52)	-	-	-0.53 (-0.56)	-	-
OTU6	Fungi	-0.28	-	-	-0.24 (-0.22)	-	-	-
OTU69	Fungi	-	-	-0.50	-	-	0.47	-
OTU17	<i>Neosetophoma</i>	-	-	-	0.24 (0.23)	-	-	-
OTU20	Phaeosphaeriaceae	-	-	-0.41	-	-	-0.40	-
OTU247	Phaeosphaeriaceae	-	-	-	-0.25	-	-	-
OTU49	Phaeosphaeriaceae	-	-	-0.41	-0.27 (-0.25)	-	0.43 (0.45)	-
OTU57	<i>Pseudoophiobolus rosae</i>	-	-	-0.45	-	-	-0.48 (-0.47)	-
OTU21	<i>Sporobolomyces roseus</i>	-	-	-	-0.21 (0.26)	-	0.51 (0.50)	-
OTU1896	<i>Vishniacozyma</i>	-	-	-	(-0.28)	-	-0.41 (0.44)	-0.48
OTU3	<i>Vishniacozyma</i>	-	-	-	-	-	0.40 (0.42)	-
OTU18	<i>Vishniacozyma carnescens</i>	-	-	-	0.26 (0.21)	-	-	-

potential large difference in aerosol microbiome over distance may also partially explain the block effects on endophytes observed in the present study.

Only a few specific microbial groups were significantly correlated with canker size or percent canopy cover. Interestingly, all significant correlations with bacterial groups indicated that higher relative abundance of these groups is associated with less canker

development, mostly with better canopy coverage and, in a few instances, negatively with canker size. In contrast, there is no such consistency in the correlation of fungal groups with canker development: both positive and negative correlation with canker development were observed. Moreover, the inconsistency exists even for the same fungal group across different canker variables or parametric or rank correlations, or at the tree or genotypic levels. Reasons

TABLE 6
Significant Pearson and Spearman (in parentheses) correlation coefficients of canker size, canopy cover and percent shoots with canker 20 months postinoculation with most abundant bacterial operational taxonomic units (OTUs) based on individual trees or F₁ genotypic means

OTU ID	Taxonomy	Quantitative PCR normalized data		Median of ratio normalized data	
		Genotypic		Individual	Genotypic
		Canker size		Canopy	Canopy
OTU58	<i>Abditibacteriota</i>	-	-	-	(0.43)
OTU93	<i>Actinobacteria</i>	-	-	-	0.47 (0.41)
OTU165	<i>Actinomycetospora</i>	-	0.25	-	-
OTU67	<i>Allobranchiibius</i>	-	-	-	(0.43)
OTU107	<i>Armatimonadetes_gp5</i>	-	-	-	0.45 (0.43)
OTU108	<i>Bacteria</i>	-	-	-	(0.47)
OTU1181	<i>Bacteria</i>	-	-	0.22	-
OTU170	<i>Dyadobacter</i>	-	-	-	0.50 (0.42)
OTU154	Methylobacteriaceae	-	-	-	(0.50)
OTU70	<i>Methylobacterium</i>	-	-	-	(0.42)
OTU106	Propionibacteriales	-0.49 (-0.53)	-	-	-
OTU85	<i>Pseudokineococcus</i>	-0.50 (-0.54)	0.22	-	-
OTU94	<i>Pseudomonas</i>	-	0.23	-	(0.41)
OTU72	<i>Sphingomonas</i>	-	-	-	0.46 (0.51)
OTU87	<i>Spirosoma</i>	-	0.23	-	-
OTU545	<i>Tepidimonas</i>	-	-	0.23	-

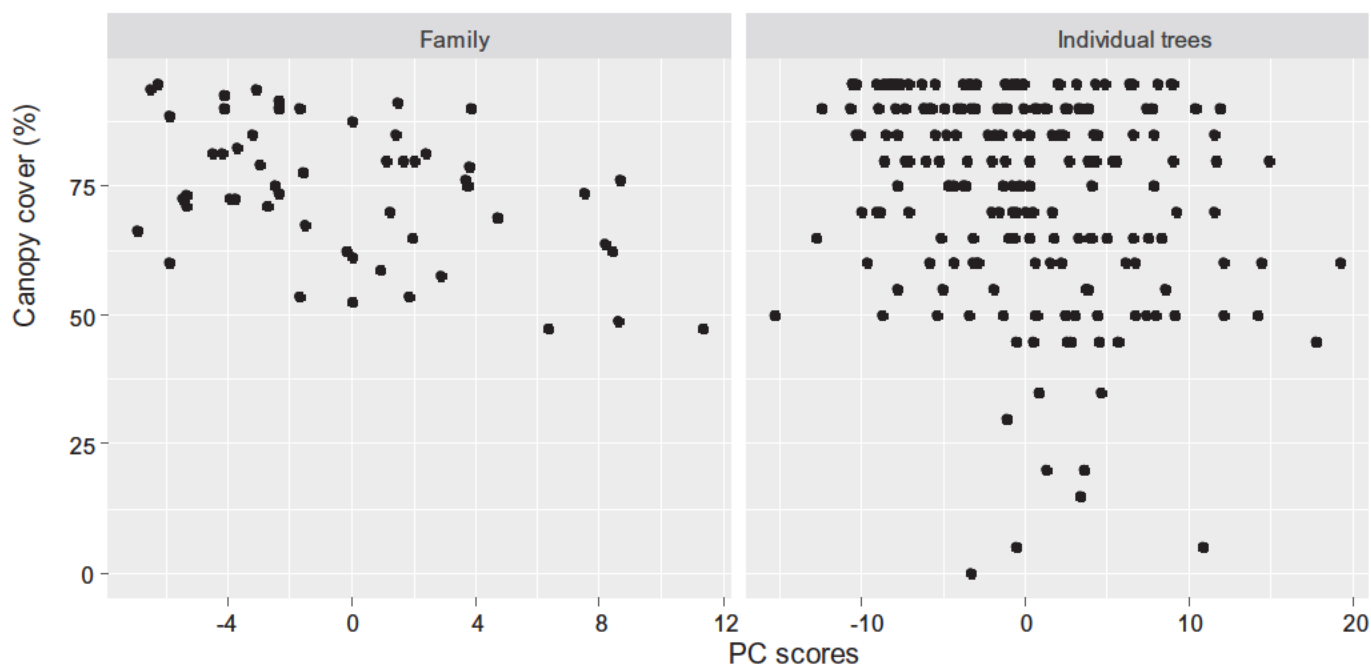


Fig. 6. Principal component 7 (PC7) scores of the median of ratio normalized bacterial operational taxonomic unit data plotted against canopy coverage 20 months postinoculation.

for these observed differences are not obvious. As discussed above, recruitment of endophytes may be considerably influenced by the local aerosol microbiome, not necessarily affected by tree genotypes. Thus, individual trees may differ greatly in relative abundance for some endophytes not because of genetics but because of variabilities in the aerosol microbiome. If these microbes have direct or indirect effects on *N. ditissima*, we may expect inconsistent correlations at the individual and genotypic levels. This may be further complicated by possible differences in the stability or persistence of individual endophytes in the leaf scar tissues at a given endophyte background. For example, fungal endophyte composition might be more easily influenced by differences in aerosol microbiome or external conditions than bacteria. Communities of endophytic fungi assembling in several plant species depend significantly on proximity to the inoculum source as well as the identity of the plant species (Ricks and Koide 2019). It is not known what fraction of the endophytic bacterial microbiome is dispersed via the atmosphere or originated from the atmosphere (Frank et al. 2017). Further research is needed to understand the relative importance of sources for plant endophytes and the effects of biotic and abiotic factors on the stability of the endophyte microbiome over time before we can amend the phytobiome with a reasonable level of predictability to improve crop performance.

Most of those bacterial groups with significant correlations with canker development cannot be classified into genus. *Dyadobacter* isolates are one of the major cohorts of bacteria in the plant phyllosphere (Delmotte et al. 2009; Reisberg et al. 2012) but what role *Dyadobacter* spp. play in these communities is currently unknown. The relative abundance of a *Pseudomonas* OTU (OTU94) and *Sphingomonas* OTU (OTU72) is positively correlated with canopy coverage in the present study. A *Pseudomonas* strain isolated from apple endophytes was shown to be antagonistic toward *N. ditissima* in in vitro tests (Liu et al. 2020). A seed-endophytic strain (*Sphingomonas melonis* ZJ26) confers rice with disease resistance against a bacterial pathogen and is vertically transmitted among plant generations via their seeds (Matsumoto et al. 2021). A couple of *Sphingomonas* groups were more abundant in canker-susceptible cultivars than in resistant cultivars (Olivieri et al. 2021a); however, that particular study did not consider the actual canker severity. *Methylobacterium* normally resides in soil and water but has also been identified as a contaminant of DNA extraction kit reagents, which may lead to its erroneous appearance in microbiota or metagenomic datasets (Salter et al. 2014). Given that these bacterial groups are mostly correlated with canopy cover but not with canker size, we may speculate that they may not be effective as direct competitors of *N. ditissima* but, rather, improve plant tolerance against consequences on plant development due to canker.

Only 3 of the 16 fungal groups with significant correlations with canker development can be classified into species: *Vishniacozyma carnescens* (syn = *Cryptococcus carnescens*), *Pseudoophiobolus rosae*, and *Sporobolomyces roseus*. Of all 16 groups, only *V. carnescens* is associated with reduced canker damage (but only at the individual tree level); unfortunately, there is no published information on its ecology in relation to plants. An *Entyloma* sp. (OTU35) is positively correlated with canker tolerance but *Entyloma* is a genus of plant-pathogenic smut fungi. Thus far, these fungal groups have not been associated with a direct antagonistic effect against *N. ditissima* (Liu et al. 2020) or associated with cultivars with differential susceptibility to *N. ditissima* (Olivieri et al. 2021a). A couple of groups appear to facilitate canker development, including *P. rosae* and Exobasidiomycetes (OTU59). Exobasidiomycetes are a class of fungi sometimes associated with galls of

plant tissues. Further metagenome sequencing and isolation combined with challenging assays against *N. ditissima* are needed to make further progress in this area.

In summary, some components of the apple endophyte microbiome as well as individual microbial groups around leaf scar tissues are partially controlled genetically by apple genotypes. Several microbial groups had significant correlation with canker development. Bacterial groups appear to be positively associated with canker tolerance. On the other hand, a few fungal groups may facilitate canker development whereas a few others may compete with the canker pathogen. The present results may be used to inform targeted approaches to further research in biocontrol of *N. ditissima* with specific microbes and breeding for resistance.

LITERATURE CITED

- Bates, D., Mächler, M., Bolker, B. M., and Walker, S. C. 2015. Fitting linear mixed-effects models using lme4. *J. Stat. Softw.* 67:1-48.
- Benjamini, Y., and Hochberg, Y. 1995. Controlling the false discovery rate: A practical and powerful approach to multiple testing. *J. Roy. Stat. Soc. B* 57:289-300.
- Bus, V. G. M., Scheper, R. W. A., Walter, M., Campbell, R. E., Kitson, B., Turner, L., Fisher, B. M., Johnston, S. L., Wu, C., Deng, C. H., Singla, G., Bowatte, D., Jesson, L. K., Hedderley, D. I., Volz, R. K., Chagné, D., and Gardiner, S. E. 2019. Genetic mapping of the European canker (*Neonectria ditissima*) resistance locus *Rnd1* from *Malus* 'Robusta 5'. *Tree Genet. Genomes* 15:25.
- Clouse, K. M., and Wagner, M. R. 2021. Plant genetics as a tool for manipulating crop microbiomes: Opportunities and challenges. *Front. Bioeng. Biotechnol.* 9.
- Cole, J. R., Wang, Q., Fish, J. A., Chai, B., McGarrell, D. M., Sun, Y., Brown, C. T., Porras-Alfaro, A., Kuske, C. R., and Tiedje, J. M. 2014. Ribosomal Database Project: Data and tools for high throughput rRNA analysis. *Nucleic Acids Res.* 42:D633-D642.
- Delmotte, N., Knief, C., Chaffron, S., Innerebner, G., Roschitzki, B., Schlapbach, R., von Mering, C., and Vorholt, J. A. 2009. Community proteogenomics reveals insights into the physiology of phyllosphere bacteria. *Proc. Natl. Acad. Sci. U.S.A.* 106:16428-16433.
- Dini-Andreote, F. 2020. Endophytes: The second layer of plant defense. *Trends Plant Sci.* 25:319-322.
- Dixon, P. 2003. VEGAN, a package of R functions for community ecology. *J. Veg. Sci.* 14:927-930.
- Edgar, R. C. 2013. UPARSE: Highly accurate OTU sequences from microbial amplicon reads. *Nat. Methods* 10:996-998.
- Edgar, R. C., and Flyvbjerg, H. 2015. Error filtering, pair assembly and error correction for next-generation sequencing reads. *Bioinformatics* 31:3476-3482.
- Frank, A. C., Guzmán, J. P. S., and Shay, J. E. 2017. Transmission of bacterial endophytes. *Microorganisms* 5:70.
- Gómez-Cortecero, A., Saville, R. J., Scheper, R. W. A., Bowen, J. K., de Medeiros, H. A., Kingsnorth, J., Xu, X., and Harrison, R. J. 2016. Variation in host and pathogen in the *Neonectria/Malus* interactions; towards an understanding of the genetic basis of resistance to European canker. *Front. Plant Sci.* 7.
- Hirakue, A., and Sugiyama, S. 2018. Relationship between foliar endophytes and apple cultivar disease resistance in an organic orchard. *Biol. Control* 127:139-144.
- Khare, E., Mishra, J., and Arora, N. K. 2018. Multifaceted interactions between endophytes and plant: Developments and prospects. *Front. Microbiol.* 9.
- Köljal, U., Nilsson, R. H., Abarenkov, K., Tedersoo, L., Taylor, A. F. S., Bahram, M., Bates, S. T., Bruns, T. D., Bengtsson-Palme, J., Callaghan, T. M., Douglas, B., Drenkhan, T., Eberhardt, U., Dueñas, M., Grebenc, T., Griffith, G. W., Hartmann, M., Kirk, P. M., Kohout, P., Larsson, E., Lindahl, B. D., Lücking, R., Martín, M. P., Matheny, P. B., Nguyen, N. H., Niskanen, T., Oja, J., Peay, K. G., Peintner, U., Peterson, M., Pöldmaa, K., Saag, L., Saar, I., Schübler, A., Scott, J. A., Senés, C., Smith, M. E., Suija, A., Taylor, D. L., Telleria, M. T., Weiss, M., and Larsson, K.-H. 2013. Towards a unified paradigm for sequence-based identification of fungi. *Mol. Ecol.* 22:5271-5277.

- Liu, J., Abdelfattah, A., Norelli, J., Burchard, E., Schena, L., Droby, S., and Wisniewski, M. 2018. Apple endophytic microbiota of different rootstock/scion combinations suggests a genotype-specific influence. *Microbiome* 6:18.
- Liu, J., Ridgway, H. J., and Jones, E. E. 2020. Apple endophyte community is shaped by tissue type, cultivar and site and has members with biocontrol potential against *Neonectria ditissima*. *J. Appl. Microbiol.* 128:1735-1753.
- Love, M. I., Huber, W., and Anders, S. 2014. Moderated estimation of fold change and dispersion for RNA-seq data with DESeq2. *Genome Biol.* 15:550.
- Matsumoto, H., Fan, X., Wang, Y., Kusstatscher, P., Duan, J., Wu, S., Chen, S., Qiao, K., Wang, Y., Ma, B., Zhu, G., Hashidoko, Y., Berg, G., Cernava, T., and Wang, M. 2021. Bacterial seed endophyte shapes disease resistance in rice. *Nat. Plants* 7:60-72.
- Olivieri, L., Saville, R. J., Gange, A. C., and Xu, X. 2021a. Apple endophyte community in relation to location, scion and rootstock genotypes and susceptibility to European canker. *FEMS Microbiol. Ecol.* 97:fiab131.
- Olivieri, L., Saville, R. J., Gange, A. C., and Xu, X. 2021b. Limited asymptomatic colonisation of apple tree shoots by *Neonectria ditissima* following infection of leaf scars and pruning wounds. *Plant Pathol.* 70: 1838-1849.
- Omomowo, O. I., and Babalola, O. O. 2019. Bacterial and fungal endophytes: Tiny giants with immense beneficial potential for plant growth and sustainable agricultural productivity. *Microorganisms* 7:481.
- Peiffer, J. A., Spor, A., Koren, O., Jin, Z., Tringe, S. G., Dangl, J. L., Bicl'er, E. S., and Ley, R. E. 2013. Diversity and heritability of the maize rhizosphere microbiome under field conditions. *Proc. Natl. Acad. Sci. U.S.A.* 110:6548-6553.
- R Core Development Team. 2019. R: A Language and Environment for Statistical Computing. R Foundation for Statistical Computing, Vienna, Austria. <https://www.R-project.org/>
- Reisberg, E. E., Hildebrandt, U., Riederer, M., and Hentschel, U. 2012. Phyllosphere bacterial communities of trichome-bearing and trichomeless *Arabidopsis thaliana* leaves. *Antonie Leeuwenhoek* 101:551-560.
- Ricks, K. D., and Koide, R. T. 2019. The role of inoculum dispersal and plant species identity in the assembly of leaf endophytic fungal communities. *PLoS One* 14:e0219832.
- Salter, S. J., Cox, M. J., Turek, E. M., Calus, S. T., Cookson, W. O., Moffatt, M. F., Turner, P., Parkhill, J., Loman, N. J., and Walker, A. W. 2014. Reagent contamination can critically impact sequence-based microbiome analyses. *BMC Biol.* 12:87.
- Saville, R. J., and Olivieri, L. 2019. Fungal diseases of fruit: Apple cankers in Europe. Pages 59-84 in: *Integrated Management of Diseases and Insect Pests of Tree Fruit*. X. Xu and M., Fountain, eds. Burleigh Dodds Science Publishing, Cambridge, U.K.
- Tkacz, A., Hortala, M., and Poole, P. S. 2018. Absolute quantitation of microbiota abundance in environmental samples. *Microbiome* 6:110.
- Wagner, M. R., Lundberg, D. S., del Rio, T. G., Tringe, S. G., Dangl, J. L., and Mitchell-Olds, T. 2016. Host genotype and age shape the leaf and root microbiomes of a wild perennial plant. *Nat. Commun.* 7:12151.
- Wagner, M. R., Roberts, J. H., Balint-Kurti, P., and Holland, J. B. 2020. Heterosis of leaf and rhizosphere microbiomes in field-grown maize. *New Phytol.* 228:1055-1069.
- Weber, R. W. S. 2014. Biology and control of the apple canker fungus *Neonectria ditissima* (syn. *N. galligena*) from a Northwestern European perspective (Biologie und Kontrolle des Obstbaumkrebs-Erregers *Neonectria ditissima* (Syn. *N. galligena*) aus der Perspektive Nordwesteuropas). *Erwerbs-Obstbau* 56:95-107.
- Wei, F., Zhao, L., Xu, X., Feng, H., Shi, Y., Deakin, G., Feng, Z., and Zhu, H. 2019. Cultivar-dependent variation of the cotton rhizosphere and endosphere microbiome under field conditions. *Front. Plant Sci.* 10.